

**Investigation on the role of Tangeretin in alleviation  
of ER stress induced diabetic complications:  
*An in vitro* approach**

by

**Eveline M Anto**  
10BB17J39011

A Thesis submitted to the  
Academy of Scientific and Innovative Research  
for the award of the degree of

**DOCTOR OF PHILOSOPHY**

in

**SCIENCE**

Under the supervision of  
**Dr. P. Jayamurthy**  
Principal Scientist



CSIR- National Institute for Interdisciplinary Science and  
Technology (CSIR-NIIST), Thiruvananthapuram

Kerala-695019, India



Academy of Scientific and Innovative Research  
AcSIR Headquarters, CSIR-HRDC campus  
Sector 19, Kamla Nehru Nagar,  
Ghaziabad, U.P. – 201 002, India

**August 2023**

**CERTIFICATE**

This is to certify that the work incorporated in this Ph.D. thesis entitled, **“Investigation on the role of Tangeretin in alleviation of ER stress induced diabetic complications: An *in vitro* approach”**, submitted by **Eveline M Anto** to the Academy of Scientific and Innovative Research (AcSIR) in partial fulfillment of the requirements for the award of the Degree of **Doctor of Philosophy in Sciences**, embodies original research work carried out by the student. We further certify that this work has not been submitted to any other University or Institution in part or full for the award of any degree or diploma. Research materials obtained from other sources and used in this research work have been duly acknowledged in the thesis. Images, illustrations, figures, tables, etc., used in the thesis from other sources, have also been duly cited and acknowledged.



Eveline M Anto



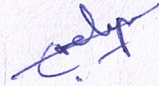
Dr. P. Jayamurthy

(Thesis Supervisor)



## STATEMENTS OF ACADEMIC INTEGRITY

I, Eveline M Anto, a Ph.D. student of the Academy of Scientific and Innovative Research (AcSIR) with Registration No. 10BB17J39011 hereby undertake that, the thesis entitled **“Investigation on the role of Tangeretin in alleviation of ER stress induced diabetic complications: An *in vitro* approach”** has been prepared by me and that the document reports original work carried out by me and is free of any plagiarism in compliance with the UGC Regulations on *“Promotion of Academic Integrity and Prevention of Plagiarism in Higher Educational Institutions (2018)”* and the CSIR Guidelines for *“Ethics in Research and in Governance (2020).”*



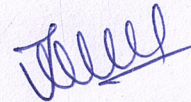
Eveline M Anto

Date 2-8-2023

Thiruvananthapuram

---

It is hereby certified that the work done by the student, under my/ our supervision, is plagiarism-free in accordance with the UGC Regulations on *“Promotion of Academic Integrity and Prevention of Plagiarism in Higher Educational Institutions, (2018)”* and the CSIR Guidelines for *“Ethics in Research and in Governance (2020).”*



Dr. P. Jayamurthy

Date 2/8/23

Thiruvananthapuram



# Acknowledgements

*First and foremost, I express my gratitude to my research supervisor, Dr. P. Jayamurthy for his constant support, guidance, and motivation throughout my PhD tenure. I thank him for his patience and calm nature that has helped me to plan my work meticulously without apprehension.*

*I take this opportunity to thank Dr. K G Raghu, my doctoral advisory committee member and former Head of the division, Agro-Processing and Technology division for his valuable expertise, insights, and encouragement that has propelled me forward in my research.*

*I am grateful to Dr. Priya S and Dr. Krishnakumar B, my doctoral advisory committee members, for their valuable suggestions and feedback that has enabled me to improve the quality of my thesis.*

*I sincerely thank Dr. C Anandharamakrishnan, Dr. A Ajayaghosh, present and former directors of CSIR-NIIST, Thiruvananthapuram for providing all the necessary lab facilities for conducting my research.*

*I express my sincere gratitude to Dr. V Karunakaran, Dr. CH Suresh, and Dr. Luxmi Varma, present and former AcSIR coordinators for efficiently managing the academic formalities and making it hassle-free for the students.*

*I would like to thank Venugopalan sir, Dr. Dileep Kumar, present and former Head of the division, Agro-Processing and Technology, for providing all the facilities and instrument access at the division for conducting my research.*

*I also thank all the scientists, technical officers, and technical staff at Agro-Processing and Technology division for their cooperation and support. I extend my gratitude to Mr. Prateesh for providing all the help regarding the proper functioning of the lab and instrumentation. I also thank Mr. Sreejith for helping with the official work.*

*My sincere thanks to all the staff members in the administration, IT lab, KRC, canteen, and the eminent scientists at CSIR-NIIST for their cooperation and support. I thank Mr. Merin and Ms. Aswathy at the AcSIR office for their humble nature and for helping with the academic documentation.*



*I express my gratitude to Dr. Rajasekaran and his student Nandhini Senthil, Vellore Institute of Technology for helping with the molecular docking studies.*

*I take this opportunity to thank my senior colleagues at APTD and NIIST. Special thanks to Dr. Lekshmy Krishnan for teaching me the basics of cell culture and related techniques with utmost patience and empathy, for selflessly sharing knowledge and research experience and for being a loyal friend. I also thank Dr. Sini S, Dr. Dhanya, Dr. Syama, Dr. Vandana, Dr. Preetha Rani, Dr. Sindhu G, Dr. Anupama, Dr. Shilpa G, Dr. Jamsheena, Dr. Sreelekshmi, Dr. Lakshmi S, Dr. Swapna and Dr. Nayana for their insightful suggestions and guidance.*

*The academic journey has been challenging and there have been instances of self-doubt and low esteem but my friends and colleagues at APTD and NIIST have been a constant source of motivation and support. Special thanks to Sruthi, my roommate and friend for being there with me during all the failed experiments, disappointments, and long working hours at the lab and for selflessly sharing all the chemicals and reagents which has enabled me to complete my work. I also thank Anaga, my research team member and friend for supporting and helping me throughout. My sincere thanks to Suchitra, Sannya, Nidhina, Shini, Suryalekshmi, Lekshmi Sundar, Sudhina, Taniya, Roopasree, Liza George, Billu, Gopika V Krishnan, Drissy, Devi Rajan, Jesmina, Jasim, Poornima, Anusha, Ashin, Raveena, Athira, and Theertha for their help and cooperation.*

*I thank the University grants commission (UGC) for providing fellowship and financial assistance during my PhD tenure.*

*I express my heartfelt gratitude to my parents, Mr. K A Anto and Mrs. Thankamma Joseph, my pillars of support for their unconditional love, for always believing in me even when I failed, and for giving me the confidence to chase my dreams and accomplish my goals.*

*I take this opportunity to thank my husband, Bibin Thomas, for being a true companion who has supported me in all my endeavors and for putting up with me at my worst. I also thank my parents-in-law and family, my sister, my brother-in-law, my nephews, my family, and my friends for their support and prayers.*

*Lastly and most importantly, I thank Lord Almighty and Mother Mary for being my guiding light and showering me with blessings and grace that has helped me to achieve this academic milestone in my life.*

*Eveline M Anto*

*Dedicated to*  
*My Parents, Husband & Daughter*



# Table of Contents

<b>Chapter 1: General Introduction and Review of Literature</b>	<b>1</b>
1.1 Diabetes mellitus	2
1.1.1 Type 1 Diabetes	2
1.1.2 Type 2 Diabetes	3
1.1.3 Gestational Diabetes	3
1.2 Pathophysiology of Diabetes mellitus	4
1.3 Currently used drugs for the treatment of Diabetes mellitus	5
1.4 Why do we need novel targets for disease intervention	8
1.5 Endoplasmic reticulum stress: an emerging target for Diabetes mellitus	9
1.5.1 IRE-1 signaling	12
1.5.2 PERK signaling	13
1.5.3 ATF6 signaling	14
1.5.4 CHOP/GADD153: indicator of maladaptive UPR	14
1.6 ER stress and Oxidative stress	16
1.6.1 ER stress and Insulin resistance	18
1.6.2 ER stress and clearance of misfolded proteins	20
1.6.2.1 ERAD	21
1.6.2.2 Autophagy	24

1.6.3 ER stress and Mitochondrial alterations	26
1.7 ER stress in skeletal muscles	28
1.7.1 Skeletal muscle atrophy	32
1.8 ER stress in pancreatic beta cells	33
1.9 Pharmacological intervention of ER stress pathways	35
1.9.1 Natural products targeting ER stress pathways	37
1.9.1.1 Apigenin	39
1.9.1.2 Luteolin	40
1.9.1.3 Tangeretin	41
1.10 Objectives of study	43
<b>Chapter 2: Effect of the selected flavones (Apigenin, Luteolin and Tangeretin) on ER stress induced redox imbalances in L6 cells</b>	<b>66</b>
2.1 Introduction	67
2.2 Materials & Methods	69
2.2.1 Chemicals	69
2.2.2 Cell culture	69
2.2.3 Experimental groups	70
2.2.4 Experimental design	70
2.2.5 Dose optimization of tunicamycin	71
2.2.5.1 Cytotoxicity studies	71



2.2.5.2 Western blot analysis for ER stress induction	71
2.2.5.3 Flow cytometry analysis for insulin resistance	72
2.2.6 Dose optimization of flavones	72
2.2.6.1 Cytotoxicity studies	72
2.2.6.2 Annexin V FITC staining	72
2.2.7 Detection of intracellular ROS generation by DHE assay and DCFH-DA assay	73
2.2.8 Antioxidant enzyme activity during ER stress	73
2.2.8.1 SOD activity	73
2.2.8.2 GR activity	74
2.2.8.3 TrxR activity	74
2.2.9 Molecular Docking Studies	75
2.2.10 Western Blot	75
2.2.11 Statistical analysis	75
2.3 Results	76
2.3.1 Optimization of tunicamycin dose	76
2.3.1.1 Cytotoxicity studies	76
2.3.1.2 Western blot analysis for upregulation of ER stress markers	76
2.3.1.3 Determination of ER stress induced insulin resistance	77
2.3.2 Optimization of dose of flavones	77

2.3.2.1 Cytotoxicity studies	78
2.3.2.2 Annexin V FITC assay	80
2.3.3 Effect of flavones on tunicamycin induced intracellular ROS generation	81
2.3.4 Antioxidant potential of flavones under ER stress	83
2.3.4.1 Structural interaction of flavones with antioxidant enzymes	85
2.3.5 Selected flavones decrease ER resident oxidoreductases, PDI and ERp72 under ER stress	86
2.3.6 Modulation of GADD153/CHOP protein by selected flavones under ER stress	89
2.3.7 Modulation of major proteins of MAP Kinase signaling cascade by selected flavones under ER stress	91
2.4 Discussion	93
2.5 Summary	97
<b>Chapter 3: Investigation &amp; elucidation of the mechanism of action of most active flavone, tangeretin in mitigation of ER stress induced insulin resistance in L6 cells</b>	<b>102</b>
3.1 Introduction	103
3.2 Materials & Methods	105
3.2.1 Chemicals	105
3.2.2 Cell Culture	106
3.2.3 Experimental Groups	106
3.2.4 Experimental design	106



3.2.5 2-NBDG uptake analysis	107
3.2.6 Western blot analysis for ER stress induction	107
3.2.7 Protein expression studies for insulin resistance induction	108
3.2.8 AMPK inhibitor studies	108
3.2.9 Statistical analysis	109
3.3 Results	109
3.3.1 Tangeretin improves 2-NBDG uptake by mitigating tunicamycin induced insulin resistance	109
3.3.2 Tangeretin suppresses the expression of tunicamycin induced ER stress markers	110
3.3.3 Tangeretin mitigates ER stress mediated insulin resistance via upregulation of AMPK	113
3.3.4 AMPK inhibitor attenuates tangeretin mediated glucose uptake under ER stress mediated insulin resistance	116
3.4 Discussion	118
3.5 Summary	121
<b>Chapter 4A: Effect of Tangeretin on ER stress induced mitochondrial alterations in L6 cells</b>	<b>126</b>
4A.1 Introduction	127
4A.2 Materials & Methods	130
4A.2.1 Chemicals	130

4A.2.2 Cell Culture	130
4A.2.3 Experimental Groups	131
4A.2.4 Experimental Design	131
4A.2.5 Intracellular mitochondrial ROS generation	131
4A.2.6 Mitochondrial Biogenesis	132
4A.2.7 Estimation of oxygen consumption rate	132
4A.2.8 Determination of mitochondrial membrane potential	132
4A.2.9 Western Blot studies	133
4A.2.10 Statistical analysis	134
4A.3 Results	134
4A.3.1 Tangeretin suppresses tunicamycin induced mitochondrial ROS generation and improves SOD levels	134
4A.3.2 Tunicamycin mediated mitochondrial alterations were independent of mitochondrial biogenesis/number, oxygen consumption rate and complex IV activity	136
4A.3.3 Tangeretin reduces tunicamycin-induced loss of mitochondrial membrane potential ( $\Delta\psi_m$ )	138
4A.3.4 Effect of tangeretin on mitochondrial dynamics during ER stress	139
4A.3.5 Effect of tangeretin on IP <sub>3</sub> R VDAC GRP75 complex at MAM junction under ER stress	140
4A.3.6 Tangeretin downregulates tunicamycin induced PACS and FUNDC1 levels	141



4A.3.7 Effect of tangeretin on XIAP and cytochrome c levels under ER stress	142
4A.4 Discussion	143
4A.5 Summary	149
<b>Chapter 4B: Effect of Tangeretin on ER stress induced autophagy and ERAD signaling in L6 Cells</b>	<b>157</b>
4B.1 Introduction	158
4B.2 Materials & Methods	160
4B.2.1 Chemicals	160
4B.2.2 Cell Culture	161
4B.2.3 Experimental Groups	161
4B.2.4 Experimental Design	161
4B.2.5 Western Blot studies	162
4B.2.6 Immunofluorescence studies	163
4B.2.7 Statistical analysis	163
4B.3 Results	163
4B.3.1 Tangeretin abrogates tunicamycin induced autophagy in L6 myotubes	163
4B.3.2 Tangeretin improves the expression of autophagy regulators	164
4B.3.3 Modulation of ERAD proteins by tangeretin	165
4B.3.4 Tangeretin upregulates the SERCA and concomitantly downregulates phospho-ryanodine receptors (p-RYR) expression levels under ER stress	168

4B.4 Discussion	170
4B.5 Summary	174
<b>Chapter 5: Effect of Tangeretin in improving the cellular function in pancreatic Beta-TC-6 cells under ER stress condition</b>	<b>181</b>
5.1 Introduction	182
5.2 Materials & Methods	185
5.2.1 Cell Culture	185
5.2.2 Experimental groups	186
5.2.3 Experimental Design	186
5.2.4 Cytotoxicity studies of tunicamycin and tangeretin	186
5.2.5 Intracellular ROS generation	187
5.2.6 Determination of mitochondrial number/biogenesis and mitochondrial membrane potential	187
5.2.7 Immunofluorescence staining of Beta-TC-6 cells	188
5.2.8 Western Blot analysis	188
5.2.9 Statistical Analysis	189
5.3 Results	189
5.3.1 Cytotoxicity studies of tunicamycin and tangeretin	189
5.3.2 Tangeretin suppresses tunicamycin induced intracellular ROS generation	
5.3.3 Changes in mitochondrial number/biogenesis and mitochondrial membrane potential	191

5.3.4 Tangeretin modulates the expression of XBP-1, ER resident chaperones and GADD153 during ER stress	194
5.3.5 Effect of tangeretin on expression levels of TRB3, p-Akt, Pdx-1, Maf A and GLUT 2 during ER stress	195
5.3.6 Effect of tangeretin on insulin expression during ER stress	198
5.4 Discussion	199
5.5 Summary	203
<b>Chapter 6: Summary &amp; Conclusion</b>	<b>212</b>

## List of Figures

<b>Figure No.</b>	<b>Title</b>	<b>Page No.</b>
Figure.1.1	Pathophysiology of diabetes mellitus	5
Figure.1.2	Endoplasmic reticulum structure	10
Figure.1.3	The activation of the three UPR sensors in response to ER stress	12
Figure.1.4	Activation of CHOP by all three ER stress sensors leads to apoptosis	15
Figure.1.5	Oxidative protein folding in the ER	17
Figure.1.6	ER stress induced ROS generation and subsequent oxidative stress	18
Figure.1.7	Endoplasmic reticulum associated degradation (ERAD) steps	23
Figure.1.8	Schematic representation of stepwise autophagy process	25
Figure.1.9	Major proteins present at the MAM junction tethering the ER to the mitochondria	27
Figure.1.10	ER stress mediated implications in skeletal muscles	31
Figure.1.11	The crosstalk between insulin resistance and skeletal muscle atrophy	33
Figure.1.12	Sustained hyperglycaemia induces ER stress disturbing the equilibrium between ER folding capacity and insulin demand	35
Figure.1.13	Natural compounds targeting ER stress pathways	38
Figure.1.14	a) Basic flavonoid structure. b) Basic flavone structure	39
Figure.1.15	Structure and natural source of selected flavones. a) Apigenin, b) Luteolin, c) Tangeretin	42

Figure.2.1	Vicious cycle between ER stress and ROS generation	67
Figure.2.2	Schematic representation of experimental design	70
Figure.2.3	Cytotoxicity studies of tunicamycin	76
Figure.2.4	Optimization of tunicamycin dose for ER stress induction	77
Figure.2.5	Dose optimization of tunicamycin for induction of insulin resistance	78
Figure.2.6	Cytotoxicity studies of selected flavones	79
Figure.2.7	Annexin V FITC assay	80
Figure.2.8	Effect of flavones on tunicamycin induced intracellular ROS generation.	82
Figure.2.9	Antioxidant potential of flavones under ER stress	84
Figure.2.10	Molecular docking	86
Figure.2.11	Protein expression studies of ER resident oxidoreductases, PDI & ERp72	88
Figure.2.12	Protein expression of GADD153/CHOP	90
Figure.2.13	Protein expression of ERK1/2, p-p38 MAP Kinase, p-JNK	92
Figure.2.14	Effect of flavones on tunicamycin induced cellular redox imbalances	97
Figure.3.1	Insulin-dependent and independent signaling pathways for glucose uptake in skeletal muscle cells	104
Figure.3.2	Schematic representation of the experimental design	107
Figure.3.3	Effect of flavones on tunicamycin induced insulin resistance	110
Figure.3.4	Effect of tangeretin on expression of tunicamycin induced major ER stress markers	112



Figure.3.5	Effect of tangeretin on tunicamycin induced insulin resistance	114
Figure.3.6	Effect of tangeretin on tunicamycin induced insulin resistance	115
Figure.3.7	AMPK inhibitor studies	117
Figure.3.8	Proposed mechanism of action of tangeretin in mitigating ER stress induced insulin resistance in skeletal muscle L6 cells	122
Figure.4A.1	Interplay between ER stress, mitochondrial dysfunction and MAMs defect contribute to insulin resistance	129
Figure.4A.2	Schematic representation of the experimental design	131
Figure.4A.3	Effect of tangeretin on mitochondrial ROS generation and SOD1 and SOD2 expression levels during tunicamycin induced ER stress	135
Figure.4A.4	Mitochondrial biogenesis/number, oxygen consumption rate COXIV and UCP3 expression under ER stress	137
Figure.4A.5	Tangeretin improves ER stress induced loss of mitochondrial membrane potential	139
Figure.4A.6	Effect of tangeretin on mitochondrial fusion and fission proteins under ER stress	140
Figure.4A.7	Effect of tangeretin on MAM proteins, IP <sub>3</sub> R, VDAC, GRP75 under ER stress	141
Figure.4A.8	Tangeretin downregulates expression of MAM proteins PACS2 and FUNDC1 under ER stress condition	142
Figure.4A.9	Effect of tangeretin on XIAP and cyt c levels under ER stress	143
Figure.4A.10	Effect of tangeretin on tunicamycin induced mitochondrial alterations in L6 myotubes	150
Figure.4B.1	Delicate balance between protein synthesis, protein folding and quality control comprise the proteostasis network	159
Figure.4B.2	Schematic representation of the experimental design	162

Figure.4B.3	Tangeretin abrogates tunicamycin induced autophagy in L6 myotubes	164
Figure.4B.4	Tangeretin improves the expression of autophagy regulators	165
Figure.4B.5	Tangeretin downregulates tunicamycin induced GRP94 and calnexin	166
Figure.4B.6	Effect of tangeretin on expression of EDEM1 and HERPUD1 during ER stress	167
Figure.4B.7	Effect of tangeretin on expression of RNF5, SYVN1, UFD1, SEL1 during ER stress	168
Figure.4B.8	Effect of tangeretin on expression of ER calcium pumps, SERCA and p-RYR	169
Figure.4B.9	Effect of tangeretin on tunicamycin induced autophagy and ERAD in L6 myotubes	175
Figure.5.1	Glucotoxicity and lipotoxicity induce ER stress in pancreatic beta cells	183
Figure.5.2	Schematic representation of the experimental design	186
Figure.5.3	Cytotoxicity analysis of tunicamycin and tangeretin	190
Figure.5.4	Determination of intracellular ROS generation	191
Figure.5.5	Tangeretin improves mitochondrial number/biogenesis under ER stress	192
Figure.5.6	Tangeretin improves tunicamycin induced loss of mitochondrial membrane potential	193
Figure.5.7	Effect of tangeretin on tunicamycin induced expression of XBP-1, GADD153, ER resident chaperones (GRP94 & calnexin)	195
Figure.5.8	Effect of tangeretin on expression levels of TRB3, p-Akt, Maf-A and GLUT 2 during ER stress	196
Figure.5.9	Tangeretin improves Pdx-1 levels during ER stress in pancreatic Beta-TC-6 cells	197

Figure.5.10	Effect of tangeretin on insulin expression during ER stress	198
Figure.5.11	Effect of tangeretin on pancreatic Beta-TC-6 function during tunicamycin induced ER stress	204
Figure.6.1	Schematic result summary in rat skeletal muscle L6 cells	218
Figure.6.2	Schematic result summary in pancreatic Beta-TC-6 cells	220

## List of Tables

<b>Table No.</b>	<b>Title</b>	<b>Page No.</b>
Table 1.1	Currently used antidiabetic drugs	6
Table 2.1	The binding energies of the docked structures	85

# Abbreviations

2-NBDG	2-[N-(7-nitrobenz-2-oxa-1,3-diazol-4-yl) amino]-2-deoxy-D-glucose
AKT	Protein kinase B
AMPK	Activated protein kinase
ANOVA	One-way analysis of variance
API	Apigenin
ASK1	Apoptosis Signal-regulating Kinase 1
ATF4	Activating transcription factor 4
ATF6	Activating transcription factor 6
BAP31	B-cell receptor-associated protein 31
BCA	Bicinchoninic acid
BIP	Immunoglobulin heavy chain binding protein
BSA	Bovine serum albumin
Ca <sup>2+</sup>	Calcium
CaMKII	Ca <sup>2+</sup> /calmodulin-dependent protein kinase II
CHOP	C/EBP homologous protein
Cyt c	Cytochrome c
DCFH-DA	2, 7-dichlorodihydrofluorescein diacetate
DHE	Dihydroethidium
DMEM	Dulbecco's modified eagle's medium
DMSO	Dimethyl sulfoxide
DPPIV	Dipeptidyl peptidase IV
DRP1	Dynamin-related protein
DTNB	5, 5'-dithio-bis-2- (nitrobenzoic acid)
ECL	Enhanced chemiluminescence
EDTA	Ethylene diamine tetra acetic acid
eIF2 $\alpha$	eukaryotic translation initiation factor 2 $\alpha$

ER	Endoplasmic reticulum
ERAD	ER-associated degradation
ERK1/2	Extracellular signal regulated kinase1/2
ERp72	Endoplasmic reticulum protein 72
ETC	Electron transport chain
FBS	Fetal bovine serum
FFAs	Free fatty acids
FIS1	Mitochondrial fission protein
FOXO	Forkhead transcription factor
FUNDC1	FUN14 Domain Containing 1
GADA	Glutamic acid decarboxylase autoantibodies
GADD153	Growth arrest-and DNA damage-inducible gene
GLP-1	Glucagon-like peptide-1
GLUT2	Glucose transporter 2
GLUT4	Glucose transporter 4
GR	Glutathione reductase
GRP75	Glucose regulatory protein 75
GRP78	Glucose regulatory protein 78
GRP94	Glucose regulatory protein 94
GSH	Reduced glutathione
GSSG	Oxidised glutathione
H <sub>2</sub> O <sub>2</sub>	Hydrogen peroxide
HBSS	Hanks' balanced salt solution
HRP	Horseradish peroxidase
IAPP	Islet amyloid precursor protein
IDDM	Insulin-dependent diabetes mellitus
IDF	International diabetes federation
INM	Inner nuclear membrane
IP <sub>3</sub> R	Inositol 1,4,5-trisphosphate receptor
IRE-1	Inositol-requiring transmembrane kinase/endoribonuclease 1



IRS1	Insulin receptor substrate 1
JNK	c-Jun N-terminal kinase
LADA	Latent autoimmune diabetes in adults
LUT	Luteolin
Maf A	Musculoaponeurotic fibrosarcoma
MAMs	Mitochondrial associated membranes
MAP Kinase	Mitogen-activated protein kinase
MAP3K5	Mitogen-Activated Protein Kinase Kinase Kinase 5
MFN2	Mitofusin 2
MIDY	Mutant insulin gene-induced diabetes of youth
MTT	(3-(4,5-Dimethylthiazol-2-yl)-2,5-diphenyltetrazolium bromide)
NIDDM	Non-insulin-dependent diabetes mellitus
OMM	Outer mitochondrial membrane
ONM	Outer nuclear membrane
OPA1	Optic atrophy 1
p38MAPK	p38 mitogen-activated protein kinase
PACS2	Phosphofurin acidic cluster sorting protein 2
PBA	4-Phenylbutyric acid
PBS	Phosphate buffered saline
PDI	Protein disulphide isomerase
Pdx-1	Pancreatic duodenal homeobox-1
PEPCK	Phosphophenolpyruvate carboxykinase
PERK	Protein kinase RNA-like endoplasmic reticulum kinase
PI3K	Phosphoinositide 3- kinase
PIP2	Phosphatidylinositol 3,4,5-triphosphate
PIP3	Phosphatidylinositol 4,5-bisphosphate
PTEN	Phosphatase and tensin homolog
PTP1P51	Protein tyrosine phosphatase interacting protein 51
PVDF	Polyvinylidene fluoride
RIPA	Radioimmunoprecipitation assay

ROS	Reactive oxygen species
RYR	Ryanodine receptors
SERCA	Sarco-endoplasmic reticulum Ca <sup>2+</sup> ATPase
SOD	Superoxide dismutase
TAN	Tangeretin
TM	Tunicamycin
TRB3	Tribbles homolog 3
TrxR	Thioredoxin reductase activity
TUDCA	Taurine-conjugated ursodeoxycholic acid
UCP3	Uncoupling Protein 3
UPR	Unfolded protein response
UPS	Ubiquitin-proteasome system
VAPB	Vesicle-associated membrane protein-associated protein B
VDAC	Voltage-dependent anion channel
WHO	World Health Organization
XBP-1	X-box binding protein 1
XIAP	X-linked inhibitor of apoptosis protein

# **Chapter 1**

## **General Introduction & Review of Literature**

## **1.1 Diabetes mellitus**

Diabetes mellitus is a progressive multifactorial metabolic disease defined by elevated blood glucose levels or hyperglycemia that in the long-term, results in injury to various organs such as kidneys, eyes, and heart and also damages the nerves and blood vessels. The International Diabetes Federation (IDF) estimates that 537 million people worldwide have diabetes, with 783 million people anticipated to have the disease by 2045 (Sun et al., 2022). Diabetes has emerged as one of the major global health issues having a significant negative impact on the socioeconomic progress of the nations and the lifespan of afflicted individuals. By 2030, diabetes is expected to be the sixth most common cause of death worldwide, according to the WHO (World Health Organization, 2010). As of 2017, the three major risk factors are high body mass index (BMI) accounting for 30.8% of mortality, dietary risk accounting for 24.7% of fatalities, and ambient particulate matter pollution responsible for 13.4% of mortality (X. Lin et al., 2020). India has emerged as one of the epicenters with a diabetic population of 74.2 million in 2021, second only to China having 140.9 million affected population which is projected to rise by 2045 to 124.9 million and 174.4 million in India and China respectively (Webber, 2021). Diabetes is mainly categorized into three types: Type 1 diabetes, Type 2 diabetes, and Gestational diabetes.

### **1.1.1 Type 1 Diabetes**

Also known as insulin-dependent diabetes mellitus (IDDM) is an autoimmune disorder which involves the T-cell mediated destruction of pancreatic beta cells, preventing them from producing insulin (Knip & Siljander, 2008). Insulin is a hormone mandatory for cellular glucose uptake and in the absence of insulin, cells fail to take up glucose resulting in hyperglycemia. It is commonly observed in children and therefore also known as

juvenile-onset diabetes. However, in some cases, type 1 diabetes may occur in adults as slowly progressing insulin dependent diabetes which can be distinguished from type 2 diabetes by the presence of autoantibodies (Banday et al., 2020) . This condition is known as the Latent autoimmune diabetes in adults (LADA). The important immune markers of this adult-onset autoimmune diabetes are the glutamic acid decarboxylase autoantibodies (GADA) (Hawa et al., 2013).

### **1.1.2 Type 2 Diabetes**

Also known as the non-insulin-dependent diabetes mellitus (NIDDM) is the predominant form accounting for more than 90% of cases and is characterized by both impaired insulin secretion and insulin resistance (Muio & Newgard, 2008). Insulin resistance is a condition in which cells fail to respond to insulin due to a defect in insulin receptor mediated signal thereby leading to diminished glucose uptake in peripheral tissues namely skeletal muscle, liver and adipose tissue (Savage et al., 2005). The main risk factors include obesity, sedentary lifestyle, lack of exercise, family history, age, diet, polycystic ovarian syndrome (Banday et al., 2020).

### **1.1.3 Gestational Diabetes**

It is a condition which develops during pregnancy in women without a prior history of diabetes. During pregnancy the placenta supports the growth of the fetus by producing certain hormones. The hormones inhibit the action of mother's insulin resulting in hyperglycemia (*Gestational Diabetes Mellitus (GDM) | Johns Hopkins Medicine*). The major risk factors are increased weight, decreased physical activity, an immediate family member with diabetes and polycystic ovarian syndrome (PCOS). Women with gestational diabetes are more prone to developing diabetes later in life (Rodriguez & Mahdy, 2022).



## **1.2 Pathophysiology of Diabetes mellitus**

As already stated, diabetes is a heterogenous, metabolic condition characterized by sustained hyperglycemia which is a consequence of reduced insulin secretion or reduced insulin sensitivity (insulin resistance) or both. The complexity of diabetes is due to the involvement of multiple organs that showcase abnormal functioning during the disease condition. The main organs implicated in the pathophysiology of diabetes are the pancreas, skeletal muscle, liver and adipose tissue (Figure.1.1). Under normal conditions, these organs are involved in maintaining the glucose homeostasis. Under physiological conditions, after a meal, glucose is absorbed into the circulation via the gastrointestinal (GI) tract, resulting in a spike in blood glucose levels. To facilitate clearance of glucose from circulation and promote cellular uptake in the peripheral tissues, pancreas release the insulin hormone. The insulin then binds to the receptors on cell surface of skeletal muscles and adipose tissue enabling the insulin dependent glucose uptake via the glucose transporter 4 (GLUT4) thereby lowering the circulating glucose levels (Röder et al., 2016). Insulin also enhances protein synthesis and glucose utilization in skeletal muscles whereas in adipose tissues, it promotes glucose utilization, fat esterification while decreasing lipolysis (Luo & Liu, 2016; Washburn et al., 2021). In liver, insulin does not directly promote glucose uptake, this is because of the presence of insulin independent glucose transporters, GLUT1 & 2 on the hepatocyte membrane. Here, insulin functions to trigger signaling pathways such as glycolysis (glucose utilization), glycogenesis (synthesis of glycogen from glucose) and lipogenesis (fatty acid synthesis) while it decreases gluconeogenesis (glucose production from de novo sources) and glycogenolysis (breakdown of glycogen) (Ribeiro & Antunes, 2018). However, under diabetic condition, the tightly regulated glucose homeostasis is disturbed resulting in impaired insulin secretion from the pancreatic islets in type 1 diabetes and later stages of

type 2 diabetes due to beta cell loss. Impaired cellular glucose uptake in skeletal muscle cells, adipose tissue and decreased glycogenesis and glycolysis in liver as a consequence of insulin resistance are also observed (Washburn et al., 2021).

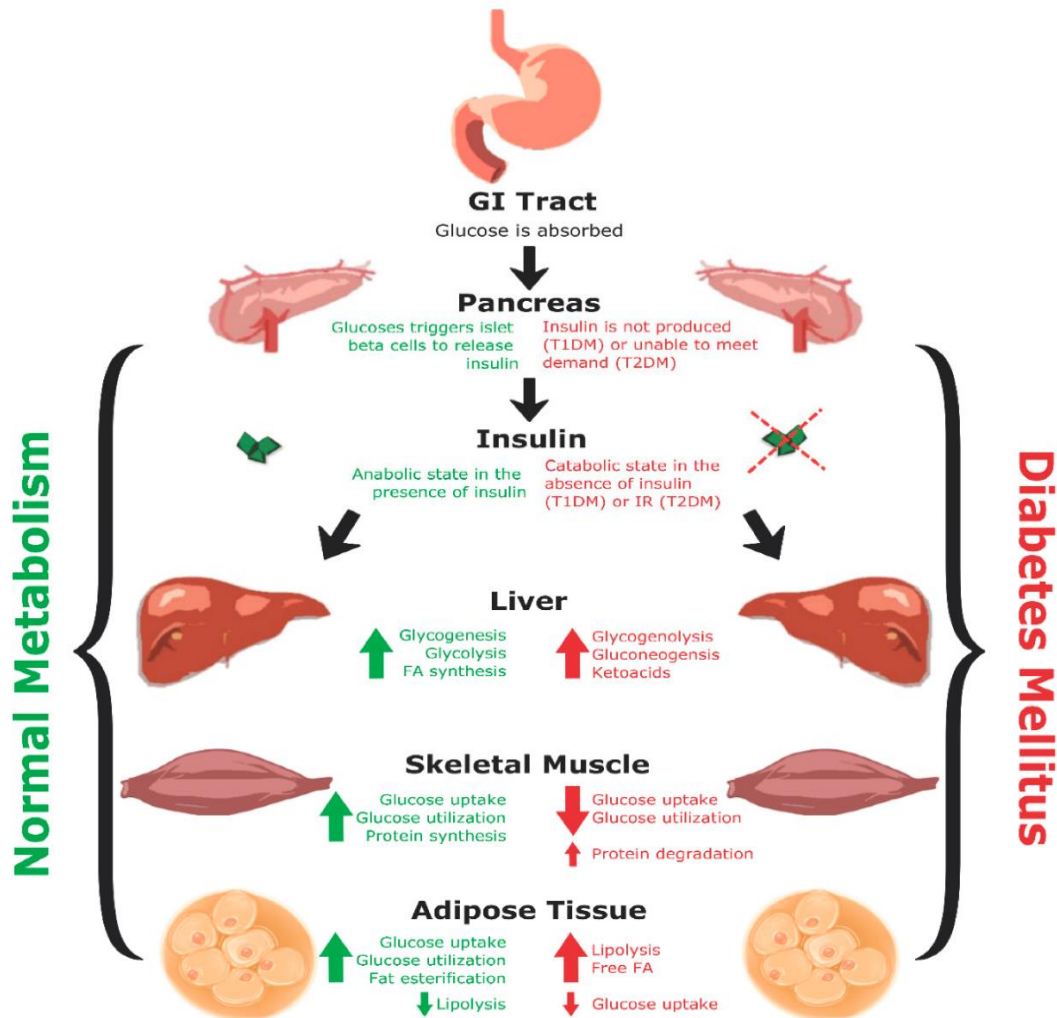


Figure.1.1. Pathophysiology of diabetes mellitus (Washburn et al., 2021)

### 1.3 Currently used drugs for treatment of Diabetes mellitus

Proper glycemic control strategies are required for effective disease management. There are several classes of antidiabetic drugs available commercially. The primary goal of these medications is to ameliorate hyperglycemia and depending on the severity of the condition, these drugs are either administered alone or in combination. The drug targets,

their mode of action and side effects are shown in Table 1.1. (Chaudhury et al., 2017; Hansen et al., 2013).

**Table 1.1 Currently used antidiabetic drugs**

<b>Class of Drug</b>	<b>Example/Brand Name</b>	<b>Mode of action</b>	<b>Side-effects</b>
Insulin	Injectable insulin a) Short acting insulin (Humulin, Novolin) b) Long-acting insulin (Detemir, Glargine) c) Rapid acting (Lispro)	Increase in endogenous insulin levels and subsequent upregulation of insulin signaling in peripheral tissues	Hypoglycemia
Biguanides	Metformin	Reduction in hepatic glucose production Increase in glucose uptake in skeletal muscle and adipose tissue by AMPK activation	Lactic acidosis, weight loss
Thiazolidinediones	Rosiglitazone, Pioglitazone	Promote insulin sensitivity via activation of peroxisome proliferator-activated receptor gamma (PPAR-gamma)	Cardiac failure, bladder cancer, weight gain

Sulfonylureas	Glimepiride, Glyburide, Glibenclamide	Promotes insulin secretion from pancreatic islets	Weight gain, hypoglycemia, increased CVD risk
Dipeptidyl peptidase IV (DPPIV)	Sitagliptin, Saxagliptin	Inhibition of Glucagon like peptide-1 (GLP-1) degradation thereby promoting insulin release	Pancreatitis
GLP-1 agonists	Liraglutide, Exenatide	Stimulate insulin secretion from pancreas while suppressing glucagon release by activating the GLP-1 receptors in pancreas	Weight loss, nausea, vomiting, pancreatitis
Alpha glucosidase inhibitors	Acarbose, Miglitol	Inhibits starch breakdown, slowing the release of glucose in circulation	Diarrhea, bloating, nausea
Sodium glucose co-transporter inhibitor (SGLT2)	Canagliflozin, Dapagliflozin, Empagliflozin	Promote glycosuria by reducing glucose reabsorption from proximal renal tubules thereby facilitating elimination of glucose from body	Acute renal injury, increased risk of bone fractures, genitourinary infections, ketoacidosis(rare)

#### **1.4 Why do we need novel targets for disease intervention**

Despite the availability of the antidiabetic drugs for management of diabetes, the disease prevalence as well as the economic burden imposed by the diabetes healthcare is increasing at an alarming rate. The annual cost globally in 2021 was estimated to be 966 billion US dollars which is a 316% increase from 232 billion dollars in 2007 and the global economic burden is projected to reach \$2-2.5 trillion by 2030 (Bommer et al., 2018; Sun et al., 2022). Due to a lack of adequate health insurance coverage for the general public and the prevalence of the ailment in both rich and poor people, emerging nations like India experience terrible economic conditions and prevalence. In 2017, the nationwide economic burden due to diabetes in India was observed to be 31 billion US dollars, placing the country at fourth position behind USA, China and Germany (Oberoi & Kansra, 2020). The diabetic population between the age 20 to 79 is expected to rise globally to 642 million (1 in 10 adults) in 2040 compared to 415 million (1 in 11 adults) in 2015 (Sun et al., 2022). The exponential growth in prevalence of diabetes can be a consequence of it being a life-long condition which despite the availability of medication worsens over time resulting in severe complications such as neuropathy, nephropathy, retinopathy and myopathy which further creates a dent in patient's pockets. This may be because the treatment strategy focuses on reprimanding the cellular outcomes namely insulin resistance and impaired insulin secretion rather than targeting the underlying mechanisms. There is a need for developing better therapeutic strategies to control the growing diabetic population as well as to curb the cost. This should involve identification of novel targets for disease intervention and cheaper alternatives than the currently used drugs.

## **1.5 Endoplasmic reticulum stress: An emerging target for Diabetes mellitus**

The complex heterogenous etiology of diabetes warrants a multitargeted therapeutic approach that should focus on gaining a deeper insight into the causes underlying insulin resistance and impaired insulin secretion. Endoplasmic reticulum (ER) stress has emerged as one of the underlying causes for diabetes pathogenesis. ER consisting of an interconnected continuous membrane network is the largest organelle distributed in the cytoplasm of the eukaryotic cells. The first description of the ER as a reticular structure was made by Emilio Veratti in 1902 by using the light microscope but it took another 50 years for researchers to rediscover it after the introduction of the electron microscope (Mazzarello et al., 2003).

The ER is a highly complex and dynamic structure consisting of two main domains, the nuclear envelope and the peripheral ER comprising the flat cisternae and reticular tubules as depicted in Figure.1.2 (Westrate et al., 2015). The nuclear envelope consists of the inner nuclear membrane and outer nuclear membrane (INM & ONM) stacked together as a flat membrane bilayer enveloping the nucleus that are separated by an internuclear membrane space while coming in contact only at the nuclear pores facilitating the diffusion of membrane proteins and molecules between the nucleus and cytoplasm (English & Voeltz, 2013). The peripheral ER extends from the ONM as a network of cisternae sheets and dynamic tubules, the ratio of the flat cisternae and tubules varies from cell to cell (Shibata et al., 2006). The main difference between the sheets and tubules lies in the membrane curvature with the former having a low membrane curvature except at the edges whereas the latter having a high membrane curvature (Westrate et al., 2015).



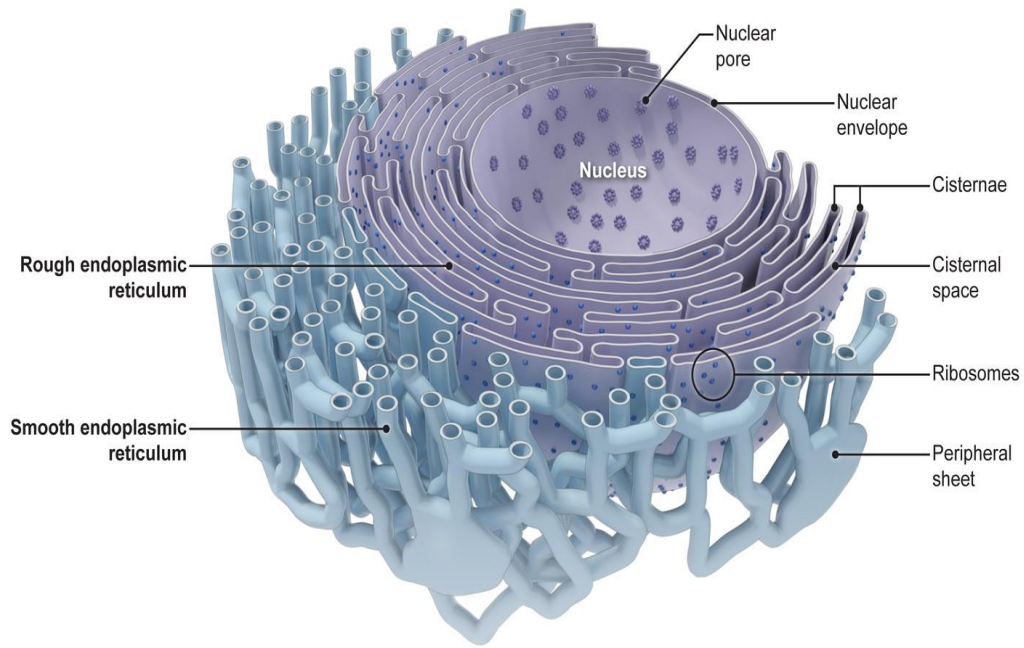


**Figure.1.2. Endoplasmic reticulum structure** (Goyal & Blackstone, 2013)

Electron microscopic studies have revealed the presence of ribosomes on the flat cisternae sheet rendering it a rough surface giving it the name rough ER (RER) while tubules have a smooth surface owing to the lack of ribosomes and therefore also known as the smooth ER (SER) (Voeltz et al., 2002). The SER is involved in lipid synthesis, steroid synthesis, calcium storage and homeostasis. It is well known that ribosomes are the site for protein synthesis or translation and the RER is involved in protein folding, translocation and post-translational modifications which is the predominant function of the ER. After the translation, the nascent polypeptide enters the ER lumen where it undergoes folding, disulfide bond formation and post translational modifications such as N-linked glycosylation and amino acid hydroxylation or carbonylation to achieve the native conformation with the help of ER resident chaperones and oxidoreductases (Schwarz and Blower 2016). After maturation, the proteins are directed to the Golgi apparatus for further processing before being transported to their ultimate destination. Being a highly

complex process, protein folding is error-prone and can result in the formation of some unfolded or misfolded protein aggregates. These aggregates are then degraded by the ubiquitin-mediated proteasome, preventing them from leaving the ER (Guerriero & Brodsky, 2012).

When the capacity for protein folding is exceeded by the demand for protein folding, a condition known as ER stress results, which causes an accumulation of misfolded proteins in the ER lumen. Any perturbations in the normal functioning of the ER leads to ER stress which then triggers a signaling cascade known as the unfolded protein response (UPR) whose primary goal is to restore the ER homeostasis by relieving the stress. The UPR is primarily an adaptive mechanism which aims to reduce the misfolded protein load and promote cell survival by attenuation of protein synthesis, degradation of unwanted misfolded protein aggregates by endoplasmic reticulum associated degradation (ERAD) and upregulation of protein folding machinery by transcriptional activation of chaperones and other folding assisting enzymes (Rajan et al., 2007). In cases of sustained or chronic ER stress, the UPR fails to restore homeostasis and becomes maladaptive or dysregulated leading to cellular apoptosis. Maladaptive UPR is associated with several pathological conditions including diabetes (J. H. Lin et al., 2007). The main stimuli for ER stress induction include high glucose, inflammatory cytokines, circulating free fatty acids, nutrient deprivation, hypoxia, reactive oxygen species (ROS) and calcium imbalance (Fonseca et al., 2011). Inositol-requiring kinase 1 alpha (IRE-1), protein kinase ribonucleic acid (RNA)-activated-like ER kinase (PERK), and activating transcription factor 6 (ATF6) are the three main arms of the UPR (Malhotra & Kaufman, 2007). These three ER stress sensors are sequestered by the BIP protein, also known as GRP78, under non-stressed conditions. These three sensors separate from BIP when ER stress is induced, activating downstream signaling pathways that, depending on how long the

stress lasts, may cause cell survival or apoptosis (Rutkowski & Kaufman, 2004) as shown in Figure.1.3.

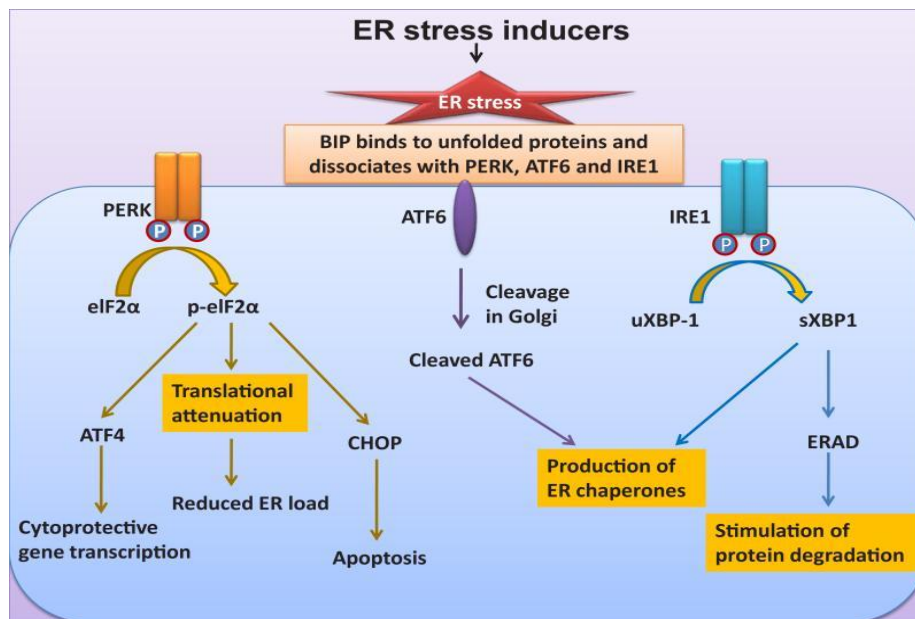


**Figure.1.3.**The activation of the three UPR sensors in response to ER stress (Mei et al., 2013)

### 1.5.1 IRE-1 signaling

It is the most conserved arm of the UPR comprising a serine/threonine kinase and an endoribonuclease domain and gets activated by dimerization and autophosphorylation following dissociation from the BIP protein (Hetz, 2012). It is a type I transmembrane protein and consists of two forms, IRE-1 $\alpha$  and IRE-1 $\beta$  sharing 39% sequence homology, the former is universally expressed whereas the expression of the latter is limited to gastrointestinal tract and pulmonary mucosal epithelium (Almanza et al., 2019; Martino et al., 2013). Upon activation, the IRE-1 $\alpha$  exerts its endoribonuclease activity by initiating the X box-binding protein 1 (XBP-1) mRNA splicing. Following this, the spliced XBP-1 (XBP-1s) then translocates to the nucleus enabling the transcriptional activation of genes involved in enhancing the protein folding and ERAD that are required for restoring the ER homeostasis and promoting survival. Besides this function, RNase activity of IRE-1 $\alpha$

is also involved in selective targeting and degradation of mRNAs coding for proteins involved in protein folding through a process known as regulated IRE-1 $\alpha$  dependent decay (RIDD) (Deldicque et al., 2013). The acute RIDD signaling aids in adaptive response whereas sustained activation leads to apoptosis. The kinase activity of the IRE-1 $\alpha$  gets triggered during the chronic ER stress, thereby activating the apoptosis signal-regulating kinase1 (ASK1) and downstream Jun-N-terminal kinase (JNK) and p38 mitogen activated protein kinase (p38 MAPK) which subsequently lead to cellular apoptosis (Ron & Hubbard, 2008).

### **1.5.2 PERK signaling**

It is an ER type I transmembrane protein which gets activated by dimerization and autophosphorylation following dissociation from BIP or GRP78 in response to ER stress. It also comprises a serine/threonine kinase domain (Bertolotti et al., 2000). The activated PERK then phosphorylates the eukaryotic translation initiation factor (eIF2 $\alpha$ ) which then attenuates the protein synthesis while also activating downstream UPR element activating transcription factor 4 (ATF4) (Harding et al., 2000). The ATF4 then translocates to the nucleus and promotes transcription of genes involved in amino acid metabolism, glutathione synthesis and reduction of oxidative stress favouring cell survival (Harding et al., 2003). Under prolonged stress conditions, PERK/ATF4 signaling becomes pro-apoptotic by activating the pro-apoptotic factor growth arrest-and DNA damage-inducible gene (GADD153) or C/EBP homologous protein (CHOP) which initiates cellular apoptosis (Sano & Reed, 2013).

### **1.5.3 ATF6 signaling**

It is an ER type II transmembrane protein comprising two subunits, ATF6 $\alpha$  and ATF6 $\beta$  with ATF6 $\alpha$  having better transcriptional activity (Thuerauf et al., 2007). During ER stress, ATF6 $\alpha$  dissociates from the GRP78 and moves to the Golgi apparatus and then undergoes cleavage by site1 and site2 proteases (Shen et al., 2002). The cleaved cytosolic form then enters the nucleus and triggers transcriptional activation of XBP-1, ER chaperones and ERAD thereby facilitating cryoprotection (Taouji et al., 2013). However, under sustained ER stress, ATF6 activates CHOP triggering apoptotic pathways (H. Yang et al., 2020).

### **1.5.4 CHOP/GADD153: indicator of maladaptive UPR**

The primary aim of the UPR is to restore ER homeostasis by alleviating ER stress and promoting cell survival. However, during chronic ER stress, the UPR fails to restore ER homeostasis resulting in cellular apoptosis. The key UPR element involved in the progression of apoptosis is the CHOP or GADD153, whose expression increases in response to maladaptive UPR activating pro-apoptotic factors (Alam et al., 2017). CHOP is a nuclear protein belonging to the CCAAT/enhancer-binding protein (C/EBP) family of transcription factors and comprises two domains, an N-terminal transcriptional activation domain and a C-terminal basic-leucine zipper domain (bZIP) with the latter domain involved in CHOP mediated apoptosis (H. Hu et al., 2019). In absence of stress conditions, CHOP is expressed at very low levels in the cytoplasm, however under chronic ER stress, CHOP expression is significantly upregulated following nuclear translocation and precedes the apoptosis induction. Under pathological conditions, CHOP is activated by all the three arms of the UPR as depicted in Figure.1.4. Apoptosis is induced by the PERK/ATF4/CHOP signaling, IRE-1/ASK-1/p-p38MAPK/CHOP

signaling and ATF6/CHOP signaling (De Bernard et al., 2019). CHOP triggers the intrinsic apoptosis by activating the genes encoding the pro-apoptotic BIM protein and suppressing the translational activation of the anti-apoptotic BCL-2 protein followed by release of cytochrome c and activation of caspases (McCullough et al., 2001; Puthalakath et al., 2007). Extrinsic apoptotic pathway is also induced by CHOP via the transcriptional activation of the TNF family member cell surface- DR-5 which activates Fas-associated death domain and caspase 8 (Y. Yang et al., 2017). CHOP can also mediate apoptosis via the activation of Tribbles homolog 3 (TRB3), an inhibitor of the Akt phosphorylation and also by the calcium mediated apoptosis through activation of ERO1 $\alpha$  and subsequent activation of Ca<sup>2+</sup>/calmodulin-dependent protein kinase II (CaMKII) (K. Du et al., 2003; Y. Yang et al., 2017).

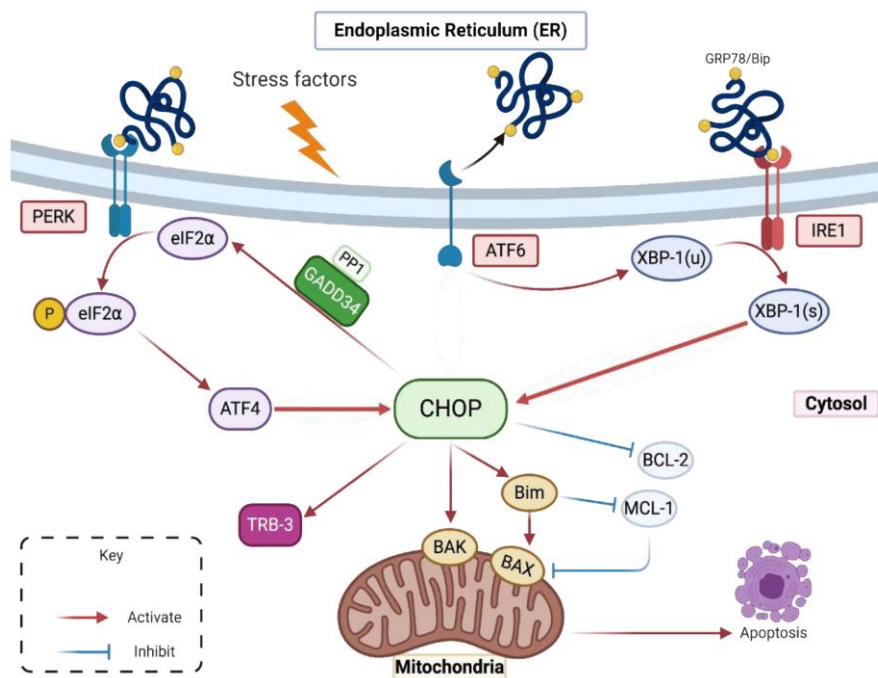


**Figure.1.4. Activation of CHOP by all three ER stress sensors leads to apoptosis (Turpin et al., 2021)**

## **1.6 ER stress and Oxidative stress**

Oxidative stress is a condition that arises due to cellular redox imbalances caused by disruption of equilibrium between the cellular antioxidant defence and ROS products due to abnormal generation of latter which is known to be associated with several pathological conditions (Henriksen et al., 2011). The primary function of the ER is folding, disulphide bond formation and maturation of protein into its native three-dimensional conformation and to facilitate the same, the ER lumen has an oxidising environment which is maintained by the high oxidised glutathione to reduced glutathione (GSSG/GSH) levels (Bass et al., 2004). Under normal conditions, protein folding machinery owing to the formation of disulphide bonds, generates a basal amount of ROS as byproducts which is scavenged by the endogenous antioxidant system. The disulphide bond formation is mediated by the ER resident oxidoreductases namely the protein disulphide isomerase (PDI) family of proteins which are involved in reduction, isomerization and formation of disulphide bonds. The substrate peptides' cysteine residues donate two electrons to the cysteine residues in the PDI active site, resulting in reduction of PDI and oxidation of substrate, the PDI then transfer the electron to an acceptor protein which transfers the electron to molecular oxygen resulting in formation of hydrogen peroxide, a ROS product (Cao & Kaufman, 2014; Hagiwara & Nagata, 2012). The oxidative protein folding in the ER is represented in the Figure.1.5. The electron acceptor for oxidative protein folding in mammalian cells include vitamin K epoxide reductase, quiescin sulphydryl oxidase (QSOX), peroxiredoxin IV, whereas in yeast cells it is the ER oxidoreductase 1 (Ero1) (Hagiwara & Nagata, 2012).

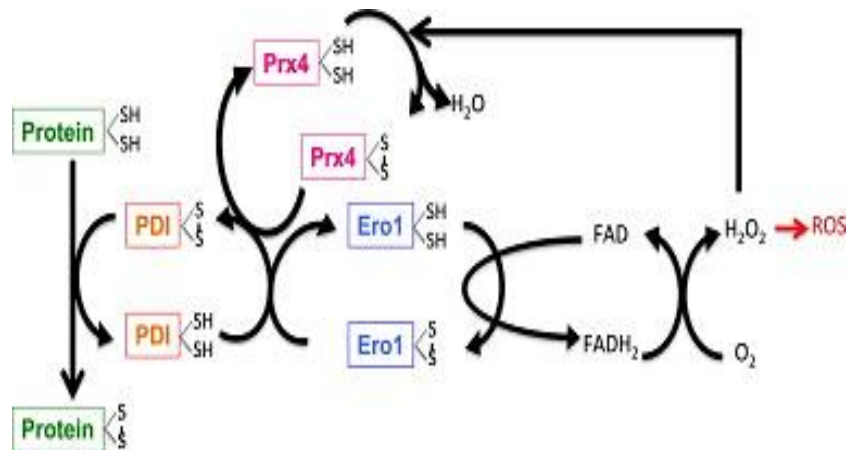


**Figure.1.5. Oxidative protein folding in the ER** (Espinosa-Diez et al., 2015)

During chronic ER stress, the protein folding machinery is upregulated to reduce the misfolded protein load in the ER lumen. The PDI family of proteins are highly expressed leading to abnormally high levels of free radicals or ROS resulting in a hyperoxidized ER lumen which worsens ER stress by impairing proper PDI action and producing more misfolded proteins (Burgos-Morón et al., 2019). There is a vicious loop between ER stress and ROS generation in which the latter can both start and feed the former (Chong et al., 2017). ROS are also known to activate the Mitogen activated protein kinase (MAP kinase) family of proteins that regulate a myriad of functions such as cell survival, proliferation and apoptosis (McCubrey et al., 2006). The MAP kinase family of proteins consist of serine/threonine kinase domains and are mainly classified into three types, the extracellular signal regulated kinase (ERK), p38 mitogen activated protein kinase (p38MAPK) and Jun N-terminal kinase (JNK). These are activated by sequential phosphorylation and all three proteins are involved in regulating cell fate decisions, both cell survival as well as dysfunction depending on the nature and duration of stress (Winter-Vann & Johnson, 2007).

In skeletal muscles, exercise induced muscle contraction and long periods of muscle disuse are associated with ROS production (Davies et al., 1982; Kondo et al., 1991). At



physiological levels, ROS are involved in regulation of signaling pathways needed for skeletal muscle adaptation whereas chronic and aberrant ROS generation in muscle cells result in oxidative damage and loss of function (Jackson et al., 2019). In pancreatic islets, the major site for synthesis and secretion of insulin peptide, a close nexus exists between ER stress and oxidative stress where both are involved in the pathogenesis of diabetes by inducing beta cell dysfunction and impaired insulin synthesis and secretion (Hasnain et al., 2016). A schematic illustration of ER stress mediated oxidative stress is shown in Figure.1.6.

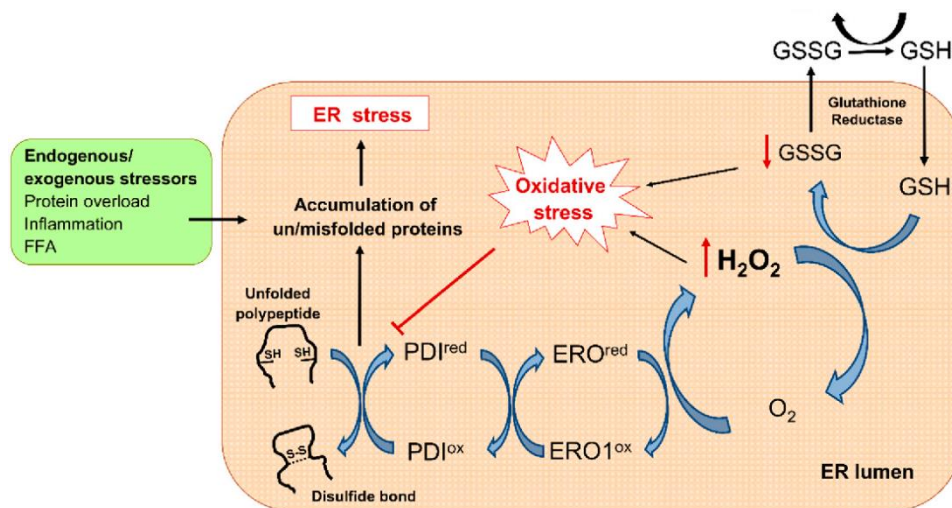


**Figure.1.6. ER stress induced ROS generation and subsequent oxidative stress** (Burgos-Morón et al., 2019)

### 1.6.1 ER stress and Insulin resistance

ER stress is one of the underlying mechanisms leading to insulin resistance, a major hallmark of type 2 diabetes. ER stress mediated insulin resistance is augmented in response to high fat diet and obesity indicating a close nexus between obesity and ER stress in diabetic condition (Eizirik et al., 2008). Under normal conditions, the binding of the insulin peptide to the insulin receptor, a member of the receptor tyrosine kinase family, initiates the insulin signaling, on the cell surface of skeletal muscle cells and

adipocytes followed by autophosphorylation and activation of the tyrosine residues (L. Chang et al., 2004). These residues are then identified by the phosphotyrosine binding domain (PTB) of the insulin receptor substrate (IRS) proteins that are then recruited and phosphorylated at the tyrosine residues by the insulin receptor (Lizcano & Alessi, 2002). The phosphorylated IRS proteins (IRS1 & IRS2) recruit the SH2 domain containing p85 regulatory subunit of phosphoinositide 3-kinase (PI3K) which subsequently activates the serine/threonine kinase Akt or protein kinase B (PKB) which then mediates the downstream signaling facilitating the glucose uptake via the GLUT4 transporters (Pessin & Saltiel, 2000).

According to a recent study, ER stress induces insulin resistance by prohibiting the maturation of insulin proreceptors by slowing their transport from the ER to the plasma membrane, which in turn inhibits Akt activation and subsequent downstream signaling (Brown et al., 2020). Earlier studies have elaborated the role of the ER stress sensors in induction of insulin resistance. The IRE-1 arm of the UPR induces IR by inducing TRAF2 and ASK1 mediated activation of the NF- $\kappa$ B and JNK which then inhibits the insulin signaling by phosphorylating the serine residues on IRS1 (P. Hu et al., 2006; Urano et al., 2000). Insulin resistance can also be induced by TRB3 following activation by PERK/ATF4 arm of the UPR (Flamment et al., 2012). Akt mediated nucleus to cytoplasmic translocation of forkhead transcription factor (FOXO) is an important event in insulin signaling (Accili & Arden, 2004). FOXO proteins are involved in metabolic regulation and regulate the expression of glucose 6 phosphatase and phosphoenolpyruvate carboxykinase (PEPCK) thereby promoting gluconeogenesis in the liver and under diabetic condition, FOXO mediates hyperglycaemia and glucose intolerance (K. Zhang et al., 2012). The PERK arm of the UPR induces insulin resistance

by mediating phosphorylation and nuclear localization of FOXO resulting in insulin resistance (W. Zhang et al., 2013).

Obesity induced lipotoxicity brought on by circulating saturated fatty acids such as palmitate, leads to ER stress-mediated insulin resistance in skeletal muscles via decrease in GLUT4 encoded by Slc2a4 gene mediated by IRE-1 $\alpha$  TRAF2 complex, it is also accompanied by myotube loss and suppression of myokine genes (FNDC5, CTRP15 and FGF21) (Ebersbach-Silva et al., 2018; M. Yang et al., 2013). Contradictions dismissing the role of ER stress in palmitate mediated skeletal muscle insulin resistance have been reported as well (Hage Hassan et al., 2012). ER stress induced muscle insulin resistance was shown to be dependent on TRB3 upregulation and its overexpression suppressed the insulin stimulated IRS1 Tyr<sup>612</sup> phosphorylation and Akt (Koh et al., 2013). Skeletal muscle and kidney-enriched inositol polyphosphate 5-phosphatase (SKIP), a PIP3 phosphatase abrogates PI3K signaling by hydrolysing PIP3 thereby acting as a negative regulator of insulin dependent signaling in skeletal muscles (Ijuin and Takenawa 2003). ER stress was reported to induce insulin resistance by enhancing the SKIP expression levels in ATF6 and XBP-1 dependent manner in skeletal muscles (Ijuin et al., 2016).

### **1.6.2 ER stress and clearance of misfolded proteins**

Proteolytic mechanisms are initiated as one of the many responses of the ER stress induced UPR in order to relieve the stress condition by decreasing the load of misfolded proteins in the ER lumen. During ER stress, the cell employs two major quality control systems for the clearance of misfolded non-native proteins, the endoplasmic reticulum associated degradation (ERAD) via ubiquitin-proteasome system (UPS) and autophagy. The major difference between these two mechanisms depends on substrate size. ERAD degrades only those proteins that can pass through the narrow channel of the proteasome

such as single unfolded proteins or soluble misfolded proteins while autophagy can degrade insoluble, large protein aggregates and damaged organelles.

### **1.6.2.1 ERAD**

ERAD can be classified as type I ERAD and type II ERAD where the former represents the UPS mediated degradation which will be discussed here while the latter represents autophagy-lysosome mediated degradation which will be discussed in Section 1.6.2.2 (Fujita et al., 2007). ERAD (I) hereafter referred to as ERAD is a complex sequential process including the following steps, protein recognition, in which the misfolded proteins are recognized by the ER resident chaperones including calnexin, calreticulin and PDI; Protein targeting, here the ERAD substrates are targeted to the retro translocation machinery and/or E3 ligases and this is mediated by the EDEMs, HERP, OS9 and XTP3-B; Retro translocation initiation, here the substrates are retro translocated to the cytoplasm and this is partly initiated by the cdc48 complex, chaperones in addition to Derlins, HERP, Sec61, VIMP, SVIP, BAP31; Ubiquitylation and further retro translocation, here following exit from the retro translocon, substrates are polyubiquitylated by E3 ubiquitin ligases promoting retro translocation aided by cytoplasmic ubiquitin-binding protein complexes and this requires UFD, HRD1-SEL1 complex, UBE1, RNF5, UBCs, TEB4, GP78, NEDD4-2; Proteasomal targeting and degradation, here the polyubiquitylated substrate is recognized by receptors in the 19S cap of 26S proteasome, de-ubiquitylating enzyme removes the polyubiquitin tag following which substrate is threaded into the 20S catalytic core of the proteasome undergoing fragmentation into peptides and this step requires p97-UFD1-NPL4, RAD23, Peptide N-Glycanase, Ataxin-3, RPNs, RPT5 (Vembar & Brodsky, 2008). A schematic illustration of the multistep ERAD process is represented in Figure.1.7. The

transcriptional induction of ERAD components in mammalian cells is mediated by the ATF6 $\alpha$  and XBP-1 pathways of UPR (Yamamoto et al., 2007). The ERAD genes are constitutively and ubiquitously expressed even in the absence of stress within the cell that not only ensures fidelity of protein production but also regulate the abundance of proteins (Bhattacharya & Qi, 2019). Therefore, any decrease in ERAD function worsens ER stress and jeopardises ER homeostasis leading to pathological consequences. Mutations or genetic deletions in ERAD components result in loss of function leading to accumulation of misfolded proteins and subsequent disease conditions such as neurological, skeletal disorders, intellectual disability, diabetes, cardio and immuno-related diseases (Badawi et al., 2023). Reports, however, also point to the overexpression of ERAD elements in pathological circumstances. In few skeletal muscle disorders such as muscle wasting or atrophy, muscular dystrophy and cachexia, enhanced UPS machinery is observed which can be treated to a certain extent by employing proteasome inhibitors owing to the multifactorial nature of the diseases (Kitajima et al., 2020).

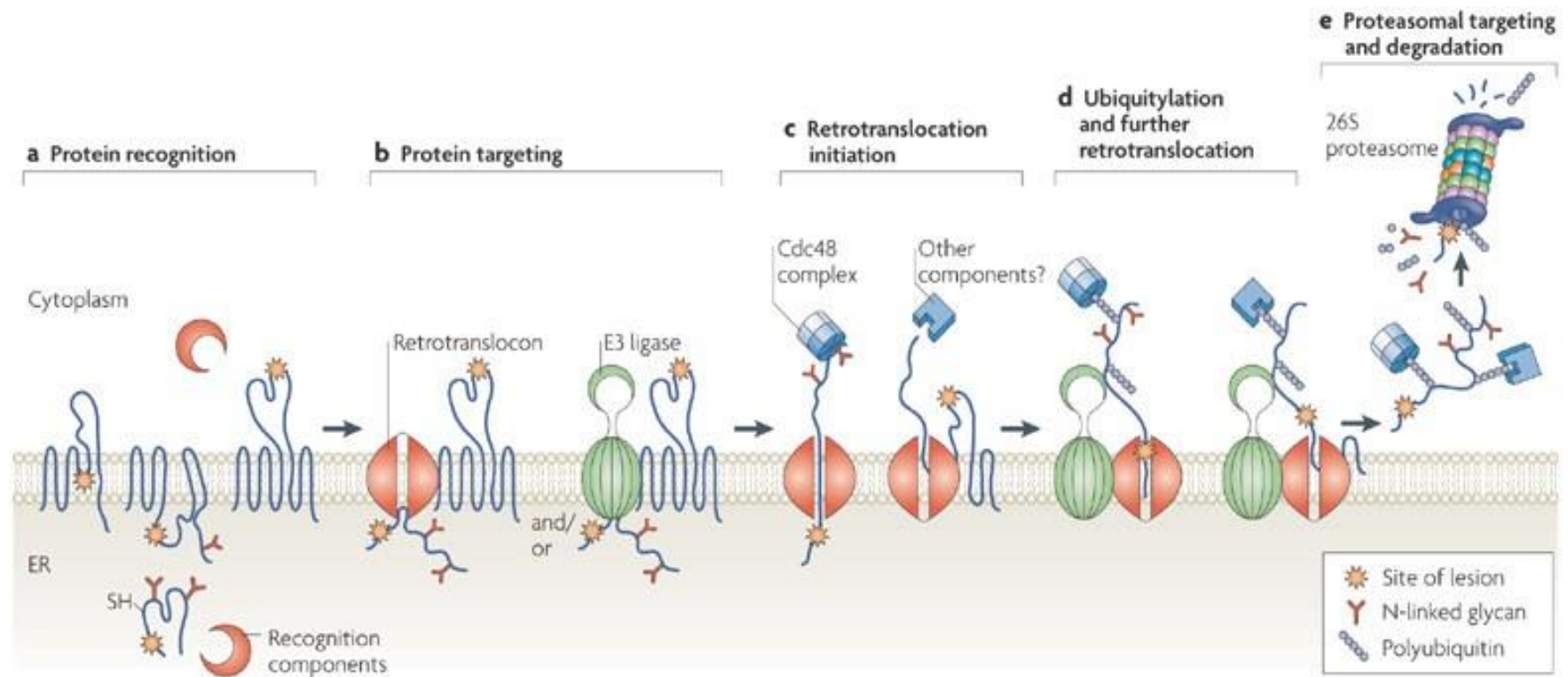


Figure 1.7. Endoplasmic reticulum associated degradation (ERAD) steps (Vembar & Brodsky, 2008)

### **1.6.2.2 Autophagy**

It is defined as a catabolic process involving the engulfment of cytoplasmic cargo comprising insoluble protein aggregates and damaged organelles by a double membrane vesicle known as the autophagosome followed by subsequent degradation of the cargo on fusion with lysosome (Beth Levine & Guido Kroemer, 2008). Autophagy, which is essential for cell proliferation, differentiation, innate and adaptive immunity, cell death and creation of new macromolecules by recycling metabolites generated by lysosomal breakdown, is maintained at a minimum basal level in healthy cells (Rashid et al., 2015). It is upregulated under stress conditions namely, nutrient starvation, low energy status, oxidative stress, ER stress, infection and hypoxia (Beth Levine & Guido Kroemer, 2008). A schematic representation of autophagy steps is shown in Figure.1.8.

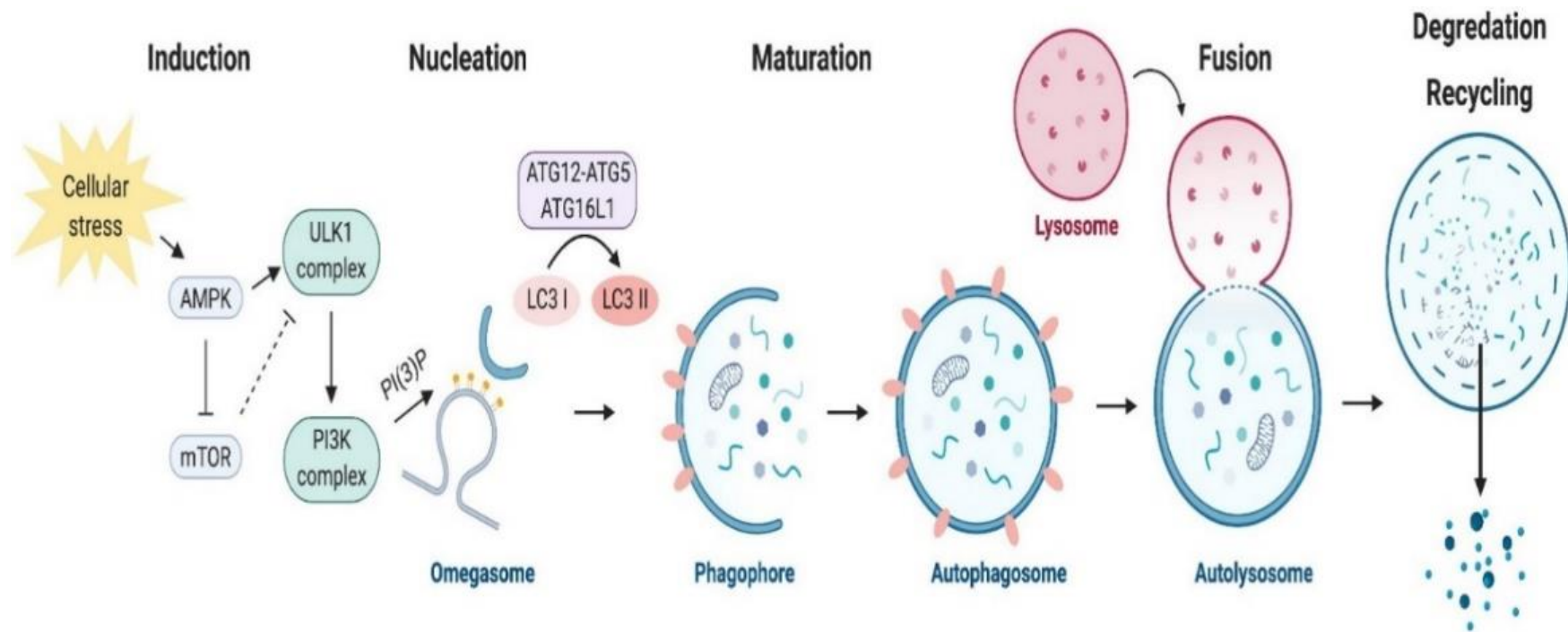


Figure.1.8. Schematic representation of stepwise autophagy process (N. C. Chang, 2020)



Under ER stress condition, autophagy is known to be triggered by all the three ER stress sensors with the primary goal of relieving the ER burden by degradation of the misfolded proteins. The IRE-1/XBP-1 pathway induces autophagy by inducing conversion of LC3-I to LC3-II and upregulation of Beclin1 (Margariti et al., 2013). Autophagy can also be triggered by the IRE-1/TRAF-2/JNK pathway which mediates the autophagosome formation (Yan et al., 2015). PERK/eIF2 $\alpha$  phosphorylation enhances ATG2 levels while expression of genes involved in autophagy namely Beclin1, ATG3, ATG12, MAP1LC3B and ATG16L1 requires downstream ATF4 activation and its interaction with DDIT3 causes transcriptional activation of autophagy markers, SQSTM1/p62, BR1 and ATG7 (B'Chir et al., 2013; Hotamisligil, 2010). CHOP is involved in the induction of ATG5, BH3 domain proteins while decreasing Bcl-2 levels which aids in disassociation of Beclin1 from Bcl-2 (Liu et al., 2014; Puthalakath et al., 2007; Rouschop et al., 2010). CHOP also enhances TRB3 levels which in turn suppress the phosphorylation of Akt and subsequently mTORC1 resulting in autophagy induction (Yan et al., 2015). ATF6 arm of UPR activates autophagy by induction of DAPK1 which drives autophagosome formation by phosphorylation of Beclin1 (Gade et al., 2012; Zalckvar et al., 2009). ATF6 initiates autophagy by enhancing expression of HSPA5 followed by suppression of activity of PKB (Yung et al., 2011).

### **1.6.3 ER stress and mitochondrial alterations**

Mitochondria are present in the cytosol as a dynamic network that undergoes fusion and fission facilitating exchange of information and catering to the energy demands of the cell. Studies over the past years have manifested the physical and functional interaction of the ER and the mitochondria. Both ER and mitochondria are dynamic in nature and undergo functional and physical modification in response to external stimuli (Malhotra &

Kaufman, 2011). Any perturbation in the ER functioning can have a negative impact on the mitochondrial function.

The ER mitochondria communication is an important example of interorganellar connection. The region of physical contact between these organelles is termed as mitochondrial associated membranes (MAMs), term coined by Vance (Rusiñol et al., 1994). MAMs are specialised regions which connect the ER surface to the outer mitochondrial membrane (OMM) and facilitate sharing of information between these two structures. The key proteins at MAMs junction that are involved in maintaining the tethering between the two organelles are the mitofusins (MFN), dynamin related protein 1 (DRP1), mitochondrial fission protein (FIS1), inositol triphosphate receptor (IP<sub>3</sub>R), Voltage dependent anion channel (VDAC), vesicle-associated membrane protein-associated protein B (VAPB), glucose regulatory protein 75 (GRP75), B-cell receptor-associated protein 31 (BAP31), protein tyrosine phosphatase interacting protein 51 (PTPIP51) (Lee & Min, 2018). The major proteins present at the MAMs junction are depicted in Figure.1.9.

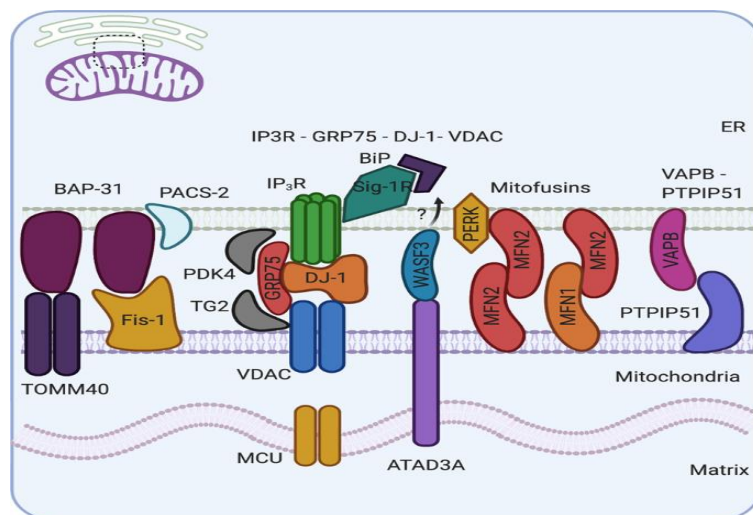


**Figure.1.9. Major proteins present at the MAMs junction tethering the ER to the mitochondria** (Wilson & Metzakopian, 2021)

The MAMs are involved in various functions such as lipid trafficking, calcium signaling, mitochondrial fusion and fission, apoptosis, cell survival, autophagy (Gordaliza-Alaguero et al., 2019). The MAMs play a major role in transport of calcium from the ER to mitochondria. The ER is the main site for storage of calcium and the inward and outward flow of calcium ions, an important second messenger, from the ER, regulates several signaling pathways. The high calcium ion levels in the ER are maintained by the sarco-endoplasmic reticulum  $\text{Ca}^{2+}$ ATPase (SERCA) pump on the ER surface which enables ATP hydrolysis coupled entry of calcium from cytosol to the ER (Gorlach et al., 2006). The calcium exit from the ER is mediated by the ryanodine receptors (RYR) and the  $\text{IP}_3\text{R}$ . Upon ER stress, the PERK/ATF4 arm of the UPR upregulates the parkin protein which tightens the contact between the ER and mitochondria thereby enhancing the calcium transport from the ER to mitochondria through the  $\text{IP}_3\text{R}$  channel (Bouman et al., 2011). Under prolonged ER stress, the increased mitochondrial calcium mediates pro-apoptotic signals including loss of mitochondrial membrane potential, increased membrane permeability, swelling of matrix and cytochrome c release (Deniaud et al., 2008). Calcium influx into the mitochondria during ER stress gives rise to increased mitochondrial ROS generation by enhancing the Krebs cycle and mitochondrial phosphorylation and electron transport chain (ETC) (Bhandary et al., 2013). Sustained ROS levels establish a vicious nexus with calcium release channels thereby augmenting calcium release from ER that can have negative implications.

### **1.7 ER stress in skeletal muscles**

Skeletal muscle is an essential organ that serves multiple functions, predominantly, body movement, thermoregulation, utilization and storage of energy metabolism substrates such as glucose, lipids and amino acids (Evans, 2010; Gallot & Bohnert, 2021). Skeletal

muscle makes up 40% of total body mass and accounts for 80% of whole body glucose metabolism making it an important target for diabetes related studies (DeFronzo et al., 1981; Zurlo et al., 1990). Moreover, the storage of 50–70% of the body's total protein occurs in skeletal muscle tissue, which is a key site for protein metabolism (Bohnert et al., 2018). Despite its limited secretory function, skeletal muscle is composed of an intricate network of specialised ER called the sarcoplasmic reticulum (SR), which serves as a calcium ion reservoir and, as a result, plays a crucial role in muscle contraction, ER stress-mediated UPR, and ultimately skeletal muscle function (Mensch & Zierz, 2020). Many factors, including a high calorie intake, exercise, lack of oxygen, disruption of redox homeostasis, and changes in calcium levels, can cause ER stress in skeletal muscle (Deldicque et al., 2013). Mild ER stress has an adaptive role in the skeletal muscles and is involved in myogenesis, calcium homeostasis, amino acid metabolism and exercise.

Myogenesis implies the formation of skeletal muscle tissue during the embryonic development or postnatal life. In the embryonic stage, the multi-potential mesodermal cells develop into myoblasts which then differentiate and fuse together to form multinucleated myotubes that mature into myofibres (Bentzinger et al., 2012). The skeletal muscles also have the ability for regeneration owing to the presence of satellite cells or muscle stem cells which remain in the quiescent state in healthy tissue and only become activated in injured tissue where these undergo multiple cell divisions and subsequent myofiber regeneration (Afroze & Kumar, 2019). ER stress associated UPR is known to control the various phases of myogenesis. During the myotube formation, the incompetent myoblasts are eliminated by apoptosis and the surviving myoblasts differentiate into myotubes, this is facilitated by the upregulation of ATF6, BIP and CHOP which in turn activate the caspases 12, 9 and 3 triggering apoptosis, eliminating the incompetent myoblasts (Nakanishi et al., 2005). The PERK/eIF2 $\alpha$  arm is involved in

harbouring the satellite cells in quiescent state whereas during muscle injury, PERK is involved in the survival and differentiation of satellite cells into myogenic lineages (Xiong et al., 2017; Zismanov et al., 2016). IRE-1 $\alpha$ /XBP-1 are activated in injured muscles and are involved in muscle regeneration by aiding proliferation of satellite cells in a cell non-autonomous manner (Roy et al., 2021).

Exercise is a physical activity associated with various health benefits making it an essential aspect of fitness regimen. Exercise elicits an adaptive UPR response in skeletal muscles and aids in improving muscle mass and function. Since exercise involves muscle contraction which in turn requires calcium ions stored in the ER/SR, therefore, exercise induced alterations in ER/SR calcium levels lead to activation of ER stress mediated UPR in skeletal muscle cells. The two extremities of exercise continuum are aerobic and resistance exercises, where the former imposes modalities of high frequency (repetition) and low power output demand on muscle contraction while the latter imposes low frequency and high resistance demand on muscle contraction and both the types activate the UPR (Egan & Zierath, 2013). Kim et al. have demonstrated the upregulation of IRE-1 $\alpha$ , XBP-1s and ATF6 in muscles after ultra endurance exercise (Kim et al., 2011). The UPR proteins, BIP, ATF4, CHOP, ATF3, eIF2 $\alpha$ , XBP-1s, GADD34, ERdj4 were observed to be upregulated after one bout of exhaustive treadmill running acute exercise (J. Wu et al., 2011). The UPR upregulation was found to be different in untrained and trained mice. The markers BIP and GRP94 were similarly expressed in both sets after a treadmill run however, CHOP and XBP-1s were found to be expressed in untrained mice whereas in trained mice these markers were not expressed indicating that moderate regular exercise protects against further stress (J. Wu et al., 2011).

Amino acid biosynthesis is another consequence of adaptive ER stress in skeletal muscles. One of the early responses of ER stress is the PERK mediated translational

repression (protein synthesis attenuation) to reduce the protein load in the ER lumen. However, Gonen et al. recently showed via ribosome footprint profiling that, upon activation of ER stress, a fraction of secreted proteins were able to evade the repression and are instead induced in a PERK dependent way (Gonen et al., 2019). This is an adaptive mechanism where increased protein synthesis demand is associated with increased amino acid biosynthesis and corresponding tRNA synthetases to meet the UPR induced protein demand (Gonen et al., 2019). During stress conditions, supply of amino acids for protein synthesis and glutathione biosynthesis is initiated in an eIF2 $\alpha$ /ATF4 dependent manner downstream of PERK to meet the protein demand and protect against oxidative stress (Harding et al., 2003). Chronic ER stress in skeletal muscles leads to several pathological scenarios including muscle wasting or atrophy, insulin resistance and myopathies (Afroze & Kumar, 2019). A schematic illustration of consequences of adaptive UPR and maladaptive UPR in skeletal muscles are depicted in Figure.1.10

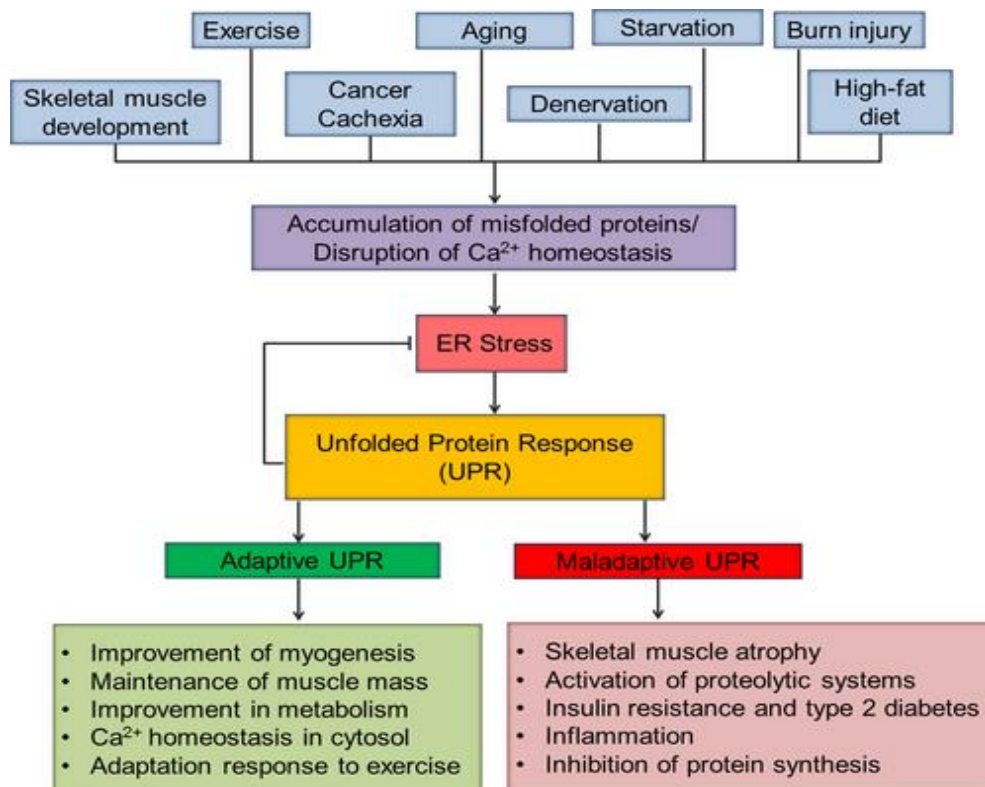


**Figure.1.10. ER stress mediated implications in skeletal muscles** (Afroze & Kumar, 2019)

### 1.7.1 Skeletal muscle Atrophy

Skeletal muscle atrophy or muscle wasting is a decrease in muscle mass which occurs when protein degradation exceeds protein synthesis and it is characterised by a reduction in cross-sectional area of myofibers along with depletion of contractile proteins and muscle strength (Fanzani et al., 2012). Accumulating evidence suggest ER stress as one of the triggers for skeletal muscle atrophy in addition to aging, prolonged disuse, inflammation, starvation, diabetes and denervation (Gallot & Bohnert, 2021). Disruption of mitochondrial network and associated oxidative stress are reported to contribute to muscle atrophy (Romanello & Sandri, 2016). Skeletal muscle diseases such myositis, insulin resistance, DMD, and myasthenia gravis are associated with muscle wasting, a major cause of morbidity and mortality. The main treatment modalities currently used are exercise, nutrient supplementation, and medication; however, for many people with severe symptoms, exercise may not be a practical choice (Yin et al., 2021). The drugs are therefore the focus, but these are constrained by the side effects (Carstens & Schmidt, 2014; Oddis, 2016; Sartori et al., 2021).

Muscle protein degradation, a key attribute of atrophy, is mediated mainly by the two major protein degradation systems, namely, the UPS and autophagy, which were observed to be upregulated in atrophied skeletal muscles (J. Du et al., 2004; A. Singh et al., 2021). A nexus between insulin resistance and muscle atrophy exists where deficiency of insulin exacerbated muscle protein degradation by suppressing the PI3K and Akt activity and increasing serine phosphorylation of IRS-1 in *db/db* mice model of insulin resistance resulting in activation of caspase-3 and ubiquitin proteasome proteolytic pathway (X. Wang et al., 2006). Targeting ER stress pathways can help in the development of improved strategies for diabetes by improving the overall muscle health

by reducing insulin resistance and skeletal muscle atrophy. The crosstalk between insulin resistance and skeletal muscle atrophy has been depicted in Figure.1.11

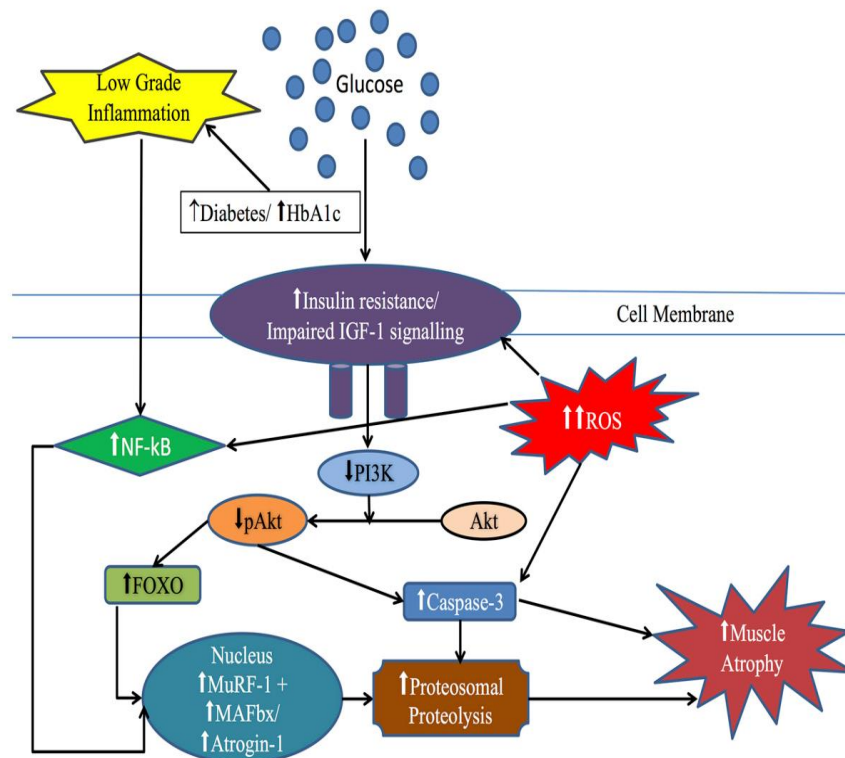


**Figure.1.11. The crosstalk between insulin resistance and skeletal muscle atrophy** (Rudrappa et al., 2016)

### 1.8 ER stress in pancreatic beta cells

In response to fluctuations in blood glucose levels, the principal function of pancreatic beta cells is to produce insulin, which accounts for half of all protein synthesis and is produced at a rate of about one million proteins per minute (Scheuner & Kaufman, 2008). Pancreatic beta cells which are secretory in nature have a well-developed ER and therefore, susceptible to perturbations in ER function. Sustained hyperglycaemia (diabetic condition) can overwhelm the ER and disturb the equilibrium between insulin demand and ER folding capacity (Figure.1.12). Pancreatic beta cells respond to both transient (1-3 hours) and chronic ER stress ( $\geq 24$  hours), the former enhances proinsulin



biosynthesis promoting adaptive UPR while the latter induces dysregulated UPR resulting in attenuation of insulin biosynthesis and loss of function(Fonseca et al., 2011). All the three UPR sensors act as binary switches depending on the nature of ER stress. Mild ER stress causes acute activation of IRE-1 $\alpha$ , PERK and ATF6 promoting cell survival whereas chronic ER stress results in maladaptive UPR culminating in cellular apoptosis. Acute IRE-1 $\alpha$  activation enhances insulin biosynthesis whereas its prolonged activation promotes maladaptive UPR by overexpression of spliced XBP-1, activation of JNK and caspase 12 (Lipson et al., 2006; Yoneda et al., 2001). Transient PERK activation promotes beta cell survival by attenuating protein production and activating anti-apoptotic effector, apoptosis antagonizing transcription factor (AATF) whereas chronic upregulation leads to apoptosis mediated by ATF4/CHOP axis (Fonseca et al., 2011). Acute activation of ATF6 improves beta cell survival by enhancing the ER folding capacity whereas chronic activation leads to insulin gene suppression and beta cell dysfunction (Seo et al., 2008). Besides hyperglycaemia, other stimuli for induction of ER stress include, circulating free fatty acids, inflammatory cytokines, oxidative stress, hypoxia, accumulation of islet amyloid precursor protein (IAPP) and mutations in insulin (Fonseca et al., 2011; Hasnain et al., 2016). Beta cell dysfunction is a main hallmark of both types of diabetes, absolute insulin insufficiency is a complication of type 1 diabetes, which is brought on by autoimmune cell destruction, type 2 diabetes is a condition in which there is a relative lack of insulin as a result of beta cell malfunction and loss. Due to the indispensable role of ER stress induced UPR in the regulation of insulin biosynthesis and pancreatic beta cell function, it has emerged as a putative target for therapeutic intervention of diabetes.

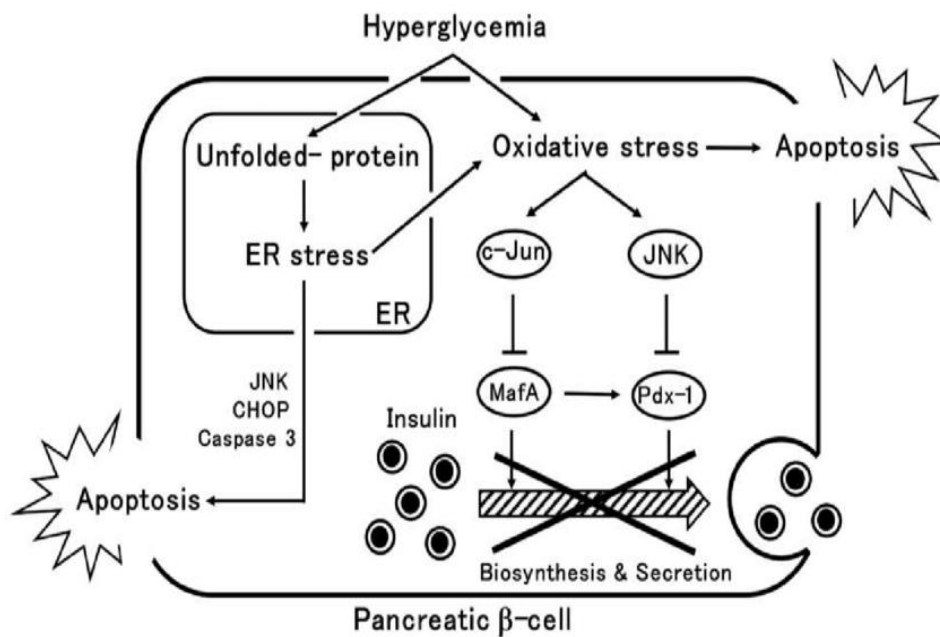


**Figure.1.12. Sustained hyperglycaemia induces ER stress disturbing the equilibrium between ER folding capacity and insulin demand (Honzawa & Fujimoto, 2021)**

### 1.9 Pharmacological intervention of ER stress pathways

Sustained ER stress and associated complications are involved in the genesis and progression of several pathological conditions including neurodegenerative diseases, diabetes, cancer, viral infections, inflammatory diseases, atherosclerosis and cardiovascular diseases (Oakes & Papa, 2015). Recent research on pre-clinical and clinical models has focussed on targeting the UPR pathways as strategies for better disease management. The role of ER stress in the complex pathophysiology of metabolic syndrome like diabetes is well established. We have already discussed the involvement of ER stress associated pathways in the progression of insulin resistance and insulin secretion impairment, the two manifestations of diabetes. Identifying compounds that modulate the individual arms of the UPR have immense therapeutic potential. These include chemical chaperones that prevent protein aggregation and misfolding by stabilising the folding intermediates. The ones with hydrophobic moiety prevent protein

aggregation by binding to the exposed hydrophobic sites of the misfolded proteins (Kitakaze et al., 2019). The examples include salubrinal, tauro-ursodeoxycholic acid (TUDCA) and 4-phenylbutyric acid (4-PBA). Pretreatment with PBA was reported to partially prevent lipid induced insulin resistance and restore pancreatic beta cell function in overweight or obese nondiabetic human subjects (Xiao et al., 2011). Taurine-conjugated ursodeoxycholic acid (TUDCA), a taurine conjugated bile acid derivative and PBA were found to suppress tunicamycin (pharmacological ER stress inducer) induced XBP-1 splicing, PERK mediated eIF2 $\alpha$  phosphorylation and JNK activation in rat hepatoma cells (Ozcan et al., 2006). In *ob/ob* mice TUDCA treatment significantly improved insulin sensitivity, glucose tolerance while suppressing PERK, IRE-1 $\alpha$  phosphorylation, JNK activation and serine phosphorylation of IRS-1 protein (Ozcan et al., 2006). TUDCA was also shown to reduce the incidence of diabetes and improve beta cell function through an ATF6 dependent mechanism (Engin et al., 2013). Salubrinal, a selective inhibitor of eIF2 $\alpha$  phosphorylation was however, reported to augment the lipotoxicity induced by free fatty acids in pancreatic beta cells by upregulation of ATF4 and CHOP resulting in dysfunction and apoptosis (Cnop et al., 2007).

Modulators of UPR elements are potential therapeutics for targeting the ER stress. In the Akita mice, a model of mutant insulin gene-induced diabetes of youth (MIDY), amelioration of diabetic parameters such as beta cell dysfunction, ER stress related inflammation, oxidative stress in islets, decreased serum insulin levels and glucose intolerance were reprimanded on administering STF and 4 $\mu$ 8c (IRE-1 $\alpha$  RNase inhibitors) (Herlea-Pana et al., 2021). In pancreatic islets isolated from arsenic treated mice, ER stress mediated autophagy and impaired glucose stimulated insulin secretion were suppressed on treating with PERK inhibitor (W. Wu et al., 2018). As ER is the major reserve of calcium ions and ER stress causes calcium homeostasis disruption, hence,

regulators of ER calcium homeostasis can also be used as therapeutic strategy for intervention of ER stress pathways. Under ER stress, depletion of calcium from ER results in loss of resident proteins via a process known as exodosis which contributes to several pathologies such as neuronal, metabolic, muscular and cardiovascular disorders (Trychta et al., 2018). Bromocriptine, a clinically used drug showed protective effects in skeletal muscle model for calcium dysregulation, Wolfram syndrome, oxygen-glucose, deprivation, type 2 diabetes and stroke by improving the ER proteostasis by exerting anti-exodosis activity (Henderson et al., 2021). Since high ER calcium levels are required for normal functioning of the ER, hence, molecules activating the SERCA pump are capable of attenuating ER stress related perturbations. CDN1163, a novel allosteric activator of SERCA was reported to improve glucose tolerance, mitochondrial biogenesis while ameliorating ER stress mediated apoptosis in *ob/ob* mice, a genetic model of insulin resistance and type 2 diabetes (Kang et al., 2015). Our knowledge regarding the ER and associated pathways has grown profoundly in the past years which has contributed to our understanding of several pathological conditions. Several compounds with ER stress modulating potential have been identified in preclinical and clinical studies, however these require detailed characterization to elucidate the mechanism of action in order to recognize the off-target effects if any. Also, clarity regarding the dose optimisation and adverse effects of these therapeutics on prolonged use needs to be ascertained for the effective translation of these therapeutics from bench to bedside.

### **1.9.1 Natural products targeting ER stress pathways**

There is a growing interest in identifying natural products that can target ER stress associated pathways owing to their bioactivity, economic feasibility, abundance and fewer adverse effects compared to synthetic analogues. Plant derived compounds have

been explored for their bioactive potential against ER stress markers in several pathologies as described in Figure.1.13. As already discussed in Section 1.4, there is a need for developing alternative therapies for management of diabetes and pharmacological targeting by natural compounds represents a compelling area of research. Studies on morin, quercetin and resveratrol have demonstrated their potential in abrogating diabetic parameters by modulation of ER stress in both *in vitro* and *in vivo* models (Prasad M et al., 2022).

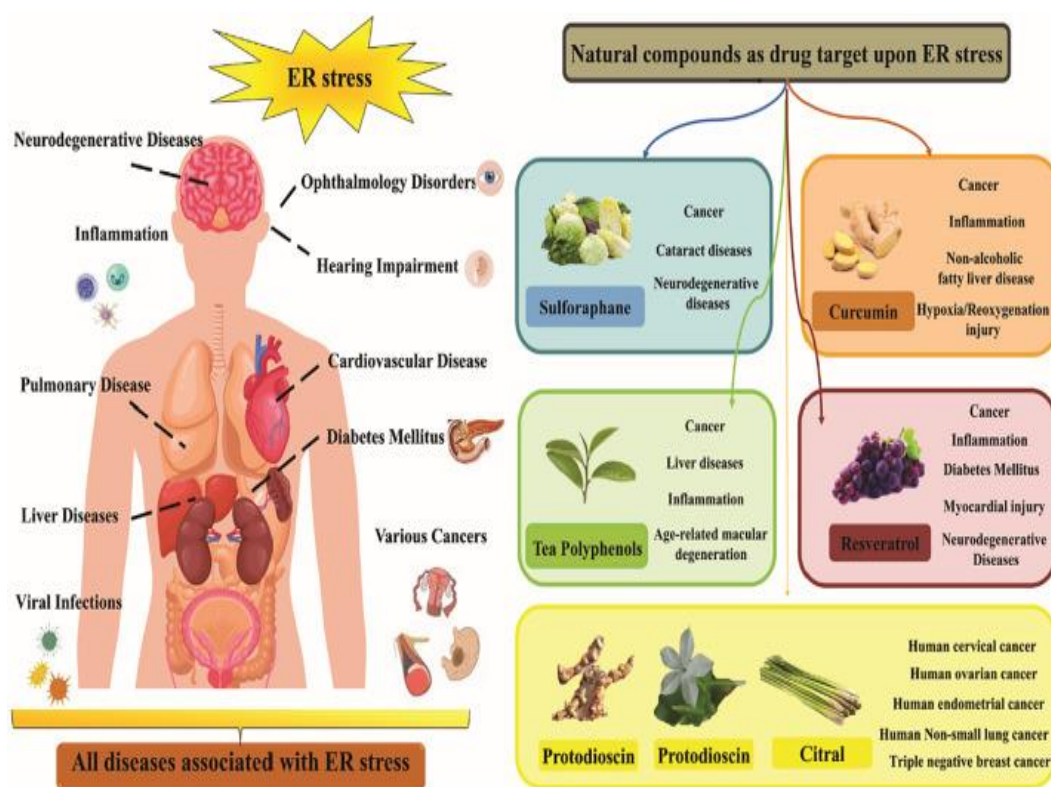


**Figure.1.13. Natural compounds targeting ER stress pathways** (Ma et al., 2020)

Flavonoids are polyphenolic compounds abundantly present in fruits and vegetables, that have gained potential in the past years due to their broad range of bioactivity including antidiabetic and nutraceutical potential (Al-Ishaq et al., 2019). However, there are limited reports regarding their therapeutic potential against ER stress mediated diabetes. The C6-C3-C6 skeleton of flavonoids is made up of two aromatic rings, A and B, connected by a

three-carbon chain, typically an oxygenated heterocyclic C ring as seen in Figure.1.14a (Beecher, 2003). Based on the structural differences, flavonoids can be classified into seven subclasses namely, flavones, flavonols, isoflavones, flavanones, flavanols, chalcones and anthocyanidins. Of importance, in this study, are the flavone subclass of flavonoids. Flavones comprising hydroxyl and carbonyl functional groups are characterised by double bond between C2 and C3 with no substitution at C3, but are oxidized at C4 (Figure.1.14b) (Martens & Mithöfer, 2005). Major sources of flavones include celery, parsley, red peppers, chamomile, mint, citrus fruit peels and *Ginkgo biloba* (Panche et al., 2016). There is a growing interest in flavones due to their significant therapeutic potential such as anti-inflammatory, antioxidant, antimicrobial, antidiabetic and antitumor activities (M. Singh et al., 2014). The three most widely studied flavones having considerable bioactivities include the apigenin, luteolin and tangeretin as shown in Figure.1.15a, b, c.

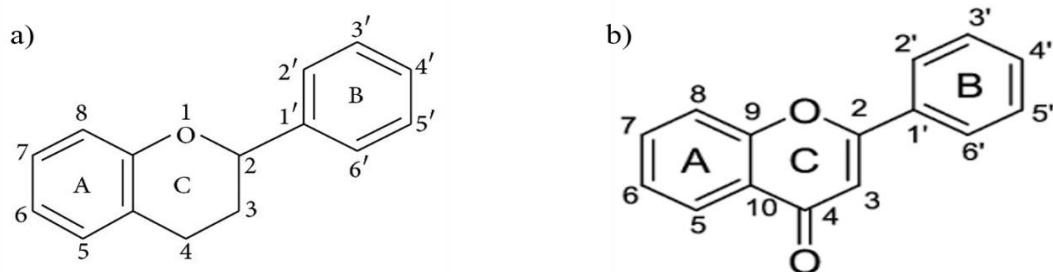


**Figure.1.14. a) Basic flavonoid structure. b) Basic flavone structure**

### 1.9.1.1 Apigenin

Also known as 4',5,7-trihydroxyflavone, apigenin is abundantly present as a secondary metabolite in parsley, celery, onions, oranges, chamomile, maize, rice, tea, wheat sprouts, grapefruit, thyme, oregano (Shukla & Gupta, 2010). Dried parsley and dried flowers of chamomile are reported to have highest quantity of apigenin, 45035 $\mu$ g/g and 3000-5000 $\mu$ g/g, respectively (Sung et al., 2016). Apigenin exists in plant sources as 7-O-

glucosides, 6-C-glucosides, 8-C-glucosides. Following ingestion, the glucosides are enzymatically metabolised into the aglycone form (free apigenin) and subsequently absorbed (Hostetler, Ralston, and Schwartz, 2017). The oral bioavailability of apigenin was observed to be 30%, it also has high molecular lipophilicity and plasma binding capability ensuring optimal tissue distribution (DeRango-Adem & Blay, 2021). The hydroxyl groups at A/B ring impart antioxidant potential to apigenin (M. Singh et al., 2014). Apigenin possesses a vast range of therapeutic potential including anti-inflammatory, anti-depressant, anti-mutagenic, anti-viral, anti-bacterial, anti-thrombotic, cardioprotective, hepatoprotective, immunostimulatory, anti-diabetic, anti-proliferative activity with regard to pancreatic, colorectal, liver, blood, lung, cervical, prostate, breast, thyroid, skin, head and throat cancers (Arya et al., 2018; Kashyap et al., 2018). Apigenin showed ER stress modulatory effects in gastric, endometrial cancer cell based systems and hyperlipidaemia animal model (Kim & Lee, 2021; Liang et al., 2022; L. Wu et al., 2021).

#### **1.9.1.2 Luteolin**

Also known as 3',4',5,6-tetrahydroxyflavone and abundantly present in carrot, cabbage, artichoke, tea, celery, broccoli, parsley, oregano, chrysanthemum flowers and apples (Pandurangan & Esa, 2014). Celery and oregano both contain significant amounts of luteolin (34.87mg/100g and 1028.75 mg/100g, respectively) (Saleem et al., 2021). Luteolin exists in plant sources as aglycone or conjugated as O or C-glycosides (Hostetler, Ralston, and Schwartz, 2017). When given orally to Sprague-Dawley rats at a dose of 100 mg/kg, luteolin showed a  $26\pm 6\%$  oral bioavailability (L. C. Lin et al., 2015). Luteolin possesses anti-inflammatory, antioxidant, neuroprotective, analgesic, antioxidant, anticancer, cardioprotective, antidiabetic and antimicrobial activities (Lopez-Lazaro,

2009). Luteolin demonstrated ER stress modulatory effects in hepatic injury and certain cancer model systems (Jegal et al., 2020; Mohi-Ud-din et al., 2022).

### **1.9.1.3 Tangeretin**

Also known as 4',5,6,7,8-pentamethoxyflavone, which is widely distributed in citrus fruit peels and juices. It is present as O-methylated aglycones and differs from apigenin and luteolin in the presence of methoxy groups (Al-Karmalawy et al., 2021). It is present at concentrations of 60 $\mu$ M in 2mg/ml tangerine peel extract (Söhretoglu & Arroo, 2018). When Tangeretin was administered orally to Sprague-Dawley rats at a dosage of 50 mg/kg, it had an absolute oral bioavailability of 27.11% (Hung et al., 2018). Its oral administration upto 3000mg/kg induced no toxicity in mice after 14 days following intake (Ting et al., 2015). Tangeretin demonstrated potential against ovarian, breast and gastric cancers and showed renoprotective, neuroprotective, hepatoprotective, antidiabetic, antioxidant and immunomodulatory activities (Ashrafizadeh et al., 2020). The therapeutic potential of tangeretin can be credited to the presence of the methoxy groups which enhances hydrophobicity and improves cellular uptake (Hung et al., 2018). Tangeretin demonstrated protective effect against ER stress induced neurotoxicity and cardiac failure (Takano et al., 2007; J. Wang et al., 2020).

These three flavones stated above are known for their broad-spectrum therapeutic potential. However, their efficacy and mode of action against ER stress mediated diabetic progression is not well known. Hence, the goal of the current investigation is to perform a detailed investigation to study the efficacy of the three selected flavones, apigenin, luteolin and tangeretin in ameliorating the ER stress induced diabetes related cellular complications such as UPR, oxidative stress, insulin resistance, mitochondrial



dysfunction, protein degradation and impaired insulin expression and to elucidate the mechanism of action of the most active flavone. We chose the mouse insulinoma pancreatic Beta-TC-6 cell line and the rat skeletal muscle L6 cell line for our investigation because these cells play a major role in the pathogenesis of diabetes and are the primary targets for therapeutic intervention.

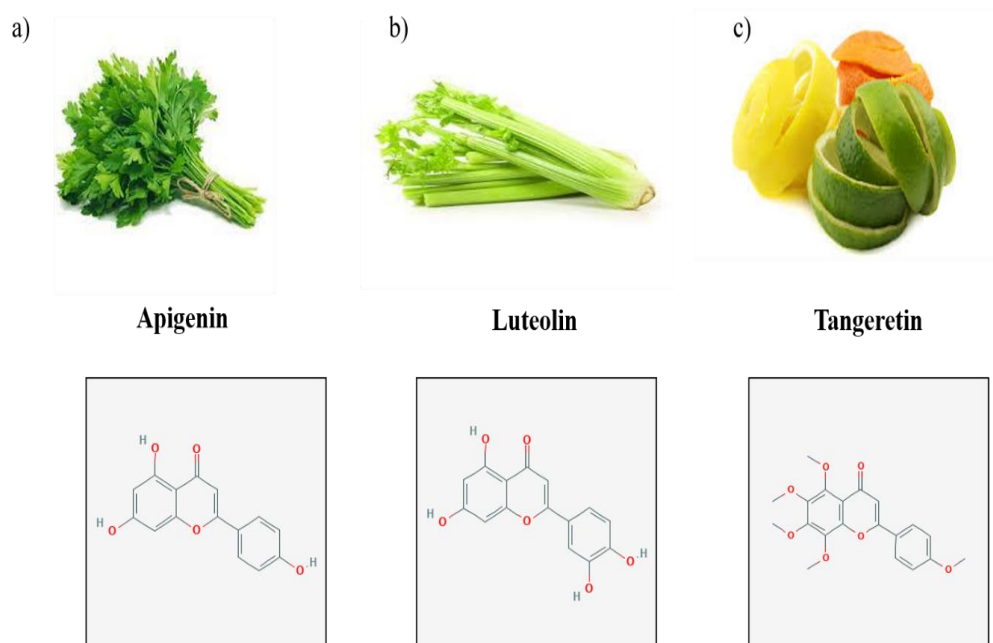


**Figure.1.15. Structure and natural source of selected flavones.** a) Apigenin, b) Luteolin, c) Tangeretin

## 1.10 Objectives of Study

The key objectives of the study include the following:

- Establishing an *in vitro* model for ER stress in rat skeletal muscle L6 cells using tunicamycin (pharmacological ER stress inducer) and screening the selected flavones based on their ability to improve the cellular redox status under ER stress.
- Evaluating the potential of most active flavone against ER stress induced UPR, insulin resistance, mitochondrial dysfunction, autophagy and ERAD signaling pathways in rat skeletal muscle L6 cells.
- Investigating the efficacy of most active flavone in alleviation of ER stress induced cellular perturbations in pancreatic Beta-TC-6 cells.

## References

- Accili, D., & Arden, K. C. (2004). FoxOs at the crossroads of cellular metabolism, differentiation, and transformation. *Cell*, *117*(4), 421–426.  
[https://doi.org/10.1016/S0092-8674\(04\)00452-0](https://doi.org/10.1016/S0092-8674(04)00452-0)
- Afroze, D., & Kumar, A. (2019). ER Stress in Skeletal Muscle Remodeling and Myopathies. *The FEBS Journal*, *286*(2), 379. <https://doi.org/10.1111/FEBS.14358>
- Al-Ishaq, R. K., Abotaleb, M., Kubatka, P., Kajo, K., & Büsselberg, D. (2019). Flavonoids and their anti-diabetic effects: Cellular mechanisms and effects to improve blood sugar levels. *Biomolecules*, *9*(9).  
<https://doi.org/10.3390/biom9090430>
- Al-Karmalawy, A. A., Farid, M. M., Mostafa, A., Ragheb, A. Y., Mahmoud, S. H., Shehata, M., Abo Shama, N. M., Gaballah, M., Mostafa-Hedeab, G., & Marzouk, M. M. (2021). Naturally Available Flavonoid Aglycones as Potential Antiviral Drug Candidates against SARS-CoV-2. *Molecules (Basel, Switzerland)*, *26*(21).  
<https://doi.org/10.3390/MOLECULES26216559>
- Alam, S., Abdullah, C. S., Aishwarya, R., Orr, A. W., Traylor, J., Miriyala, S., Panchatcharam, M., Pattillo, C. B., & Shenuarin Bhuiyan, M. (2017). Sigmar1 regulates endoplasmic reticulum stress-induced C/EBP-homologous protein expression in cardiomyocytes. *Bioscience Reports*.  
<https://doi.org/10.1042/BSR20170898>
- Almanza, A., Carlesso, A., Chintia, C., Creedican, S., Doultinos, D., Leuzzi, B., Luís, A., McCarthy, N., Montibeller, L., More, S., Papaioannou, A., Püschel, F., Sassano, M. L., Skoko, J., Agostinis, P., de Bellerocche, J., Eriksson, L. A., Fulda, S., Gorman, A. M., ... Samali, A. (2019). Endoplasmic reticulum stress signalling – from basic mechanisms to clinical applications. *FEBS Journal*, *286*(2), 241–278.  
<https://doi.org/10.1111/febs.14608>
- Arya, D. V., Alik, S. M., Suchal, K., & Bhatia, J. (2018). A18239 Apigenin ameliorates streptozotocin induced diabetic nephropathy in rats by modulation of oxidative stress, apoptosis and inflammation through MAPK pathway. *Journal of Hypertension*, *36*, e63. <https://doi.org/10.1097/01.HJH.0000548245.36355.2B>

- Ashrafizadeh, M., Ahmadi, Z., Mohammadinejad, R., & Ghasemipour Afshar, E. (2020). Tangeretin: a mechanistic review of its pharmacological and therapeutic effects. *Journal of Basic and Clinical Physiology and Pharmacology*, *31*(4). <https://doi.org/10.1515/JBCPP-2019-0191>
- B'Chir, W., Maurin, A. C., Carraro, V., Averous, J., Jousse, C., Muranishi, Y., Parry, L., Stepien, G., Fafournoux, P., & Bruhat, A. (2013). The eIF2 $\alpha$ /ATF4 pathway is essential for stress-induced autophagy gene expression. *Nucleic Acids Research*, *41*(16), 7683–7699. <https://doi.org/10.1093/NAR/GKT563>
- Badawi, S., Mohamed, F. E., Varghese, D. S., & Ali, B. R. (2023). Genetic disruption of mammalian endoplasmic reticulum-associated protein degradation: Human phenotypes and animal and cellular disease models. *Traffic*. <https://doi.org/10.1111/TRA.12902>
- Banday, M. Z., Sameer, A. S., & Nissar, S. (2020). Pathophysiology of diabetes: An overview. *Avicenna Journal of Medicine*, *10*(4), 174. [https://doi.org/10.4103/AJM.AJM\\_53\\_20](https://doi.org/10.4103/AJM.AJM_53_20)
- Bass, R., Ruddock, L. W., Klappa, P., & Freedman, R. B. (2004). A Major Fraction of Endoplasmic Reticulum-located Glutathione Is Present as Mixed Disulfides with Protein. *Journal of Biological Chemistry*, *279*(7), 5257–5262. <https://doi.org/10.1074/JBC.M304951200>
- Beecher, G. R. (2003). Overview of Dietary Flavonoids: Nomenclature, Occurrence and Intake. *The Journal of Nutrition*, *133*(27), 3255–3261. <http://www.ncbi.nlm.nih.gov/pubmed/17073577>
- Bentzinger, C. F., Wang, Y. X., & Rudnicki, M. A. (2012). Building Muscle: Molecular Regulation of Myogenesis. *Cold Spring Harbor Perspectives in Biology*, *4*(2). <https://doi.org/10.1101/CSHPERSPECT.A008342>
- Bertolotti, A., Zhang, Y., Hendershot, L. M., Harding, H. P., & Ron, D. (2000). *Sci-Hub / Dynamic interaction of BiP and ER stress transducers in the unfolded-protein response. Nature Cell Biology*, *2*(6), 326–332 | 10.1038/35014014. <https://sci-hub.se/10.1038/35014014>
- Beth Levine, & Guido Kroemer. (2008). Autophagy in the Pathogenesis of Disease. *Cell*,

132(1), 27–42. <https://doi.org/10.1016/j.cell.2007.12.018>

- Bhandary, B., Marahatta, A., Kim, H. R., & Chae, H. J. (2013). An involvement of oxidative stress in endoplasmic reticulum stress and its associated diseases. *International Journal of Molecular Sciences*, *14*(1), 434–456. <https://doi.org/10.3390/ijms14010434>
- Bhattacharya, A., & Qi, L. (2019). *ER-associated degradation in health and disease – from substrate to organism*. <https://doi.org/10.1242/jcs.232850>
- Bohnert, K. R., McMillan, J. D., & Kumar, A. (2018). Emerging roles of ER stress and unfolded protein response pathways in skeletal muscle health and disease. *Journal of Cellular Physiology*, *233*(1), 67–78. <https://doi.org/10.1002/jcp.25852>
- Bommer, C., Sagalova, V., Heesemann, E., Manne-Goehler, J., Atun, R., Bärnighausen, T., Davies, J., & Vollmer, S. (2018). Global Economic Burden of Diabetes in Adults: Projections From 2015 to 2030. *Diabetes Care*, *41*(5), 963–970. <https://doi.org/10.2337/dc17-1962>
- Bouman, L., Schlierf, A., Lutz, A. K., Shan, J., Deinlein, A., Kast, J., Galehdar, Z., Palmisano, V., Patenge, N., Berg, D., Gasser, T., Augustin, R., Trümbach, D., Irrcher, I., Park, D. S., Wurst, W., Kilberg, M. S., Tatzelt, J., & Winklhofer, K. F. (2011). Parkin is transcriptionally regulated by ATF4: evidence for an interconnection between mitochondrial stress and ER stress. *Cell Death and Differentiation*, *18*(5), 769–782. <https://doi.org/10.1038/CDD.2010.142>
- Burgos-Morón, E., Abad-Jiménez, Z., de Marañón, A. M., Iannantuoni, F., Escribano-López, I., López-Domènech, S., Salom, C., Jover, A., Mora, V., Roldan, I., Solá, E., Rocha, M., & Víctor, V. M. (2019). Relationship between Oxidative Stress, ER Stress, and Inflammation in Type 2 Diabetes: The Battle Continues. *Journal of Clinical Medicine* 2019, Vol. 8, Page 1385, *8*(9), 1385. <https://doi.org/10.3390/JCM8091385>
- Cao, S. S., & Kaufman, R. J. (2014). *Endoplasmic Reticulum Stress and Oxidative Stress in Cell Fate Decision and Human Disease*. <https://doi.org/10.1089/ars.2014.5851>
- Carstens, P. O., & Schmidt, J. (2014). Diagnosis, pathogenesis and treatment of myositis: Recent advances. *Clinical and Experimental Immunology*, *175*(3), 349–358.

<https://doi.org/10.1111/cei.12194>

Chang, L., Chiang, S. H., & Saltiel, A. R. (2004). Insulin signaling and the regulation of glucose transport. *Molecular Medicine*, 10(7–12), 65–71. <https://doi.org/10.2119/2005-00029.Saltiel>

Chang, N. C. (2020). Autophagy and Stem Cells: Self-Eating for Self-Renewal. *Frontiers in Cell and Developmental Biology*, 8, 526120. <https://doi.org/10.3389/FCELL.2020.00138/BIBTEX>

Chaudhury, A., Duvoor, C., Reddy Dendi, V. S., Kraleti, S., Chada, A., Ravilla, R., Marco, A., Shekhawat, N. S., Montales, M. T., Kuriakose, K., Sasapu, A., Beebe, A., Patil, N., Musham, C. K., Lohani, G. P., & Mirza, W. (2017). Clinical Review of Antidiabetic Drugs: Implications for Type 2 Diabetes Mellitus Management. *Frontiers in Endocrinology*, 8(January). <https://doi.org/10.3389/fendo.2017.00006>

Cnop, M., Ladriere, L., Hekerman, P., Ortis, F., Cardozo, A. K., Dogusan, Z., Flamez, D., Boyce, M., Yuan, J., & Eizirik, D. L. (2007). Selective inhibition of eukaryotic translation initiation factor 2 alpha dephosphorylation potentiates fatty acid-induced endoplasmic reticulum stress and causes pancreatic beta-cell dysfunction and apoptosis. *The Journal of Biological Chemistry*, 282(6), 3989–3997. <https://doi.org/10.1074/JBC.M607627200>

Davies, K. J. A., Quintanilha, A. T., Brooks, G. A., & Packer, L. (1982). Free radicals and tissue damage produced by exercise. *Biochemical and Biophysical Research Communications*, 107(4), 1198–1205. [https://doi.org/10.1016/S0006-291X\(82\)80124-1](https://doi.org/10.1016/S0006-291X(82)80124-1)

De Bernard, M., Robson, M. J., Kruyt, F., Yu, S., Hu, H., Tian, M., & Ding, C. (2019). The C/EBP Homologous Protein (CHOP) Transcription Factor Functions in Endoplasmic Reticulum Stress-Induced Apoptosis and Microbial Infection. *Frontiers in Immunology | Www.Frontiersin.Org*, 1, 3083. <https://doi.org/10.3389/fimmu.2018.03083>

DeFronzo, R. A., Jacot, E., Jequier, E., Maeder, E., Wahren, J., & Felber, J. P. (1981). The effect of insulin on the disposal of intravenous glucose. Results from indirect calorimetry and hepatic and femoral venous catheterization. *Diabetes*, 30(12), 1000–1007. <https://doi.org/10.2337/DIAB.30.12.1000>

- Deldicque, L., Guimarães-Ferreira, L., & Paolocci, N. (2013). *Endoplasmic reticulum stress in human skeletal muscle: any contribution to sarcopenia?* <https://doi.org/10.3389/fphys.2013.00236>
- Deniaud, Sharaf, Maillier, Poncet, Kroemer, Lemaire, & Brenner. (2008). *Endoplasmic reticulum stress induces calcium-dependent permeability transition, mitochondrial outer membrane permeabilization and apoptosis.* *Oncogene*. <https://scihub.se/10.1038/sj.onc.1210638>
- DeRango-Adem, E. F., & Blay, J. (2021). Does Oral Apigenin Have Real Potential for a Therapeutic Effect in the Context of Human Gastrointestinal and Other Cancers? In *Frontiers in Pharmacology* (Vol. 12). <https://doi.org/10.3389/fphar.2021.681477>
- Du, J., Wang, X., Miereles, C., Bailey, J. L., Debigare, R., Zheng, B., Price, S. R., & Mitch, W. E. (2004). Activation of caspase-3 is an initial step triggering accelerated muscle proteolysis in catabolic conditions. *The Journal of Clinical Investigation*, *113*(1), 115–123. <https://doi.org/10.1172/JCI18330>
- Du, K., Herzig, S., & Kulkarni, R. N. (2003). *TRB3: A tribbles Homolog That Inhibits Akt / PKB Activation by.* *300*(June), 1574–1578.
- Ebersbach-Silva, P., Poletto, A. C., David-Silva, A., Seraphim, P. M., Anhê, G. F., Passarelli, M., Furuya, D. T., & Machado, U. F. (2018). Palmitate-induced Slc2a4/GLUT4 downregulation in L6 muscle cells: Evidence of inflammatory and endoplasmic reticulum stress involvement. *Lipids in Health and Disease*, *17*(1), 2–9. <https://doi.org/10.1186/s12944-018-0714-8>
- Egan, B., & Zierath, J. R. (2013). Exercise metabolism and the molecular regulation of skeletal muscle adaptation. *Cell Metabolism*, *17*(2), 162–184. <https://doi.org/10.1016/j.cmet.2012.12.012>
- Eizirik, D. L., Cardozo, A. K., & Cnop, M. (2008). *The Role for Endoplasmic Reticulum Stress in Diabetes Mellitus.* *29*(July), 42–61. <https://doi.org/10.1210/er.2007-0015>
- Engin, F., Yermalovich, A., Ngyuen, T., Hummasti, S., Fu, W., Eizirik, D. L., Mathis, D., & Hotamisligil, G. S. (2013). Restoration of the unfolded protein response in pancreatic  $\beta$  cells protects mice against type 1 diabetes. *Science Translational Medicine*, *5*(211). <https://doi.org/10.1126/scitranslmed.3006534>

- English, A. R., & Voeltz, G. K. (2013). Endoplasmic reticulum structure and interconnections with other organelles. *Cold Spring Harbor Perspectives in Biology*, 5(4), 1–16. <https://doi.org/10.1101/cshperspect.a013227>
- Espinosa-Diez, C., Miguel, V., Mennerich, D., Kietzmann, T., Sánchez-Pérez, P., Cadenas, S., & Lamas, S. (2015). Antioxidant responses and cellular adjustments to oxidative stress. *Redox Biology*, 6, 183–197. <https://doi.org/10.1016/j.redox.2015.07.008>
- Evans, W. (2010). Skeletal muscle loss: cachexia, sarcopenia, and inactivity. *American Journal of Clinical Nutrition*. <https://academic.oup.com/ajcn/article-abstract/91/4/1123S/4597225>
- Fanzani, A., Conraads, V. M., Penna, F., & Martinet, W. (2012). Molecular and cellular mechanisms of skeletal muscle atrophy: An update. *Journal of Cachexia, Sarcopenia and Muscle*, 3(3), 163–179. <https://doi.org/10.1007/s13539-012-0074-6>
- Flamment, M., Hajduch, E., Ferré, P., & Foufelle, F. (2012). New insights into ER stress-induced insulin resistance. *Trends in Endocrinology and Metabolism*, 23(8), 381–390. <https://doi.org/10.1016/j.tem.2012.06.003>
- Fonseca, S. G., Gromada, J., & Urano, F. (2011). Endoplasmic reticulum stress and pancreatic  $\beta$ -cell death. *Trends in Endocrinology and Metabolism*, 22(7), 266–274. <https://doi.org/10.1016/j.tem.2011.02.008>
- Fujita, E., Kouroku, Y., Isoai, A., Kumagai, H., Misutani, A., Matsuda, C., Hayashi, Y. K., & Momoi, T. (2007). Two endoplasmic reticulum-associated degradation (ERAD) systems for the novel variant of the mutant dysferlin: ubiquitin/proteasome ERAD(I) and autophagy/lysosome ERAD(II). *Human Molecular Genetics*, 16(6), 618–629. <https://doi.org/10.1093/HMG/DDM002>
- Gade, P., Ramachandran, G., Maachani, U. B., Rizzo, M. A., Okada, T., Prywes, R., Cross, A. S., Mori, K., & Kalvakolanu, D. V. (2012). An IFN- $\gamma$ -stimulated ATF6-C/EBP- $\beta$ -signaling pathway critical for the expression of death associated protein kinase 1 and induction of autophagy. *Proceedings of the National Academy of Sciences of the United States of America*, 109(26), 10316–10321. <https://doi.org/10.1073/PNAS.1119273109/-/DCSUPPLEMENTAL>



- Gallot, Y. S., & Bohnert, K. R. (2021). Confounding roles of ER stress and the unfolded protein response in skeletal muscle atrophy. *International Journal of Molecular Sciences*, 22(5), 1–18. <https://doi.org/10.3390/ijms22052567>
- Gestational Diabetes Mellitus (GDM) | Johns Hopkins Medicine*. (n.d.). Retrieved June 28, 2023, from <https://www.hopkinsmedicine.org/health/conditions-and-diseases/diabetes/gestational-diabetes>
- Gonen, N., Meller, A., Sabath, N., & Shalgi, R. (2019). Amino Acid Biosynthesis Regulation during Endoplasmic Reticulum Stress Is Coupled to Protein Expression Demands. *ISCIENCE*, 19, 204–213. <https://doi.org/10.1016/j.isci.2019.07.022>
- Gordaliza-Alaguero, I., Cantó, C., & Zorzano, A. (2019). Metabolic implications of organelle-mitochondria communication. *EMBO Reports*, 20(9). <https://doi.org/10.15252/EMBR.201947928>
- Gorlach, Klappa, & Kietzmann. (2006). *Sci-Hub | The Endoplasmic Reticulum: Folding, Calcium Homeostasis, Signaling, and Redox Control. Antioxidants & Redox Signaling*, 8(9-10), 1391–1418 | 10.1089/ars.2006.8.1391. Antioxidants & Redox Signaling. <https://sci-hub.se/https://doi.org/10.1089/ars.2006.8.1391>
- Goyal, U., & Blackstone, C. (2013). *Sci-Hub | Untangling the web: Mechanisms underlying ER network formation. Biochimica et Biophysica Acta (BBA) - Molecular Cell Research*, 1833(11), 2492–2498 | 10.1016/j.bbamcr.2013.04.009. <https://sci-hub.se/https://doi.org/10.1016/j.bbamcr.2013.04.009>
- Guerriero, C. J., & Brodsky, J. L. (2012). The delicate balance between secreted protein folding and endoplasmic reticulum-associated degradation in human physiology. *Physiological Reviews*, 92(2), 537–576. <https://doi.org/10.1152/physrev.00027.2011>
- Hage Hassan, R., Hainault, I., Vilquin, J.-T., Samama, C., Lasnier, F., Ferré, P., Fougère, F., & Hajduch, E. (2012). Endoplasmic reticulum stress does not mediate palmitate-induced insulin resistance in mouse and human muscle cells. *Diabetologia*, 55(1), 204–214. <https://doi.org/10.1007/s00125-011-2328-9>
- Hagiwara, & Nagata. (2012). *Sci-Hub | Redox-Dependent Protein Quality Control in the Endoplasmic Reticulum: Folding to Degradation. Antioxidants & Redox Signaling*,

16(10), 1119–1128 / 10.1089/ars.2011.4495. <https://sci-hub.se/https://doi.org/10.1089/ars.2011.4495>

Hansen, D., Peeters, S., Zwaenepoel, B., Verleyen, D., Wittebrood, C., Timmerman, N., & Schotte, M. (2013). Exercise assessment and prescription in patients with type 2 diabetes in the private and home care setting: Clinical recommendations from AXXON (Belgian Physical Therapy Association). *Physical Therapy*, 93(5), 597–610. <https://doi.org/10.2522/ptj.20120400>

Harding, H. P., Zhang, Y., Bertolotti, A., Zeng, H., & David, R. (2000). Perk Is Essential for Translational Regulation and Cell Survival during the Unfolded Protein Response. *Molecular Cell*.

Harding, H. P., Zhang, Y., Zeng, H., Novoa, I., Lu, P. D., Calton, M., Sadri, N., Yun, C., Popko, B., Paules, R., Stojdl, D. F., Bell, J. C., Hettmann, T., Leiden, J. M., & Ron, D. (2003). An integrated stress response regulates amino acid metabolism and resistance to oxidative stress. *Molecular Cell*, 11(3), 619–633. [https://doi.org/10.1016/S1097-2765\(03\)00105-9](https://doi.org/10.1016/S1097-2765(03)00105-9)

Hasnain, S. Z., Prins, J. B., & McGuckin, M. A. (2016). Oxidative and endoplasmic reticulum stress in  $\beta$ -cell dysfunction in diabetes. *Journal of Molecular Endocrinology*, 56(2), R33–R54. <https://doi.org/10.1530/JME-15-0232>

Hawa, M. I., Kolb, H., Schloot, N., Beyan, H., Paschou, S. A., Buzzetti, R., Mauricio, D., De Leiva, A., Yderstraede, K., Beck-Neilsen, H., Tuomilehto, J., Sarti, C., Thivolet, C., Hadden, D., Hunter, S., Scherthaner, G., Scherbaum, W. A., Williams, R., Brophy, S., ... Leslie, R. D. (2013). Adult-onset autoimmune diabetes in Europe is prevalent with a broad clinical phenotype: Action LADA 7. *Diabetes Care*, 36(4), 908–913. <https://doi.org/10.2337/DC12-0931/-/DC1>

Henderson, M. J., Trychta, K. A., Yang, S. M., Bäck, S., Yasgar, A., Wires, E. S., Danchik, C., Yan, X., Yano, H., Shi, L., Wu, K. J., Wang, A. Q., Tao, D., Zahoránszky-Kóhalmi, G., Hu, X., Xu, X., Maloney, D., Zakharov, A. V., Rai, G., ... Harvey, B. K. (2021). A target-agnostic screen identifies approved drugs to stabilize the endoplasmic reticulum-resident proteome. *Cell Reports*, 35(4). <https://doi.org/10.1016/j.celrep.2021.109040>

Henriksen, E. J., Diamond-Stanic, M. K., & Marchionne, E. M. (2011). Oxidative stress

- and the etiology of insulin resistance and type 2 diabetes. *Free Radical Biology and Medicine*, 51(5), 993–999. <https://doi.org/10.1016/j.freeradbiomed.2010.12.005>
- Herlea-Pana, O., Eeda, V., Undi, R. B., Lim, H. Y., & Wang, W. (2021). Pharmacological Inhibition of Inositol-Requiring Enzyme 1 $\alpha$  RNase Activity Protects Pancreatic Beta Cell and Improves Diabetic Condition in Insulin Mutation-Induced Diabetes. *Frontiers in Endocrinology*, 12(October), 1–14. <https://doi.org/10.3389/fendo.2021.749879>
- Hetz, C. (2012). The unfolded protein response: Controlling cell fate decisions under ER stress and beyond. *Nature Reviews Molecular Cell Biology*, 13(2), 89–102. <https://doi.org/10.1038/nrm3270>
- Honzawa, N., & Fujimoto, K. (2021). The Plasticity of Pancreatic  $\beta$ -Cells. *Metabolites*, 11(4). <https://doi.org/10.3390/METABO11040218>
- Hostetler, G. L., Ralston, R. A., & Schwartz, S. J. (n.d.). *Flavones: Food Sources, Bioavailability, Metabolism, and Bioactivity 1,2*. <https://doi.org/10.3945/an.116.012948>
- Hotamisligil, G. S. (2010). Endoplasmic Reticulum Stress and the Inflammatory Basis of Metabolic Disease. *Cell*, 140(6), 900–917. <https://doi.org/10.1016/j.cell.2010.02.034>
- Hu, H., Tian, M., Ding, C., & Yu, S. (2019). The C/EBP homologous protein (CHOP) transcription factor functions in endoplasmic reticulum stress-induced apoptosis and microbial infection. *Frontiers in Immunology*, 10(JAN), 1–13. <https://doi.org/10.3389/fimmu.2018.03083>
- Hu, P., Han, Z., Couvillon, A. D., Kaufman, R. J., & Exton, J. H. (2006). Autocrine tumor necrosis factor alpha links endoplasmic reticulum stress to the membrane death receptor pathway through IRE1 $\alpha$ -mediated NF- $\kappa$ B activation and down-regulation of TRAF2 expression. *Molecular and Cellular Biology*, 26(8), 3071–3084. <https://doi.org/10.1128/MCB.26.8.3071-3084.2006>
- Hung, W. L., Chang, W. S., Lu, W. C., Wei, G. J., Wang, Y., Ho, C. T., & Hwang, L. S. (2018). Pharmacokinetics, bioavailability, tissue distribution and excretion of tangeretin in rat. *Journal of Food and Drug Analysis*, 26(2), 849–857.

<https://doi.org/10.1016/j.jfda.2017.08.003>

Ijuin, T., Hosooka, T., & Takenawa, T. (2016). Phosphatidylinositol 3,4,5-Trisphosphate Phosphatase SKIP Links Endoplasmic Reticulum Stress in Skeletal Muscle to Insulin Resistance. *Molecular and Cellular Biology*, 36(1), 108–118. <https://doi.org/10.1128/mcb.00921-15>

Ijuin, T., & Takenawa, T. (2003). SKIP Negatively Regulates Insulin-Induced GLUT4 Translocation and Membrane Ruffle Formation. *https://Doi.Org/10.1128/MCB.23.4.1209-1220.2003*, 23(4), 1209–1220. <https://doi.org/10.1128/MCB.23.4.1209-1220.2003>

Jackson, M. J., Pollock, N., Staunton, C. A., Stretton, C., Vasilaki, A., & McArdle, A. (2019). Oxidative stress in skeletal muscle: Unraveling the potential beneficial and deleterious roles of reactive oxygen species. In *Oxidative Stress: Eustress and Distress*. Elsevier Inc. <https://doi.org/10.1016/B978-0-12-818606-0.00034-1>

Jegal, K. H., Kim, E. O., Kim, J. K., Park, S. M., Jung, D. H., Lee, G. H., Ki, S. H., Byun, S. H., Ku, S. K., Cho, I. J., & Kim, S. C. (2020). Luteolin prevents liver from tunicamycin-induced endoplasmic reticulum stress via nuclear factor erythroid 2-related factor 2-dependent sestrin 2 induction. *Toxicology and Applied Pharmacology*, 399, 115036. <https://doi.org/10.1016/J.TAAP.2020.115036>

Kang, S., Dahl, R., Hsieh, W., Shin, A., Zsebo, M. K., Buettner, C., Hajjar, J. R., & Lebeche Djamel. (2015). *Small Molecular Allosteric Activator of the Sarco/Endoplasmic Reticulum Ca<sup>2</sup>-ATPase (SERCA) Attenuates Diabetes and Metabolic Disorders*. The Journal of Biological Chemistry. <https://www.jbc.org/action/showPdf?pii=S0021-9258%2820%2943156-4>

Kashyap, D., Sharma, A., Tuli, H. S., Sak, K., Garg, V. K., Buttar, H. S., Setzer, W. N., & Sethi, G. (2018). Apigenin: A natural bioactive flavone-type molecule with promising therapeutic function. *Journal of Functional Foods*, 48, 457–471. <https://doi.org/10.1016/J.JFF.2018.07.037>

Kim, Jamart, & Deldicque. (2011). *Sci-Hub | Endoplasmic Reticulum Stress Markers and Ubiquitin-Proteasome Pathway Activity in Response to a 200-km Run*. *Medicine & Science in Sports & Exercise*, 43(1), 18–25 | [10.1249/mss.0b013e3181e4c5d1](https://doi.org/10.1249/mss.0b013e3181e4c5d1). <https://sci-hub.se/https://doi.org/10.1249/mss.0b013e3181e4c5d1>

- Kim, T. W., & Lee, H. G. (2021). Apigenin Induces Autophagy and Cell Death by Targeting EZH2 under Hypoxia Conditions in Gastric Cancer Cells. *International Journal of Molecular Sciences* 2021, Vol. 22, Page 13455, 22(24), 13455. <https://doi.org/10.3390/IJMS222413455>
- Kitajima, Y., Yoshioka, K., & Suzuki, N. (2020). The ubiquitin-proteasome system in regulation of the skeletal muscle homeostasis and atrophy: From basic science to disorders. *Journal of Physiological Sciences*, 70(1). <https://doi.org/10.1186/s12576-020-00768-9>
- Kitakaze, K., Taniuchi, S., Kawano, E., Hamada, Y., Miyake, M., Oyadomari, M., Kojima, H., Kosako, H., Kuribara, T., Yoshida, S., Hosoya, T., & Oyadomari, S. (2019). Cell-based hts identifies a chemical chaperone for preventing er protein aggregation and proteotoxicity. *ELife*, 8. <https://doi.org/10.7554/ELIFE.43302>
- Knip, M., & Siljander, H. (2008). Autoimmune mechanisms in type 1 diabetes. *Autoimmunity Reviews*, 7(7), 550–557. <https://doi.org/10.1016/J.AUTREV.2008.04.008>
- Koh, H. J., Toyoda, T., Didesch, M. M., Lee, M. Y., Sleeman, M. W., Kulkarni, R. N., Musi, N., Hirshman, M. F., & Goodyear, L. J. (2013). Tribbles 3 mediates endoplasmic reticulum stress-induced insulin resistance in skeletal muscle. *Nature Communications*, 4(May), 1–11. <https://doi.org/10.1038/ncomms2851>
- Kondo, H., Miura, M., & Itokawa, Y. (1991). Oxidative stress in skeletal muscle atrophied by immobilization. *Acta Physiologica Scandinavica*, 142(4), 527–528. <https://doi.org/10.1111/J.1748-1716.1991.TB09191.X>
- Lee, S., & Min, K. T. (2018). The Interface Between ER and Mitochondria: Molecular Compositions and Functions. *Molecules and Cells*, 41(12), 1000. <https://doi.org/10.14348/MOLCELLS.2018.0438>
- Liang, Y. C., Zhong, Q., Ma, R. H., Ni, Z. J., Thakur, K., Khan, M. R., Busquets, R., Zhang, J. G., & Wei, Z. J. (2022). Apigenin inhibits migration and induces apoptosis of human endometrial carcinoma Ishikawa cells via PI3K-AKT-GSK-3 $\beta$  pathway and endoplasmic reticulum stress. *Journal of Functional Foods*, 94, 105116. <https://doi.org/10.1016/J.JFF.2022.105116>

- Lin, J. H., Walter, P., & Benedict Yen, T. S. (2007). *Endoplasmic Reticulum Stress in Disease Pathogenesis*.  
<https://doi.org/10.1146/annurev.pathmechdis.3.121806.151434>
- Lin, L. C., Pai, Y. F., & Tsai, T. H. (2015). Isolation of Luteolin and Luteolin-7-O-glucoside from *Dendranthema morifolium* Ramat Tzvel and Their Pharmacokinetics in Rats. *Journal of Agricultural and Food Chemistry*, 63(35), 7700–7706.  
[https://doi.org/10.1021/JF505848Z/SUPPL\\_FILE/JF505848Z\\_SI\\_001.PDF](https://doi.org/10.1021/JF505848Z/SUPPL_FILE/JF505848Z_SI_001.PDF)
- Lin, X., Yufeng, Pan, X., Xu, J., Ding, Y., Sun, X., Song, X., Ren, Y., & Peng-Fei Shan, &. (2020). *Global, regional, and national burden and trend of diabetes in 195 countries and territories: an analysis from 1990 to 2025*. 10, 14790.  
<https://doi.org/10.1038/s41598-020-71908-9>
- Lipson, K. L., Fonseca, S. G., Ishigaki, S., Nguyen, L. X., Foss, E., Bortell, R., Rossini, A. A., & Urano, F. (2006). Regulation of insulin biosynthesis in pancreatic beta cells by an endoplasmic reticulum-resident protein kinase IRE1. *Cell Metabolism*, 4(3), 245–254. <https://doi.org/10.1016/j.cmet.2006.07.007>
- Liu, K., Shi, Y., Guo, X., Wang, S., Ouyang, Y., Hao, M., Liu, D., Qiao, L., Li, N., Zheng, J., & Chen, D. (2014). CHOP mediates ASPP2-induced autophagic apoptosis in hepatoma cells by releasing Beclin-1 from Bcl-2 and inducing nuclear translocation of Bcl-2. *Cell Death & Disease*, 5(7). <https://doi.org/10.1038/CDDIS.2014.276>
- Lizcano, J. M., & Alessi, D. R. (2002). The insulin signalling pathway. *Current Biology*, 12(7), 236–238. [https://doi.org/10.1016/S0960-9822\(02\)00777-7](https://doi.org/10.1016/S0960-9822(02)00777-7)
- Lopez-Lazaro, M. (2009). Distribution and biological activities of the flavonoid luteolin. *Mini Reviews in Medicinal Chemistry*, 9(1), 31–59.  
<https://doi.org/10.2174/138955709787001712>
- Luo, L., & Liu, M. (2016). Adipose tissue in control of metabolism. *Journal of Endocrinology*, 231(3), R77–R99. <https://doi.org/10.1530/JOE-16-0211>
- Ma, R.-H., Ni, Z.-J., Thakur, K., Zhang, F., Zhang, Y.-Y., Zhang, J.-G., & Wei, Z.-J. (2020). Natural Compounds Play Therapeutic Roles in Various Human Pathologies via Regulating Endoplasmic Reticulum Pathway. *Medicine in Drug Discovery*, 8, 100065. <https://doi.org/10.1016/J.MEDIDD.2020.100065>

- Malhotra, J. D., & Kaufman, R. J. (2007). Endoplasmic Reticulum Stress and Oxidative Stress: A Vicious Cycle or a Double-Edged Sword? *https://Home.Liebertpub.Com/Ars*, 9(12), 2277–2293.  
<https://doi.org/10.1089/ARS.2007.1782>
- Malhotra, J. D., & Kaufman, R. J. (2011). ER stress and Its functional link to mitochondria: Role in cell survival and death. *Cold Spring Harbor Perspectives in Biology*, 3(9), 1–13. <https://doi.org/10.1101/cshperspect.a004424>
- Margariti, A., Li, H., Chen, T., Martin, D., Vizcay-Barrena, G., Alam, S., Karamariti, E., Xiao, Q., Zampetaki, A., Zhang, Z., Wang, W., Jiang, Z., Gao, C., Ma, B., Chen, Y. G., Cockerill, G., Hu, Y., Xu, Q., & Zeng, L. (2013). XBP1 mRNA splicing triggers an autophagic response in endothelial cells through BECLIN-1 transcriptional activation. *Journal of Biological Chemistry*, 288(2), 859–872. <https://doi.org/10.1074/jbc.M112.412783>
- Martens, S., & Mithöfer, A. (2005). Flavones and flavone synthases. *Phytochemistry*, 66(20), 2399–2407. <https://doi.org/10.1016/J.PHYTOCHEM.2005.07.013>
- Martino, M., Jones, L., Brighton, B., Ehre, C., Abdulah, L., Davies, C., Ron, D., O’Neal, W., & Ribiero, C. (2013). The ER stress transducer IRE1 $\beta$  is required for airway epithelial mucin production. *Mucosal Immunology*, 23(1), 1–7. <https://doi.org/10.1038/mi.2012.105>.The
- Mazzarello, P., Calligaro, A., Vannini, V., & Muscatello, U. (2003). The sarcoplasmic reticulum: Its discovery and rediscovery. *Nature Reviews Molecular Cell Biology*, 4(1), 69–74. <https://doi.org/10.1038/nrm1003>
- McCubrey, J. A., LaHair, M. M., & Franklin, R. A. (2006). Reactive oxygen species-induced activation of the MAP kinase signaling pathways. *Antioxidants and Redox Signaling*, 8(9–10), 1775–1789. <https://doi.org/10.1089/ars.2006.8.1775>
- McCullough, K. D., Martindale, J. L., Klotz, L.-O., Aw, T.-Y., & Holbrook, N. J. (2001). Gadd153 Sensitizes Cells to Endoplasmic Reticulum Stress by Down-Regulating Bcl2 and Perturbing the Cellular Redox State. *Molecular and Cellular Biology*, 21(4), 1249. <https://doi.org/10.1128/MCB.21.4.1249-1259.2001>
- Mei, Y., Thompson, M. D., Cohen, R. A., & Tong, X. (2013). Endoplasmic Reticulum

- Stress and Related Pathological Processes. *Journal of Pharmacological & Biomedical Analysis*, 1(2), 1000107–1000107. <https://doi.org/10.4172/2327-4638.1000107>
- Mensch, A., & Zierz, S. (2020). Cellular stress in the pathogenesis of muscular disorders—from cause to consequence. *International Journal of Molecular Sciences*, 21(16), 1–27. <https://doi.org/10.3390/ijms21165830>
- Mohi-Ud-din, R., Mir, R. H., Wani, T. U., Alsharif, K. F., Alam, W., Albrakati, A., Saso, L., & Khan, H. (2022). The Regulation of Endoplasmic Reticulum Stress in Cancer: Special Focuses on Luteolin Patents. *Molecules*, 27(8). <https://doi.org/10.3390/MOLECULES27082471>
- Muoio, D. M., & Newgard, C. B. (2008). Molecular and metabolic mechanisms of insulin resistance and  $\beta$ -cell failure in type 2 diabetes. *Nature Reviews Molecular Cell Biology* 2008 9:3, 9(3), 193–205. <https://doi.org/10.1038/nrm2327>
- Nakanishi, K., Sudo, T., & Morishima, N. (2005). Endoplasmic reticulum stress signaling transmitted by ATF6 mediates apoptosis during muscle development. *The Journal of Cell Biology*, 169(4), 555–560. <https://doi.org/10.1083/jcb.200412024>
- Oakes, S. A., & Papa, F. R. (2015). *The Role of Endoplasmic Reticulum Stress in Human Pathology*. October 2014, 173–194. <https://doi.org/10.1146/annurev-pathol-012513-104649>
- Oberoi, S., & Kansra, P. (2020). Economic menace of diabetes in India: a systematic review. *International Journal of Diabetes in Developing Countries*, 40(4), 464–475. <https://doi.org/10.1007/s13410-020-00838-z>
- Oddis, C. V. (2016). *Update on the pharmacological treatment of adult myositis*. <https://doi.org/10.1111/joim.12511>
- Ozcan, U., Erkan, Y., Furuhashi, M., Vaillancourt, E., Smith, R., Gorgun, C., & Hotamisligil, G. (2006). Chemical Chaperones Reduce ER Stress and Restore Glucose Homeostasis in a Mouse Model of Type 2 Diabetes. *Science*, 176(1), 139–148. <https://doi.org/10.1126/science.1128294>.Chemical
- Panche, A. N., Diwan, A. D., & Chandra, S. R. (2016). Flavonoids: an overview. *Journal of Nutritional Science*, 5, 1–15. <https://doi.org/10.1017/jns.2016.41>



- Pandurangan, A. K., & Esa, N. M. (2014). Luteolin, a bioflavonoid inhibits colorectal cancer through modulation of multiple signaling pathways: A review. *Asian Pacific Journal of Cancer Prevention*, *15*(14), 5501–5508.  
<https://doi.org/10.7314/APJCP.2014.15.14.5501>
- Pessin, J. E., & Saltiel, A. R. (2000). Signaling pathways in insulin action: molecular targets of insulin resistance. *Journal of Clinical Investigation*, *106*(2), 165.  
<https://doi.org/10.1172/JCI10582>
- Prasad M, K., Mohandas, S., & Ramkumar, K. M. (2022). Role of ER stress inhibitors in the management of diabetes. *European Journal of Pharmacology*, *922*(January), 174893. <https://doi.org/10.1016/j.ejphar.2022.174893>
- Puthalakath, H., O'Reilly, L. A., Gunn, P., Lee, L., Kelly, P. N., Huntington, N. D., Hughes, P. D., Michalak, E. M., McKimm-Breschkin, J., Motoyama, N., Gotoh, T., Akira, S., Bouillet, P., & Strasser, A. (2007). ER stress triggers apoptosis by activating BH3-only protein Bim. *Cell*, *129*(7), 1337–1349.  
<https://doi.org/10.1016/J.CELL.2007.04.027>
- Rajan, S. S., Srinivasan, V., Balasubramanyam, M., & Tatu, U. (2007). *Endoplasmic reticulum ( ER ) stress & diabetes. March*, 411–424.
- Rashid, H. O., Yadav, R. K., Kim, H. R., & Chae, H. J. (2015). ER stress: Autophagy induction, inhibition and selection. *Autophagy*, *11*(11), 1956–1977.  
<https://doi.org/10.1080/15548627.2015.1091141>
- Ribeiro, I. M. R., & Antunes, V. R. (2018). The role of insulin at brain-liver axis in the control of glucose production. *American Journal of Physiology - Gastrointestinal and Liver Physiology*, *315*(4), G538–G543.  
<https://doi.org/10.1152/ajpgi.00290.2017>
- Röder, P. V, Wu, B., Liu, Y., & Han, W. (2016). Pancreatic regulation of glucose homeostasis. *Experimental & Molecular Medicine*, 219.  
<https://doi.org/10.1038/emm.2016.6>
- Rodriguez, B. S. Q., & Mahdy, H. (2022). *Gestational Diabetes*.  
<https://www.ncbi.nlm.nih.gov/books/NBK545196/>

- Romanello, V., & Sandri, M. (2016). Mitochondrial quality control and muscle mass maintenance. *Frontiers in Physiology*, 6(JAN), 1–21. <https://doi.org/10.3389/fphys.2015.00422>
- Ron, D., & Hubbard, S. R. (2008). How IRE1 Reacts to ER Stress. *Cell*, 132(1), 24–26. <https://doi.org/10.1016/J.CELL.2007.12.017>
- Rouschop, K. M. A., Van Den Beucken, T., Dubois, L., Niessen, H., Bussink, J., Savelkoul, K., Keulers, T., Mujcic, H., Landuyt, W., Voncken, J. W., Lambin, P., Van Der Kogel, A. J., Koritzinsky, M., & Wouters, B. G. (2010). The unfolded protein response protects human tumor cells during hypoxia through regulation of the autophagy genes MAP1LC3B and ATG5. *The Journal of Clinical Investigation*, 120(1), 127. <https://doi.org/10.1172/JCI40027>
- Roy, A., Da Silva, M. T., Bhat, R., Bohnert, K. R., Iwawaki, T., & Kumar, A. (2021). The IRE1/XBP1 signaling axis promotes skeletal muscle regeneration through a cell non-autonomous mechanism. *ELife*, 10. <https://doi.org/10.7554/ELIFE.73215>
- Rudrappa, S. S., Wilkinson, D. J., Greenhaff, P. L., Smith, K., Idris, I., & Atherton, P. J. (2016). Human skeletal muscle disuse atrophy: Effects on muscle protein synthesis, breakdown, and insulin resistance-A qualitative review. *Frontiers in Physiology*, 7(AUG), 1–10. <https://doi.org/10.3389/fphys.2016.00361>
- Rusiñol, A. E., Cui, Z., Chen, M. H., & Vance, J. E. (1994). A unique mitochondria-associated membrane fraction from rat liver has a high capacity for lipid synthesis and contains pre-Golgi secretory proteins including nascent lipoproteins. *Journal of Biological Chemistry*, 269(44), 27494–27502. [https://doi.org/10.1016/s0021-9258\(18\)47012-3](https://doi.org/10.1016/s0021-9258(18)47012-3)
- Rutkowski, D. T., & Kaufman, R. J. (2004). A trip to the ER: Coping with stress. *Trends in Cell Biology*, 14(1), 20–28. <https://doi.org/10.1016/j.tcb.2003.11.001>
- Saleem, H., Anwar, S., Alafnan, A., & Ahemad, N. (2021). Luteolin. *A Centum of Valuable Plant Bioactives*, 509–523. <https://doi.org/10.1016/B978-0-12-822923-1.00022-4>
- Sano, R., & Reed, J. C. (2013). ER stress-induced cell death mechanisms. *Biochimica et Biophysica Acta (BBA) - Molecular Cell Research*, 1833(12), 3460–3470.

<https://doi.org/10.1016/J.BBAMCR.2013.06.028>

Sartori, R., Romanello, V., & Sandri, M. (2021). *Mechanisms of muscle atrophy and hypertrophy: implications in health and disease*. <https://doi.org/10.1038/s41467-020-20123-1>

Savage, D. B., Petersen, K. F., & Shulman, G. I. (2005). *Mechanisms of Insulin Resistance in Humans and Possible Links With Inflammation*. <https://doi.org/10.1161/01.HYP.0000163475.04421.e4>

Scheuner, D., & Kaufman, R. J. (2008). The Unfolded Protein Response: A Pathway That Links Insulin Demand with  $\beta$ -Cell Failure and Diabetes. *Endocrine Reviews*, 29(3), 317–333. <https://doi.org/10.1210/ER.2007-0039>

Schwarz, D. S., & Blower, M. D. (2002). The endoplasmic reticulum: structure, function and response to cellular signaling. *Cellular and Molecular Life Sciences*, 73. <https://doi.org/10.1007/s00018-015-2052-6>

Seo, H. Y., Yong, D. K., Lee, K. M., Min, A. K., Kim, M. K., Kim, H. S., Won, K. C., Park, J. Y., Lee, K. U., Choi, H. S., Park, K. G., & Lee, I. K. (2008). Endoplasmic Reticulum Stress-Induced Activation of Activating Transcription Factor 6 Decreases Insulin Gene Expression via Up-Regulation of Orphan Nuclear Receptor Small Heterodimer Partner. *Endocrinology*, 149(8), 3832. <https://doi.org/10.1210/EN.2008-0015>

Shen, J., Chen, X., Hendershot, L., & Prywes, R. (2002). *ER Stress Regulation of ATF6 Localization by Dissociation of BiP/GRP78 Binding and Unmasking of Golgi Localization Signals*.

Shibata, Y., Voeltz, G. K., & Rapoport, T. A. (2006). Rough Sheets and Smooth Tubules. *Cell*, 126(3), 435–439. <https://doi.org/10.1016/j.cell.2006.07.019>

Shukla, S., & Gupta, S. (2010). *Apigenin: A Promising Molecule for Cancer Prevention*. <https://doi.org/10.1007/s11095-010-0089-7>

Singh, A., Phogat, J., Yadav, A., & Dabur, R. (2021). The dependency of autophagy and ubiquitin proteasome system during skeletal muscle atrophy. *Biophysical Reviews*, 13(2), 203. <https://doi.org/10.1007/S12551-021-00789-7>

Singh, M., Kaur, M., & Silakari, O. (2014). Flavones: An important scaffold for medicinal

- chemistry. *European Journal of Medicinal Chemistry*, 84, 206–239.  
<https://doi.org/10.1016/J.EJMECH.2014.07.013>
- Söhretoglu, D., & Arroo, R. (2018). Plant-Derived Antiinflammatory Steroid Analogs for Neuroprotection: A Recent Update. *Discovery and Development of Neuroprotective Agents from Natural Products: Natural Product Drug Discovery*, 321–358.  
<https://doi.org/10.1016/B978-0-12-809593-5.00007-0>
- Sun, H., Saeedi, P., Karuranga, S., Pinkepank, M., Ogurtsova, K., Duncan, B. B., Stein, C., Basit, A., Chan, J. C. N., Mbanya, J. C., Pavkov, M. E., Ramachandaran, A., Wild, S. H., James, S., Herman, W. H., Zhang, P., Bommer, C., Kuo, S., Boyko, E. J., & Magliano, D. J. (2022). IDF Diabetes Atlas: Global, regional and country-level diabetes prevalence estimates for 2021 and projections for 2045. *Diabetes Research and Clinical Practice*, 183, 109119. <https://doi.org/10.1016/j.diabres.2021.109119>
- Sung, B., Chung, H. Y., & Kim, N. D. (2016). Role of Apigenin in Cancer Prevention via the Induction of Apoptosis and Autophagy. *21*(4), 216–226.
- Takano, K., Tabata, Y., Kitao, Y., Murakami, R., Suzuki, H., Yamada, M., Inuma, M., Yoneda, Y., Ogawa, S., & Hori, O. (2007). Methoxyflavones protect cells against endoplasmic reticulum stress and neurotoxin. *American Journal of Physiology - Cell Physiology*, 292(1), 353–361.  
[https://doi.org/10.1152/AJPCELL.00388.2006/SUPPL\\_FILE/FIGURE](https://doi.org/10.1152/AJPCELL.00388.2006/SUPPL_FILE/FIGURE)
- Taouji, S., Wolf, S., & Chevet, E. (2013). Oligomerization in endoplasmic reticulum stress signaling. *Progress in Molecular Biology and Translational Science*, 117, 465–484. <https://doi.org/10.1016/B978-0-12-386931-9.00017-9>
- Thuerauf, D. J., Marcinko, M., Belmont, P. J., & Glembotski, C. C. (2007). Effects of the isoform-specific characteristics of ATF6 $\alpha$  and ATF6 $\beta$  on endoplasmic reticulum stress response gene expression and cell viability. *Journal of Biological Chemistry*, 282(31), 22865–22878. <https://doi.org/10.1074/jbc.M701213200>
- Ting, Y., Chiou, Y. S., Jiang, Y., Pan, M. H., Lin, Z., & Huang, Q. (2015). Safety evaluation of tangeretin and the effect of using emulsion-based delivery system: Oral acute and 28-day sub-acute toxicity study using mice. *Food Research International*, 74, 140. <https://doi.org/10.1016/j.foodres.2015.04.031>

- Trychta, K. A., Bäck, S., Henderson, M. J., & Harvey, B. K. (2018). KDEL Receptors Are Differentially Regulated to Maintain the ER Proteome under Calcium Deficiency. *Cell Reports*, 25(7), 1829-1840.e6.  
<https://doi.org/10.1016/j.celrep.2018.10.055>
- Turpin, J., El-Safadi, D., Lebeau, G., Frumence, E., Desprès, P., Viranaïcken, W., & Krejbich-Trotot, P. (2021). Chop pro-apoptotic transcriptional program in response to er stress is hacked by zika virus. *International Journal of Molecular Sciences*, 22(7). <https://doi.org/10.3390/ijms22073750>
- Urano, F., Wang, X. Z., Bertolotti, A., Zhang, Y., Chung, P., Harding, H. P., & Ron, D. (2000). Coupling of stress in the ER to activation of JNK protein kinases by transmembrane protein kinase IRE1. *Science (New York, N.Y.)*, 287(5453), 664–666.  
<https://doi.org/10.1126/SCIENCE.287.5453.664>
- Vembar, S. S., & Brodsky, J. L. (2008). One step at a time: Endoplasmic reticulum-associated degradation. *Nature Reviews Molecular Cell Biology*, 9(12), 944–957.  
<https://doi.org/10.1038/NRM2546>
- Voeltz, G. K., Rolls, M. M., & Rapoport, T. A. (2002). Structural organization of the endoplasmic reticulum. *EMBO Reports*, 3(10), 944–950.  
<https://doi.org/10.1093/embo-reports/kvf202>
- Wang, J., Sci, A. M., Zhang, C., Hou, X., Kong, Y., & Liu, Y. (2020). Tangeretin prevents cardiac failure induced by reperfusion/ischaemia by inhibiting apoptosis, endoplasmic reticulum stress, and JNK/ERK pathway. *Archives of Medical Science*.  
<https://doi.org/10.5114/AOMS.2020.97052>
- Wang, X., Hu, Z., Hu, J., Du, J., & Mitch, W. E. (2006). Insulin resistance accelerates muscle protein degradation: Activation of the ubiquitin-proteasome pathway by defects in muscle cell signaling. *Endocrinology*, 147(9), 4160–4168.  
<https://doi.org/10.1210/en.2006-0251>
- Washburn, R. L., Mueller, K., Kaur, G., Moreno, T., Moustaid-moussa, N., Ramalingam, L., & Dufour, J. M. (2021). C-Peptide as a Therapy for Type 1 Diabetes Mellitus. *Biomedicines*, 9(3), 1–24. <https://doi.org/10.3390/BIOMEDICINES9030270>
- Webber, S. (2021). International Diabetes Federation. In *Diabetes Research and Clinical*

*Practice* (Vol. 102, Issue 2). <https://doi.org/10.1016/j.diabres.2013.10.013>

Westrate, L. M., Lee, J. E., Prinz, W. A., & Voeltz, G. K. (2015). Form follows function: The importance of endoplasmic reticulum shape. *Annual Review of Biochemistry*, 84, 791–811. <https://doi.org/10.1146/annurev-biochem-072711-163501>

Wilson, E. L., & Metzakopian, E. (2021). ER-mitochondria contact sites in neurodegeneration: genetic screening approaches to investigate novel disease mechanisms. *Cell Death & Differentiation*, 28, 1804–1821. <https://doi.org/10.1038/s41418-020-00705-8>

Winter-Vann, A. M., & Johnson, G. L. (2007). Integrated activation of MAP3Ks balances cell fate in response to stress. *Journal of Cellular Biochemistry*, 102(4), 848–858. <https://doi.org/10.1002/JCB.21522>

World Health Organization. (2010). Global status report on noncommunicable diseases. *World Health Organization*, 53(9), 1689–1699.

<https://doi.org/10.1017/CBO9781107415324.004>

Wu, J., Ruas, J. L., Estall, J. L., Rasbach, K. A., Choi, J. H., Ye, L., Boström, P., Tyra, H. M., Crawford, R. W., Campbell, K. P., Rutkowski, D. T., Kaufman, R. J., & Spiegelman, B. M. (2011). The unfolded protein response mediates adaptation to exercise in skeletal muscle through a PGC-1 $\alpha$  /ATF6 $\alpha$  complex. *Cell Metabolism*, 13(2), 160. <https://doi.org/10.1016/J.CMET.2011.01.003>

Wu, L., Guo, T., Deng, R., Liu, L., & Yu, Y. (2021). Apigenin Ameliorates Insulin Resistance and Lipid Accumulation by Endoplasmic Reticulum Stress and SREBP-1c/SREBP-2 Pathway in Palmitate-Induced HepG2 Cells and High-Fat Diet-Fed Mice. *The Journal of Pharmacology and Experimental Therapeutics*, 377(1), 146–156. <https://doi.org/10.1124/JPET.120.000162>

Wu, W., Yao, X., Jiang, L., Zhang, Q., Bai, J., Qiu, T., Yang, L., Gao, N., Yang, G., Liu, X., Chen, M., & Sun, X. (2018). Pancreatic islet-autonomous effect of arsenic on insulin secretion through endoplasmic reticulum stress-autophagy pathway. *Food and Chemical Toxicology*, 111(May 2017), 19–26.

<https://doi.org/10.1016/j.fct.2017.10.043>

Xiao, C., Giacca, A., & Lewis, G. F. (2011). *Sodium Phenylbutyrate, a Drug With Known*

*Capacity to Reduce Endoplasmic Reticulum Stress, Partially Alleviates Lipid-Induced Insulin Resistance and  $\beta$ -Cell Dysfunction in Humans.*  
<https://doi.org/10.2337/db10-1433>

Xiong, G., Hindi, S. M., Mann, A. K., Gallot, Y. S., Bohnert, K. R., Cavener, D. R., Whittemore, S. R., & Kumar, A. (2017). The PERK arm of the unfolded protein response regulates satellite cell-mediated skeletal muscle regeneration. *ELife*, 6. <https://doi.org/10.7554/ELIFE.22871>

Yamamoto, K., Sato, T., Matsui, T., Sato, M., Okada, T., Yoshida, H., Harada, A., & Mori, K. (2007). Transcriptional Induction of Mammalian ER Quality Control Proteins Is Mediated by Single or Combined Action of ATF6 $\alpha$  and XBP1. *Developmental Cell*, 13(3), 365–376.  
<https://doi.org/10.1016/J.DEVCEL.2007.07.018>

Yan, M. M., Ni, J. D., Song, D., Ding, M., & Huang, J. (2015). Interplay between unfolded protein response and autophagy promotes tumor drug resistance (Review). *Oncology Letters*, 10(4), 1959–1969. <https://doi.org/10.3892/ol.2015.3508>

Yang, H., Niemeijer, M., van de Water, B., & Beltman, J. B. (2020). ATF6 Is a Critical Determinant of CHOP Dynamics during the Unfolded Protein Response. *IScience*, 23(2). <https://doi.org/10.1016/J.ISCI.2020.100860>

Yang, M., Wei, D., Mo, C., Zhang, J., Wang, X., Han, X., Wang, Z., & Xiao, H. (2013). Saturated fatty acid palmitate-induced insulin resistance is accompanied with myotube loss and the impaired expression of health benefit myokine genes in C2C12 myotubes. <https://doi.org/10.1186/1476-511X-12-104>

Yang, Y., Liu, L., Naik, I., Braunstein, Z., Zhong, J., & Ren, B. (2017). Transcription factor C/EBP homologous protein in health and diseases. *Frontiers in Immunology*, 8(NOV), 1612. <https://doi.org/10.3389/FIMMU.2017.01612/BIBTEX>

Yin, L., Li, N., Jia, W., Wang, N., Liang, M., Yang, X., & Du, G. (2021). Skeletal muscle atrophy: From mechanisms to treatments. *Pharmacological Research*, 172(August). <https://doi.org/10.1016/j.phrs.2021.105807>

Yoneda, T., Imaizumi, K., Oono, K., Yui, D., Gomi, F., Katayama, T., & Tohyama, M. (2001). Activation of Caspase-12, an Endoplasmic Reticulum (ER) Resident Caspase,

- through Tumor Necrosis Factor Receptor-associated Factor 2-dependent Mechanism in Response to the ER Stress. *Journal of Biological Chemistry*, 276(17), 13935–13940. <https://doi.org/10.1074/jbc.M010677200>
- Yung, H. W., Charnock-Jones, D. S., & Burton, G. J. (2011). Regulation of AKT phosphorylation at Ser473 and Thr308 by endoplasmic reticulum stress modulates substrate specificity in a severity dependent manner. *PloS One*, 6(3). <https://doi.org/10.1371/JOURNAL.PONE.0017894>
- Zalckvar, E., Berissi, H., Mizrachi, L., Idelchuk, Y., Koren, I., Eisenstein, M., Sabanay, H., Pinkas-Kramarski, R., & Kimchi, A. (2009). DAP-kinase-mediated phosphorylation on the BH3 domain of beclin 1 promotes dissociation of beclin 1 from Bcl-XL and induction of autophagy. *EMBO Reports*, 10(3), 285. <https://doi.org/10.1038/EMBOR.2008.246>
- Zhang, K., Li, L., Qi, Y., Zhu, X., Gan, B., DePinho, R. A., Averitt, T., & Guo, S. (2012). Hepatic suppression of Foxo1 and Foxo3 causes hypoglycemia and hyperlipidemia in mice. *Endocrinology*, 153(2), 631–646. <https://doi.org/10.1210/en.2011-1527>
- Zhang, W., Hietakangas, V., Wee, S., Lim, S. C., Gunaratne, J., & Cohen, S. M. (2013). ER stress potentiates insulin resistance through PERK-mediated FOXO phosphorylation. *Genes and Development*, 27(4), 441–449. <https://doi.org/10.1101/gad.201731.112>
- Zismanov, V., Chichkov, V., Colangelo, V., Jamet, S., Wang, S., Syme, A., Koromilas, A. E., & Crist, C. (2016). Phosphorylation of eIF2 $\alpha$  Is a Translational Control Mechanism Regulating Muscle Stem Cell Quiescence and Self-Renewal. *Cell Stem Cell*, 18(1), 79–90. <https://doi.org/10.1016/J.STEM.2015.09.020>
- Zurlo, F., Larson, K., Bogardus, C., & Ravussin, E. (1990). Skeletal muscle metabolism is a major determinant of resting energy expenditure. *The Journal of Clinical Investigation*, 86(5), 1423–1427. <https://doi.org/10.1172/JCI114857>



# **Chapter 2**

**Effect of the selected flavones  
(Apigenin, Luteolin & Tangeretin) on  
ER stress induced redox imbalances  
in L6 cells**

## 2.1 Introduction

The development and progression of a number of skeletal muscle pathologies, including myositis, atrophy or muscle wasting, and diabetes, are influenced by ER stress and associated oxidative stress in skeletal muscle cells (Burgos-Morón et al., 2019; Rayavarapu et al., 2012). Skeletal muscles are the major protein reservoirs in the body accounting for 50% of total protein and hence susceptible to ER stress related perturbations (Yin et al., 2021). PDI-mediated disulfide bond formation is the major source of cellular ROS and it gets augmented in response to sustained ER stress. ER stress and ROS production are mutually reinforcing processes that can both start and intensify one another in a vicious cycle as depicted in Figure.2.1 (Ong & Logue, 2023). High ROS production impairs redox equilibrium and decreases antioxidant defense in cells, which is a precursor to several pathological conditions. Sustained ER stress triggers the maladaptive unfolded protein response (UPR) which leads to cellular dysfunction.

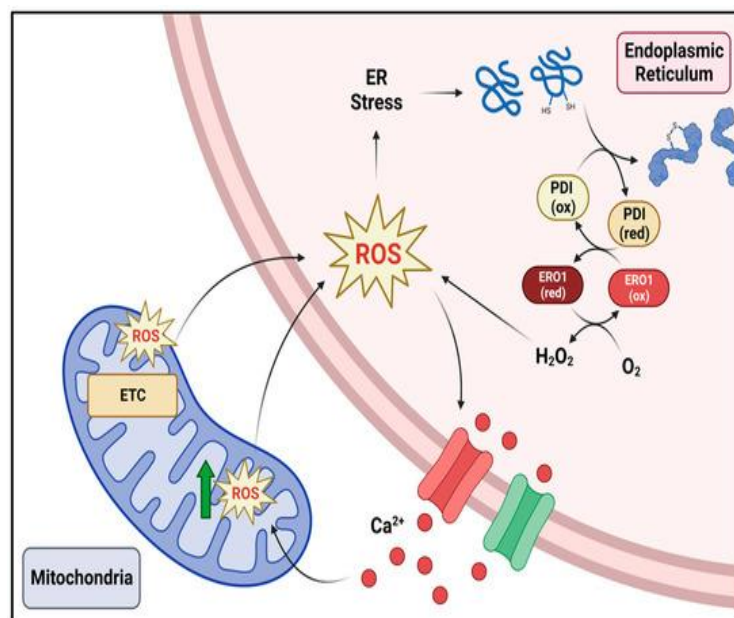


**Figure.2.1. Vicious cycle between ER stress and ROS generation (Ong & Logue, 2023)**

One of the major outcomes of chronic ER stress and oxidative stress in skeletal muscles is the loss of muscle mass (atrophy) due to the enhanced rate of protein degradation (Afroze & Kumar, 2019; Powers et al., 2012). Previous studies also suggest the involvement of insulin resistance in the muscle wasting or atrophy by suppressing the PI3K/Akt signaling which in turn enhances the degradation of muscle proteins (Wang et al., 2006). Studies have also reported the association of poor muscle quality, a consequence of imbalance between rate of protein synthesis and protein degradation with diabetic condition that may affect the daily activities, quality of living and increase risk of fatality (Ostler et al., 2014; Perry et al., 2016). Skeletal muscle mass loss is a serious pathological abnormality with no specific therapeutic strategy. The current treatment options include exercise, nutrient supplement and administration of androgen receptor modulators, ghrelin and anti-inflammatory drugs (Cheng et al., 2016). However, people who are bedridden or have severe symptoms may find it impossible to engage in exercise (Yin et al., 2021). Hence, treatment with medication is a crucial therapeutic strategy but a main drawback of this approach is the related side effects (Carstens & Schmidt, 2014; Oddis, 2016; Sartori et al., 2021).

Pharmacological treatment of ER stress and accompanying oxidative damage can help restore the health of the weakened skeletal muscles. This can be a better approach than the current treatment strategies of diabetes which only focus on improving the cellular outcomes of insulin resistance and insulin secretion impairment rather than focusing on improving the overall health of the targeted tissue. In the present study, the three selected flavones, apigenin, luteolin and tangeretin were analysed for their potential against ER stress mediated oxidative stress including ROS generation, antioxidant potential, protein expression of ER resident oxidoreductases, GADD153/CHOP and MAP kinases in

skeletal muscle L6 cells. For ER stress induction, tunicamycin, a chemical ER stress inducer was used (Osowski & Urano, 2013).

## **2.2 Materials & Methods**

### **2.2.1 Chemicals**

Dulbecco's modified Eagle's medium (4.5g/L glucose and 1.5g/L sodium bicarbonate) (DMEM), antimycotic antibiotic mix, fetal bovine serum, glycine, dimethyl sulfoxide (DMSO), sodium dodecyl sulphate, triton X, horse serum, skimmed milk, tris base, were purchased from Himedia (Mumbai, India). HPLC grade methanol, tangeritin, 4-phenyl butyric acid (PBA), tunicamycin, protease inhibitor cocktail tablets were bought from Sigma Aldrich Chemical (St. Louis Missouri, USA). Dichlorodihydrofluorescein diacetate (DCFH-DA), glutathione reductase (GR) assay kit, dihydroethidium (DHE) assay kit, superoxide dismutase (SOD) assay kit, annexin V FITC assay kit, thioredoxin reductase (TrxR) assay kit was purchased from Cayman Chemicals (Michigan, USA). Radioimmunoprecipitation assay (RIPA) buffer, 2-NBDG (2-(N-(7-Nitrobenz-2-oxa-1,3-diazol-4-yl) Amino)-2-Deoxyglucose), bicinchoninic acid assay kit (BCA kit) was purchased from Thermo Fisher Scientific (Waltham, Massachusetts, USA). The antibodies PDI, IRE-1 $\alpha$ , beta actin, GADD153, p38MAPK, HRP conjugated secondary antibodies were purchased from Cell Signaling Technologies (Danvers, Massachusetts, USA). Antibodies ATF6, GRP78, p-p38MAPK, p-JNK, JNK, ERK1/2 were purchased from Santa Cruz Biotechnology (Dallas, Texas, USA). ERp72 was purchased from Gbiosciences (St. Louis MO, USA). Rat skeletal muscle cell line, L6 myoblasts were procured from National Centre for Cell Sciences, Pune, India.

### **2.2.2 Cell Culture**

L6 myoblasts were cultured in DMEM containing 10% fetal bovine serum and 1% antibiotic antimycotic mix and kept in incubator at 37°C (5% carbon dioxide). When

myoblasts reached 80% confluency, the culture medium was removed and differentiation medium consisting of 2% horse serum was added to induce differentiation. The differentiation was induced for 4 days by giving alternative media change. All the experiments were performed in differentiated myotubes after the cell viability assays.

### 2.2.3 Experimental Groups

- **CON-** untreated or control cells
- **TM-** tunicamycin (0.25µg/ml) treated cells
- **TM+API-** tunicamycin (0.25µg/ml) & apigenin (20µM) co-treated cells
- **TM+LUT-** tunicamycin (0.25µg/ml) & luteolin (10µM) co-treated cells
- **TM+TAN-** tunicamycin (0.25µg/ml) & tangeretin (50µM) co-treated cells
- **TM+PBA-** tunicamycin (0.25µg/ml) & PBA (1mM) co-treated cells (Positive control)

### 2.2.4 Experimental design

The work flow of this chapter is depicted in Figure.2.2.

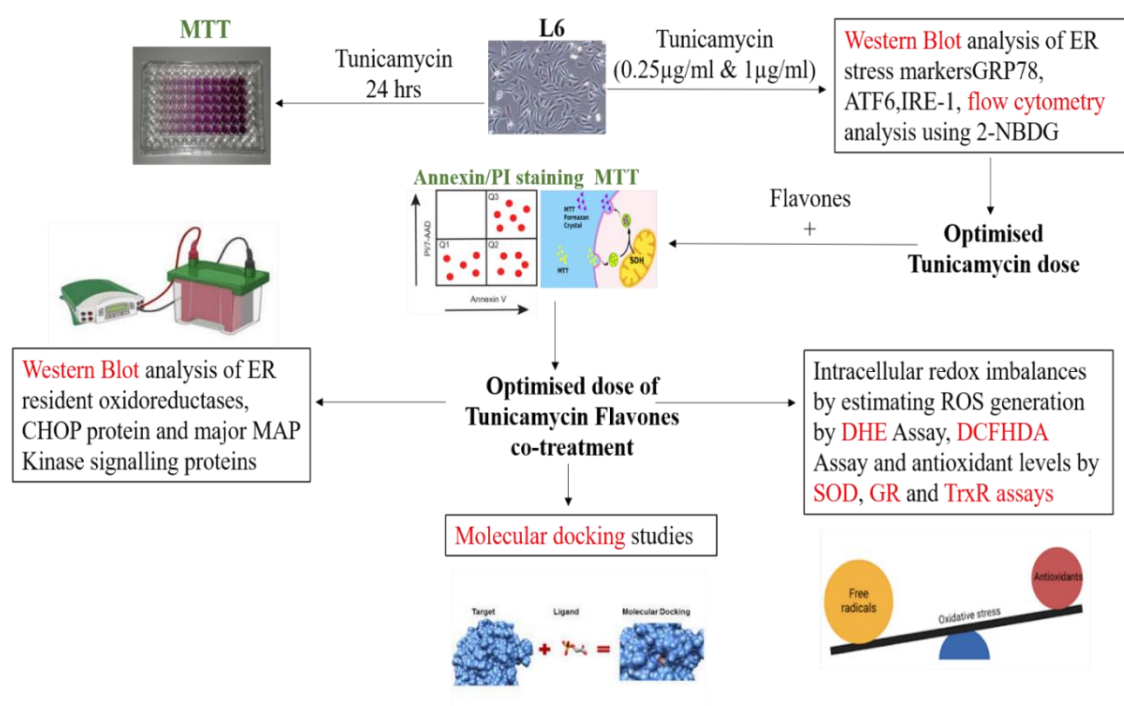


**Figure. 2.2. Schematic representation of experimental design**

## **2.2.5 Dose Optimization of tunicamycin**

### **2.2.5.1 Cytotoxicity studies**

Tunicamycin's cytotoxicity was assessed using the MTT assay (Mosmann 1983). Myoblasts were seeded at a density of  $5 \times 10^3$  cells per well in a 96-well plate. After becoming confluent, myoblasts were given different doses of tunicamycin (0.25  $\mu$ g/ml to 4  $\mu$ g/ml) for 24 hours. Cells were rinsed with HBSS following treatment, and incubated with MTT solution (0.5 mg/ml) dissolved in serum-free DMEM for 4 hours. After incubation, MTT solution was discarded and 100  $\mu$ L DMSO was added to each well. To ensure that the formazan crystals were completely dissolved, the plate was incubated on the shaker for 20 minutes and the absorbance was estimated at 570nm in multimode plate reader (Tecan infinite 200 PRO, Austria).

### **2.2.5.2 Western blot analysis for ER stress induction**

Myotubes were rinsed with HBSS following a 24-hour treatment with the appropriate doses of tunicamycin, and then proteins were extracted using RIPA lysis buffer. The BCA assay kit was used to quantitate and normalise the protein samples using bovine serum albumin (BSA) as the standard. Protein samples were separated on 10% sodium dodecyl sulphate polyacrylamide gels. Proteins were then transferred onto PVDF membranes (Millipore, Merck, USA) and blocking in skimmed milk (5%) was carried out for 1 hour. Membranes were given TBST wash thrice followed by incubation with the appropriate primary antibodies (dilution 1:1000) for ER stress markers such as GRP78, ATF6, and IRE-1 $\alpha$  at 4°C with overnight agitation. The loading control used was beta actin (dilution 1:1000). After that, membranes were incubated with the proper dilution (1:1000 to 1:2000) of HRP-conjugated secondary antibodies for 2 to 3 hours at room temperature. The blot images were obtained by adding the ECL substrate (Thermo Fisher Scientific,

Massachusetts, USA) to the membranes in Chemidoc MP Imaging systems (Bio-Rad, USA). The resultant bands were quantified by densitometric analysis using the Image lab software version 6.1 (Bio-Rad, USA).

### **2.2.5.3 Flow cytometry analysis for insulin resistance**

The ER stress induced insulin resistance was determined by treating the cells with the appropriate doses of tunicamycin for 24 hours followed by stimulation with 100 nmol insulin for 30 minutes. The cells were then incubated with 2-NBDG, a fluorescent glucose analog for 30 minutes followed by estimation of the percentage of 2-NBDG uptake by flow cytometry analysis using BD FACS Aria II (BD Biosciences).

## **2.2.6 Dose optimization of Flavones**

### **2.2.6.1 Cytotoxicity studies**

Myoblasts were seeded in 96 well plate at a density of  $5 \times 10^3$  cells per well. After becoming confluent, cells were given different concentrations (10 $\mu$ M to 100 $\mu$ M) of selected flavones, apigenin, luteolin and tangeretin for 24 hours and MTT assay was performed (please refer to Section 2.2.5.1). The doses of the flavones, apigenin, luteolin and tangeretin for co-treatment with tunicamycin was also determined. For this, the cells were treated with the different doses (10 $\mu$ M to 100 $\mu$ M) of the flavones, apigenin, luteolin and tangeretin in the presence of the optimised dose of tunicamycin for 24 hours followed by MTT assay. The absorbance was estimated by reading the plate at 570nm in multimode plate reader (Tecan infinite 200 PRO, Austria).

### **2.2.6.2 Annexin V FITC Staining**

After a 24-hour treatment with the experimental groups, myotubes were collected by centrifugation and stained with Annexin V FITC/Propidium iodide staining solution for

10 minutes according to the manufacturer's protocol. This was followed by the addition of 150µl 1X binding buffer to the cells and immediate analysis by flow cytometry.

### **2.2.7 Detection of intracellular ROS generation by DHE assay and DCFH-DA assay**

L6 myoblasts were seeded at a density of  $5 \times 10^3$  in 96 black well plate. After differentiation, myotubes were subjected to treatment with the experimental groups for 24 hours. The positive control used for all experiments was PBA (1mM), a chemical chaperone approved by the FDA. After the treatment, cells were evaluated in accordance with the manufacturer's instructions (Cayman chemicals, USA). DHE staining solution was added to myotubes for 1.5 hours at 37°C in dark conditions. After this, the DHE solution was replaced with 100µl cell-based assay buffer in each well. Fluorescence intensity was estimated using a multimode plate reader (Tecan infinite 200 PRO, Austria) at an excitation and emission wavelength of 480-520nm and 570-600nm, respectively.

Alternatively, myotubes were treated with a 10µM DCFH-DA staining solution for 20 minutes following a 24-hour co-treatment. After that, cells were rinsed with HBSS and covered with 100µl plain DMEM. Fluorescence images were then acquired in fluorescence microscope and the cell sense software (Olympus Life Science, Japan) was used to measure the fluorescence intensity.

### **2.2.8 Antioxidant enzyme activity during ER stress**

#### **2.2.8.1 SOD activity**

Cellular SOD levels were measured in accordance with the manufacturer's protocol (Cayman chemicals, USA). After 24 hours treatment with the experimental groups, myotubes were centrifuged at 1000×g for 5 minutes at 4°C. The cell pellets were then homogenised in 20mM cold HEPES buffer (pH 7.2). The samples were then centrifuged at 1,500×g for 5 minutes at 4°C and the supernatant was collected. To 10µl supernatant



sample, 200µl radical detector was added. To start the reaction, 20µl xanthine oxidase was added to each well. The absorbance was determined at 440 nm in a multimode plate reader (Tecan infinite 200 PRO, Austria) following a 30-minute incubation period at room temperature.

#### **2.2.8.2 GR activity**

GR activity was determined according to the manufacturer's instructions (Cayman chemicals, USA). GR mediated rate of oxidation of NADPH to NADP<sup>+</sup> was measured and this was indicated by a decrease in absorbance. After a 24-hour treatment period, myotubes were homogenised in ice cold 50mM potassium phosphate buffer containing 1mM EDTA (pH 7.5) and centrifuged at 10000×g for 15 minutes at 4°C. Sample supernatants belonging to the different experimental groups were collected and analysed. The reaction was triggered by adding NADPH (50µl) to assay mix in wells containing sample supernatant (20µl), assay buffer (100µl) and GSSG (20µl). Absorbance was kinetically read at 340nm (Tecan infinite 200 PRO, Austria) at an interval of 1 minute for 5 timepoints.

#### **2.2.8.3 TrxR activity**

TrxR activity was determined in accordance with the manufacturer's protocol (Cayman chemicals, USA). Myotubes were obtained by centrifugation at 1000×g for 5 minutes after a 24-hour co-treatment, and homogenisation of cell pellets was carried out in cold buffer (50mM potassium phosphate buffer, pH 7.4, containing 1mM EDTA). Centrifugation at 10000×g for 15 minutes at 4°C was then performed. By adding NADPH and 5,5'-dithio-bis (2-dinitro benzoic acid) (DTNB) to an assay mixture comprising diluted assay buffer (140µl) and sample supernatants (20µl), the TrxR activity of the supernatants was measured. To acquire 5 timepoints, kinetic readings of the absorbance

at 405 nm were made at intervals of 1 minute in multimode plate reader (Tecan infinite 200 PRO, Austria).

### **2.2.9 Molecular Docking Studies**

To determine the antioxidant potential of the selected flavones, molecular docking was performed using the autodock 1.5.6 software to study the binding interaction of the flavones with different antioxidant enzymes, namely, catalase, glutathione peroxidase, superoxide dismutase1 (SOD1) and superoxide dismutase 2 (SOD2). Initially, the three-dimensional structures of Catalase (PDB ID: **1DGB**), Glutathione peroxidase (PDB ID: **2F8A**), SOD1 (PDB ID: **1CB4**), SOD2 (PDB ID: **1AP5**) were retrieved from Protein Data Bank and structures of apigenin (CID: 5280443), luteolin (CID: 5280445) and tangeretin (CID: 68077) were obtained from PubChem database. The protein ligand interaction was optimised using the pyMol software.

### **2.2.10 Western Blot**

To investigate the expression of proteins connected to ER stress and oxidative damage, western blotting was used. Myotubes, after a 24-hour treatment with the experimental groups were lysed for protein extraction. The sample proteins were then taken for western blot analysis as described in Section 2.2.5.2. The proteins studied included PDI, ERp72, GADD153, p38MAP kinase, p-p38MAP kinase, ERK1/2, p-JNK, JNK and beta actin.

### **2.2.11 Statistical analysis**

Three independent triplicate runs of each experiment were performed. In SPSS software, all data were statistically analysed using one-way ANOVA and the Duncan post hoc test. Every result is shown as a mean $\pm$ SEM. A p value  $\leq$  0.05 was considered statistically significant in each experiment.

## 2.3 Results

### 2.3.1 Optimization of tunicamycin dose

#### 2.3.1.1 Cytotoxicity studies

Cells were cultured with several doses (0.25 $\mu$ g/ml to 4 $\mu$ g/ml) of tunicamycin for a total of 24 hours in order to determine the optimal dose for our investigation. Viable concentrations were those that produced less than 20% toxicity. Less than 20% cytotoxicity was reported to be induced by tunicamycin up to 1 $\mu$ g/ml as shown in Figure.

2.3.

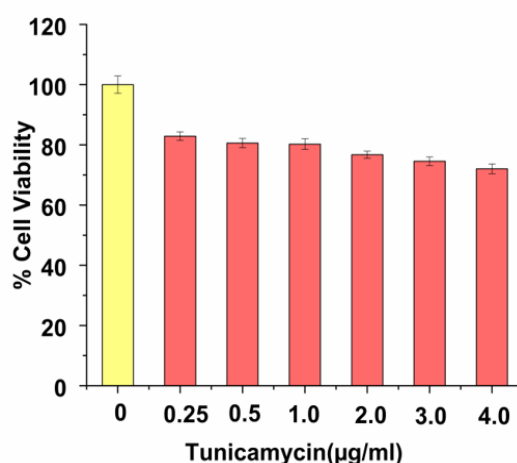


**Figure.2.3. Cytotoxicity studies of tunicamycin.** L6 cells were treated with different concentrations of tunicamycin (0.25 $\mu$ g/ml to 4 $\mu$ g/ml) for 24 hours. Values are expressed as mean $\pm$ SEM where n=3.

#### 2.3.1.2 Western blot analysis for upregulation of ER stress markers

Chronic tunicamycin exposure increases the expression of the ER stress markers GRP78, IRE-1 $\alpha$  and ATF6; these levels were considerably higher when treated with both doses of tunicamycin (highest viable dose of 1 $\mu$ g/ml and lowest dose of 0.25 $\mu$ g/ml) compared

to control cells as shown in Figure.2.4a, b. Tunicamycin treatment increased the GRP78 expression to 359.9% and 314.8%, at concentrations of 0.25 $\mu$ g/ml and 1.0 $\mu$ g/ml respectively (Figure.2.4a, b). Exposure to both doses of tunicamycin upregulated the IRE-1 $\alpha$  expression (176.9% with 0.25 $\mu$ g/ml and 173.1% with 1.0 $\mu$ g/ml) (Figure.2.4a, b). After treatment with both doses of tunicamycin, the active cleaved form of ATF6 was also expressed, reaching 125.4% and 131.9% for 0.25 $\mu$ g/ml and 1 $\mu$ g/ml, respectively (Figure.2.4a, b).

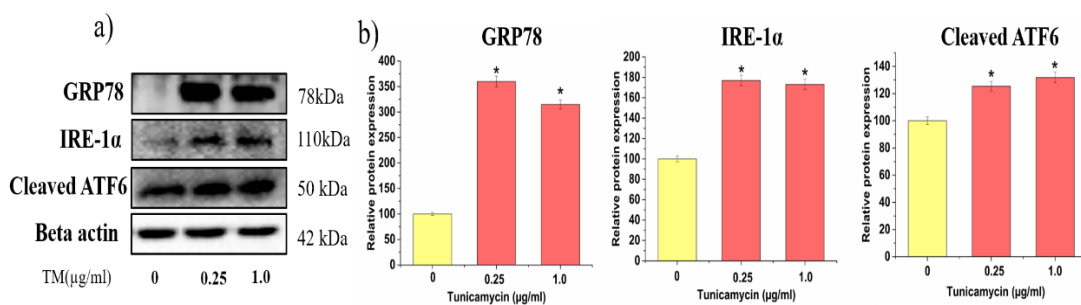


**Figure.2.4. Optimization of tunicamycin dose for ER stress induction.** a) After treating L6 myotubes with 0.25 $\mu$ g/ml and 1.0 $\mu$ g/ml tunicamycin respectively for 24 hours. ER stress markers, GRP78, IRE-1 $\alpha$  and cleaved ATF6 were analysed using western blot. The loading control was beta actin. b) Densitometric analysis of the proteins normalised to beta actin. Values are expressed as mean $\pm$ SEM where n=3. \*p $\leq$ 0.05 significantly different from control cells.

### 2.3.1.3 Determination of ER stress induced insulin resistance

The ER stress induced insulin resistance was determined by the 2-NBDG uptake flow cytometry analysis. In untreated cells, the uptake was recorded as 37.6% as seen in Figure.2.5. On treatment with the lower dose of tunicamycin (0.25 $\mu$ g/ml), the uptake diminished to 21% and on treatment with the highest viable dose of tunicamycin, the uptake was recorded as 24.3% (Figure.2.5). From the results, it was observed that the

lower dose of tunicamycin, 0.25 $\mu$ g/ml was sufficient for induction of ER stress as well as insulin resistance for a period of 24 hours without inducing significant cytotoxicity in L6 cells, therefore, this concentration was chosen for all subsequent experiments.

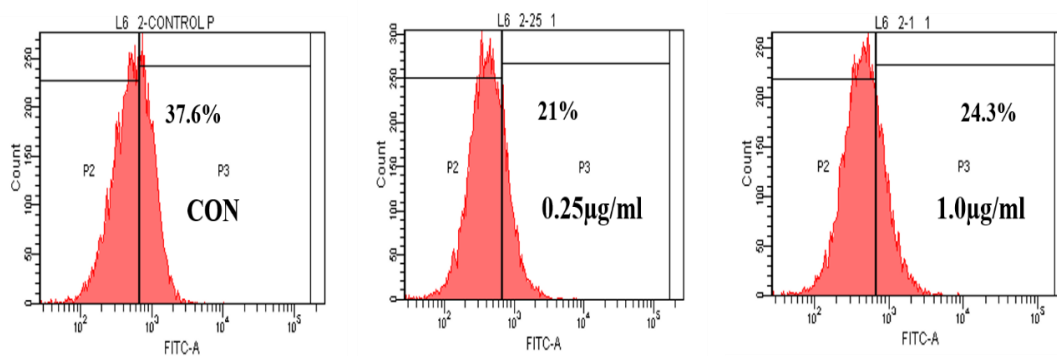


**Figure.2.5. Dose optimization of tunicamycin for induction of insulin resistance.** L6 myotubes were treated with 0.25 $\mu$ g/ml and 1 $\mu$ g/ml tunicamycin respectively for 24 hours followed by 100nmol insulin stimulation for 30 min. Cells were then incubated with 2-NBDG for 30min and then taken for flow cytometry analysis. CON-untreated cells, 0.25 $\mu$ g/ml-0.25 $\mu$ g/ml tunicamycin, 1 $\mu$ g/ml-1 $\mu$ g/ml tunicamycin. Values are expressed as mean $\pm$ SEM where n=3. \*p $\leq$ 0.05 significantly different from control cells.

### 2.3.2 Optimization of dose of flavones

#### 2.3.2.1 Cytotoxicity studies

Cytotoxicity of the selected flavones, apigenin, luteolin and tangeretin was determined by the MTT assay by treating cells with different concentrations (10 $\mu$ M to 100 $\mu$ M) for 24 hours. Concentrations that induced less than 20% cytotoxicity were considered viable doses and hence, cells were found to be viable upto 50 $\mu$ M apigenin, 10 $\mu$ M luteolin and 100 $\mu$ M tangeretin (Figure.2.6a, b, c). Cytotoxicity of the flavones in the presence of tunicamycin was evaluated by treating cells with different concentrations (10 $\mu$ M to 100 $\mu$ M) of apigenin, luteolin and tangeretin respectively along with 0.25 $\mu$ g/ml

tunicamycin for 24 hours. Cells were found to be viable upto 20 $\mu$ M apigenin, 10 $\mu$ M luteolin and 50 $\mu$ M tangeretin upon co-treatment with optimized dose of tunicamycin. Based on the results of MTT assay, 20 $\mu$ M apigenin, 10 $\mu$ M luteolin and 50 $\mu$ M tangeretin were selected for co-treatment studies as shown in Figure.2.6d, e, f.

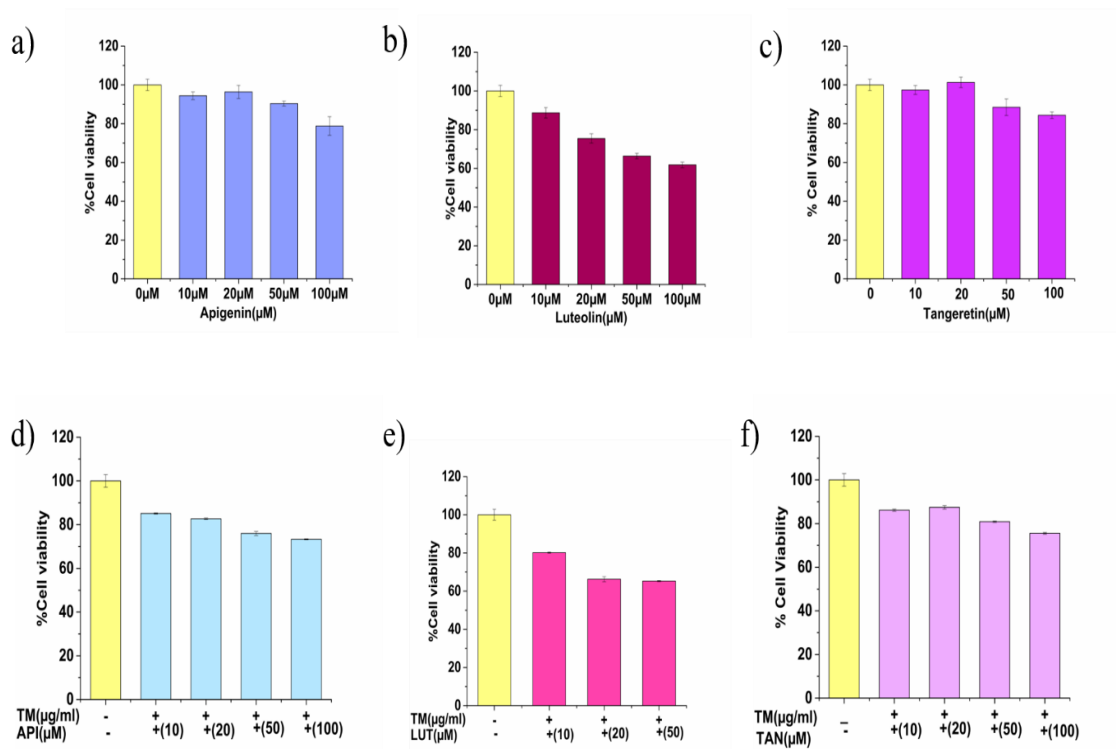


**Figure.2.6. Cytotoxicity studies of selected flavones.** L6 cells treated with different concentrations of a) apigenin (10 $\mu$ M to 100 $\mu$ M), b) luteolin (10 $\mu$ M to 100 $\mu$ M), c) tangeretin (10 $\mu$ M to 100 $\mu$ M) followed by MTT assay. L6 cells treated in the presence of 0.25 $\mu$ g/ml tunicamycin with different concentrations of d) apigenin (10 $\mu$ M to 100 $\mu$ M), e) luteolin (10 $\mu$ M to 50 $\mu$ M), f) tangeretin (10 $\mu$ M to 100 $\mu$ M) and subjected to MTT assay. Values are expressed as mean $\pm$ SEM where n=3.

### 2.3.2.2 Annexin V FITC assay

To further confirm the low cytotoxicity of the co-treatment doses, Annexin V FITC/ PI staining assay was performed. Based on variations in plasma membrane integrity and permeability, the annexin V FITC/PI labelling analyses cellular viability, apoptosis, and necrosis (Rieger et al., 2011). The representative graphs consist of four quadrants namely, Q1, Q2, Q3 and Q4 where Q1 indicates percentage of necrotic cells, Q2 indicates late apoptosis, Q3 indicates the percentage of live/viable cells, Q4 indicates early apoptosis. Here, most of the cells were seen in Q3 quadrant indicating cellular viability. In untreated cells, percentage of live cells was 99.9% while in cells treated with tunicamycin, it was 86.1%; in apigenin co-treated cells, it was 88.5%; in luteolin co-treated cells, it was 91.4%; in tangeretin co-treated cells it was 93%; in PBA co-treated cells, it was 90.2% (Figure.2.7). In all experimental groups, the percentage toxicity was below 20% indicating the low cytotoxicity of the co-treatment doses.

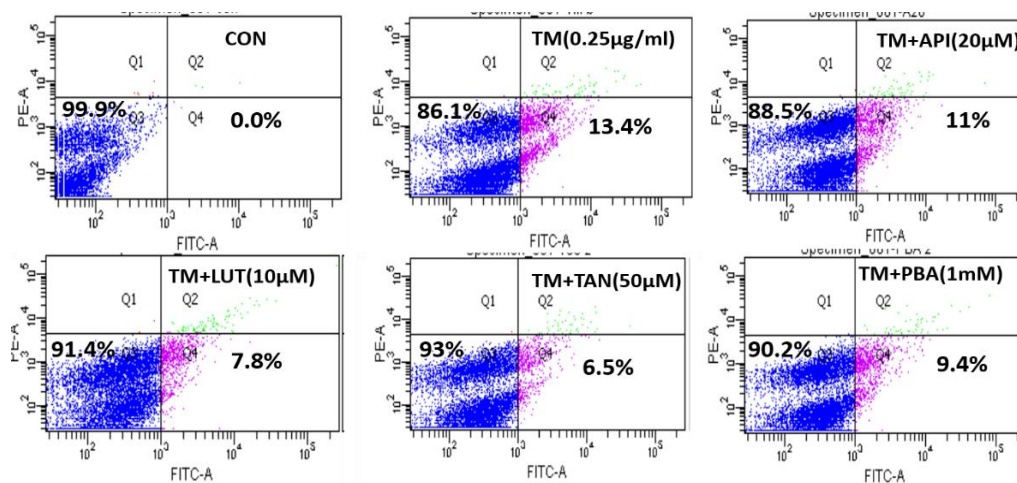


**Figure.2.7. Annexin V FITC assay.** L6 myotubes treated with selected flavones in presence of 0.25µg/ml tunicamycin and taken for flow cytometry analysis after staining with annexin V/PI. Representative flow cytometry images show four quadrants, Q1 indicating necrotic cells, Q2 indicating late apoptosis, Q3 indicating live cells, Q4 indicating early apoptosis. CON-untreated cells, TM-0.25µg/ml tunicamycin treated cells, TM+API- 0.25µg/ml tunicamycin apigenin (20µM) co-treated, TM+LUT-0.25µg/ml tunicamycin luteolin (10µM) co-treated, TM+TAN-0.25µg/ml tangeretin (50µM) co-treated, TM+PBA-0.25µg/ml tunicamycin PBA (1mM) co-treated cells.

### **2.3.3 Effect of flavones on tunicamycin induced intracellular ROS generation**

Reactive oxygen species are produced as a result of oxidative damage caused by ER stress. Tunicamycin induced ROS production was determined by the DCFH-DA and DHE assays. In tunicamycin treated cells, there was a significant increase in ROS generation to 14413.02 a.u. (arbitrary units) compared to the untreated cells (5989.79 a.u.) on incubation with DCFH-DA dye as evident from the fluorescence images in Figure.2.8a and fluorescence intensity histogram in Figure.2.8b. Apigenin decreased the ROS levels to 11008.78 a.u. but it was not significant. Co-treatment with luteolin remarkably reduced the ROS levels to 6375.03a.u. compared to tunicamycin treated cells. Co-treatment with tangeretin significantly lowered the ROS levels to 8284.019a.u. whereas PBA suppressed the ROS levels to 9501.8014a.u. compared to tunicamycin treated cells (Figure.2.8b). The cellular ROS generation under ER stress was also determined by the DHE assay where DHE served as a fluorescent probe for estimation of cellular ROS levels. Cells treated with tunicamycin showed an increase in intracellular ROS generation (1203.67 a.u.) compared to the control cells (737.33 a.u.) as shown in fluorescence intensity graph in Figure.2.8c. Co-treatment with apigenin did not significantly suppress the ROS levels (1070.33 a.u.). Luteolin and tangeretin significantly suppressed the ROS levels to 876.66 a.u. and 785 a.u. respectively while PBA co-treatment brought down the ROS levels to 840 a.u. compared to the tunicamycin treated cells as seen in Figure.2.8c.



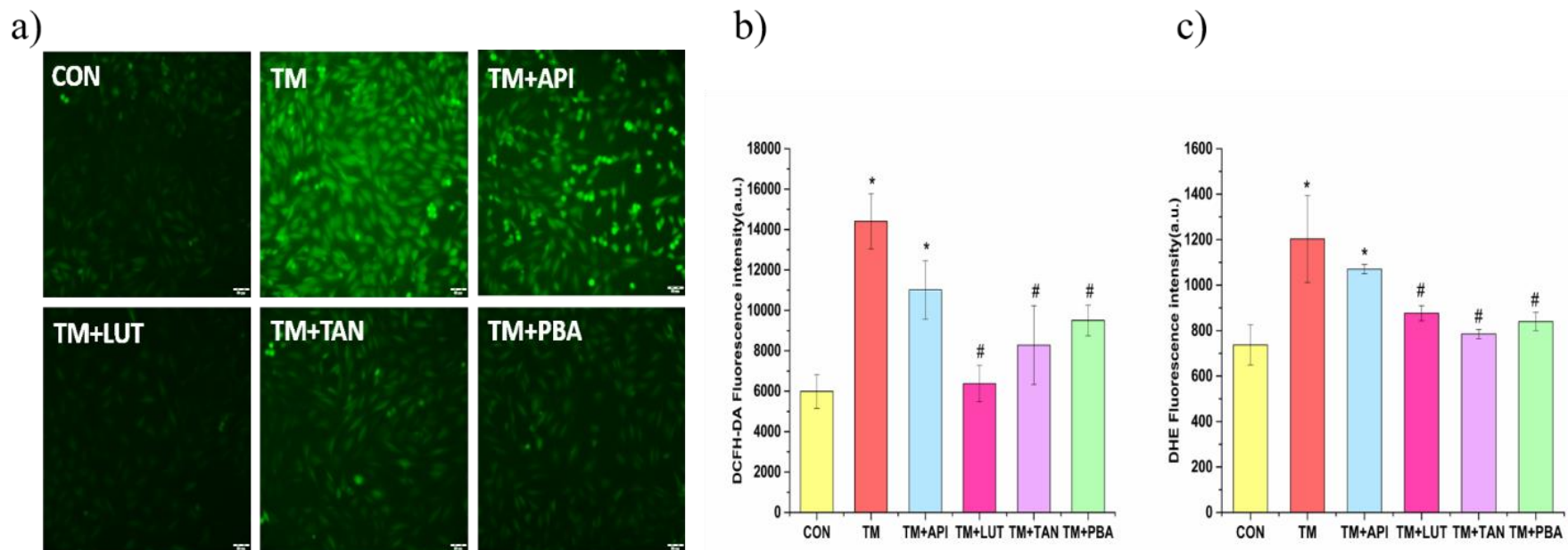


**Figure.2.8. Effect of flavones on tunicamycin induced intracellular ROS generation.** L6 myotubes were treated with selected flavones in presence of tunicamycin. This was followed by DCFH-DA staining. a) Fluorescence images indicative of ROS generated. Magnification 20X. Scale corresponds to 50 $\mu$ m. b) Intensity histogram of fluorescence. c) DHE assay indicative of ROS levels. CON-untreated cells, TM-0.25 $\mu$ g/ml tunicamycin treated cells, TM+API-0.25 $\mu$ g/ml tunicamycin apigenin (20 $\mu$ M) co-treated, TM+LUT-0.25 $\mu$ g/ml tunicamycin luteolin (10 $\mu$ M) co-treated, TM+TAN-0.25 $\mu$ g/ml tangeretin (50 $\mu$ M) co-treated, TM+PBA-0.25 $\mu$ g/ml tunicamycin PBA (1mM) co-treated cells. Values are expressed as mean $\pm$ SEM where n=3. \* $p\leq 0.05$  significantly different from control cells, # $p\leq 0.05$  significantly different from tunicamycin treated cells.

### **2.3.4 Antioxidant potential of flavones under ER stress**

Oxidative stress is accompanied by concomitant decrease in innate antioxidant status resulting in disruption of redox homeostasis. Here, the effect of ER stress on antioxidants, SOD, GR and TrxR was studied. In tunicamycin treated cells SOD activity significantly decreased to 37.2% compared to the control (Figure.2.9a). Treatment with apigenin improved the SOD activity to 84.4%, luteolin improved the activity to 56.22%, tangeretin improved the SOD activity to 69.3% while PBA improved the activity to 68.4% significantly compared to tunicamycin treated cells (Figure.2.9a). Treatment with tunicamycin, reduced the GR activity by 29.3 % (5.66nmol/min/ml) compared to the control cells (8.01nmol/min/ml) whereas treatment with apigenin increased the activity by 45.82% (9.327nmol/min/ml), luteolin increased the GR levels by 21.06% (7.344nmol/min/ml), tangeretin remarkably improved the same by 62 % (10.623nmol/min/ml) and PBA improved the GR activity by 22.6 % (7.473nmol/min/ml) compared to the tunicamycin treated cells as depicted in Figure.2.9b. In cells treated with tunicamycin, TrxR activity was significantly increased to 211.62% as compared to the control group. Apigenin reduced the enzyme levels to 98.01%, luteolin decreased the levels to 128.9%. TrxR levels were decreased to 90.5% on treatment with tangeretin while on treatment with PBA it decreased to 175.7% as compared to tunicamycin treated cells (Figure.2.9c).

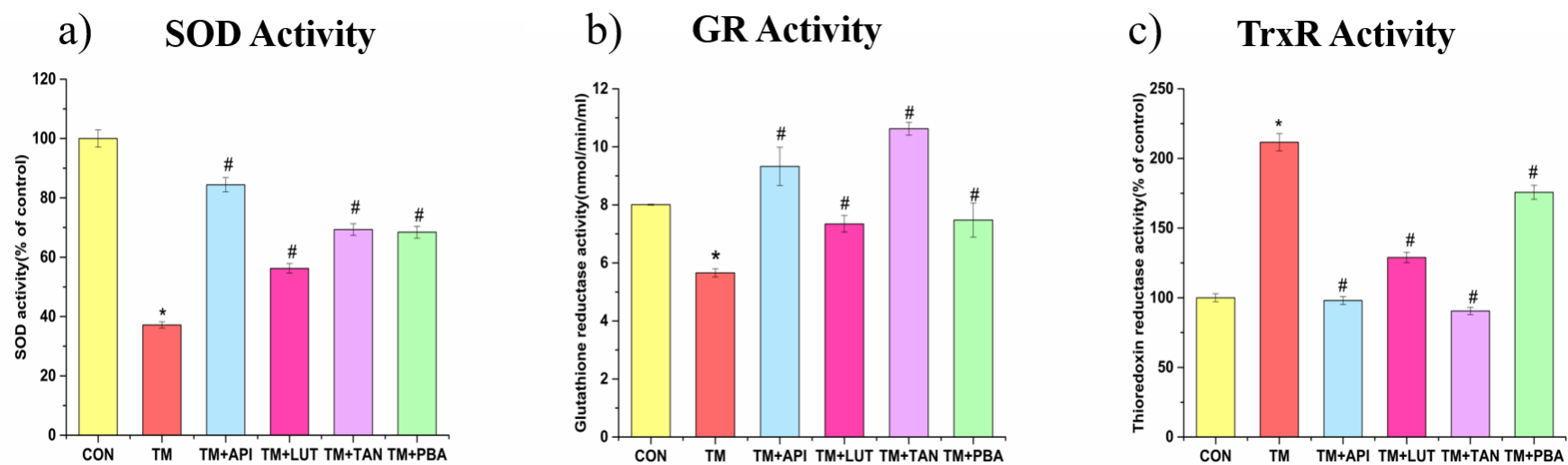


**Figure.2.9. Antioxidant potential of flavones under ER stress.** Effect of apigenin, luteolin and tangeretin on a) SOD activity, b) GR activity, c) TrxR activity during ER stress was analysed. CON-untreated cells, TM-0.25 $\mu$ g/ml tunicamycin treated cells, TM+API- 0.25 $\mu$ g/ml tunicamycin apigenin (20 $\mu$ M) co-treated, TM+LUT-0.25 $\mu$ g/ml tunicamycin luteolin (10 $\mu$ M) co-treated, TM+TAN-0.25 $\mu$ g/ml tangeretin (50 $\mu$ M) co-treated, TM+PBA-0.25 $\mu$ g/ml tunicamycin PBA (1mM) co-treated cells. Values are expressed as mean $\pm$ SEM where n=3. \*p $\leq$ 0.05 significantly different from control cells, #p $\leq$ 0.05 significantly different from tunicamycin treated cells.

### 2.3.4.1 Structural interaction of flavones with antioxidant enzymes

To confirm the antioxidant potential of the selected flavones, docking studies of flavones with antioxidant enzymes such as catalase, glutathione peroxidase, SOD1 and SOD2 was performed to determine the binding interactions. The binding energies indicate the strong interaction of the flavones with the antioxidant enzymes (Table 2.1). The best conformation of the ligand (flavone) protein (antioxidant) interaction is represented in Figure.2.10a, b, c.

**Table 2.1: The binding energies of the docked structures**

Protein	Ligand	Binding energy in Kcal/mol
Catalase (PDB ID: 1DGB)	Apigenin	-7.28
	Luteolin	-5.95
	Tangeretin	-5.68
Glutathione peroxidase (PDB ID: 2F8A)	Apigenin	-5.29
	Luteolin	-4.79
	Tangeretin	-6.1
Superoxide Dismutase 1 (PDB ID:1CB4)	Apigenin	-6.29
	Luteolin	-6.16
	Tangeretin	-5.42
Superoxide Dismutase 2 (PDB ID: 1AP5)	Apigenin	-5.69
	Luteolin	-5.39
	Tangeretin	-5.04

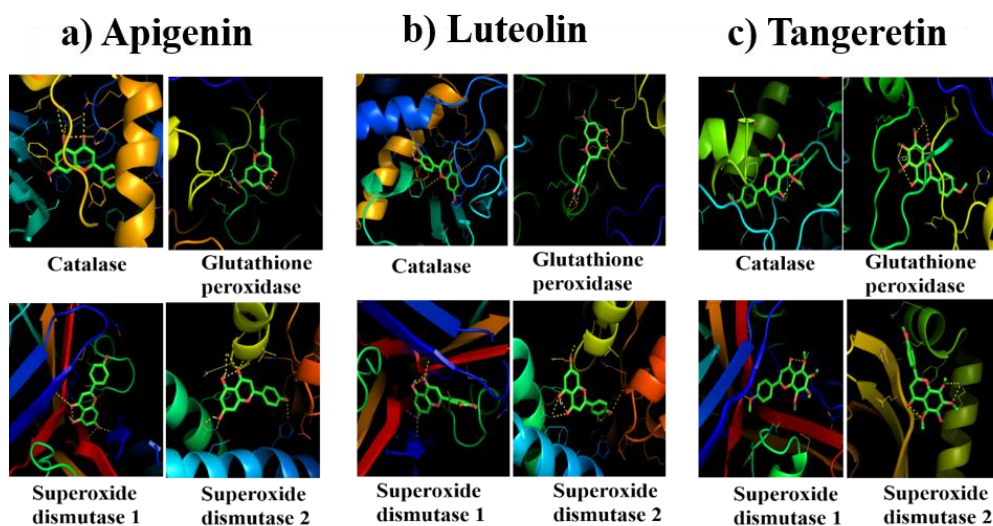


**Figure.2.10. Molecular docking.** a) Docked structures of apigenin with catalase, glutathione peroxidase, SOD1 and SOD2. b) Docked structures of luteolin with catalase, glutathione peroxidase, SOD1 and SOD2, c) Docked structures of tangeretin with catalase, glutathione peroxidase, SOD1 and SOD2.

### 2.3.5 Selected flavones decrease ER resident oxidoreductases, PDI and ERp72 under ER stress

Under ER stress condition, the ER resident oxidoreductases are upregulated to enhance the reduction of misfolded proteins which in turn generates excess ROS as byproducts. The protein expression studies for the flavones were carried out independently and in different experimental sets. In the first set of experiment, the tunicamycin treatment significantly upregulated the PDI and ERp72 levels to 119.1% and 126.11% respectively compared to the control cells as observed in Figure.2.11a. Apigenin downregulated the PDI levels and ERp72 levels to 108.6% and 114.1% while PBA decreased the PDI levels to 91.3% and ERp72 levels to 110.24% respectively compared to tunicamycin treated cells (Figure.2.11a). In the second set as shown in Figure.2.11b, on treatment with tunicamycin, PDI and ERp72 levels were increased to 141.5% and 199.5% respectively compared to the control cells. Luteolin significantly reduced the PDI and ERp72 levels

to 93.75% and 135.9% while PBA downregulated the PDI levels to 84.6% and ERp72 levels to 98.4% respectively compared to tunicamycin treated cells (Figure.2.11b). In the third set, tunicamycin upregulated the PDI and ERp72 levels to 126% and 145.7% respectively compared to control cells. Tangeretin remarkably downregulated the PDI and ERp72 levels to 99.8% and 129.9% respectively while PBA reduced the levels of PDI to 92.5% and ERp72 levels to 109.7% compared to tunicamycin treated cells as shown in Figure.2.11c.

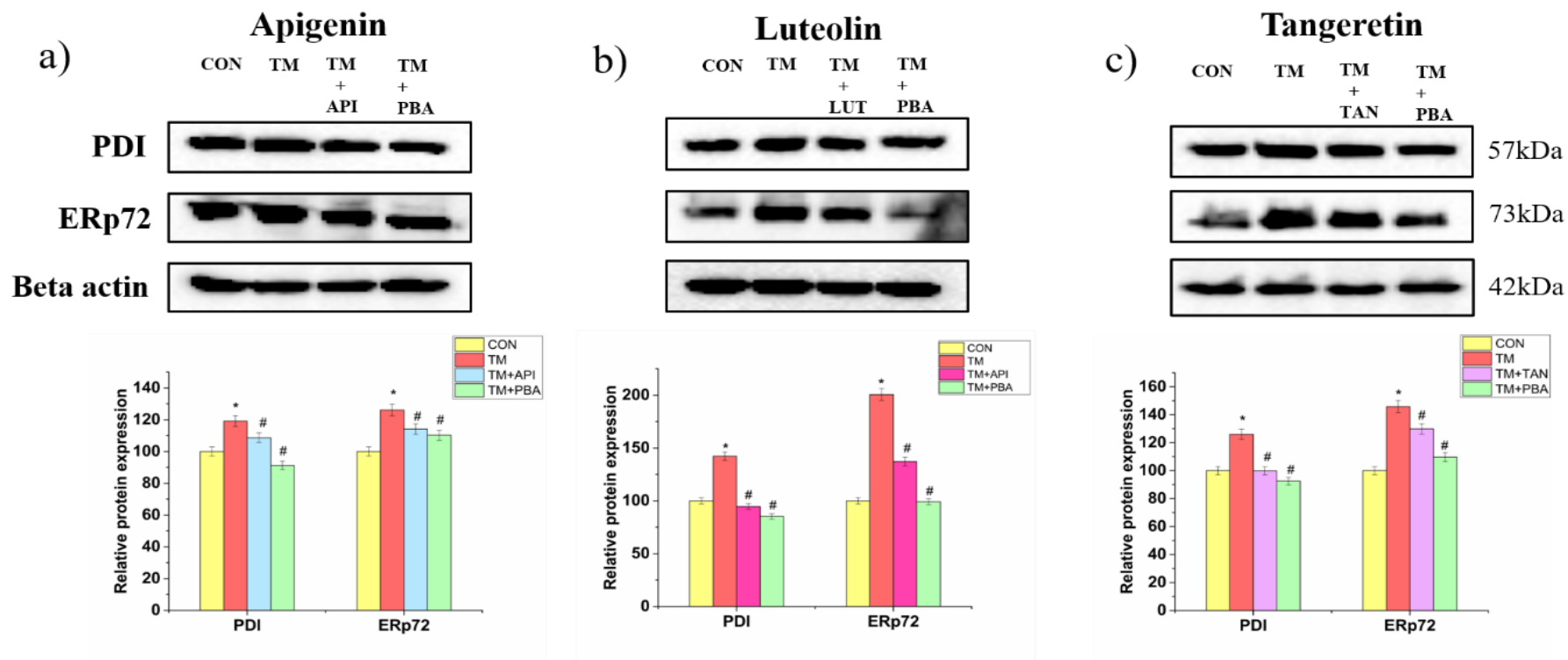


**Figure.2.11. Protein expression studies of ER resident oxidoreductases, PDI & ERp72.** Western blot and densitometric analysis of proteins on treatment with a) apigenin, b) luteolin, c) tangeretin under ER stress condition with beta actin as loading control. CON-untreated cells, TM-0.25 $\mu$ g/ml tunicamycin treated cells, TM+API- 0.25 $\mu$ g/ml tunicamycin apigenin (20 $\mu$ M) co-treated, TM+LUT-0.25 $\mu$ g/ml tunicamycin luteolin (10 $\mu$ M) co-treated, TM+TAN-0.25 $\mu$ g/ml tangeretin (50 $\mu$ M) co-treated, TM+PBA-0.25 $\mu$ g/ml tunicamycin PBA (1mM) co-treated cells. Values are expressed as mean $\pm$ SEM where n=3. \*p $\leq$ 0.05 significantly different from control treated cells, #p $\leq$ 0.05 significantly different from tunicamycin treated cells.

### **2.3.6 Modulation of GADD153/CHOP protein by selected flavones under ER stress**

GADD153 or CHOP is an indicator of maladaptive UPR and subsequent cellular dysfunction. The protein expression study was carried out independently for the flavones (Figure.2.12a, b, c). In the first set, tunicamycin significantly increased the GADD153 expression to 131.5% compared to the control cells. In apigenin treated cells, GADD153 expression was 135.4% while in PBA treated cells, the protein expression decreased to 99.7% compared to tunicamycin treated cells (Figure.2.12a). In the second set, tunicamycin upregulated the GADD153 expression to 156.7% compared to the control cells. Luteolin remarkably decreased the GADD153 levels to 116.6% whereas PBA treatment reduced the levels to 105.7% compared to tunicamycin treated cells (Figure.2.12b). In the third set, GADD153 expression increased to 264.9% in tunicamycin treated cells compared to the control cells. Tangeretin treatment remarkably suppressed the levels to 91.2% while PBA treatment decreased the levels to 168.6% compared to the tunicamycin treated cells (Figure.2.12c).



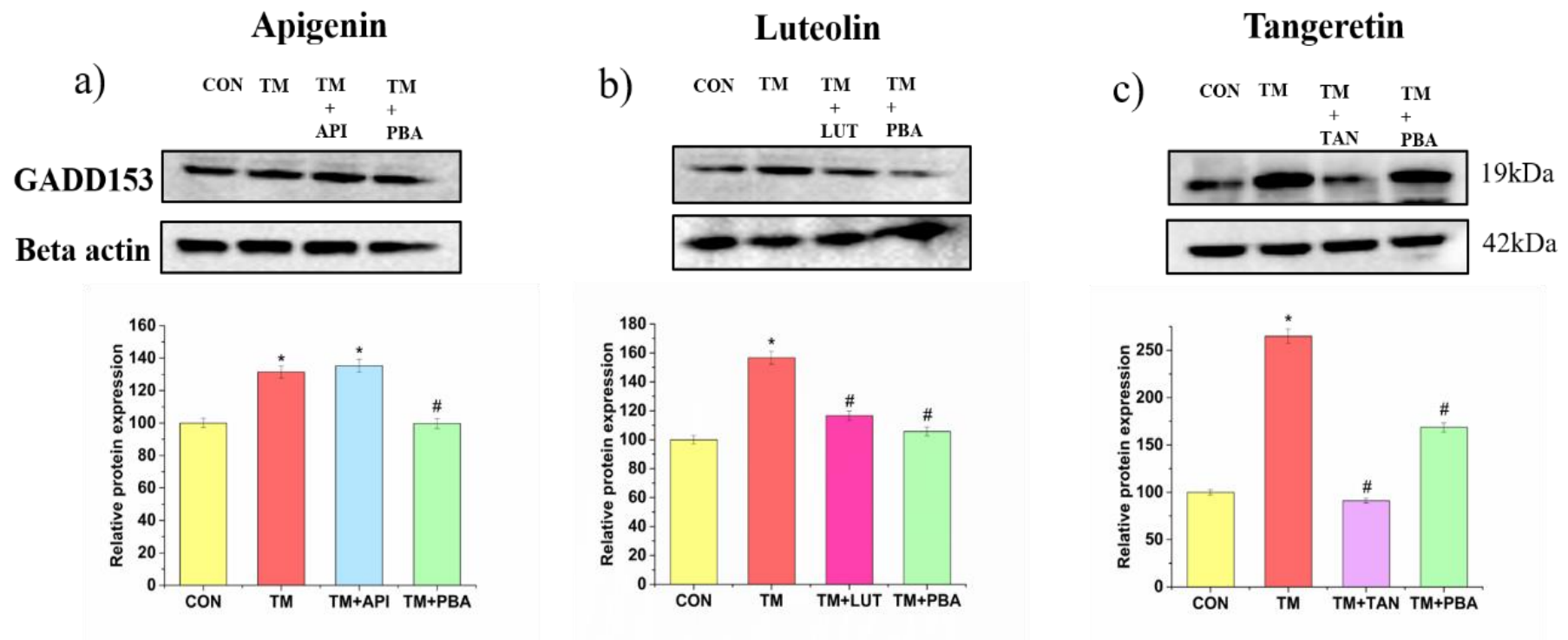


**Figure.2.12. Protein expression of GADD153/CHOP.** Western blot and densitometric analysis of GADD153 on treatment with a) apigenin, b) luteolin, c) tangeretin under ER stress condition with beta actin as loading control. CON-untreated cells, TM-0.25 $\mu$ g/ml tunicamycin treated cells, TM+API- 0.25 $\mu$ g/ml tunicamycin apigenin (20 $\mu$ M) co-treated, TM+LUT-0.25 $\mu$ g/ml tunicamycin luteolin (10 $\mu$ M) co-treated, TM+TAN-0.25 $\mu$ g/ml tangeretin (50 $\mu$ M) co-treated, TM+PBA-0.25 $\mu$ g/ml tunicamycin PBA (1mM) co-treated cells. Values are expressed as mean $\pm$ SEM where n=3. \* $p\leq 0.05$  significantly different from control cells, # $p\leq 0.05$  significantly different from tunicamycin treated cells.

### **2.3.7 Modulation of major proteins of MAP kinase signaling cascade by selected flavones under ER stress**

The MAP kinase proteins are activated in response to pathological insults such as oxidative stress and ER stress and mediate cellular dysfunction. The expression of major MAP kinase proteins namely, ERK1/2, p-p38 MAP kinase and p-JNK was studied and it was carried out independently for the selected flavones (Figure.2.13a, b, c). In the first experiment, tunicamycin significantly upregulated the ERK1/2 to 177.9%, p-p38MAP kinase to 126.9% and p-JNK to 122.4% compared to control cells. In apigenin treated cells, ERK1/2 expression was 194.3%, p-p38 MAP kinase was 225.7%, p-JNK was 136.2% while in PBA treated cells, the expression of ERK1/2 was 116.3%, p-p38 MAP Kinase was 140.7% and p-JNK was 166.3% compared to tunicamycin treated cells as shown in Figure.2.13a. In the second set, tunicamycin remarkably increased the expression of ERK1/2 to 161.8%, p-p38MAP kinase to 212.1% and p-JNK to 136.2% compared to control. In luteolin treated cells, the expression of ERK1/2 was 72.9%, p-p38MAP kinase was 323.84% and p-JNK was 136.1% compared to tunicamycin treated cells (Figure.2.13b). PBA co-treatment altered the expression of ERK1/2 to 39.83%, p-p38 MAP kinase to 140.73%, p-JNK to 110.4% respectively compared to tunicamycin treated cells. In the third set, tunicamycin treatment elevated the ERK1/2 levels to 128.8%, p-p38 MAP kinase to 139.47%, p-JNK to 185.3% compared to control. Tangeretin treatment altered the expression of ERK1/2 to 90.8%, p-p38 MAP kinase to 112.4% and p-JNK to 156.6% while treatment with PBA altered the ERK1/2 levels to 102.6%, p-p38MAP kinase to 105.7% and p-JNK to 229.7% respectively compared to tunicamycin treated cells (Figure.2.13c).

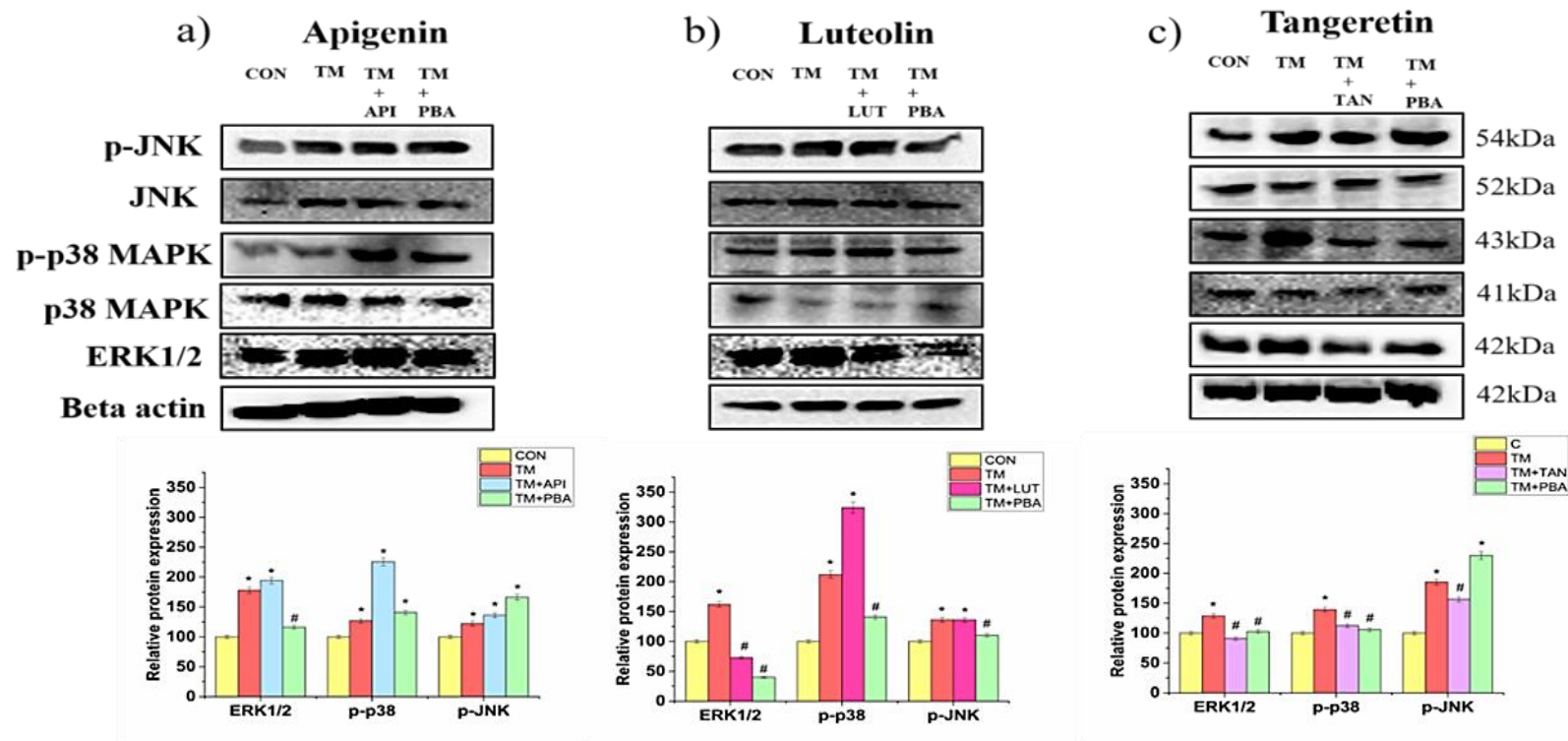


**Figure.2.13. Protein expression of ERK1/2, p-p38 MAP kinase, p-JNK.** Western blot and densitometric analysis of ERK1/2, p-p38 MAP kinase and p-JNK on treatment with a) apigenin, b) luteolin, c) tangeretin under ER stress condition with beta actin as loading control for ERK1/2, p38 MAP kinase as loading control for p-p38 MAP kinase and JNK as loading control for p-JNK. CON-untreated cells, TM-0.25 $\mu$ g/ml tunicamycin treated cells, TM+API- 0.25 $\mu$ g/ml tunicamycin apigenin (20 $\mu$ M) co-treated, TM+LUT-0.25 $\mu$ g/ml tunicamycin luteolin (10 $\mu$ M) co-treated, TM+TAN-0.25 $\mu$ g/ml tangeretin (50 $\mu$ M) co-treated, TM+PBA-0.25 $\mu$ g/ml tunicamycin PBA (1mM) co-treated cells. Values are expressed as mean $\pm$ SEM where n=3. \* $p\leq 0.05$  significantly different from control cells, # $p\leq 0.05$  significantly different from tunicamycin treated cells.

## 2.4 Discussion

In this study, prolonged treatment of myotubes with tunicamycin at the recommended dose (0.25 g/ml) increased the expression of ER stress indicators, as shown by the elevation of UPR-related proteins such as GRP78, IRE-1 $\alpha$  and ATF6. This is in agreement with previous studies where upregulation of GRP78, the ER stress master regulator protein was reported in muscle biopsies with inclusion body myositis (Cullinan & Diehl, 2006; Vattemi et al., 2004). In a Lewis lung cancer mouse model, Bohnert et al. showed that the IRE-1 and downstream XBP-1 signaling is a mediator of muscle atrophy (Bohnert, McMillan, and Kumar 2018). Our results demonstrated upregulation of ATF6 protein. ATF6 disassociates from the BIP protein under ER stress and moves to the Golgi apparatus where it undergoes cleavage by site 1 and site 2 proteases. The cleaved form moves to the nucleus and triggers a series of signaling cascades (Taouji, Wolf, and Chevet 2013). The cleaved form then enters the nucleus and triggers downstream signaling pathways (Taouji et al., 2013).

We also optimized the dose of tunicamycin for induction of insulin resistance. In the present study, the optimised dose of 0.25 $\mu$ g/ml tunicamycin was sufficient for induction of insulin resistance. This is in concordance with studies that report ER stress as a major underlying cause of insulin resistance (Brown et al., 2020; Kim et al., 2015). In this study, the concentration of tunicamycin was optimised based on its ability to induce ER stress and insulin resistance without causing significant cell death. The doses of selected flavones were also optimized. Here, the doses of flavones for co-treatment with tunicamycin were optimised by MTT assay and Annexin V FITC staining to determine the low cytotoxicity of the experimental groups in L6 myotubes.

The oxidative stress, which is characterised by abnormal ROS formation and disrupts redox homeostasis, is one of the effects as well as the cause of ER stress. Low quantities of ROS are produced in skeletal muscles during exercise induced muscular contraction (Davies et al. 1982). The low level of ROS helps in improving muscle health (Scicchitano et al., 2018). Increased ROS generation, though, may cause skeletal muscle damage by activating signalling pathways and aggravating inflammatory mediators and mitochondrial dysfunction (Marzetti et al. 2013). Here, we evaluated the potential of the flavones in suppressing the ER stress mediated ROS generation using DCFH-DA and DHE assays. Luteolin and tangeretin were effective in suppressing the tunicamycin induced ROS levels whereas apigenin could not significantly reduce the ROS levels. This is in agreement with Wu et al. who have reported the inefficacy of apigenin in attenuating the 4-hydroxy-2-Nonenal mediated ROS generation in PC12 cells (Wu et al., 2015).

Increased ROS levels also disrupt the redox homeostasis by weakening the antioxidant defense and from the results it was observed that tunicamycin lowered the activity of antioxidants SOD and GR which were improved on treatment with apigenin, luteolin and tangeretin. TrxR activity, however, was upregulated on treatment with tunicamycin while flavones brought down the levels. This is because the TrxR is involved in reducing the non-native disulphide bonds which would be higher during the ER stress. This accounts for the aberrant upregulation of the enzyme activity in tunicamycin treated cells. SOD decreases the amounts of ROS in cells by converting superoxide to oxygen and hydrogen peroxide, respectively while GR is connected with the reduction of oxidised glutathione (GSSG) to reduced glutathione (Couto, Wood, and Barber 2016; Y. Wang et al. 2018). The molecular docking of the selected flavones with antioxidant enzymes, catalase, glutathione peroxidase, SOD1 and SOD2 further confirmed the antioxidant potential of

the flavones as evident from the comparable binding energies which reveals the interaction of the flavones with the antioxidant enzymes.

The disulphide bond reduction, synthesis, and isomerization that occurs during protein folding is normally mediated by the ER-resident oxidoreductase PDI under normal conditions (Malhotra and Kaufman 2007). In response to ER stress, the PDI expression is increased which promotes the protein folding machinery and also reprimands the non-native disulphide linkages (Franca et al. 2019; Khan and Mutus 2014). As a result, the PDI itself experiences an abnormal cycle of oxidation-reduction that results in an excess of ROS being produced as byproducts and a hyperoxidized ER lumen, which worsens ER stress by impairing appropriate PDI activity and causing additional misfolded proteins (Burgos-Morón et al. 2019). An increase in cellular ROS production is associated with escalated PDI levels (Khan & Mutus, 2014). In our study, we observed that PDI and ERp72, a member of the PDI family with comparable activities to PDI, were considerably increased in expression when treated with tunicamycin (Zhou et al. 2017). Here, significant downregulation in PDI and ERp72 levels was observed on co-treatment with apigenin, luteolin and tangeretin respectively. The findings support the research of Pan et al., who found that bioactives from *Scutellariae radix* and *Rhei rhizoma* were effective in suppressing oxidative damage through downregulation of the dimethylnitrosamine-induced PDI expression in an *in vivo* model (Pan et al. 2015).

The maladaptive nature of the UPR is indicated by the expression of the CHOP/GADD153 protein, an important ER stress marker that indicates the cellular dysfunction (Oyadomari & Mori, 2004). Here in the present study, tunicamycin treated cells showed significant upregulation of GADD153 levels. Apigenin did not exert any lowering effect on the upregulated GADD153 levels whereas luteolin and tangeretin significantly suppressed the GADD153 levels indicating alleviation of maladaptive UPR.

The MAP kinase signaling is also triggered by changes in redox homeostasis. ERK1/2, p38MAP Kinase, and JNK are the three main MAP kinase proteins. Previous study reports sustained upregulation of ERK1/2 in hydrogen peroxide treated rat neuronal cells resulting in cell death (Zakharova et al., 2015). Increased mitochondrial ROS and downstream activation of several pathways, including inflammatory response, insulin resistance, and mitochondrial dysfunction, are driven by p38MAPK (Ashraf et al. 2014; A. E. Brown et al. 2014; Yu et al. 2017). It is known that both ROS production and the IRE-1 $\alpha$  arm of the UPR activate p38MAPK (Jia et al. 2007). JNK is activated in response to ROS and sustained activation is linked to mitochondrial malfunction, elevation of pro-apoptotic transcription factors, and ultimately apoptosis while simultaneously promoting the production of more ROS (Chambers and LoGrasso 2011). JNK is also activated by the IRE-1 $\alpha$  arm of the UPR through the TRAF2 ASK1 complex formation and sustained activation of JNK after 12 hours or more of ER stress supports pro-apoptotic induction (Brown et al., 2016). ERK1/2, p38 MAPK and JNK are also associated with skeletal muscle atrophy and inhibition of MAP kinase proteins may be an effective treatment option (Belova et al., 2020; Mulder et al., 2020; Ryu et al., 2019).

In the present study, it was observed that tunicamycin induced significant upregulation in ERK1/2, p38MAPK and JNK expression and the selected flavones differently modulated the MAP kinase expression. Apigenin could not suppress the expression of the major MAP kinase proteins which is in concordance with its inefficacy in significantly lowering the ROS levels and GADD153 upregulation. Luteolin was only effective in downregulating the ERK1/2 levels while having no lowering effect on the p38MAP kinase and JNK expression. Tangeretin was effective in lowering ERK1/2, p38MAP kinase, and JNK levels. This is consistent with its potential to reduce the redox imbalances caused by ER stress by decreasing ROS levels and GADD153 expression.

## 2.5 Summary

ER stress and associated oxidative stress are mediators of skeletal muscle atrophy, a comorbidity associated with diabetes. Targeting these pathways may provide an avenue for the development of better therapeutic approaches aimed at enhancing the overall function of the skeletal muscle, which will aid in better management of diabetes. In our study, three flavones were analyzed for their potential against ER stress mediated redox perturbations and were observed to exhibit varying efficacy against tunicamycin induced ER stress and associated redox disturbances in skeletal muscle L6 cells. Based on the results, tangeretin was observed to have a better potential than apigenin and luteolin in mitigating the ER stress induced redox imbalances in L6 cells. A schematic summary of the results is depicted in Figure.2.14.

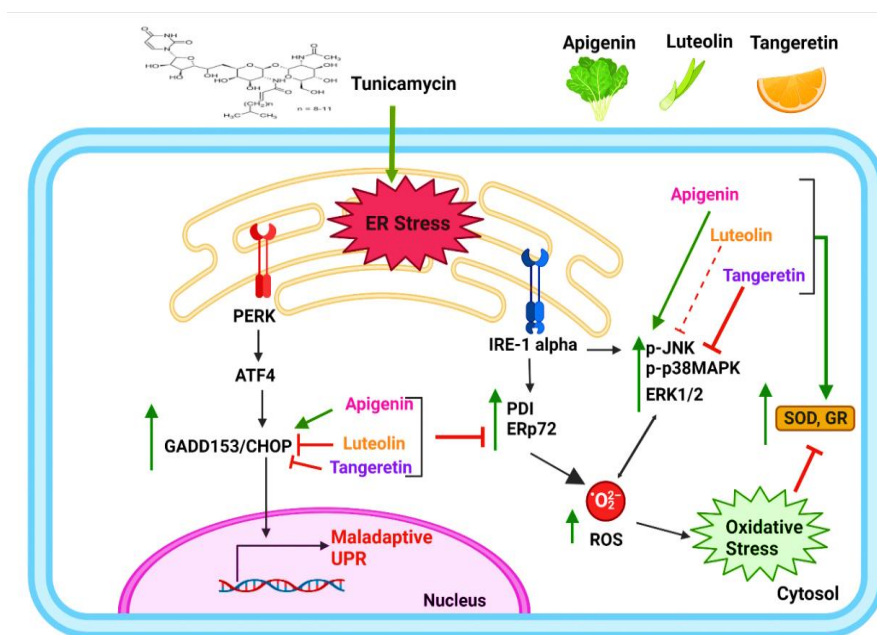


**Figure.2.14. Effect of flavones on tunicamycin induced cellular redox imbalances.** Tunicamycin treatment in L6 myotubes induced ER stress mediated redox imbalances by increasing the CHOP/GADD153 levels, indicator of maladaptive UPR. Exposure to tunicamycin resulted in upregulation of ER resident oxidoreductases and MAP kinase proteins, increased ROS generation and decreased antioxidant activity. Flavones exhibited varying efficacy against ER stress mediated redox disturbances. Tangeretin was observed to be most effective in mitigating the ER stress induced oxidative stress in L6 myotubes.



## References

- Afroze, D., & Kumar, A. (2019). ER Stress in Skeletal Muscle Remodeling and Myopathies. *The FEBS Journal*, 286(2), 379. <https://doi.org/10.1111/FEBS.14358>
- Belova, S. P., Mochalova, E. P., Kostrominova, T. Y., Shenkman, B. S., & Nemirovskaya, T. L. (2020). P38 $\alpha$ -MAPK Signaling Inhibition Attenuates Soleus Atrophy during Early Stages of Muscle Unloading. *International Journal of Molecular Sciences*, 21(8). <https://doi.org/10.3390/IJMS21082756>
- Brown, M., Dainty, S., Strudwick, N., Mihai, A. D., Watson, J. N., Dendooven, R., Paton, A. W., Paton, J. C., & Schröder, M. (2020). Endoplasmic reticulum stress causes insulin resistance by inhibiting delivery of newly synthesized insulin receptors to the cell surface. *Molecular Biology of the Cell*, 31(23), 2597–2629. <https://doi.org/10.1091/MBC.E18-01-0013>
- Brown, M., Strudwick, N., Suwara, M., Sutcliffe, L. K., Mihai, A. D., Ali, A. A., Watson, J. N., & Schröder, M. (2016). An initial phase of JNK activation inhibits cell death early in the endoplasmic reticulum stress response. *Journal of Cell Science*, 129(12), 2317. <https://doi.org/10.1242/JCS.179127>
- Burgos-Morón, E., Abad-Jiménez, Z., de Marañón, A. M., Iannantuoni, F., Escribano-López, I., López-Domènech, S., Salom, C., Jover, A., Mora, V., Roldan, I., Solá, E., Rocha, M., & Víctor, V. M. (2019). Relationship between Oxidative Stress, ER Stress, and Inflammation in Type 2 Diabetes: The Battle Continues. *Journal of Clinical Medicine* 2019, Vol. 8, Page 1385, 8(9), 1385. <https://doi.org/10.3390/JCM8091385>
- Carstens, P. O., & Schmidt, J. (2014). Diagnosis, pathogenesis and treatment of myositis: Recent advances. *Clinical and Experimental Immunology*, 175(3), 349–358. <https://doi.org/10.1111/cei.12194>
- Cheng, Y.-L., Lee, C.-Y., Huang, Y.-L., Buckner, C. A., Lafrenie, R. M., Dénomée, J. A., Caswell, J. M., Want, D. A., Gan, G. G., Leong, Y. C., Bee, P. C., Chin, E., Teh, A. K. H., Picco, S., Villegas, L., Tonelli, F., Merlo, M., Rigau, J., Diaz, D., ... Mathijssen, R. H. J. (2016). <https://www.intechopen.com/books/advanced-biometric-technologies/liveness-detection-in-biometrics>

- Cullinan, S. B., & Diehl, J. A. (2006). Coordination of ER and oxidative stress signaling: The PERK/Nrf2 signaling pathway. *International Journal of Biochemistry and Cell Biology*, 38(3), 317–332. <https://doi.org/10.1016/J.BIOCEL.2005.09.018>
- Khan, H. A., & Mutus, B. (2014). Protein disulfide isomerase a multifunctional protein with multiple physiological roles. *Frontiers in Chemistry*, 2(AUG), 70. <https://doi.org/10.3389/FCHEM.2014.00070/BIBTEX>
- Kim, O.-K., Jun, W., & Lee, J. (2015). Mechanism of ER Stress and Inflammation for Hepatic Insulin Resistance in Obesity. *Annals of Nutrition and Metabolism*, 67(4), 218–227. <https://doi.org/10.1159/000440905>
- Mulder, S. E., Dasgupta, A., King, R. J., Abrego, J., Attri, K. S., Murthy, D., Shukla, S. K., & Singh, P. K. (2020). JNK signaling contributes to skeletal muscle wasting and protein turnover in pancreatic cancer cachexia. *Cancer Letters*, 491, 70–77. <https://doi.org/10.1016/J.CANLET.2020.07.025>
- Oddis, C. V. (2016). *Update on the pharmacological treatment of adult myositis*. <https://doi.org/10.1111/joim.12511>
- Ong, G., & Logue, S. E. (2023). Unfolding the Interactions between Endoplasmic Reticulum Stress and Oxidative Stress. *Antioxidants 2023, Vol. 12, Page 981*, 12(5), 981. <https://doi.org/10.3390/ANTIOX12050981>
- Osowski, C. M., & Urano, F. (2013). Measuring ER stress and the unfolded protein response using mammalian tissue culture system. *Methods in Enzymology*, 490(508), 71–92. <https://doi.org/10.1016/B978-0-12-385114-7.00004-0.Measuring>
- Ostler, J. E., Maurya, S. K., Dials, J., Roof, S. R., Devor, S. T., Ziolo, M. T., & Periasamy, M. (2014). Effects of insulin resistance on skeletal muscle growth and exercise capacity in type 2 diabetic mouse models. *Am J Physiol Endocrinol Metab*, 306, 592–605. <https://doi.org/10.1152/ajpendo.00277.2013>.
- Oyadomari, S., & Mori, M. (2004). Roles of CHOP/GADD153 in endoplasmic reticulum stress. *Cell Death and Differentiation*, 11, 381–389. <https://doi.org/10.1038/sj.cdd.4401373>
- Perry, B. D., Caldow, M. K., Brennan-Speranza, T. C., Sbaraglia, M., Jerums, G., Garnham, A., Wong, C., Levinger, P., Asrar Ul Haq, M., Hare, D. L., Price, S. R.,

- & Levinger, I. (2016). Muscle atrophy in patients with Type 2 Diabetes Mellitus: roles of inflammatory pathways, physical activity and exercise HHS Public Access. *Exerc Immunol Rev*, 22, 94–109.
- Powers, S. K., Smuder, A., & Judge, A. (2012). *Oxidative stress and disuse muscle atrophy: cause or consequence?* <https://doi.org/10.1097/MCO.0b013e328352b4c2>
- Rayavarapu, S., Coley, W., & Nagaraju, K. (2012). Endoplasmic reticulum stress in skeletal muscle homeostasis and disease. *Current Rheumatology Reports*, 14(3), 238–243. <https://doi.org/10.1007/s11926-012-0247-5>
- Rieger, A. M., Nelson, K. L., Konowalchuk, J. D., & Barreda, D. R. (2011). Modified Annexin V/Propidium Iodide Apoptosis Assay For Accurate Assessment of Cell Death. *J. Vis. Exp*, 50, 2597. <https://doi.org/10.3791/2597>
- Ryu, Y., Lee, D., Jung, S. H., Lee, K.-J., Jin, H., Kim, S. J., Lee, H. M., Kim, B., & Won, K.-J. (2019). Sabinene Prevents Skeletal Muscle Atrophy by Inhibiting the MAPK-MuRF-1 Pathway in Rats. *International Journal of Molecular Sciences Article*. <https://doi.org/10.3390/ijms20194955>
- Sartori, R., Romanello, V., & Sandri, M. (2021). *Mechanisms of muscle atrophy and hypertrophy: implications in health and disease*. <https://doi.org/10.1038/s41467-020-20123-1>
- Scicchitano, B. M., Pelosi, L., Sica, G., & Musarò, A. (2018). The physiopathologic role of oxidative stress in skeletal muscle. *Mechanisms of Ageing and Development*, 170, 37–44. <https://doi.org/10.1016/J.MAD.2017.08.009>
- Taouji, S., Wolf, S., & Chevet, E. (2013). Oligomerization in endoplasmic reticulum stress signaling. *Progress in Molecular Biology and Translational Science*, 117, 465–484. <https://doi.org/10.1016/B978-0-12-386931-9.00017-9>
- Vattemi, G., Engel, W. K., McFerrin, J., & Askanas, V. (2004). Endoplasmic Reticulum Stress and Unfolded Protein Response in Inclusion Body Myositis Muscle. *American Journal of Pathology*, 164(1), 1–7. [https://doi.org/10.1016/S0002-9440\(10\)63089-1](https://doi.org/10.1016/S0002-9440(10)63089-1)
- Wang, X., Hu, Z., Hu, J., Du, J., & Mitch, W. E. (2006). Insulin resistance accelerates muscle protein degradation: Activation of the ubiquitin-proteasome pathway by

defects in muscle cell signaling. *Endocrinology*, 147(9), 4160–4168.  
<https://doi.org/10.1210/en.2006-0251>

Wu, P. S., Yen, J. H., Kou, M. C., & Wu, M. J. (2015). Luteolin and Apigenin Attenuate 4-Hydroxy-2-Nonenal-Mediated Cell Death through Modulation of UPR, Nrf2-ARE and MAPK Pathways in PC12 Cells. *PLOS ONE*, 10(6), e0130599.  
<https://doi.org/10.1371/JOURNAL.PONE.0130599>

Yin, L., Li, N., Jia, W., Wang, N., Liang, M., Yang, X., & Du, G. (2021). Skeletal muscle atrophy: From mechanisms to treatments. *Pharmacological Research*, 172(August).  
<https://doi.org/10.1016/j.phrs.2021.105807>

Zakharova, I. O., Sokolova, T. V., Akhmetshina, A. O., & Avrova, N. F. (2015). Alpha-tocopherol prevents long-term activation of ERK1/2 in neurons of the brain cortex under conditions of oxidative stress. *Neurochemical Journal*, 9(4), 319–322.  
<https://doi.org/10.1134/S1819712415040170>

# **Chapter 3**

**Investigation & elucidation of the  
mechanism of action of most active  
flavone, tangeretin, in mitigation of ER  
stress induced insulin resistance in L6  
cells**

### 3.1 Introduction

Type 2 diabetes is the predominant form of diabetes, and insulin resistance is a significant attribute of this condition with most treatment strategies focusing on targeting insulin resistance for disease amelioration. Insulin resistance is an important manifestation of type 2 diabetes and a primary target for antidiabetic drugs. The complex pathophysiology of this disease makes monotherapy inadequate and warrants the identification of alternative targets and therapies for disease intervention. ER stress has emerged as a negative regulator of insulin signaling as evident from the earlier studies (Brown et al., 2020; Flamment et al., 2012; Urano et al., 2000). Skeletal muscle is the primary tissue involved in insulin-stimulated glucose metabolism making it a relevant target for insulin resistance studies (Gallot & Bohnert, 2021). Moreover, it possesses a complex ER that regulates the activity of skeletal muscles as well as acts as a store for calcium ions necessary for muscular contraction (Rayavarapu et al., 2012). Hence, therapeutic intervention of the ER stress-related pathways for alleviation of insulin resistance in skeletal muscles can contribute to new targets for disease management.

The glucose uptake in skeletal muscles can occur by the insulin-stimulated pathway mediated by PI3K and/or even independent of the insulin signaling pathway mediated by AMPK activation as depicted in Figure.3.1 (Deshmukh, 2016). The insulin-stimulated pathway is the canonical signaling pathway for cellular glucose uptake which is triggered by the binding of insulin to the cell surface receptor followed by tyrosine phosphorylation of IRS proteins and subsequent activation of PI3K and downstream Akt which facilitates the translocation of glucose transporter GLUT4 to the plasma membrane of muscle cells (Pessin & Saltiel, 2000). It is negatively regulated by phosphatase and tensin homolog (PTEN), which is known to suppress insulin-stimulated signaling by dephosphorylating

phosphatidylinositol 3,4,5-triphosphate (PIP3) to phosphatidylinositol 4,5-bisphosphate (PIP2) in the PI3K pathway (Nakashima et al., 2000).

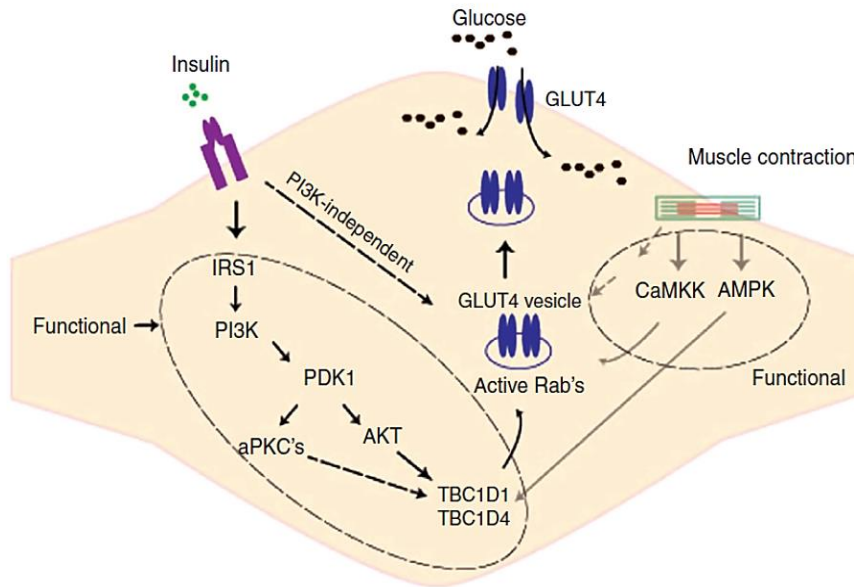


**Figure.3.1. Insulin-dependent and independent signaling pathways for glucose uptake in skeletal muscle cells** (Deshmukh, 2016)

Alternatively, glucose uptake can occur independent of the PI3K activation via the AMPK signaling cascade. AMPK is a heterotrimer comprising  $\alpha$  catalytic subunit and  $\beta\gamma$  regulatory subunits and it can be independently activated by two upstream kinases, LKB1 and calcium/calmodulin dependent protein kinases (CaMKK) by phosphorylation on T172 loop on  $\alpha$  subunit with the former being the main AMPK activator in skeletal muscles (Dyck et al., 1996; Sakamoto et al., 2005; Woods et al., 2005). Low energy status such as in exercise is a trigger for AMPK activation that suppresses the ATP consuming pathways such as fatty acid synthesis and upregulates the ATP producing pathways, namely, glucose uptake and metabolism and fatty acid oxidation (O’neill, 2013). In skeletal muscles, AMPK facilitates GLUT4 translocation by phosphorylation and

activation of downstream AS160, a Rab GTPase activating protein also known as TBC1D4, however, AS160 is also known to be stimulated by insulin dependent signaling component, Akt (Deshmukh, 2016). Thus, making it an important link between insulin dependent and independent signaling mediated glucose uptake (Thong et al., 2007; Treebak et al., 2006). ER stress is shown to impair glucose uptake by suppressing insulin stimulated signaling components via upregulation of IRE-1 $\alpha$ /ASK1/MAP3K5/JNK and/or TRB3 as well as insulin independent AMPK expression (Flamment et al., 2012; Hwang et al., 2013; Urano et al., 2000). In the present study, the potential of apigenin, luteolin and tangeretin in mitigating tunicamycin induced insulin resistance in L6 myotubes was evaluated. The study focused on identifying the most active flavone against tunicamycin induced insulin resistance and elucidation of its mechanism of action in alleviating the same by investigating the effect of the flavone on the expression of proteins involved in the insulin dependent as well as independent signaling pathways for glucose uptake during ER stress.

## **3.2 Materials & Methods**

### **3.2.1 Chemicals**

DMEM containing 4.5g/L glucose and 1.5g/L sodium bicarbonate, fetal bovine serum, horse serum, antimycotic antibiotic mix, DMSO, triton X, glycine, tris base, skimmed milk, sodium dodecyl sulphate, HBSS were purchased from Himedia (Mumbai, India). Tangeretin, luteolin, tunicamycin, PBA, HPLC grade methanol, protease inhibitor cocktail tablets, dorsomorphin, bovine insulin were purchased from Sigma Aldrich Chemical (St. Louis Missouri, USA). Apigenin was purchased from Cayman Chemicals (Michigan, USA). RIPA lysis buffer, BCA kit, 2-NBDG were purchased from Thermo Fisher Scientific (Waltham, Massachusetts, USA). The antibodies IRE-1 $\alpha$ , beta actin, ATF4, p-IRS-1(Tyr), IRS-1, p-AMPK, AMPK, GLUT4, PI3K, AS160, p-LKB1,



antirabbit and antimouse HRP conjugated antibodies were purchased from Cell Signaling Technologies (Danvers, Massachusetts, USA). Antibodies ATF6, GRP78, PTEN were purchased from Santa Cruz Biotechnology (Dallas, Texas, USA). p-PERK, XBP-1, MAP3K5 were purchased from Gbiosciences (St. Louis MO, USA). Rat skeletal muscle cell line, L6 myoblasts were purchased from National Centre for Cell Sciences, Pune, India.

### **3.2.2 Cell Culture**

L6 myoblasts were maintained in DMEM containing 10% fetal bovine serum and 1% antibiotic antimycotic mix at 37°C (5% carbon dioxide). When myoblasts reached 80% confluency, growth medium was replaced with DMEM containing 2% horse serum to induce differentiation into myotubes. Alternative medium change was given for 4 days. All the experiments were carried out in differentiated myotubes.

### **3.2.3 Experimental Groups**

- **CON-** untreated or control cells
- **TM-** tunicamycin (0.25µg/ml) treated cells
- **TM+API-** tunicamycin (0.25µg/ml) & apigenin (20µM) co-treated cells
- **TM+LUT-** tunicamycin (0.25µg/ml) & luteolin (10µM) co-treated cells
- **TM+TAN-** tunicamycin (0.25µg/ml) & tangeretin (50µM) co-treated cells
- **TM+PBA-** tunicamycin (0.25µg/ml) & PBA (1mM) co-treated cells (Positive control)

### **3.2.4 Experimental design**

The workflow of this chapter is described in Figure.3.2.

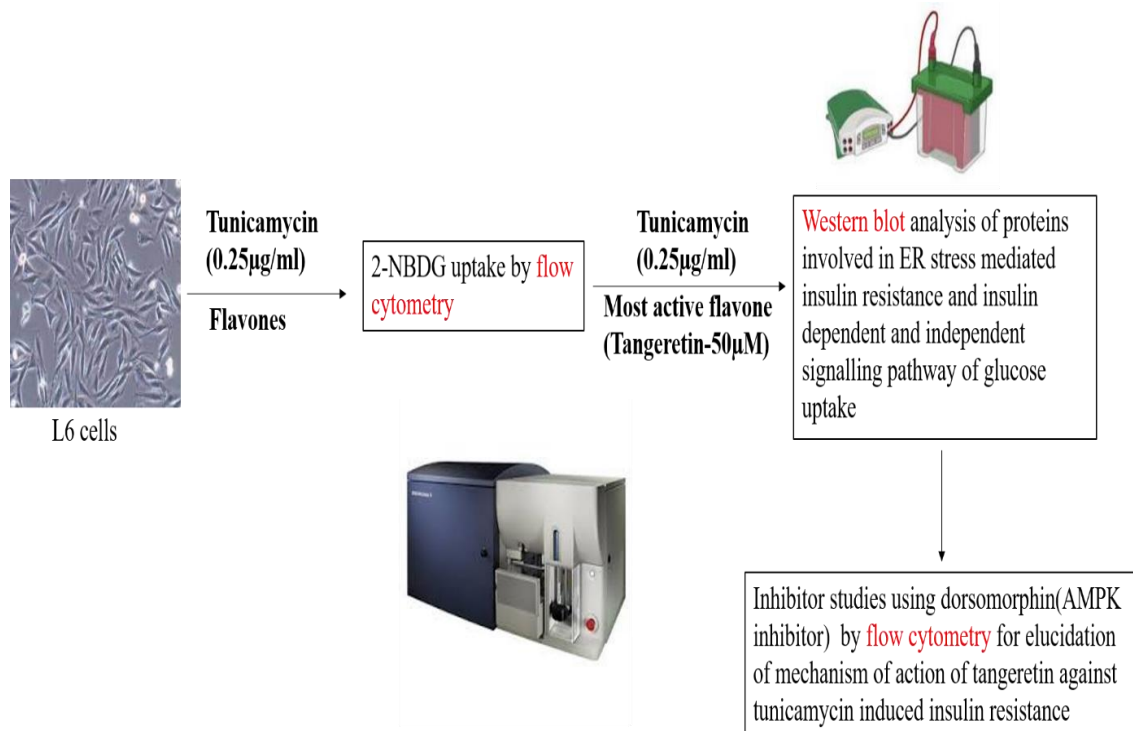


**Figure.3.2. Schematic representation of the experimental design**

### 3.2.5 2-NBDG uptake analysis

L6 myoblasts were seeded in 6 well plates at  $1 \times 10^5$  density, the cells were then differentiated for four days and analysed for myotube formation. The myotubes were then treated with the experimental groups for 24 hours followed by stimulation with 100 nmol insulin for 30 minutes. The cells were then incubated with the fluorescent glucose analog, 2-NBDG for 30 minutes following which cells were washed with HBSS, trypsinized, centrifuged and resuspended in HBSS and taken for flow cytometry analysis using BD FACS Aria II (BD Biosciences).

### 3.2.6 Western blot analysis for ER stress induction

L6 myoblasts were seeded in T25 flasks and grown to 80% confluency. The cells were then differentiated for 4 days followed by co-treatment studies with most active flavone

and positive control (PBA). Myotubes were then rinsed with HBSS and proteins were extracted using RIPA lysis buffer. Protein samples were quantitated and normalised with the BCA assay kit using BSA as the standard. Protein samples were separated on 10% sodium dodecyl sulphate polyacrylamide gels. Proteins were then transferred onto PVDF membranes (Millipore, Merck, USA) and blocked for 1 hour in 5% skimmed milk. Membranes were then washed thrice with TBST and incubated with the appropriate primary antibodies (dilution 1:1000) against ER stress markers such as GRP78, ATF6, IRE-1 $\alpha$ , p-PERK, XBP-1, ATF4 with beta actin as the loading control at 4°C with overnight agitation. Membranes were then incubated with appropriate HRP conjugated secondary antibodies (dilution 1:1000 to 1:2000) for 2 to 3 hours at room temperature. The blot images were obtained by adding the ECL substrate (Thermo Fisher Scientific, Massachusetts, USA) to the membranes in Chemidoc MP Imaging systems (Bio-Rad, USA). The resultant bands were quantified by densitometric analysis using the Image lab software version 6.1 (Bio-Rad, USA).

### **3.2.7 Protein expression studies for insulin resistance induction**

After 24-hour co-treatment studies with most active flavone and positive control (PBA), proteins from myotubes were extracted by RIPA lysis buffer. The protein samples were quantified using the BCA kit with BSA as the standard. Protein samples were subjected to western blotting as elaborated in Section 3.2.6. The proteins studied were p-IRS-1(Tyr), IRS-1, PI3K, GLUT4, p-AMPK, AMPK, AS160, p-LKB1, PTEN, MAP3K5 and beta actin.

### **3.2.8 AMPK inhibitor studies**

L6 myotubes, following differentiation, were starved in serum free medium for 1.5 hours followed by incubation with AMPK inhibitor, dorsomorphin (20 $\mu$ M) for 0.5 hours. The

cells were then treated with tunicamycin, positive control and most active flavone with or without AMPK inhibitor for 24 hours. The cells were then stimulated with 100 nmol insulin for 30 minutes followed by incubation with 2-NBDG for 30 minutes and subjected to flow cytometry analysis as described in Section 3.2.5.

### **3.2.9 Statistical analysis**

Three independent triplicate runs of each experiment were performed. In SPSS software, all data were statistically analysed using one-way ANOVA and the Duncan post hoc test. Every result is shown as a mean±SEM. A value of  $p \leq 0.05$  was considered statistically significant in each experiment.

## **3.3 Results**

### **3.3.1 Tangeretin improves 2-NBDG uptake by mitigating tunicamycin induced insulin resistance**

The ER stress is reported to be involved in skeletal muscle insulin resistance. In the present study, ER stress induced insulin resistance was determined by the 2-NBDG flow cytometry uptake analysis as seen in Figure.3.3. In untreated cells, the 2-NBDG uptake was recorded as 62.5%. On treatment with 0.25µg/ml tunicamycin only, the 2-NBDG uptake decreased to 40.8% which mimics insulin resistance condition. Apigenin co-treated cells showed 2-NBDG uptake of 42.4%. Luteolin co-treated cells showed 2-NBDG uptake of 40.5%. Co-treatment with tangeretin showed an improved uptake of 60.8%. PBA treated cells showed an uptake of 48.1%. Of the three selected flavones, only tangeretin showed an increased glucose uptake under ER stress condition. Also based on results from the previous chapter, tangeretin was shown to have considerable potential against tunicamycin induced oxidative stress condition in L6 myotubes, hence, tangeretin was selected for future studies.

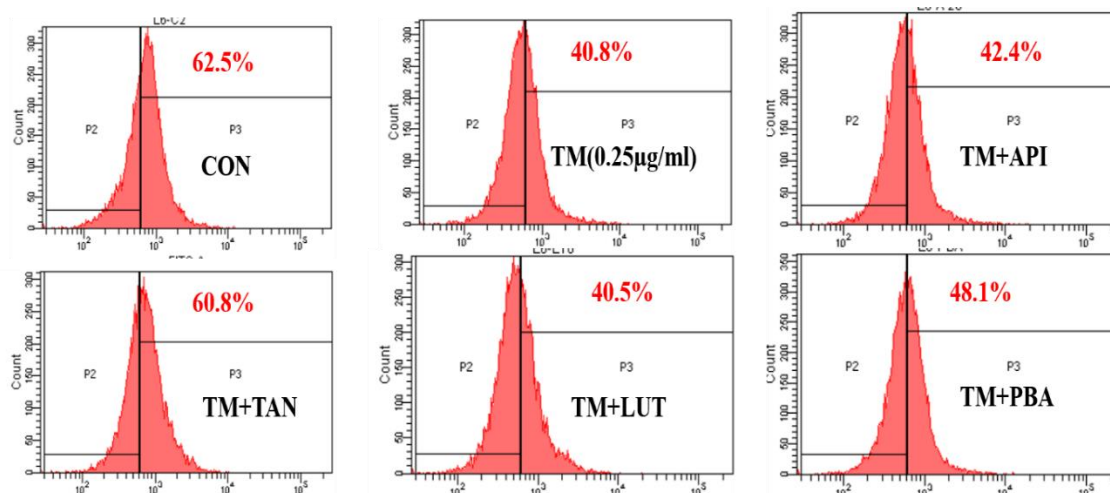


**Figure.3.3. Effect of flavones on tunicamycin induced insulin resistance.** L6 myotubes were treated with respective experimental groups for 24 hours followed by stimulation with 100nmol insulin for 30 minutes. Cells were incubated with 2-NBDG for 30 minutes and subjected to flow cytometry analysis. CON-untreated cells, TM-0.25µg/ml tunicamycin treatment, TM+API-0.25µg/ml tunicamycin apigenin (20µM) co-treatment, TM+LUT-0.25µg/ml tunicamycin luteolin (10µM) co-treatment, TM+TAN-0.25µg/ml tangeretin (50µM) co-treatment, TM+PBA-0.25µg/ml tunicamycin PBA (1mM) co-treatment.

### 3.3.2 Tangeretin suppresses the expression of tunicamycin induced ER stress markers

Prolonged treatment with tunicamycin causes maladaptive UPR which was evident from the significant upregulation of the major ER stress markers (Figure.3.4a, b). On prolonged exposure to tunicamycin GRP78 was remarkably upregulated to 638% compared to control cells. Tangeretin co-treatment significantly downregulated the levels to 547.6% while PBA co-treatment brought down the levels to 466.17%, respectively, compared to the tunicamycin treated cells (Figure.3.4a, b). Tunicamycin treatment increased the IRE-1α levels to 180.5% compared to the control. Tangeretin co-treatment suppressed the levels to 108.3% remarkably while PBA reduced the expression greatly to 65.5%,

respectively, compared to tunicamycin treated cells as shown in Figure.3.4a, b. p-PERK levels were enhanced to 187.2% on treatment with tunicamycin alone. Co-treatment with tangeretin significantly brought down the levels to 142.8% while co-treatment with PBA remarkably reduced the levels to 121.3% compared to tunicamycin treated cells (Figure.3.4a, b). Upon induction of ER stress by tunicamycin, IRE-1 $\alpha$  induces splicing of XBP-1. Here, in cells treated with tunicamycin, there was an increase in the expression of spliced (138.2%) and unspliced (123.2%) variants of XBP-1 respectively. Co-treatment with tangeretin remarkably reduced the expression of both unspliced and spliced forms of XBP-1 to 87.24% and 106.57%, respectively, compared to tunicamycin treated cells (Fig.3.4a, b). PBA co-treatment downregulated the expression levels to 98.89% and 57.09% respectively compared to tunicamycin treated cells. Another ER stress sensor, ATF6 was notably upregulated to 152.3% in tunicamycin treated cells compared to the control. Tangeretin co-treatment remarkably decreased the expression levels to 136.4% while PBA treatment suppressed the expression to 143.95%, respectively, compared to the tunicamycin treated cells. Tunicamycin treated myotubes augmented the ATF4 expression to 145.09% compared to the control cells. In cells co-treated with tangeretin, the expression levels were downregulated to 97.7% and with PBA, it was reduced to 120.7%, respectively, compared to the tunicamycin treated cells as shown in Figure.3.4a, b.

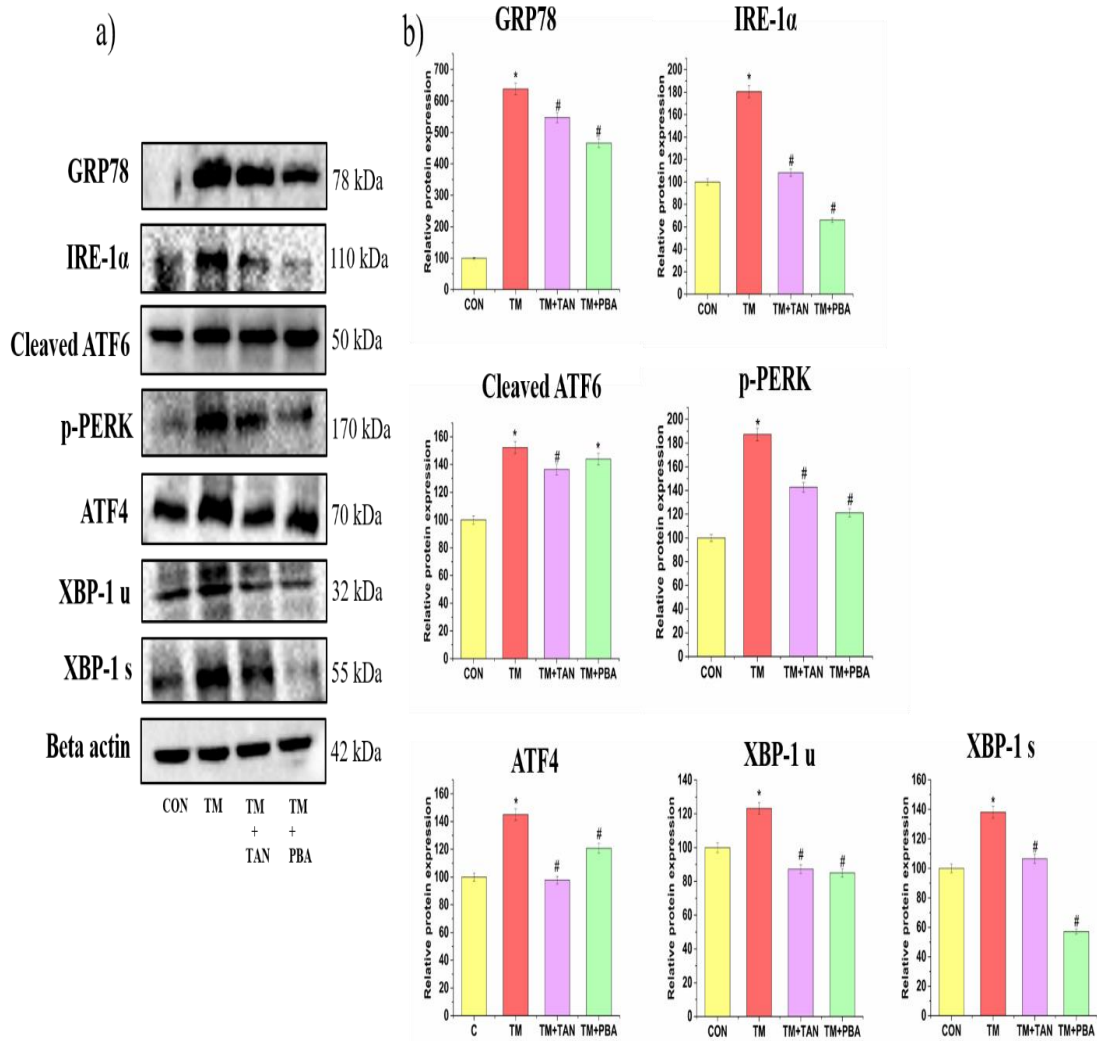


**Figure 3.4. Effect of tangeretin on expression of tunicamycin induced major ER stress markers.** a) Western blot analysis of ER stress markers, GRP78, IRE-1 $\alpha$ , ATF6, p-PERK, ATF4, unspliced and spliced XBP-1 was performed with beta actin as the loading control. b) Densitometric analysis of all proteins relative to beta actin. CON-untreated cells, TM-0.25 $\mu$ g/ml tunicamycin treatment, TM+TAN-0.25 $\mu$ g/ml tunicamycin tangeretin (50 $\mu$ M) co-treatment, TM+PBA-0.25 $\mu$ g/ml tunicamycin PBA (1mM) co-treatment. Values are expressed as mean $\pm$ SEM where n=3. \*p $\leq$ 0.05 significantly different from control cells, #p $\leq$ 0.05 significantly different from tunicamycin treated cells.

### **3.3.3 Tangeretin mitigates ER stress mediated insulin resistance via upregulation of AMPK**

Chronic treatment of differentiated L6 myotubes with tunicamycin resulted in insulin resistance as evident from decreased 2-NBDG uptake. This was further confirmed by expression studies of proteins involved in insulin dependent (PI3K) and independent (AMPK) signaling pathway for glucose uptake. Under ER stress condition, the expression of p-IRS-1(Tyr), PI3K, p-AMPK, GLUT4 were significantly decreased to 87.93%, 79.23%, 69.57% and 85.04% respectively as compared to the untreated cells (Figure.3.5a, b). Tangeretin could not improve the levels of p-IRS-1(Tyr) (82.49%) and PI3K (71.26%) that are components of the insulin dependent signaling for cellular glucose uptake (Figure.3.5a, b). PBA co-treatment did not improve the p-IRS-1(Tyr) (76.23%) and PI3K (79.64%) levels. Co-treatment with tangeretin, however, could significantly improve the p-AMPK and GLUT4 levels to 90.75% and 92.35% respectively compared to tunicamycin treated group. PBA however did not induce any significant improvement in the expression of p-AMPK (64.2%) and GLUT4 (87.9%) levels compared to tunicamycin group under ER stress as depicted in Figure.3.5a, b. The above findings, indicate the role of tangeretin in mitigating ER stress mediated IR via AMPK mediated GLUT4 translocation while failing to upregulate the insulin dependent signaling.



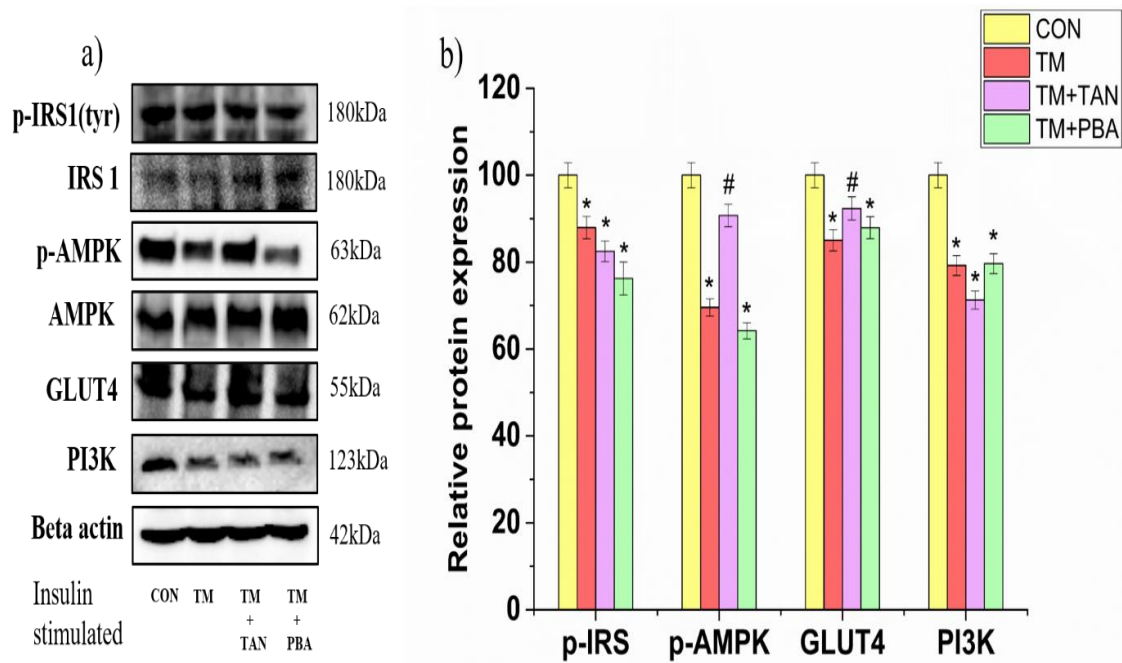


**Figure.3.5. Effect of tangeretin on tunicamycin induced insulin resistance.** a) Western blot analysis of proteins involved in insulin dependent and independent signaling, namely, p-IRS(Tyr), p-AMPK, GLUT4, PI3K was performed. Beta actin was the loading control for all non-phosphorylated proteins. For the phosphorylated proteins, the loading control was their non-phosphorylated forms. b) Densitometric analysis of proteins relative to the respective loading controls. CON-untreated cells, TM-0.25 $\mu$ g/ml tunicamycin treatment, TM+TAN-0.25 $\mu$ g/ml tunicamycin tangeretin (50 $\mu$ M) co-treatment, TM+PBA-0.25 $\mu$ g/ml tunicamycin PBA (1mM) co-treatment. Values are expressed as mean $\pm$ SEM where n=3. \*p $\leq$ 0.05 significantly different from control cells, #p $\leq$ 0.05 significantly different from tunicamycin treated cells.

The role of AMPK was confirmed by expression studies of proteins involved in AMPK signaling (Figure.3.6a, b). The expression of p-LKB1 and AS160 involved in AMPK signaling were significantly downregulated to 72.39% and 52.52% respectively compared to untreated cells on exposure to tunicamycin. Tangeretin significantly improved the levels of p-LKB1 to 138.57% and AS160 to 67.57% while PBA could not significantly

enhance the suppressed p-LKB1 (49.08%) and AS160 (58.72%) levels compared to tunicamycin treated group as seen in Figure.3.6a, b. The MAP3K5 or ASK1 which is downstream of IRE-1 $\alpha$  (mediator of the ER stress induced insulin resistance) was upregulated to 180.27% on treatment with tunicamycin compared to untreated cells. Tangeretin and PBA significantly suppressed the levels to 98.98% and 116.83% respectively compared to tunicamycin treated group. PTEN, a negative regulator of insulin dependent signaling was significantly increased to 114.46% in tunicamycin treated cells compared to untreated cells. Tangeretin augmented the PTEN levels to 140.33% while PBA also increased the expression to 134.86% compared to tunicamycin treated group as shown in Figure.3.6a, b.

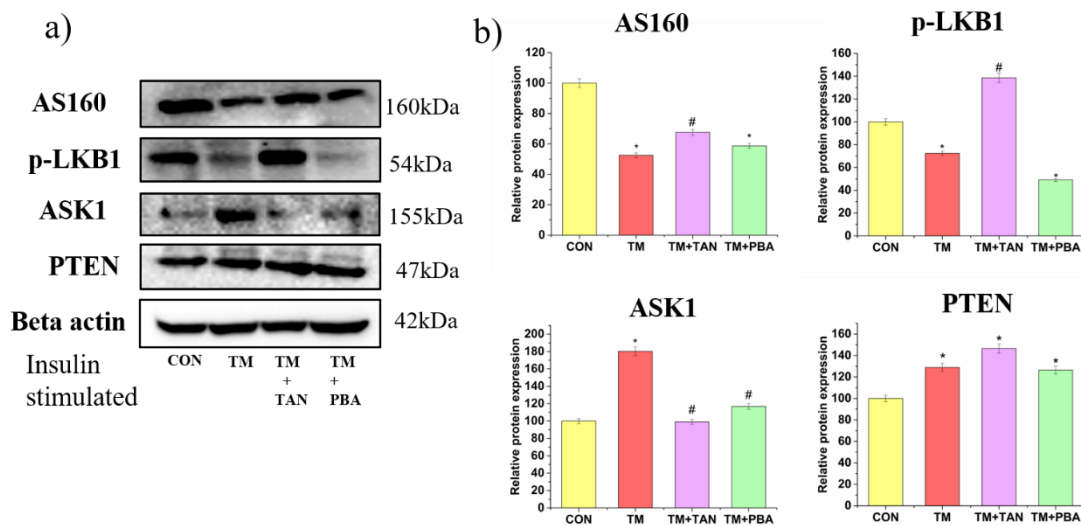
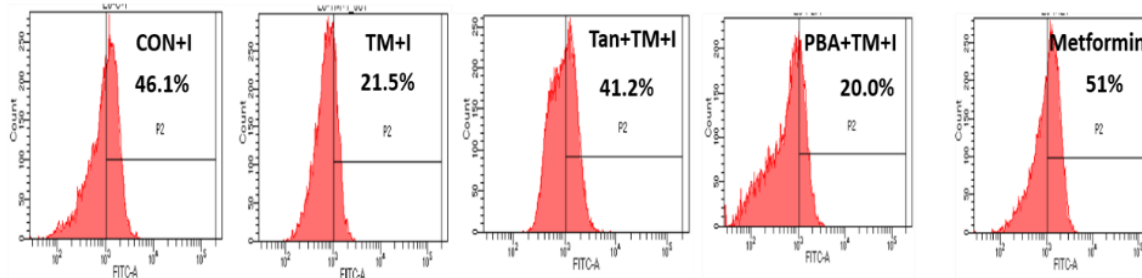


**Figure.3.6. Effect of tangeretin on tunicamycin induced insulin resistance.** a) Western blot analysis of MAP3K5, p-LKB1, AS160, PTEN was performed with beta actin as the loading control. b) Densitometric analysis of proteins relative to beta actin. CON-untreated cells, TM-0.25 $\mu$ g/ml tunicamycin treatment, TM+TAN-0.25 $\mu$ g/ml tunicamycin tangeretin (50 $\mu$ M) co-treatment, TM+PBA-0.25 $\mu$ g/ml tunicamycin PBA (1mM) co-treatment. Values are expressed as mean $\pm$ SEM where n=3. \*p $\leq$ 0.05 significantly different from control cells, #p $\leq$ 0.05 significantly different from tunicamycin treated cells.

### **3.3.4 AMPK inhibitor attenuates tangeretin mediated glucose uptake under ER stress mediated insulin resistance**

From the protein expression studies, it is evident that tangeretin alleviates tunicamycin induced insulin resistance and improves glucose uptake by activating the AMPK pathway. To validate the findings, tangeretin mediated 2-NBDG (glucose analog) uptake during tunicamycin induced insulin resistance was evaluated in the presence and absence of AMPK inhibitor, dorsomorphin. In the absence of inhibitor, in untreated cells, the uptake was 46.1% while in tunicamycin treated cells, uptake was reduced to 21.5% and in tangeretin co-treated cells, the uptake was 41.2% while in PBA co-treated group, the uptake was 24.5% respectively as depicted in Figure.3.7. Metformin, an AMPK activator was used as the standard for comparison and the uptake in this group was recorded as 51% in the absence of inhibitor. In the presence of dorsomorphin, the uptake in control cells was observed to be 19.2% and tunicamycin treated group was 24.6%. The uptake in tangeretin co-treated group reduced to 13.7% while in PBA co-treated cells, the uptake was 30% and in metformin treated cells the uptake was 23.4% in presence of inhibitor (Figure.3.7). The decreased uptake in presence of AMPK inhibitor, dorsomorphin in tangeretin co-treated cells confirm the role of AMPK in tangeretin mediated glucose uptake under ER stress.

**(-) Dorsomorphin**



**(+) Dorsomorphin**

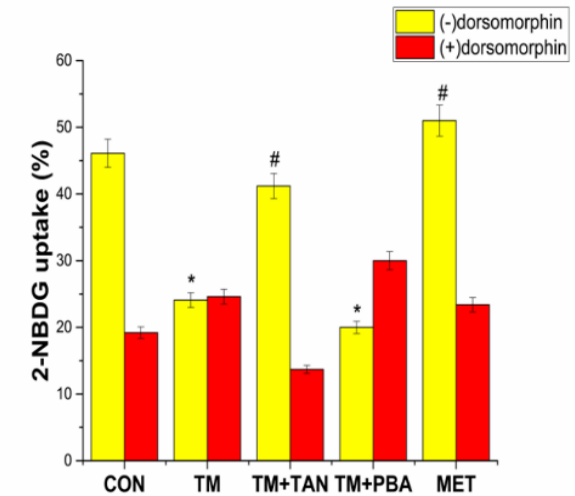
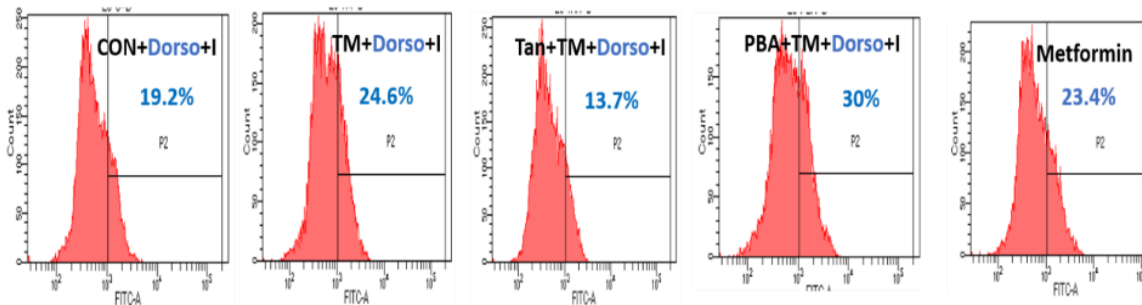


**Figure.3.7. AMPK inhibitor studies.** The 2-NBDG uptake in the presence and absence of AMPK inhibitor was evaluated to determine the role of AMPK signaling in tangeretin mediated uptake during tunicamycin induced insulin resistance. L6 myotubes were pre-treated with/without dorsomorphin followed by co-incubation with TM (0.25µg/ml), TM+TAN (TM-0.25µg/ml, TAN-50µM), TM+PBA (TM-0.25µg/ml, PBA-1mM) and metformin (100µM). All the groups were insulin stimulated. Values are expressed as mean±SEM where n=3. \*p≤0.05 significantly different from control cells, #p≤0.05 significantly different from tunicamycin treated cells.

### 3.4 Discussion

In the present study, the protective effects of selected flavones, apigenin, luteolin and tangeretin in mitigating tunicamycin induced insulin resistance in skeletal muscle L6 myotubes were analyzed. The findings demonstrated the role of tangeretin in improving tunicamycin induced impaired glucose uptake. Initially, selected flavones were screened for their ability to improve ER stress induced impaired glucose uptake. From the results, it was evident that only tangeretin could significantly improve the 2-NBDG uptake under ER stress condition and therefore, only tangeretin was taken for future studies.

In this study, prolonged exposure to tunicamycin at a dose of 0.25µg/ml was found to upregulate the expression of the ER stress markers, GRP78, IRE-1α, p-PERK, ATF6, ATF4 and splicing of XBP-1. This was in concordance with previous reports that have demonstrated the induction of ER stress in skeletal muscle cells on prolonged exposure to tunicamycin (Eo & Valentine, 2021; Thoma et al., 2020). During ER stress, the three ER stress sensors (IRE-1α, PERK and ATF6) dissociate from GRP78 and subsequently activate downstream elements. IRE-1α exerts its endoribonuclease activity by increasing splicing of XBP-1 and also its kinase activity by upregulation of downstream MAP3K5/ASK1 that is followed by JNK activation which subsequently suppresses the insulin stimulated signaling inducing insulin resistance (Urano et al., 2000). The results from the present study demonstrated the upregulation of XBP-1 and MAP3K5 on prolonged treatment of L6 cells with tunicamycin. The PERK arm of the UPR triggers insulin resistance under ER stress via ATF4/TRB3 signaling (Flamment et al., 2012). Here, the results showed an upregulation of p-PERK and ATF4 on chronic treatment with tunicamycin. Co-treatment with tangeretin significantly abrogated the levels of GRP78, IRE-1α, p-PERK, ATF6, ATF4 and splicing of XBP-1 which confirms the ER protective effects of tangeretin in skeletal muscle cells. This is in agreement with Takano et al. who

have demonstrated the ER protective potential of tangeretin in F9 Herp null cells, insulinoma MIN-6 cells and PC-12 cells exposed to tunicamycin (Takano et al., 2007). From the findings here, it was observed that the MAP3K5/ASK1 levels were downregulated on co-treatment with tangeretin. ASK1 forms a nexus between ER stress and insulin resistance via upregulation of IRE-1 $\alpha$  and downstream JNK activity and its suppression indicates alleviation of ER stress mediated insulin resistance.

Impaired glucose uptake is a consequence of insulin resistance and it is regulated by signaling pathways that either require insulin stimulation and/or can function independent of insulin. Here, the expression of proteins involved in cellular glucose uptake under ER stress condition was studied. Chronic exposure to tunicamycin significantly downregulated the levels of phospho-IRS-1(Tyr), PI3K, p-AMPK and GLUT4. Tyrosine phosphorylation of IRS-1 aids in insulin stimulated glucose uptake by enabling its binding to PI3K while phosphorylation at its serine residue correlates with insulin resistance (Hançer et al., 2014). The downregulation of p-IRS-1(Tyr) and PI3K by tunicamycin in this study indicates downregulation of insulin stimulated response and subsequent induction of insulin resistance. Quan et al. have reported a similar decrease in IRS-1 tyrosine phosphorylation in C2C12 myotubes on treatment with 0.5 $\mu$ g/ml tunicamycin for 16 hours (Quan et al., 2015). In this study, tangeretin could not improve the expression levels of phospho-IRS-1(Tyr) and PI3K under ER stress. These findings indicate the inability of tangeretin in modulating the insulin stimulated signaling cascade under ER stress condition. The downregulated GLUT4 levels, however were improved on co-treatment with tangeretin indicating improvement in impaired glucose uptake. To confirm the inability of tangeretin in modulating the insulin dependent glucose uptake, the PTEN levels under ER stress was measured. Prolonged incubation with tunicamycin resulted in increased PTEN levels which is a negative regulator of insulin signaling. It was observed

here that tangeretin exacerbated the PTEN levels in response to ER stress indicating its inability in improving the insulin stimulated signaling. Since, tangeretin improved the glucose uptake, despite failing to improve insulin stimulated signaling, the effect of tangeretin on expression of components involved in insulin independent glucose uptake during ER stress was determined. Tunicamycin suppressed the AMPK activation, an important mediator of insulin independent signaling. Tangeretin significantly improved the p-AMPK levels as evident from the results. This is consistent with the findings of Kim et al., who found that tangeretin treatment enhanced glucose uptake in C2C12 myotubes via the activation of AMPK (Kim et al., 2012). The proteins upstream and downstream of AMPK activation were studied. LKB1, a major kinase upstream of AMPK activation in skeletal muscles was downregulated under ER stress and its activity was significantly enhanced on treatment with tangeretin. AS160, downstream of AMPK and mediator of GLUT4 translocation in skeletal muscle cells was suppressed on exposure to tunicamycin. AS160 is also reported to be downstream of Akt, a component of insulin stimulated signal. Thus, AS160 serves a dual role in insulin dependent and insulin independent glucose uptake (Thong et al., 2007). In this study, tangeretin successfully upregulated the compromised AS160 levels but it was not comparable to the control levels. This could be due to the dual role of AS160 in insulin dependent and insulin independent glucose uptake and inability of tangeretin to improve the former. The protein expression studies manifest the role of tangeretin in alleviation of ER stress induced insulin resistance via AMPK activation.

To validate the findings, 2-NBDG flow cytometry analysis was performed in the absence and presence of AMPK inhibitor, dorsomorphin. In the absence of inhibitor, tangeretin ameliorated the ER stress mediated insulin resistance and showed an enhanced uptake, however, in the presence of inhibitor, the uptake was reduced indicating the inability of

tangeretin to improve the glucose uptake when AMPK is attenuated completely. This further provides evidence for the involvement of AMPK activation in tangeretin mediated alleviation of insulin resistance during ER stress.

### **3.5 Summary**

ER stress has been identified as a key mechanism driving insulin resistance, and its modulation may provide novel targets for the management of diabetes. In the present study, the efficacy of the selected flavones in mitigating tunicamycin mediated insulin resistance in skeletal muscle L6 myotubes was studied. Tangeretin remarkably suppressed the tunicamycin induced UPR induction as evident from the decreased expression of the ER stress marker proteins. Tangeretin also improved the cellular glucose uptake via the activation of the AMPK signaling cascade while having no significant effect on the insulin stimulated signaling pathway during tunicamycin induced insulin resistance. The proposed mechanism of action has been illustrated in Figure.3.8. This is the first report elucidating the mechanism of action of tangeretin in ameliorating tunicamycin induced insulin resistance.



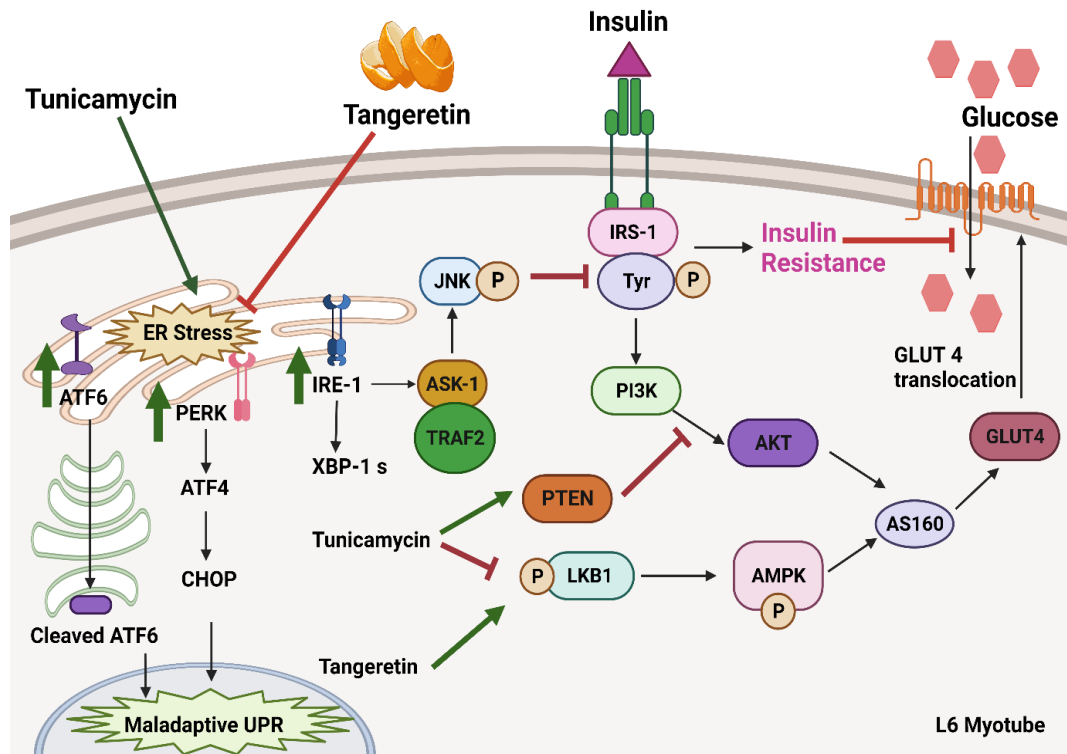


**Figure.3.8. Proposed mechanism of action of tangeretin in mitigating ER stress induced insulin resistance in skeletal muscle L6 cells.** Prolonged exposure to tunicamycin induced insulin resistance by suppressing p-IRS-1 (tyr) and PI3K activity via IRE-1 $\alpha$ /ASK1/JNK signal. Tunicamycin also upregulated PTEN while suppressing GLUT4 translocation and AMPK signaling. Tangeretin improved ER stress mediated impaired glucose uptake via the suppression of maladaptive UPR and activation of AMPK signaling.

## References

- Brown, M., Dainty, S., Strudwick, N., Mihai, A. D., Watson, J. N., Dendooven, R., Paton, A. W., Paton, J. C., & Schröder, M. (2020). Endoplasmic reticulum stress causes insulin resistance by inhibiting delivery of newly synthesized insulin receptors to the cell surface. *Molecular Biology of the Cell*, *31*(23), 2597–2629. <https://doi.org/10.1091/MBC.E18-01-0013>
- Deshmukh, A. S. (2016). Insulin-stimulated glucose uptake in healthy and insulin-resistant skeletal muscle. *Hormone Molecular Biology and Clinical Investigation*, *26*(1), 13–24. <https://doi.org/10.1515/hmbci-2015-0041>
- Dyck, J. R. B., Gao, G., Widmer, J., Stapleton, D., Fernandez, C. S., Kemp, B. E., & Witters, L. A. (1996). Regulation of 5'-AMP-activated protein kinase activity by the noncatalytic beta and gamma subunits. *The Journal of Biological Chemistry*, *271*(30), 17798–17803. <https://doi.org/10.1074/JBC.271.30.17798>
- Eo, H., & Valentine, R. J. (2021). Imoxin inhibits tunicamycin-induced endoplasmic reticulum stress and restores insulin signaling in C2C12 myotubes. *American Journal of Physiology - Cell Physiology*, *321*(2), C221–C229. <https://doi.org/10.1152/ajpcell.00544.2020>
- Flamment, M., Hajduch, E., Ferré, P., & Foufelle, F. (2012). New insights into ER stress-induced insulin resistance. *Trends in Endocrinology and Metabolism*, *23*(8), 381–390. <https://doi.org/10.1016/j.tem.2012.06.003>
- Gallot, Y. S., & Bohnert, K. R. (2021). Confounding roles of er stress and the unfolded protein response in skeletal muscle atrophy. *International Journal of Molecular Sciences*, *22*(5), 1–18. <https://doi.org/10.3390/ijms22052567>
- Hançer, N. J., Qiu, W., Cherella, C., Li, Y., Copps, K. D., & White, M. F. (2014). *Insulin and Metabolic Stress Stimulate Multisite Serine/Threonine Phosphorylation of Insulin Receptor Substrate 1 and Inhibit Tyrosine Phosphorylation* \*. <https://doi.org/10.1074/jbc.M114.554162>
- Hwang, S. L., Jeong, Y. T., Li, X., Kim, Y. D., Lu, Y., Chang, Y. C., Lee, I. K., & Chang, H. W. (2013). Inhibitory cross-talk between the AMPK and ERK pathways mediates endoplasmic reticulum stress-induced insulin resistance in skeletal muscle. *British*

*Journal of Pharmacology*, 169(1), 69–81. <https://doi.org/10.1111/bph.12124>

Kim, M. S., Hur, H. J., Kwon, D. Y., & Hwang, J. T. (2012). Tangeretin stimulates glucose uptake via regulation of AMPK signaling pathways in C2C12 myotubes and improves glucose tolerance in high-fat diet-induced obese mice. *Molecular and Cellular Endocrinology*, 358(1), 127–134. <https://doi.org/10.1016/j.mce.2012.03.01>

Nakashima, N., Sharma, P. M., Imamura, T., Bookstein, R., & Olefsky, J. M. (2000). The tumor suppressor PTEN negatively regulates insulin signaling in 3T3-L1 adipocytes. *The Journal of Biological Chemistry*, 275(17), 12889–12895.

<https://doi.org/10.1074/JBC.275.17.12889>

O’neill, H. M. (2013). *AMPK and Exercise: Glucose Uptake and Insulin Sensitivity*. <https://doi.org/10.4093/dmj.2013.37.1.1>

Pessin, J. E., & Saltiel, A. R. (2000). Signaling pathways in insulin action: molecular targets of insulin resistance. *Journal of Clinical Investigation*, 106(2), 165. <https://doi.org/10.1172/JCI10582>

Quan, X., Wang, J., Liang, C., Zheng, H., & Zhang, L. (2015). Melatonin inhibits tunicamycin-induced endoplasmic reticulum stress and insulin resistance in skeletal muscle cells. *Biochemical and Biophysical Research Communications*, 463(4), 1102–1107. <https://doi.org/10.1016/J.BBRC.2015.06.065>

Rayavarapu, S., Coley, W., & Nagaraju, K. (2012). Endoplasmic reticulum stress in skeletal muscle homeostasis and disease. *Current Rheumatology Reports*, 14(3), 238–243. <https://doi.org/10.1007/s11926-012-0247-5>

Sakamoto, K., McCarthy, A., Smith, D., Green, K. A., Hardie, D. G., Ashworth, A., & Alessi, D. R. (2005). Deficiency of LKB1 in skeletal muscle prevents AMPK activation and glucose uptake during contraction. *The EMBO Journal*, 24(10), 1810. <https://doi.org/10.1038/SJ.EMBOJ.7600667>

Takano, K., Tabata, Y., Kitao, Y., Murakami, R., Suzuki, H., Yamada, M., Iinuma, M., Yoneda, Y., Ogawa, S., & Hori, O. (2007). Methoxyflavones protect cells against endoplasmic reticulum stress and neurotoxin. *American Journal of Physiology - Cell Physiology*, 292(1), 353–361.

[https://doi.org/10.1152/AJPCELL.00388.2006/SUPPL\\_FILE/FIGURE](https://doi.org/10.1152/AJPCELL.00388.2006/SUPPL_FILE/FIGURE)

- Thoma, A., Lyon, M., Al-Shanti, N., Nye, G. A., Cooper, R. G., & Lightfoot, A. P. (2020). Eukarion-134 attenuates endoplasmic reticulum stress-induced mitochondrial dysfunction in human skeletal muscle cells. *Antioxidants*, 9(8), 1–19. <https://doi.org/10.3390/antiox9080710>
- Thong, F. S. L., Bilan, P. J., & Klip, A. (2007). The Rab GTPase-Activating Protein AS160 Integrates Akt, Protein Kinase C, and AMP-Activated Protein Kinase Signals Regulating GLUT4 Traffic. *Diabetes*, 56, 414–423. <https://doi.org/10.2337/db06-0900>
- Treebak, J. T., Glund, S., Deshmukh, A., Klein, D. K., Long, Y. C., Jensen, T. E., Jørgensen, S. B., Viollet, B., Andersson, L., Neumann, D., Wallimann, T., Richter, E. A., Chibalin, A. V., Zierath, J. R., & Wojtaszewski, J. F. P. (2006). *AMPK-Mediated AS160 Phosphorylation in Skeletal Muscle Is Dependent on AMPK Catalytic and Regulatory Subunits*. <https://doi.org/10.2337/db06-0175>
- Urano, F., Wang, X. Z., Bertolotti, A., Zhang, Y., Chung, P., Harding, H. P., & Ron, D. (2000). Coupling of stress in the ER to activation of JNK protein kinases by transmembrane protein kinase IRE1. *Science (New York, N.Y.)*, 287(5453), 664–666. <https://doi.org/10.1126/SCIENCE.287.5453.664>
- Woods, A., Dickerson, K., Heath, R., Hong, S. P., Momcilovic, M., Johnstone, S. R., Carlson, M., & Carling, D. (2005). Ca<sup>2+</sup>/calmodulin-dependent protein kinase kinase-beta acts upstream of AMP-activated protein kinase in mammalian cells. *Cell Metabolism*, 2(1), 21–33. <https://doi.org/10.1016/J.CMET.2005.06.005>

# **Chapter 4 A**

**Effect of Tangeretin on ER stress  
induced mitochondrial alterations in L6  
cells**

#### **4A.1 Introduction**

The ER and mitochondria are both dynamic organelles that undergo changes in morphology and function in response to cellular stresses. Around 20% of the mitochondrial surface is in direct contact with the ER via the MAMs which implies that ER stress and maladaptive UPR can exert debilitating consequences on the mitochondrial function (Kornmann et al., 2009). Mitochondria are rightly termed the powerhouses of the cells. They are involved in various functions such as energy metabolism through ATP production, regulation of cellular apoptosis, calcium homeostasis, and ROS generation (Wai & Langer, 2016). ER stress conditions result in exacerbated mitochondrial ROS which contribute to mitochondrial dysfunction. Elevated mitochondrial ROS is a consequence of the ER calcium leak into the mitochondria via the protein channels namely the IP<sub>3</sub>R and ryanodine receptors (RYR) at the MAM junction (Zeeshan et al., 2016). The upregulated ROS alters the metabolism and interferes with mitochondrial respiration resulting in altered electron transport chain (ETC) complex activities and disrupted ATP production (Tirichen et al., 2021). Mitochondrial ROS also affects mitochondrial dynamics and promotes fragmentation (X. Li et al., 2013).

The dynamic nature of mitochondria comprises fission and fusion processes which are essential for facilitating the exchange of information and content between different mitochondria and maintaining mitochondrial function (Chan, 2020). Under physiological conditions, a balanced fusion and fission cycle are essential for ensuring mitochondrial quality, and disturbances in this equilibrium can lead to several pathologies including diabetes, myopathies, neurological disorders, and cardiomyopathies (Djalalvandi & Scorrano, 2022; Ojaimi et al., 2022; Rovira-Llopis et al., 2017). Mitochondrial fission is associated with the growth and division of mitochondria while fusion is involved in

elongation and promotes an interconnected mitochondrial network. The fusion and fission events are controlled by the highly conserved dynamin family of GTPases which include the optic atrophy 1 (OPA1) on the inner mitochondrial membrane and mitofusin 1/2 (MFN1/2) on the outer mitochondrial membrane for mediating fusion whereas dynamin-related protein 1 (DRP1) and mitochondrial fission protein (FIS1) mediate the fission process (H. Chen & Chan, 2005). Prolonged ER stress is associated with escalated mitochondrial fission resulting in fragmentation and damaged mitochondria (Rocha et al., 2020). The dysfunctional mitochondria are then removed by a process known as mitophagy which involves engulfment by autophagosomes (Rovira-Llopis et al., 2017).

Between the ER and mitochondria, calcium is a key intracellular messenger that controls a variety of functions. ER mitochondria interaction is essential for maintaining the calcium homeostasis and any disruptions in their function can lead to calcium overload or depletion (Panda et al., 2021). Calcium is transported from the ER to mitochondria via the IP<sub>3</sub>R and RYR receptors at the MAMs junction and the transport is augmented in response to chronic ER stress resulting in excess mitochondrial calcium levels. Excess mitochondrial calcium is associated with increased ROS, opening of mitochondrial permeability transport pore, loss of membrane potential and apoptosis (Antonio Navarro-Langa et al., 2022). Interplay between ER stress, mitochondrial dysfunction and defects in MAMs organization can alter the calcium homeostasis which ultimately leads to insulin resistance (Figure.4A.1) (Wang et al., 2015).

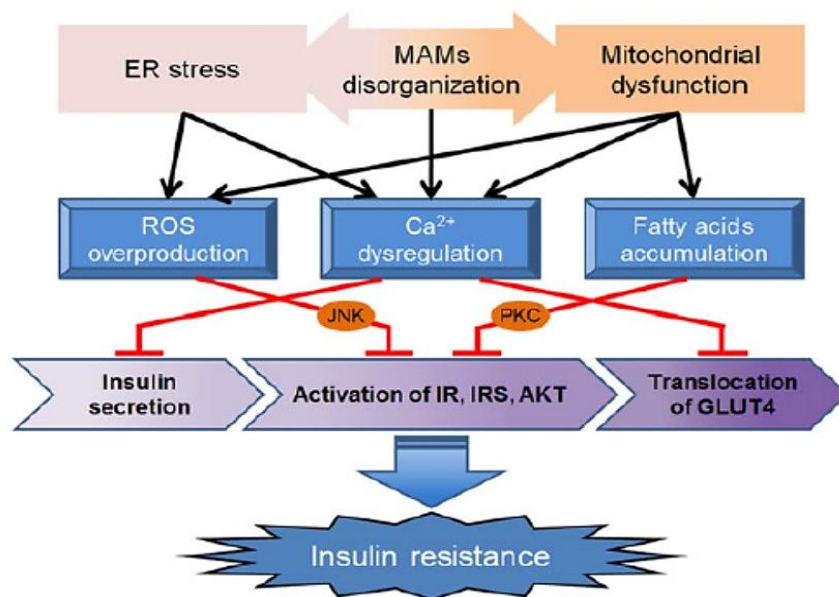


**Figure.4A.1. Interplay between ER stress, mitochondrial dysfunction and MAMs defect contribute to insulin resistance (Wang et al., 2015)**

The putative interdependence of the ER and mitochondria is well known due to their tethering at the MAMs region which harbours several proteins essential for regulating various processes in both organelles and hence, pharmacological manipulation of ER stress associated mitochondrial dysfunction can aid in development of better therapeutic strategies for diabetes management. Skeletal muscle is reported to be a highly energy consuming and metabolically active tissue, making it more susceptible to changes in mitochondrial function which mainly caters to the cellular energy demand (Ignatieva et al., 2021). Therefore, targeting the mitochondria can help in amelioration of muscle pathologies such as atrophy, a comorbidity associated with diabetes. In the present study, the potential of tangeretin in alleviation of tunicamycin induced mitochondrial alterations with emphasis on redox status, mitochondrial dynamics and MAM proteins in skeletal muscle L6 myotubes was studied.



## **4A.2 Materials & Methods**

### **4A.2.1 Chemicals**

DMEM containing 4.5g/L glucose and 1.5g/L sodium bicarbonate, fetal bovine serum, horse serum, antimycotic antibiotic mix, DMSO, triton X, glycine, tris base, skimmed milk, sodium dodecyl sulphate, HBSS was purchased from Himedia (Mumbai, India). Tangeretin, tunicamycin, PBA, HPLC grade methanol, protease inhibitor cocktail tablets were purchased from Sigma Aldrich Chemicals (St. Louis Missouri, USA). JC-1 staining kit, oxygen consumption kit was purchased from Cayman Chemicals (Michigan, USA). RIPA lysis buffer, BCA kit, Mito SOX dye, Mito tracker dye were purchased from Thermo Fisher Scientific (Waltham, Massachusetts, USA). The antibodies SOD1, SOD2, Fis1, Mfn2, Opa1, complex IV (COXIV), VDAC, GRP75, beta actin, Antirabbit and Antimouse HRP conjugated antibodies were purchased from Cell Signaling Technologies (Danvers, Massachusetts, USA). FUN14 Domain Containing 1 protein (FUNDC1), phosphofurin acidic cluster sorting protein 2 (PACS2), X-linked inhibitor of apoptosis protein (XIAP), cytochrome c (cyt c), IP<sub>3</sub>R were purchased from Gbiosciences (St. Louis MO, USA). Rat skeletal muscle cell lines, L6 myoblasts were procured from National Centre for Cell Sciences, Pune, India.

### **4A.2.2 Cell Culture**

L6 myoblasts were maintained in DMEM containing 10% fetal bovine serum and 1% antibiotic antimycotic mix at 37°C (5% carbon dioxide). Myoblasts were cultured to 80% confluency and the media was replaced with DMEM containing 2% horse serum to induce differentiation into myotubes. Alternative media change was given every 4 days to obtain differentiated myotubes. All of the experiments were carried out in differentiated myotubes.

### 4A.2.3 Experimental Groups

- **CON-** untreated or control cells
- **TM-** tunicamycin (0.25µg/ml) treated cells
- **TM+TAN-** tunicamycin (0.25µg/ml) & tangeretin (50µM) co-treated cells
- **TM+PBA-** tunicamycin (0.25µg/ml) & PBA (1mM) co-treated cells (Positive control)

### 4A.2.4 Experimental Design

The work flow of this chapter is represented schematically in Figure. 4A.2.

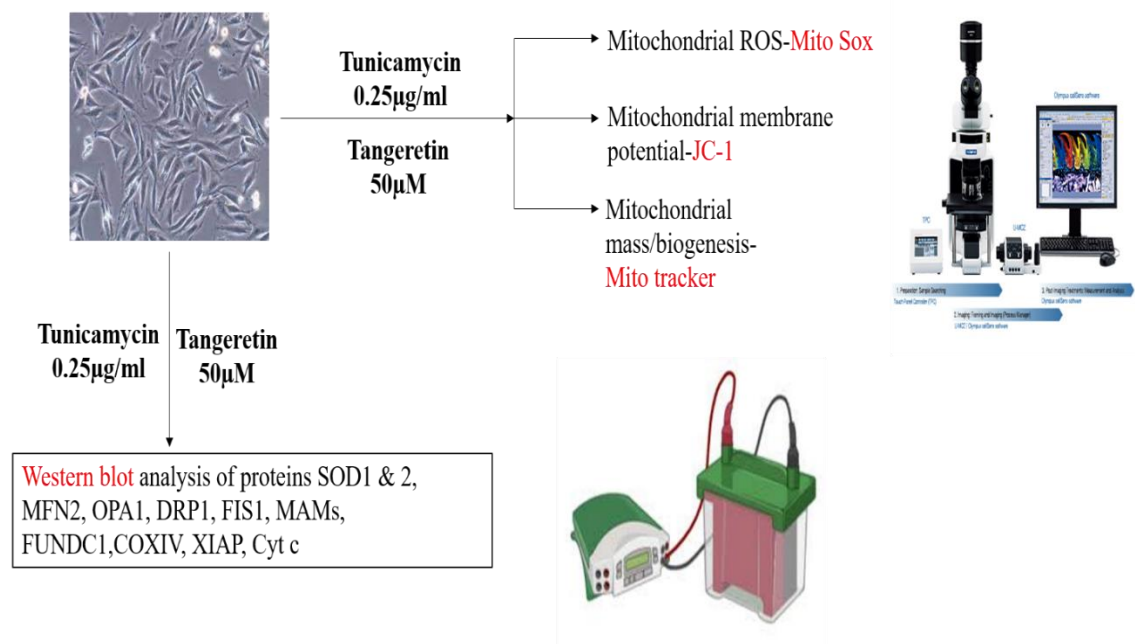


Figure.4A. 2. Schematic representation of the experimental design

### 4A.2.5 Intracellular mitochondrial ROS generation

L6 myoblasts were seeded in 96 well plates at  $5 \times 10^3$  density, the cells were then differentiated for four days and analysed for myotube formation. The myotubes were then treated with respective experimental groups for 24 hours followed by incubation with

5 $\mu$ M Mito SOX dye for 10-20 minutes. The cells were washed with HBSS, twice and taken for imaging in fluorescence microscope using TRITC filter and fluorescence intensity was quantitated using the cell sense software (Olympus Life Science, Japan).

#### **4A.2.6 Mitochondrial Biogenesis**

After 24 hours treatment with designated experimental groups, myotubes were incubated with 5 $\mu$ M Mito tracker red dye for 20 minutes followed by HBSS wash. Cells were then taken for imaging in fluorescence microscope using TRITC filter and fluorescence intensity was quantified using cell Sens software (Olympus Life Science, Japan).

#### **4A.2.7 Estimation of oxygen consumption rate**

L6 myoblasts were seeded in 96 well plate at a density of  $5 \times 10^3$ . After attaining 80% confluency, cells were differentiated by replacing the growth medium with medium containing 2% horse serum. Media change was given alternatively for four days following which, the myotubes were treated with the experimental groups for 24 hours. The oxygen consumption rate was then determined according to the manufacturer's protocol (Cayman Chemical, Michigan, USA). The spent culture medium was replaced with 150 $\mu$ l fresh medium. 10 $\mu$ l of Glucose oxidase and Antimycin A stock solution were added to the designated wells respectively. This was followed by addition of 10 $\mu$ l of phosphorescent oxygen probe solution. The cells were then overlaid with HS mineral oil. The plate was then read kinetically for  $\geq 120$  minutes in a plate reader (Tecan infinite 200 PRO, Austria).

#### **4A.2.8 Determination of mitochondrial membrane potential**

Myoblasts were seeded in 96 black-well plate and after reaching 80% confluency differentiation was induced. Myotubes were then treated with the experimental groups for 24 hours following which, cells were stained with JC-1 dye (Cayman Chemicals, USA) and kept in CO<sub>2</sub> incubator at 37 °C for 20 min. Fluorescence images were acquired in the

fluorescence microscope (Olympus Life Science, Japan). JC-1 exists as red aggregates in the mitochondria in normal conditions and it can be detected at an excitation/emission wavelength of 540/570 nm. In disease condition, JC-1 exists as green monomers in stressed conditions due to mitochondrial membrane potential dissipation. The green fluorescence can be detected at an excitation/emission of 485/535 nm and quantitated using Cell sense software (Olympus Life Science, Japan).

#### **4A.2.9 Western Blot studies**

L6 myoblasts were seeded in T25 flasks and grown to 80% confluency. The cells were then differentiated for 4 days followed by a 24-hour treatment with the experimental groups. Myotubes were then rinsed with HBSS and proteins were extracted using RIPA lysis buffer. Estimation and normalisation of the protein samples was done with BCA assay kit using BSA as the standard. Protein samples were separated on 10% sodium dodecyl sulphate polyacrylamide gels. Proteins were then transferred onto PVDF membranes (Millipore, Merck, USA) and blocked for 1 hour in 5% skimmed milk. Membranes were then washed thrice with TBST before being incubated at 4°C overnight with the appropriate primary antibodies SOD1, SOD2, Complex IV (COXIV), UCP3, MFN2, DRP1, FIS1, OPA1, IP3R, GRP75, VDAC, PACS2, FUNDC1, XIAP, cytochrome c (dilution 1:1000). Beta actin was used as the loading control. Membranes were then incubated with appropriate HRP conjugated secondary antibodies (dilution 1:1000 to 1:2000) for 2 to 3 hours at room temperature. The blot images were obtained by adding the ECL substrate (Thermo Fisher Scientific, Massachusetts, USA) to the membranes in Chemidoc MP Imaging systems (Bio-Rad, USA). The resultant bands were quantified by densitometric analysis using the Image lab software version 6.1 (Bio-Rad, USA).

#### **4A.2.10 Statistical analysis**

All experiments were performed independently in triplicates. The data were statistically analysed using one-way ANOVA and the Duncan post hoc test in the SPSS software. Each result is presented as a mean±SEM. In each trial, a p value of 0.05 or lower ( $p \leq 0.05$ ) was regarded as statistically significant.

### **4A.3 Results**

#### **4A.3.1 Tangeretin suppressed tunicamycin induced mitochondrial ROS generation and improved SOD levels**

Prolonged exposure of L6 myotubes to tunicamycin remarkably exacerbated the mitochondrial ROS production to 126.75% (643.9 a.u.) compared to the control group (508 a.u.) as evident from fluorescence images (Figure.4A.3a) and intensity histogram (Figure.4A.3b). Co-treatment with tangeretin and PBA significantly suppressed the levels to 98.03% (497.98 a.u.) and 103.26% (524.55 a.u.) respectively compared to tunicamycin treated group (Figure.4A.3a, b). SODs are part of the innate antioxidant system within the cells and are responsible for keeping the ROS levels under control. SOD1 is localized in the cytoplasm while SOD2 is localized in the mitochondria. In the present study, tunicamycin suppressed the levels of both SOD1 and SOD2 to 89.84% and 81.94% respectively as shown in Figure.4A.3c, d. Tangeretin co-treatment remarkably improved the levels of SOD1 to 108.03% and SOD2 to 98.53% while PBA co-treatment also improved the levels SOD1 to 105.48% and SOD2 to 96.2% respectively (Figure.4A.3c, d).

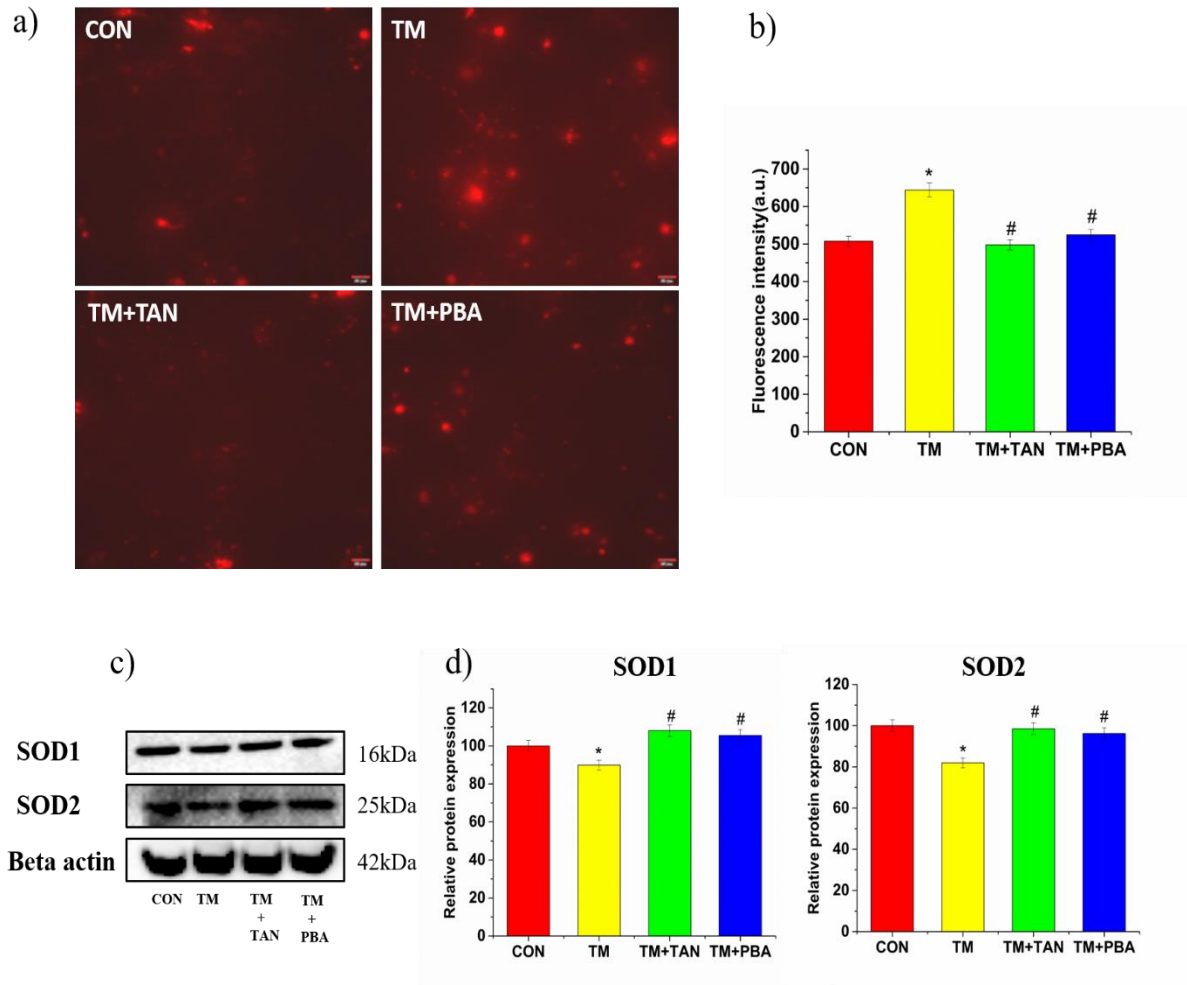


**Figure.4A.3. Effect of tangeretin on mitochondrial ROS generation and SOD1 and SOD2 expression levels during tunicamycin induced ER stress.** a) Mito SOX-stained fluorescence images. Magnification 20X. Scale corresponds to 20 $\mu$ m. b) Fluorescence intensity histogram in arbitrary units (a.u.). c) Western blot analysis of SOD1 and SOD2. The loading control was beta actin. d) Densitometric analysis of SOD1 and SOD2 normalised to beta actin. CON-untreated cells, TM-0.25 $\mu$ g/ml tunicamycin treatment, TM+TAN-0.25 $\mu$ g/ml tunicamycin tangeretin (50 $\mu$ M) co-treatment, TM+PBA-0.25 $\mu$ g/ml tunicamycin PBA (1mM) co-treatment. Values are expressed as mean $\pm$ SEM where n=3. \* $p\leq 0.05$  significantly different from control cells, # $p\leq 0.05$  significantly different from tunicamycin treated cells.

### **4A.3.2 Tunicamycin mediated mitochondrial alterations were independent of mitochondrial biogenesis/number, oxygen consumption rate and complex IV activity**

L6 myotubes treated with tunicamycin did not show any significant change in mitochondrial biogenesis/number compared to the control group following staining with Mito tracker red as seen in fluorescence images in Figure.4A.4a and intensity histogram in Figure.4A.4b. Similarly, co-treatment with tangeretin and PBA did not induce any remarkable change compared to control and tunicamycin treated cells (Figure.4A.4a, b). There was no significant variation in the oxygen consumption rate, an indicator of the oxidative phosphorylation or ETC, among the experimental groups as seen in the Figure.4A.4c. The COXIV levels, which facilitates the last step of ETC by reducing molecular oxygen to water was studied under ER stress. Tunicamycin treatment did not elicit any significant change in the activity compared to control as shown in Figure.4A.4d, e. Tangeretin and PBA co-treatment did not induce any significant change in the COXIV expression compared to control and tunicamycin treated cells (Figure.4A.4d, e). Here, the expression of the uncoupling protein, UCP3 was analysed and it was observed that in tunicamycin treated group, the expression escalated to 198.4% compared to untreated cells (Figure.4A.4d, e). Co-treatment with tangeretin and PBA augmented the levels to 258.6% and 223.2% respectively compared to tunicamycin treated cells as shown in Figure.4A.4d, e.

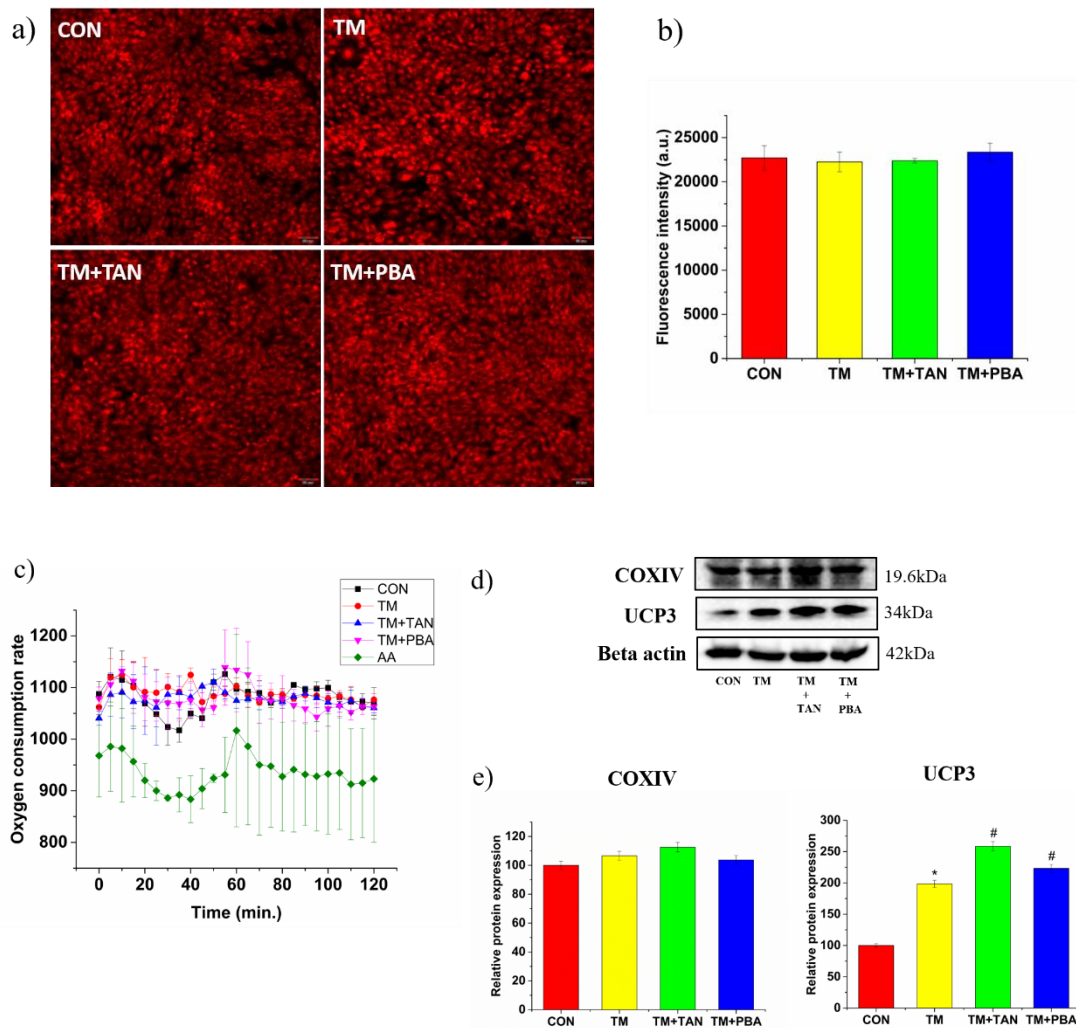


**Figure 4A.4. Mitochondrial biogenesis/number, oxygen consumption rate, COXIV and UCP3 expression under ER stress.** a) Mito tracker-stained fluorescence images. Magnification 20X. Scale corresponds to 20 $\mu$ m. b) Fluorescence intensity histogram in arbitrary units (a.u.). c) measurement of oxygen consumption rate kinetically. AA represents antimycin A, a blocker of oxidative phosphorylation. d) Western blot analysis of COXIV and UCP3. Beta actin was the loading control. e) Densitometric analysis of proteins normalised to beta actin. CON-untreated cells, TM-0.25 $\mu$ g/ml tunicamycin treatment, TM+TAN-0.25 $\mu$ g/ml tunicamycin tangeretin (50 $\mu$ M) co-treatment, TM+PBA-0.25 $\mu$ g/ml tunicamycin PBA (1mM) co-treatment. Values are expressed as mean $\pm$ SEM where n=3. \* $p\leq 0.05$  significantly different from control cells, # $p\leq 0.05$  significantly different from tunicamycin treated cells.



### **4A.3.3 Tangeretin reduced tunicamycin induced loss of mitochondrial membrane potential**

Here, changes in membrane potential were determined using the JC-1 staining dye. Under normal conditions JC-1 (cationic, lipophilic dye) enters the mitochondria and accumulates to form aggregates which emit fluorescence in the red spectrum. In unhealthy cells, JC-1 accumulates to a lesser extent as monomers inside the mitochondria due to loss of membrane potential and increased membrane permeability thereby emitting green fluorescence (Sivandzade et al. 2019). Chronic exposure to tunicamycin resulted in loss of membrane potential compared to the control. Co-treatment with tangeretin significantly improved the membrane potential (Figure.4A.5a). The red to green fluorescence ratio or the JC-1 aggregate to monomer ratio is an indicator for mitochondrial function. Treatment with tunicamycin, results in membrane depolarization as observed by significant decrease in percentage aggregate to monomer ratio to 60.5% (1.4702 ratio) compared to the control (2.4292 ratio). Remarkable improvement in aggregate to monomer percentage ratio to 96.2% (2.3392 ratio) was seen on treatment with tangeretin compared to tunicamycin treated cells. In PBA treated cells, the JC-1 aggregate to monomer percentage ratio was improved to 78.1% (1.8971 ratio) compared to tunicamycin treated group as depicted in Figure.4A.5b.

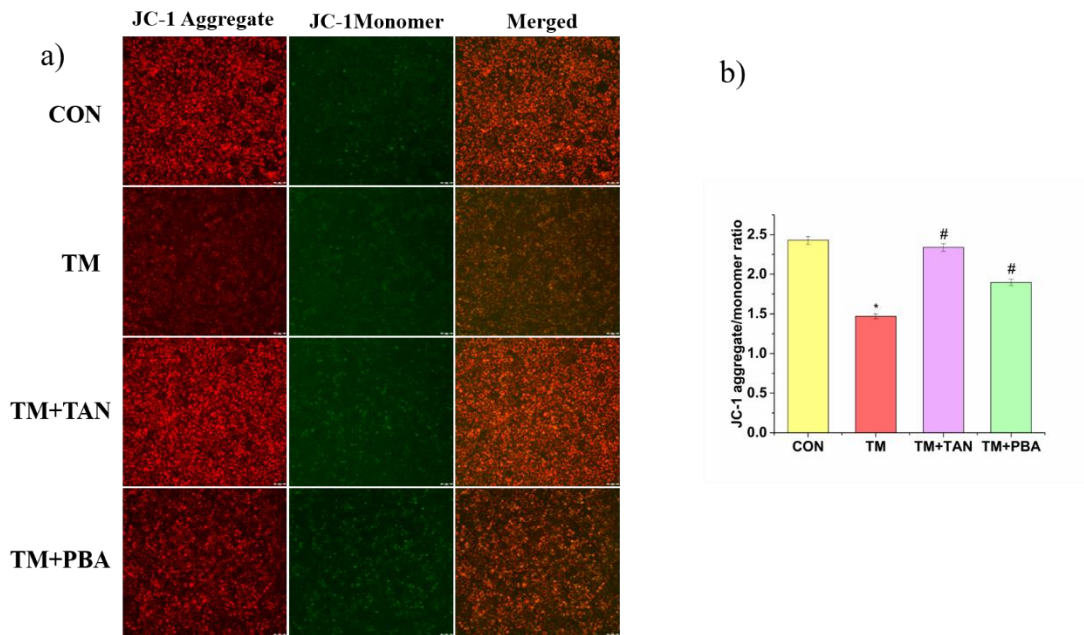


**Figure.4A.5. Tangeretin improves ER stress induced loss of mitochondrial membrane potential.** a) L6 myotubes after treatment with respective groups for 24 hrs were incubated with JC-1 staining solution for 20 min. Imaging was performed in fluorescence microscope. Magnification 20X. Scale corresponds to 50 $\mu$ m. b) Red to green fluorescent intensity ratio. CON-untreated cells, TM-0.25 $\mu$ g/ml tunicamycin treatment, TM+TAN-0.25 $\mu$ g/ml tunicamycin tangeretin (50 $\mu$ M) co-treatment, TM+PBA-0.25 $\mu$ g/ml tunicamycin PBA (1mM) co-treatment. Values are expressed as mean $\pm$ SEM where n=3. \* $p\leq 0.05$  significantly different from control cells, # $p\leq 0.05$  significantly different from tunicamycin treated cells.

#### 4A.3.4 Effect of tangeretin on mitochondrial dynamics during ER stress

Chronic exposure of L6 myotubes to tunicamycin resulted in significant upregulation of proteins involved in mitochondrial fusion and fission. MFN2 was upregulated to 126.11%, OPA1 to 124.01%, DRP1 to 144.1% and FIS1 to 153.9% respectively compared to the control (Figure.4A.6a, b). Co-treatment with tangeretin could not downregulate the MFN2 levels (125.04%), however, OPA1, DRP1 and FIS1 levels were reduced to 84.37%, 92.3% and 105.69% respectively compared to tunicamycin group as shown in Figure.4A.6a, b. PBA co-treatment significantly downregulated the MFN2

(80.44%), OPA1 (88.57%), DRP1 (78.42%) and Fis1(110.13%) respectively compared to tunicamycin group (Figure.4A.6a, b).

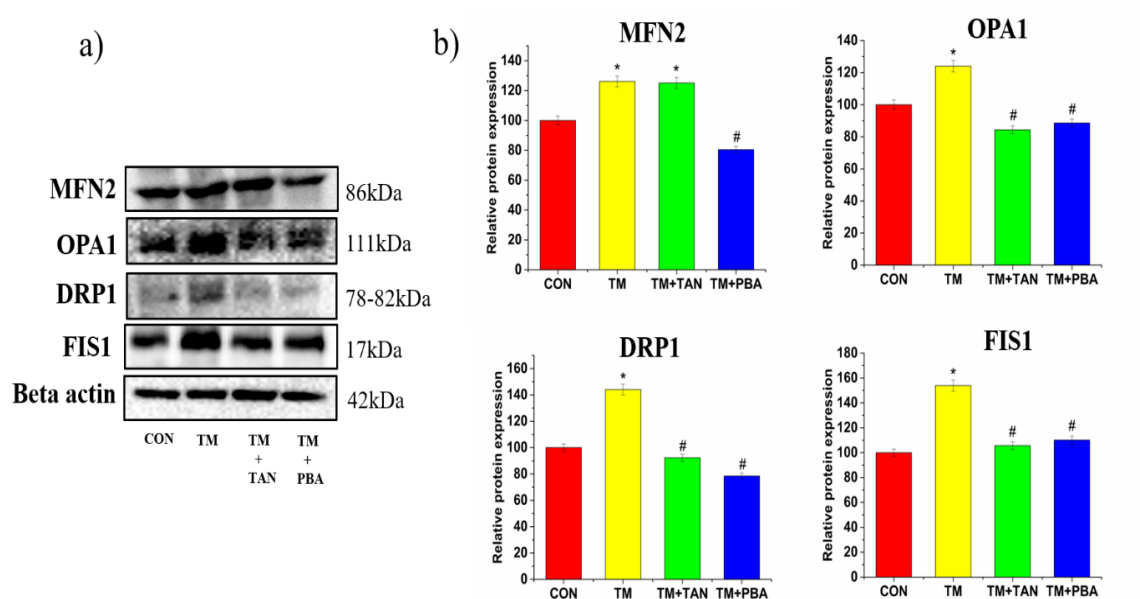


**Figure.4A.6. Effect of tangeretin on mitochondrial fusion and fission proteins under ER stress.** a) Western blot analysis of Mfn2, Opa1 and Fis1 with beta actin as loading control. b) Densitometric analysis of proteins normalised to beta actin. CON-untreated cells, TM-0.25 $\mu$ g/ml tunicamycin treatment, TM+TAN-0.25 $\mu$ g/ml tunicamycin tangeretin (50 $\mu$ M) co-treatment, TM+PBA-0.25 $\mu$ g/ml tunicamycin PBA (1mM) co-treatment. Values are expressed as mean $\pm$ SEM where n=3. \*p<0.05 significantly different from control cells, #p<0.05 significantly different from tunicamycin treated cells.

#### 4A.3.5 Effect of tangeretin on IP<sub>3</sub>R VDAC GRP75 complex at MAMs junction under ER stress

The IP<sub>3</sub>R, VDAC and GRP75 form a complex at the MAMs junction and are involved in the transport of calcium ions from the ER to the mitochondria. Chronic treatment with tunicamycin upregulated the IP<sub>3</sub>R moderately but not significantly to 112.36% compared

to untreated cells (Figure.4A.7a, b). VDAC and GRP75 expression was downregulated on treatment with tunicamycin treatment to 64.87% and 82.07% respectively compared to untreated cells (Figure.4A.7a, b). In tangeretin co-treated cells, IP<sub>3</sub>R levels were 107.66%, VDAC levels increased to 76.77% and GRP75 to 93.43% while in PBA co-treated cells, IP<sub>3</sub>R levels were 109.65%, VDAC levels were improved to 78.68% and GRP75 99.67% compared to the tunicamycin treated cells as depicted in Figure.4A.7a, b.

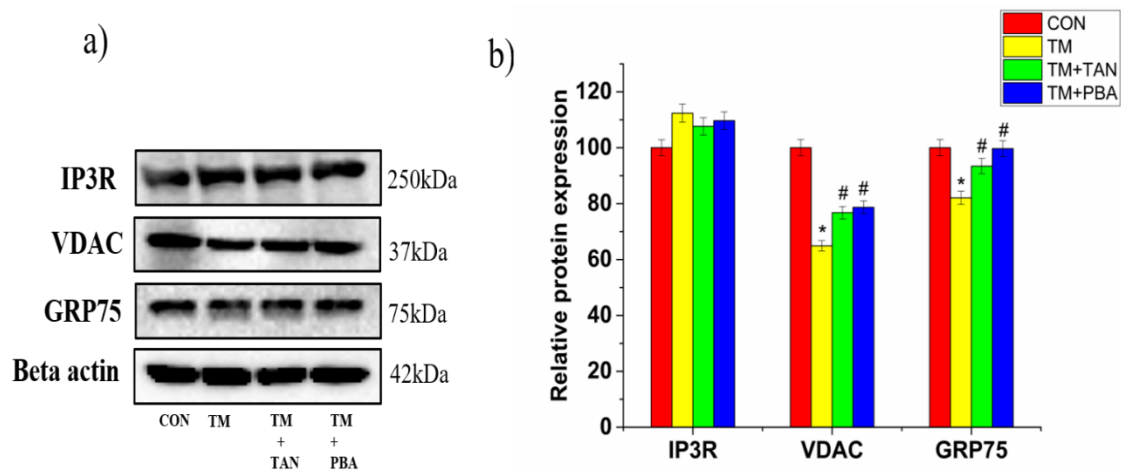


**Figure.4A.7. Effect of tangeretin on MAM proteins, IP<sub>3</sub>R, VDAC, GRP75 under ER stress.**

a) Western blot analysis of IP<sub>3</sub>R, VDAC and GRP75 with beta actin as loading control. b) Densitometric analysis of proteins normalised to Beta actin. CON-untreated cells, TM-0.25µg/ml tunicamycin treatment, TM+TAN-0.25µg/ml tunicamycin tangeretin (50µM) co-treatment, TM+PBA-0.25µg/ml tunicamycin PBA (1mM) co-treatment. Values are expressed as mean±SEM where n=3. \*p≤0.05 significantly different from control cells, #p≤0.05 significantly different from tunicamycin treated cells.

#### 4A.3.6 Tangeretin downregulates tunicamycin induced PACS2 and FUNDC1 levels

Treatment with tunicamycin significantly upregulated the levels of MAM proteins PACS2 and FUNDC1 as shown in Figure.4A.8a, b to 134.91% and 328.39% respectively

compared to untreated L6 cells. Co-treatment with tangeretin significantly brought down the levels of PACS2 to 112.23% and FUNDC1 to 171.85% while PBA treatment remarkably suppressed the PACS2 levels to 99.78% while augmenting FUNDC1 levels to 263.87% respectively compared to tunicamycin treated cells (Figure.4A.8a, b).

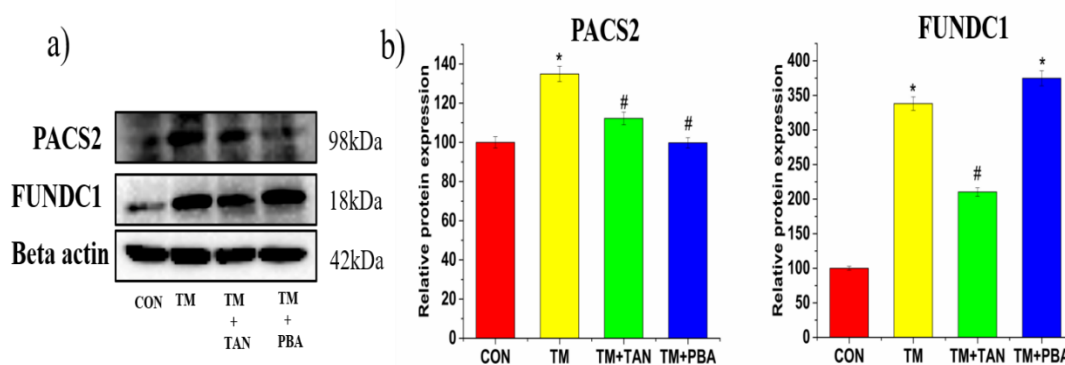


**Figure.4A.8. Tangeretin downregulates expression of MAM proteins PACS2 and FUNDC1 under ER stress condition.** a) Western blot analysis of PACS2 and FUNDC1 with beta actin as loading control. b) Densitometric analysis of proteins normalised to Beta actin. CON-untreated cells, TM-0.25 $\mu$ g/ml tunicamycin treated cells, TM+TAN-TM tangeretin (50 $\mu$ M) co-treatment, TM+PBA-TM 4-phenylbutyric acid (1mM) co-treatment. Values are expressed as mean $\pm$ SEM where n=3. \*p $\leq$ 0.05 significantly different from control cells, #p $\leq$ 0.05 significantly different from tunicamycin treated cells.

#### 4A.3.7 Effect of tangeretin on XIAP and cytochrome c levels under ER stress

Under ER stress, XIAP, an anti-apoptotic factor was observed to be upregulated to 172.57% and cyt c, a component of the intrinsic apoptotic pathway was upregulated slightly but insignificantly (104.35%) on exposure to tunicamycin compared to control group (Figure.4A.9a, b). In tangeretin treated cells, XIAP expression was downregulated to 139.91% while cyt c levels were brought down to 92.44% compared to tunicamycin

treated group (Figure.4A.9a, b). In PBA treated cells, XIAP levels were downregulated to 139.27% and cyt c levels to 100.99% compared to tunicamycin treated group as shown in Figure.4A.9a, b.

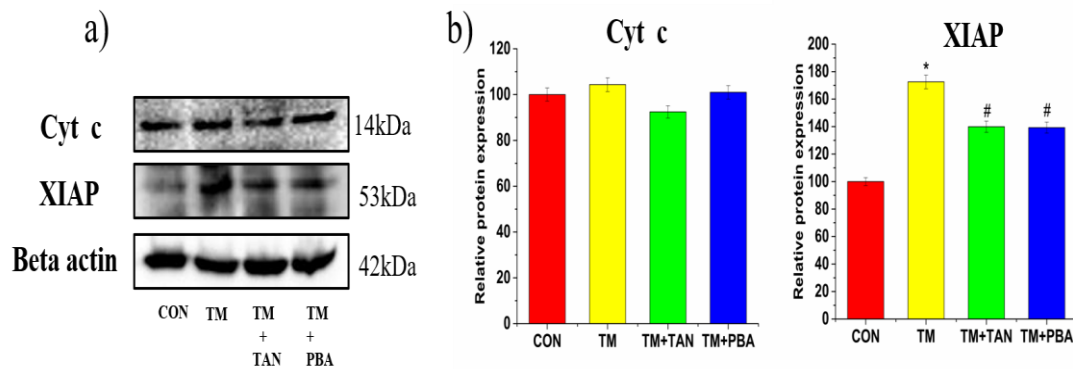


**Figure.4A.9. Effect of tangeretin on XIAP and cyt c levels under ER stress.** a) Western blot analysis of XIAP and cyt c with beta actin as loading control. b) Densitometric analysis of proteins normalised to beta actin. CON-untreated cells, TM-0.25 $\mu$ g/ml tunicamycin treatment, TM+TAN-0.25 $\mu$ g/ml tunicamycin tangeretin (50 $\mu$ M) co-treatment, TM+PBA-0.25 $\mu$ g/ml tunicamycin PBA (1mM) co-treatment. Values are expressed as mean $\pm$ SEM where n=3. \*p $\leq$ 0.05 significantly different from control cells, #p $\leq$ 0.05 significantly different from tunicamycin treated cells.

#### 4A.4 Discussion

In this study, the efficacy of tangeretin in alleviation of tunicamycin induced mitochondrial alterations was evaluated. Due to the close physical and functional interaction between ER and mitochondria, any disturbances in normal functioning of the former can negatively regulate the latter. Mitochondrial dysfunction is associated with skeletal muscle atrophy and insulin resistance and hence, investigating the related mechanisms can improve our understanding of these myopathologies (Genders et al., 2020; Hood et al., 2019; Lee et al., 2021; Romanello & Sandri, 2016). In the present study, the mitochondrial ROS production was studied since ER stress induced oxidative

stress and calcium influx are known to directly mediate the same (Cao & Kaufman, 2014). Within the mitochondria, oxidative phosphorylation coupled to ATP production facilitated by O<sub>2</sub> consumption serves as a source of ROS production. Aberrant generation of mitochondrial ROS is associated with oxidative damage of mitochondrial proteins, membranes, DNA that hamper its metabolic functions and subsequently activate the apoptotic machinery by releasing cytochrome c into the cytosol (Murphy, 2009). Mitochondrial ROS is mainly in the form of superoxide ion and under physiological conditions it is scavenged by SODs, catalase, glutathione peroxidase, thioredoxin peroxidase, thioredoxin 2, glutaredoxin 2, complex IV, coenzyme Q and oxidised cytochrome c (Bou-Teen et al., 2021). SOD2 is localized in the mitochondrial matrix and actively involved in converting superoxide ions to hydrogen peroxide that is then reduced to water by catalases and glutathione peroxidases (Flynn & Melov, 2013). Here, in this study, exposure to tunicamycin augmented the mitochondrial ROS production which was accompanied by concomitant decrease in SOD1 and SOD2 expression levels. Tangeretin suppressed the ROS levels within the mitochondria by improving the SOD1 and SOD2 levels.

Next, the mitochondrial number/biogenesis was analysed by staining the L6 myotubes with Mito Tracker dye. It was observed that exposure to tunicamycin did not induce any remarkable change in the mitochondrial number/biogenesis. Similarly, co-treatment with tangeretin also did not induce any significant changes as well. This is in agreement with Lightfoot et al. who have demonstrated that incubation of C2C12 myotubes with tunicamycin did not induce any changes in genes associated with mitochondrial biogenesis (Lightfoot et al., 2018). The oxygen consumption rate which is a measure of cellular metabolism and mitochondrial function was also studied (Divakaruni & Jastroch, 2022). The oxygen consumption occurs during the oxidative phosphorylation and

involves the reduction of O<sub>2</sub> to drive the generation of ATP. The oxidative phosphorylation can be divided into two processes, namely the mitochondrial ETC and chemiosmosis (Ahmad et al., 2022). The ETC consists of four protein complexes (I, II, III, IV) that facilitate electron transfer through redox reactions for generating an electrochemical gradient for energy release which is utilised to generate a proton gradient that can be used for generation of ATP through the final complex V/ATP synthase (Deshpande & Mohiuddin, 2022). Here, treatment with tunicamycin did not induce any significant change in the oxygen consumption rate. This is in contradiction to prior reports in myotubes where oxygen consumption rate was significantly altered on exposure to tunicamycin. This could be because those studies had used sensitive instruments namely oxytherm clark electrode and seahorse extracellular flux analyser respectively for measurement of different parameters of oxygen consumption rate including respiratory control ratio, phosphate oxygen ratio, basal respiration, maximal respiration, non-mitochondrial respiration and spare respiratory capacity (Lightfoot et al., 2018; Thoma et al., 2020).

On the other hand, in the current study, a simple kit-based method using a phosphorescent oxygen probe solution was used to monitor the oxygen consumption rate changes over a period of 2 hours. The subtoxic dose of tunicamycin used here, may not have been sufficient to elicit a detectable difference over limited period of time. This study is limited by the lack of detailed estimation of the oxygen consumption rate parameters that may have yielded a better analysis. To confirm the findings here, protein expression study of COXIV or cytochrome c oxidase which is responsible for consumption of O<sub>2</sub> by its reduction to water by transfer of electrons from cytochrome c to O<sub>2</sub>, the last electron acceptor of ETC was studied (Deshpande & Mohiuddin, 2022). Here, synonymous with oxygen consumption rate, the COXIV expression did not show any significant difference



between the experimental groups indicating that tunicamycin at the dose and duration used in this study induced mitochondrial dysfunction independent of the mitochondrial biogenesis, the overall oxygen consumption rate and COXIV activity.

Under stress conditions, mitochondria undergo uncoupling, a phenomenon involving dissociation of oxidative phosphorylation from ATP synthesis which is mediated by uncoupling proteins (UCPs) and specifically UCP3 in skeletal muscle cells (Cadenas, 2018). Uncoupling can be an adaptive mechanism against increased ROS production (R. Z. Zhao et al., 2019). Here, chronic treatment of myotubes with tunicamycin augmented the UCP3 expression that was further exacerbated on co-treatment with tangeretin. This increase could be a protective mechanism for suppressing the increased ROS levels.

The depolarization of mitochondrial membrane is an indicator of mitochondrial malfunction (Sivandzade et al., 2019). Data from atrophying muscles revealed reduced mitochondrial membrane potential and compromised mitochondria quality (Li Ji et al., 2019). From the results, here, it is evident that tunicamycin induced a loss of potential or membrane depolarisation which was improved on treatment with tangeretin.

Here, the expression of proteins involved in mitochondrial fusion and fission in L6 myotubes under ER stress was evaluated. The mitochondrial fusion proteins, MFN2 and OPA1 as well as the fission proteins, DRP1 and FIS1 were exacerbated on treatment with tunicamycin. This is in agreement with Thoma et al., who have reported an increase in fusion and fission processes in myotubes on exposure to tunicamycin (Thoma et al., 2020). Overexpression of MFN2 enhances the ER mitochondria tethering promoting mitochondrial calcium uptake (Han et al., 2021). OPA1 is involved in preserving the inner mitochondrial membrane and cristae (fold in the inner mitochondrial membrane) structure and function (Jang & Javadov, 2020). The overexpression may increase mitochondrial

network formation but may not necessarily protect against apoptosis (L. Chen et al., 2009). DRP1 overexpression is associated with impaired skeletal muscle development and also known to contribute to insulin resistance in obese and type 2 diabetic animal models (Touvier et al., 2015). Excess stress exacerbates the ROS levels that may lead to abnormal mitochondrial dynamics. FIS1 upregulation is involved in mitochondrial fragmentation, mitophagy, apoptosis and enhanced calcium flux and it also contributes to diabetic progression (Kelvin Ihenacho et al., 2021). Upregulation of fusion under excess stress may indicate highly fused mitochondrial network with compromised function and upregulated fission may indicate mitochondrial fragmentation with damaged mitochondria (Ren et al., 2020). Tangeretin could not lower the MFN2 levels, however, OPA1, DRP1 and FIS1 were suppressed on co-treatment indicating its potential in modulating mitochondrial dynamics under ER stress condition.

The expression of the proteins at the MAMs junction on exposure of L6 myotubes to tunicamycin was evaluated in this study. On treatment with tunicamycin, the IP<sub>3</sub>R levels were slightly upregulated, while the VDAC and GRP75 levels were suppressed. The IP<sub>3</sub>R VDAC and GRP75 form a complex at MAMs junction that facilitates the transport of calcium from the ER to mitochondria with VDAC at the outer mitochondrial membrane being tethered to the IP<sub>3</sub>R via the chaperone GRP75 (Basso et al., 2020; Pauly et al., 2017). Decreased IP<sub>3</sub>R VDAC GRP75 interaction in muscle cells was observed on exposure to tunicamycin and reported in muscle dystrophy (Pauly et al., 2017). Suppressed GRP75 was reported in insulin resistant *in vitro* and *in vivo* models and its upregulation led to improved insulin sensitivity and improved mitochondrial function (Q. Zhao et al., 2022). Here, Tangeretin did not significantly alter the IP<sub>3</sub>R levels, however, VDAC and GRP75 expression were improved indicating an improvement in mitochondrial function.

In the current study, the expression levels of MAM proteins PACS2 and FUNDC1 in L6 myotubes in response to tunicamycin treatment was determined. Here, both the proteins were found to be upregulated under prolonged ER stress condition and these were suppressed on co-treatment with tangeretin. PACS2 is a key regulator of MAMs that is required for membrane trafficking, calcium signaling, apoptosis and autophagy (C. Li et al., 2020). Enhanced PACS2 was shown to be associated with obesity, insulin resistance and mitochondrial dysfunction in *in vivo* models and knockdown of PACS2 was demonstrated to improve insulin sensitivity and mitochondrial function (Arruda et al., 2014). FUNDC1 located on the outer mitochondrial membrane is involved in mitophagy and found to be increased at MAMs regions under stress conditions (G. Li et al., 2021). FUNDC1 is also known to disrupt calcium homeostasis, augment mitochondrial fission and ROS generation (Liu et al., 2022). Both PACS2 and FUNDC1 under stress conditions contribute to metabolic syndrome and hence, these can be promising therapeutic targets for disease intervention.

Cytochrome c is a mitochondrial protein that participates in the electron transfer in the ETC (Hüttemann et al., 2010). Dysfunctional or damaged mitochondria are known to release cytochrome c into the cytosol, where it facilitates induction of apoptosis protease activating factor 1 (APAF1) which is required for maturation of caspases triggering the intrinsic pathway of apoptosis (Garrido et al., 2006). In this study, the expression levels of cytochrome c on chronic treatment with tunicamycin was monitored and it was observed that the expression levels were only slightly upregulated. This could be due to the subtoxic dose of inducer used that is sufficient for inducing mitochondrial dysfunction but not apoptosis. Tangeretin co-treatment slightly suppressed the cytochrome c level indicating its potential in alleviating the mitochondrial dysfunction. Here, the expression of X-linked inhibitor of apoptosis protein (XIAP), an inhibitor of caspases 3 and 7 was

also studied (Scott et al., 2005). It was observed that prolonged exposure to tunicamycin significantly upregulated the XIAP levels indicating the increased stress levels in response to tunicamycin. Tangeretin brought down the XIAP levels which implies alleviation of the stress conditions.

#### **4A.5 Summary**

In the current study, the potential of tangeretin in ameliorating tunicamycin induced mitochondrial alterations was monitored with special emphasis on mitochondrial redox status, oxygen consumption, mitochondrial dynamics, membrane potential and MAMs protein expression. Tangeretin was able to improve the mitochondrial redox state by suppressing the mitochondrial ROS levels and upregulating the SOD levels. Tangeretin also aided in suppressing the mitochondrial fusion, fission, PACS2, FUNDC1 and improved VDAC, GRP75 and mitochondrial membrane potential. A schematic summary of the findings is depicted in Figure.4A.10. Mitochondrial dysfunction is a direct consequence of chronic ER stress and known to be associated with insulin resistance as well as muscle atrophy. Pharmacological intervention of the mitochondrial alterations can aid in development of better therapeutic strategies for disease management.



## References

- Ahmad, M., Wolberg, A., & Kahwaji, C. I. (2022). Biochemistry, Electron Transport Chain. *StatPearls*. <https://www.ncbi.nlm.nih.gov/books/NBK526105/>
- Antonio Navarro-Langa, J., Matuz-Mares, D., González-Andrade, M., Georgina Araiza-Villanueva, M., Magdalena Vilchis-Landeros, M., & Vázquez-Meza, H. (2022). *Mitochondrial Calcium: Effects of Its Imbalance in Disease*. <https://doi.org/10.3390/antiox11050801>
- Arruda, A. P., M Pers, B., Parlakgul, G., Guney, E., Inouye, K., & Hotamisligil, G. S. (2014). *Sci-Hub | Chronic enrichment of hepatic endoplasmic reticulum–mitochondria contact leads to mitochondrial dysfunction in obesity. Nature Medicine, 20(12), 1427–1435 | 10.1038/nm.3735*. Nature Medicine. <https://sci-hub.se/10.1038/nm.3735>
- Basso, V., Marchesan, E., & Ziviani, E. (2020). A trio has turned into a quartet: DJ-1 interacts with the IP3R-Grp75-VDAC complex to control ER-mitochondria interaction. *Cell Calcium, 87*, 102186. <https://doi.org/10.1016/j.ceca.2020.102186>
- Bou-Teen, D., Kaludercic, N., Weissman, D., Turan, B., Maack, C., Di Lisa, F., & Ruiz-Meana, M. (2021). Mitochondrial ROS and mitochondria-targeted antioxidants in the aged heart. *Free Radical Biology and Medicine, 167*(March), 109–124. <https://doi.org/10.1016/j.freeradbiomed.2021.02.043>
- Cadenas, S. (2018). Mitochondrial uncoupling, ROS generation and cardioprotection. *Biochimica et Biophysica Acta - Bioenergetics, 1859*(9), 940–950. <https://doi.org/10.1016/j.bbabi.2018.05.019>
- Cao, S. S., & Kaufman, R. J. (2014). *Endoplasmic Reticulum Stress and Oxidative Stress in Cell Fate Decision and Human Disease*. <https://doi.org/10.1089/ars.2014.5851>
- Chan, D. C. (2020). Mitochondrial Dynamics and Its Involvement in Disease. *Annual Review of Pathology: Mechanisms of Disease, 15*, 235–259. <https://doi.org/10.1146/annurev-pathmechdis-012419-032711>
- Chen, H., & Chan, D. C. (2005). Emerging functions of mammalian mitochondrial fusion

- and fission. *Human Molecular Genetics*, 14 Spec No. 2(SUPPL. 2).  
<https://doi.org/10.1093/HMG/DDI270>
- Chen, L., Gong, Q., Stice, J. P., & Knowlton, A. A. (2009). Mitochondrial OPA1, apoptosis, and heart failure. *Cardiovascular Research*.  
<https://doi.org/10.1093/cvr/cvp181>
- Deshpande, O. A., & Mohiuddin, S. S. (2022). Biochemistry, Oxidative Phosphorylation. *StatPearls*. <https://www.ncbi.nlm.nih.gov/books/NBK553192/>
- Divakaruni, A. S., & Jastroch, M. (2022). *A practical guide for the analysis, standardization, and interpretation of oxygen consumption measurements*.  
<https://doi.org/10.1038/s42255-022-00619-4>
- Djalalvandi, A., & Scorrano, L. (2022). Mitochondrial dynamics: roles in exercise physiology and muscle mass regulation. *Current Opinion in Physiology*, 27, 100550.  
<https://doi.org/10.1016/J.COPHYS.2022.100550>
- Flynn, J. M., & Melov, S. (2013). SOD2 in mitochondrial dysfunction and neurodegeneration. *Free Radical Biology and Medicine*, 62, 4–12.  
<https://doi.org/10.1016/j.freeradbiomed.2013.05.027>
- Garrido, C., Galluzzi, L., Brunet, M., Puig, P. E., Didelot, C., & Kroemer, G. (2006). Mechanisms of cytochrome c release from mitochondria. *Cell Death and Differentiation*, 13(9), 1423–1433. <https://doi.org/10.1038/sj.cdd.4401950>
- Genders, A. J., Holloway, G. P., & Bishop, D. J. (2020). *Molecular Sciences Are Alterations in Skeletal Muscle Mitochondria a Cause or Consequence of Insulin Resistance?* <https://doi.org/10.3390/ijms21186948>
- Han, S., Zhao, F., Hsia, J., Ma, X., Liu, Y., Torres, S., Fujioka, H., & Zhu, X. (2021). The role of Mfn2 in the structure and function of endoplasmic reticulum-mitochondrial tethering in vivo. *Journal of Cell Science*, 134(13).  
<https://doi.org/10.1242/JCS.253443>
- Hood, D. A., Memme, J. M., Oliveira, A. N., & Triolo, M. (2019). The Annual Review of Physiology is online at. *Annu. Rev. Physiol*, 81, 19–41.  
<https://doi.org/10.1146/annurev-physiol-020518>
- Hüttemann, M., Pecina, P., Rainbolt, M., Sanderson ||, T. H., Kagan, V. E., Samavati, L.,

- Doan, J. W., & Lee, I. (2010). *The multiple functions of cytochrome c and their regulation in life and death decisions of the mammalian cell: from respiration to apoptosis*. <https://doi.org/10.1016/j.mito.2011.01.010>
- Ignatieva, E., Smolina, N., Kostareva, A., & Dmitrieva, R. (2021). Skeletal muscle mitochondria dysfunction in genetic neuromuscular disorders with cardiac phenotype. *International Journal of Molecular Sciences*, 22(14). <https://doi.org/10.3390/ijms22147349>
- Jang, S., & Javadov, S. (2020). OPA1 regulates respiratory supercomplexes assembly: The role of mitochondrial swelling. *Mitochondrion*, 51, 30–39. <https://doi.org/10.1016/J.MITO.2019.11.006>
- Kelvin Ihenacho, U., Meacham, K. A., Cleland Harwig, M., Widlansky, M. E., & Blake Hill, R. (2021). Mitochondrial Fission Protein 1: Emerging Roles in Organellar Form and Function in Health and Disease. *Frontiers in Endocrinology*. <https://doi.org/10.3389/fendo.2021.660095>
- Kornmann, B., Currie, E., Collins, S. R., Schuldiner, M., Nunnari, J., Weissman, J. S., & Walter, P. (2009). An ER-Mitochondria Tethering Complex Revealed by a Synthetic Biology Screen. *Science (New York, N.Y.)*, 325(5939), 477. <https://doi.org/10.1126/SCIENCE.1175088>
- Lee, H., Ha, T. Y., Jung, C. H., Nirmala, F. S., Park, S. Y., Huh, Y. H., & Ahn, J. (2021). Mitochondrial dysfunction in skeletal muscle contributes to the development of acute insulin resistance in mice. *Journal of Cachexia, Sarcopenia and Muscle*, 12(6), 1925–1939. <https://doi.org/10.1002/JCSM.12794>
- Li, C., Li, L., Yang, M., Zeng, L., & Sun, L. (2020). PACS-2: A key regulator of mitochondria-associated membranes (MAMs). <https://doi.org/10.1016/j.phrs.2020.105080>
- Li, G., Li, J., Shao, R., Zhao, J., & Chen, M. (2021). FUNDC1: A Promising Mitophagy Regulator at the Mitochondria-Associated Membrane for Cardiovascular Diseases. *Frontiers in Cell and Developmental Biology*, 9(December), 1–11. <https://doi.org/10.3389/fcell.2021.788634>
- Li Ji, L., Yeo, D., & Hood Canada, D. A. (2019). *Open Peer Review Mitochondrial*



*dysregulation and muscle disuse atrophy [version 1; peer review: 2 approved]*.  
<https://doi.org/10.12688/f1000research.19139.1>

Li, X., Fang, P., Mai, J., Choi, E. T., Wang, H., & Yang, X. F. (2013). Targeting mitochondrial reactive oxygen species as novel therapy for inflammatory diseases and cancers. *Journal of Hematology and Oncology*, 6(1), 1–19.  
<https://doi.org/10.1186/1756-8722-6-19>

Lightfoot, A. P., Morgan, R. S., Parkes, J. E., Thoma, A., Iwanejko, L. A., & Cooper, R. G. (2018). 17-(Allylamino)-17-demethoxygeldanamycin reduces Endoplasmic Reticulum (ER) stress-induced mitochondrial dysfunction in C2C12 myotubes. *BioRxiv*, 350702. <https://doi.org/10.1101/350702>

Liu, H., Zang, C., Yuan, F., Ju, C., Shang, M., Ning, J., Yang, Y., Ma, J., Li, G., Bao, X., & Zhang, D. (2022). The role of FUNDC1 in mitophagy, mitochondrial dynamics and human diseases. *Biochemical Pharmacology*, 197, 114891.  
<https://doi.org/10.1016/J.BCP.2021.114891>

Murphy, M. P. (2009). How mitochondria produce reactive oxygen species. *Biochemical Journal*, 417(Pt 1), 1. <https://doi.org/10.1042/BJ20081386>

Ojaimi, A., Salah, M. ;, El-Hattab, A. ;, Mitochondrial, A. W., Sarkadi, B., Al Ojaimi, M., Salah, A., & El-Hattab, A. W. (2022). *Citation: membranes Review Mitochondrial Fission and Fusion: Molecular Mechanisms, Biological Functions, and Related Disorders*. <https://doi.org/10.3390/membranes12090893>

Panda, S., Behera, S., Faraz, M., #a, A., & Hussain Syed, G. (2021). *Endoplasmic reticulum & mitochondrial calcium homeostasis: The interplay with viruses*.  
<https://doi.org/10.1016/j.mito.2021.03.008>

Pauly, M., Angebault-Prouteau, C., Dridi, H., Notarnicola, C., Scheuermann, V., Lacampagne, A., Matecki, S., & Fauconnier, J. (2017). ER stress disturbs SR/ER-mitochondria Ca<sup>2+</sup> + transfer: Implications in Duchenne muscular dystrophy. *Biochimica et Biophysica Acta - Molecular Basis of Disease*, 1863(9), 2229–2239.  
<https://doi.org/10.1016/j.bbadis.2017.06.009>

Ren, L., Chen, X., Chen, X., Li, J., Cheng, B., & Xia, J. (2020). Mitochondrial Dynamics: Fission and Fusion in Fate Determination of Mesenchymal Stem Cells. *Frontiers in*

*Cell and Developmental Biology*, 8(October), 1–18.

<https://doi.org/10.3389/fcell.2020.580070>

Rocha, M., Apostolova, N., Diaz-Rua, R., Muntane, J., & Victor, V. M. (2020). Mitochondria and T2D: Role of Autophagy, ER Stress, and Inflammasome. *Trends in Endocrinology and Metabolism*, 31(10), 725–741.

<https://doi.org/10.1016/j.tem.2020.03.004>

Romanello, V., & Sandri, M. (2016). Mitochondrial quality control and muscle mass maintenance. *Frontiers in Physiology*, 6(JAN), 1–21.

<https://doi.org/10.3389/fphys.2015.00422>

Rovira-Llopis, S., Bañuls, C., Diaz-Morales, N., Hernandez-Mijares, A., Rocha, M., & Victor, V. M. (2017). Mitochondrial dynamics in type 2 diabetes: Pathophysiological implications. *Redox Biology*, 11, 637–645.

<https://doi.org/10.1016/J.REDOX.2017.01.013>

Scott, F. L., Denault, J. B., Riedl, S. J., Shin, H., Renatus, M., & Salvesen, G. S. (2005). XIAP inhibits caspase-3 and -7 using two binding sites: evolutionarily conserved mechanism of IAPs. *The EMBO Journal*, 24(3), 645–655.

<https://doi.org/10.1038/SJ.EMBOJ.7600544>

Sivandzade, F., Bhalerao, A., & Cucullo, L. (2019). Analysis of the Mitochondrial Membrane Potential Using the Cationic JC-1 Dye as a Sensitive Fluorescent Probe. *Bio-Protocol*, 9(1). <https://doi.org/10.21769/BIOPROTOC.3128>

Thoma, A., Lyon, M., Al-Shanti, N., Nye, G. A., Cooper, R. G., & Lightfoot, A. P. (2020). Eukarion-134 attenuates endoplasmic reticulum stress-induced mitochondrial dysfunction in human skeletal muscle cells. *Antioxidants*, 9(8), 1–19.

<https://doi.org/10.3390/antiox9080710>

Tirichen, H., Yaigoub, H., Xu, W., Wu, C., Li, R., & Li, Y. (2021). Mitochondrial Reactive Oxygen Species and Their Contribution in Chronic Kidney Disease Progression Through Oxidative Stress. *Frontiers in Physiology*, 12, 627837.

<https://doi.org/10.3389/FPHYS.2021.627837/BIBTEX>

Touvier, T., De Palma, C., Rigamonti, E., Scagliola, A., Incerti, E., Mazelin, L., Thomas, J. L., D'Antonio, M., Politi, L., Schaeffer, L., Clementi, E., & Brunelli, S. (2015).

Muscle-specific Drp1 overexpression impairs skeletal muscle growth via translational attenuation. *Cell Death and Disease*, 6(2), 1–11. <https://doi.org/10.1038/cddis.2014.595>

Wai, T., & Langer, T. (2016). Mitochondrial Dynamics and Metabolic Regulation. *Trends in Endocrinology and Metabolism*, 27(2), 105–117. <https://doi.org/10.1016/j.tem.2015.12.001>

Wang, C. H., Tsai, T. F., & Wei, Y. H. (2015). Role of mitochondrial dysfunction and dysregulation of Ca<sup>2+</sup> homeostasis in insulin insensitivity of mammalian cells. *Annals of the New York Academy of Sciences*, 1350(1), 66–76. <https://doi.org/10.1111/nyas.12838>

Zeeshan, H. M. A., Lee, G. H., Kim, H. R., & Chae, H. J. (2016). Endoplasmic reticulum stress and associated ROS. *International Journal of Molecular Sciences*, 17(3), 1–20. <https://doi.org/10.3390/ijms17030327>

Zhao, Q., Luo, T., Gao, F., Fu, Y., Li, B., Shao, X., Chen, H., Zhou, Z., Guo, S., Shen, L., Jin, L., Cen, D., Zhou, H., Lyu, J., & Fang, H. (2022). GRP75 Regulates Mitochondrial-Supercomplex Turnover to Modulate Insulin Sensitivity. *Diabetes*, 71(2), 233–248. <https://doi.org/10.2337/db21-0173>

Zhao, R. Z., Jiang, S., Zhang, L., & Yu, Z. Bin. (2019). Mitochondrial electron transport chain, ROS generation and uncoupling (Review). *International Journal of Molecular Medicine*, 44(1), 3–15. <https://doi.org/10.3892/ijmm.2019.4188>

# **Chapter 4 B**

**Effect of Tangeretin on ER stress  
induced autophagy and ERAD signaling  
in L6 Cells**

## 4B.1 Introduction

One of the cellular responses during ER stress is the clearance of unfolded/misfolded protein load from the ER lumen. The two main protein degradation systems include the ERAD or UPS and the autophagy where the former involves the degradation of soluble, short-lived misfolded proteins while the latter degrades insoluble, long-lived protein aggregates and both the proteolytic systems know their targets through the ubiquitin tags (Kocaturk & Gozuacik, 2018). Disruption of calcium homeostasis is a significant trigger for both autophagy and ERAD owing to the abundance of calcium in the ER lumen (Daverkausen-Fischer & Pröls, 2022; Sun et al., 2016). The ER calcium homeostasis is maintained by ER  $\text{Ca}^{2+}$  uptake pump, SERCA, ER  $\text{Ca}^{2+}$  release channels,  $\text{IP}_3\text{R}$ , RYR, and  $\text{Ca}^{2+}$  binding proteins (Park et al., 2021). Suppression of the SERCA or overexpression of  $\text{IP}_3\text{R}$  or RYR leads to depletion of  $\text{Ca}^{2+}$  from the ER and this may lead to ER stress and subsequent activation of protein degradation (Vervliet, 2018; Wong et al., 2013).

Due to the error-prone nature of protein folding and the presence of proteotoxic stressors, cells have a protein quality control mechanism that is necessary for the clearance of misfolded proteins. Hence, with a delicate balance between protein synthesis and degradation, cells contain a proteostasis network that includes protein synthesis, folding, and quality control as depicted in Figure.4B.1 (Johnston & Samant, 2021). All proteins required for translation, chaperone proteins required for correct folding, the UPS, and the autophagy mechanisms that break down proteins are all part of this network (Whittemore et al., 2022).

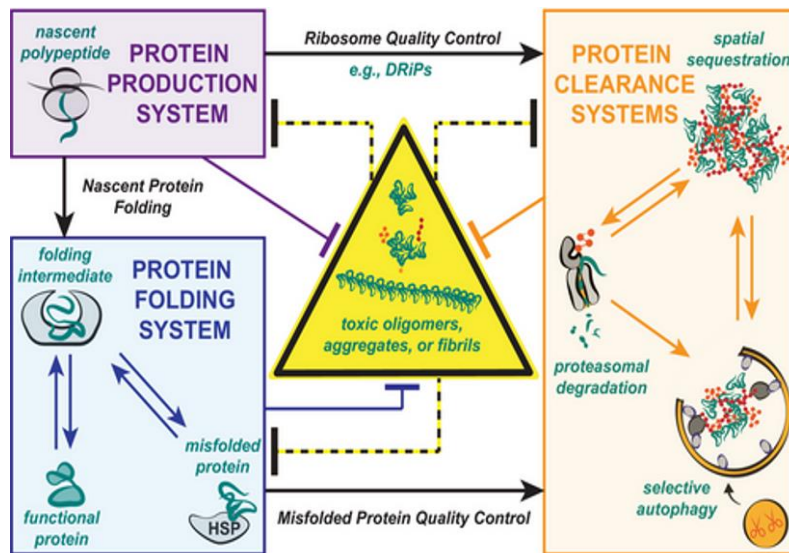


**Figure.4B.1. Delicate balance between protein synthesis, protein folding and quality control comprise the proteostasis network (Johnston & Samant, 2021)**

Protein folding and maturation in the ER involve oxidative and glycosylation changes that are intimately connected to the cell's metabolic state and this complex posttranslational processing of proteins makes the ER extremely susceptible to disruption of proteostasis networks (Medinas et al., 2021). During mild ER stress, the proteostasis network is maintained by an interplay between protein translation, chaperone activity, and degradation machinery promoting cellular adaptation (Hetz et al., 2020). However, unresolved ER stress leads to disruption of the proteostasis network which is linked to a number of diseases, including neurological disorders and muscular pathologies (Sandri, 2013; Whittemore et al., 2022). Skeletal muscle wasting which is a comorbidity associated with the diabetic condition is a serious ailment with no specific therapies and therefore, pharmacological manipulation of the proteostasis network may provide new strategies for disease management.

In atrophying muscles, increased proteolysis (autophagy and ERAD) are associated with enhanced loss of muscle mass (Sandri, 2013). Muscles from obese, insulin-resistant individuals displayed markers of metabolic stress, protein misfolding, and UPS, suggesting disruptions in the proteostasis network (Siekman et al., 2023). Autophagy plays a dubious role in insulin sensitivity as evident from two different reports that suggest contribution of exercise induced autophagy in protection against high fat diet induced glucose intolerance and amelioration of diet induced obesity and insulin resistance on muscle specific deletion of autophagy related gene Atg7 (He et al., 2012; Kim et al., 2013).

From the reports, it is evident that therapeutic strategies for improvement of muscle wasting as well as insulin sensitivity must focus on targeting the protein degradation systems. The present study attempted to unravel the potential of tangeretin in modulating the different proteins implicated in autophagy and ERAD pathways under ER stress in L6 myotubes.

## **4B.2 Materials & Methods**

### **4B.2.1 Chemicals**

DMEM containing 4.5g/L glucose and 1.5g/L sodium bicarbonate, fetal bovine serum, horse serum, antimycotic antibiotic mix, DMSO, triton X, glycine, tris base, skimmed milk, sodium dodecyl sulphate, HBSS were purchased from Himedia (Mumbai, India). Tangeretin, tunicamycin, PBA, HPLC grade methanol, protease inhibitor cocktail tablets were purchased from Sigma Aldrich Chemical (St. Louis Missouri, USA). RIPA lysis buffer, BCA kit, were purchased from Thermo Fisher Scientific (Waltham, Massachusetts, USA). The antibodies LC3, Beclin1, p-RYR1, GRP94, Calnexin, EDEM1, RNF5, SYVN1, UFD1, SEL1 and ATP2A2/SERCA2 were purchased from Gbiosciences (St. Louis MO, USA). HERPUD1, p-Akt, Akt, mTOR, beta actin, HRP

conjugated secondary antibodies, Antirabbit Alexa fluor conjugated antibodies were purchased from Cell Signaling Technologies (Danvers, Massachusetts, USA). Rat skeletal muscle cell lines, L6 myoblasts were procured from National Centre for Cell Sciences, Pune, India.

#### **4B.2.2 Cell Culture**

L6 myoblasts were maintained in DMEM containing 10% fetal bovine serum and 1% antibiotic antimycotic mix at 37°C (5% carbon dioxide). Myoblasts were cultured to 80% confluency and growth medium was replaced with DMEM containing 2% horse serum to induce differentiation. Alternative media change was given for 4 days to obtain differentiated myotubes. All the experiments were carried out in differentiated myotubes.

#### **4B.2.3 Experimental Groups**

- **CON-** untreated or control cells
- **TM-** tunicamycin (0.25µg/ml) treated cells
- **TM+TAN-** tunicamycin (0.25µg/ml) & tangeretin (50µM) co-treated cells
- **TM+PBA-** tunicamycin (0.25µg/ml) & PBA (1mM) co-treated cells (Positive control)

#### **4B.2.4 Experimental Design**

The workflow of this chapter is represented in Figure.4B.2.



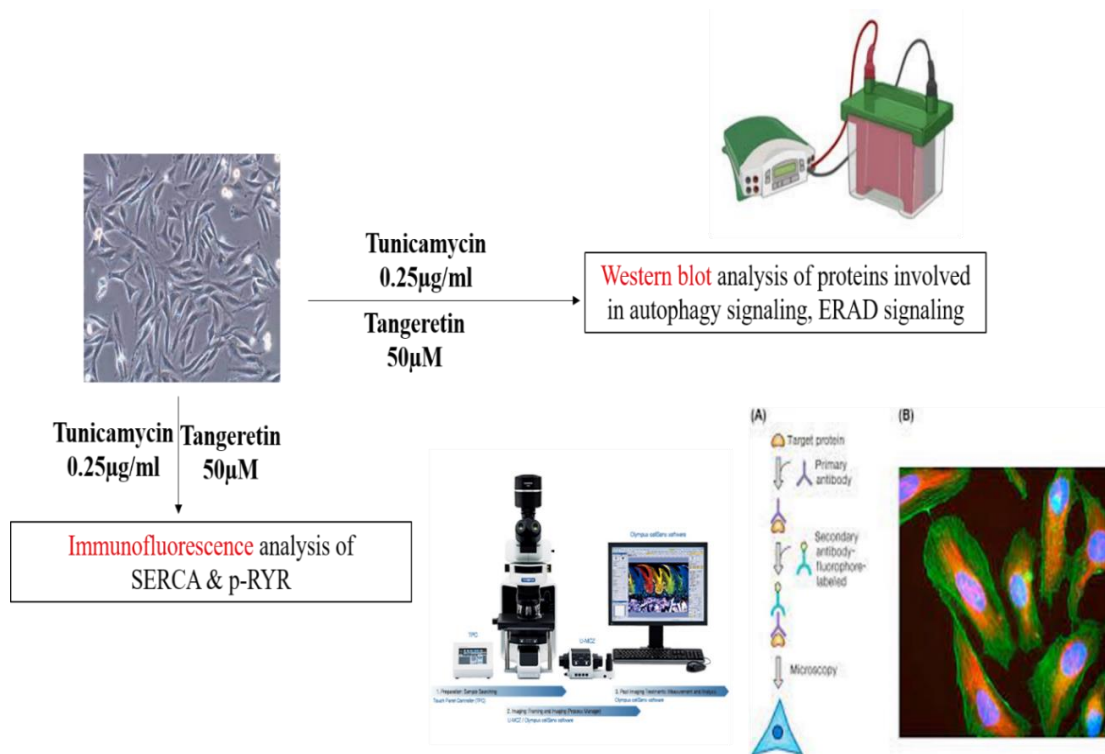


**Figure.4B.2. Schematic representation of the experimental design**

#### 4B.2.5 Western Blot studies

L6 myoblasts were seeded in T25 flasks and grown to 80% confluency. The cells were then differentiated for 4 days followed by a 24-hour treatment with the experimental groups. Myotubes were then rinsed with HBSS and proteins were extracted using RIPA lysis buffer. Using the BCA assay kit and BSA as the standard, the extracted protein samples were quantitated and normalised. Protein samples were separated on 10% sodium dodecyl sulphate polyacrylamide gels. Proteins were then transferred onto PVDF membranes (Millipore, Merck, USA) and blocked for 1 hour in 5% skimmed milk. Membranes were then washed thrice with TBST before being incubated with the appropriate primary antibodies LC3, Beclin1, p-Akt, Akt, mTOR, Calnexin, GRP94, EDEM1, HERPUD1, RNF5, SYVN1, UFD1, SEL1, ATP2A2/SERCA2, beta actin (dilution 1:1000) at 4°C overnight with agitation. This was followed by incubation of

membranes for 2 to 3 hours at room temperature with the appropriate HRP-conjugated secondary antibodies (dilution 1:1000 to 1:2000). The blot images were obtained by adding the ECL substrate (Thermo Fisher Scientific, Massachusetts, USA) to the membranes in Chemidoc MP Imaging systems (Bio-Rad, USA). The resultant bands were quantified by densitometric analysis using the Image lab software version 6.1 (Bio-Rad, USA).

#### **4B.2.6 Immunofluorescence studies**

After the treatment period, cells were fixed in 4% paraformaldehyde solution for 15 minutes followed by permeabilization in 0.1% Triton X for 10 minutes. Fixed cells were then incubated with the following antibodies, SERCA (1:400) and p-RYR (1:400) antibodies, respectively. This was followed by incubation with a specific secondary antibody conjugated with Alexa fluor (1:500). The fluorescence images were acquired using a fluorescence microscope (Olympus Life Science, Japan).

#### **4B.2.7 Statistical analysis**

The triplicates of each experiment were run independently. The one-way ANOVA and Duncan post hoc test in the SPSS software was used to statistically analyze the data that is represented as mean $\pm$ SEM. Each trial with a p-value of 0.05 or less ( $p\leq 0.05$ ) was considered statistically significant.

### **4B.3 Results**

#### **4B.3.1 Tangeretin abrogates tunicamycin induced autophagy in L6 myotubes**

ER stress triggers autophagy for the clearance of misfolded proteins. Here, in this study prolonged exposure to tunicamycin, resulted in significant upregulation of autophagy proteins LC3-II (121.21%) and Beclin1 (125.55%) compared to the control cells as

depicted in Figure.4B.3a, b. Co-treatment with tangeretin remarkably suppressed the LC3-II levels to 102.34% and Beclin1 levels to 95.34% while PBA treatment decreased the LC3-II expression to 91.88% and Beclin1 to 69.43% compared to tunicamycin treated cells (Figure.4B.3a, b).

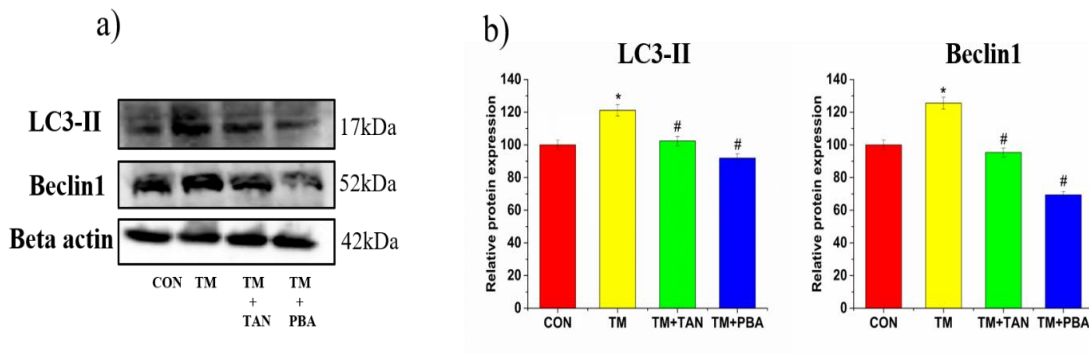


**Figure.4B.3. Tangeretin abrogates tunicamycin induced autophagy in L6 myotubes.** a) Western blot analysis of LC3 and Beclin1 with beta actin as loading control. b) Densitometric analysis of proteins relative to beta actin. CON-untreated cells, TM-0.25µg/ml tunicamycin treatment, TM+TAN-0.25µg/ml tunicamycin tangeretin (50µM) co-treatment, TM+PBA-0.25µg/ml tunicamycin PBA (1mM) co-treatment. Values are expressed as mean±SEM where n=3. \*p≤0.05 significantly differs from control cells, #p≤0.05 significantly different from tunicamycin treated cells.

#### 4B.3.2 Tangeretin improves the expression of autophagy regulators

Akt and downstream mTOR are negative regulators of autophagy and in this study exposure to tunicamycin suppressed the expression of p-Akt to 67.04% and mTOR to 73.18% compared to control group (Figure.4B.4a, b). Tangeretin improved the expression of p-Akt (80.32%) and mTOR (107.56%) while PBA improved the p-Akt to 81.68% and mTOR to 92.36% compared to tunicamycin treated cells (Figure.4B.4a, b).

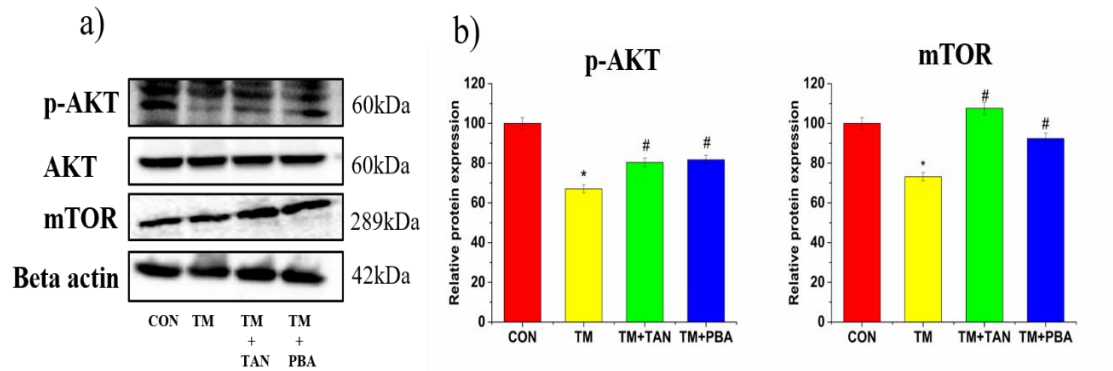


**Figure.4B.4. Tangeretin improves the expression of autophagy regulators.** a) Western blot analysis of p-AKT and mTOR. b) Densitometric analysis of proteins relative to AKT and beta actin respectively. CON-untreated cells, TM-0.25 $\mu$ g/ml tunicamycin treatment, TM+TAN-0.25 $\mu$ g/ml tunicamycin tangeretin (50 $\mu$ M) co-treatment, TM+PBA-0.25 $\mu$ g/ml tunicamycin PBA (1mM) co-treatment. Values are expressed as mean $\pm$ SEM where n=3. \* $p\leq 0.05$  significantly differs from control cells, # $p\leq 0.05$  significantly different from tunicamycin treated cells.

### 4B.3.3 Modulation of ERAD proteins by tangeretin

Here, chronic treatment with tunicamycin resulted in significant upregulation of proteins involved in various steps of ERAD, proteolytic degradation machinery. GRP94 and calnexin are part of the ER quality control machinery and are involved in the protein recognition step of ERAD. Both GRP94 and calnexin were significantly upregulated to 163.46% and 120.28% respectively on exposure to tunicamycin (Figure.4B.5a, b). Co-treatment with tangeretin reduced the expression of GRP94 to 116.95% and calnexin to 92.90% while PBA treatment reduced GRP94 to 122.3% and calnexin to 105.60% compared to tunicamycin treated cells (Figure.4B.5a, b).

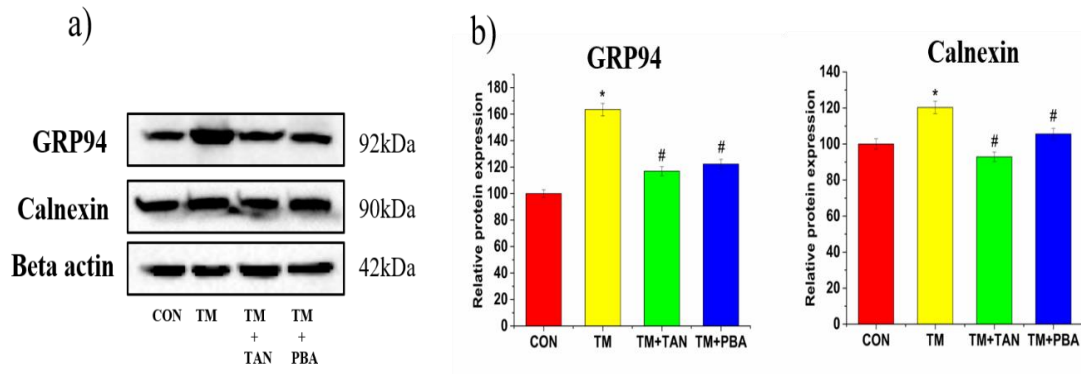


**Figure.4B.5.Tangeretin downregulates tunicamycin induced GRP94 and calnexin.** a) Western blot analysis of GRP94 and calnexin with beta actin as loading control. b) Densitometric analysis of proteins relative to beta actin. CON-untreated cells, TM-0.25 $\mu$ g/ml tunicamycin treatment, TM+TAN-0.25 $\mu$ g/ml tunicamycin tangeretin (50 $\mu$ M) co-treatment, TM+PBA-0.25 $\mu$ g/ml tunicamycin PBA (1mM) co-treatment. Values are expressed as mean $\pm$ SEM where n=3. \* $p\leq 0.05$  significantly different from untreated group, # $p\leq 0.05$  significantly different from tunicamycin treated cells.

EDEM1 and HERPUD1 proteins involved in the protein targeting and retro translocation step of ERAD were observed to be upregulated on treatment with tunicamycin. EDEM1 expression was increased to 125.85% and HERPUD1 was upregulated to 481.94% compared to untreated cells as depicted in Figure.4B.6a, b. Co-treatment with tangeretin could not suppress the EDEM1 expression (133.19%), however, HERPUD1 was downregulated to 298.53% while in PBA co-treated cells, EDEM1 expression was 135.04% and HERPUD1 levels were 286.59% compared to tunicamycin group (Figure.4B.6a, b).

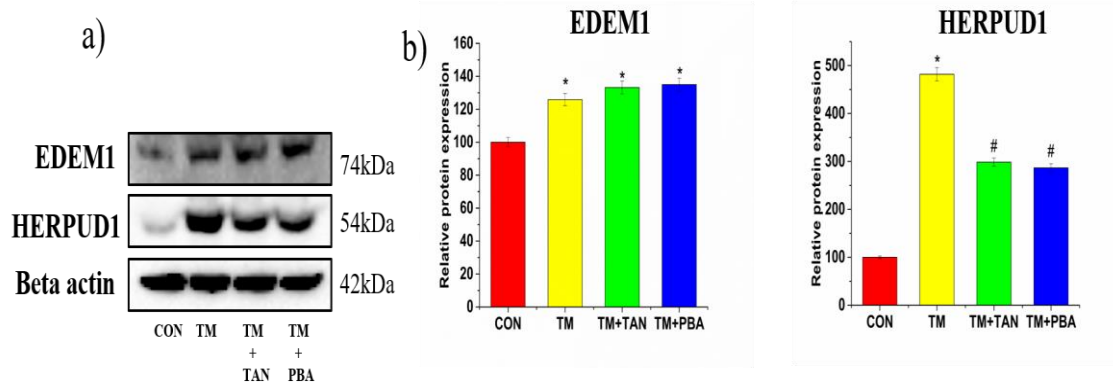


**Figure.4B.6. Effect of tangeretin on expression of EDEM1 and HERPUD1 during ER stress.**

a) Western blot analysis of EDEM1 and HERPUD1 with beta actin as loading control. b) Densitometric analysis of proteins relative to beta actin. CON-untreated cells, TM-0.25µg/ml tunicamycin treatment, TM+TAN-0.25µg/ml tunicamycin tangeretin (50µM) co-treatment, TM+PBA-0.25µg/ml tunicamycin PBA (1mM) co-treatment. Values are expressed as mean±SEM where n=3. \*p≤0.05 significantly different from untreated cells, #p≤0.05 significantly different from tunicamycin treated cells.

Next, the expression of proteins involved in the final steps of ERAD involving ubiquitination and proteasomal degradation were also studied. The expression of RNF5, SYVN1, UFD1 and SEL1 were significantly upregulated on chronic treatment with tunicamycin (Figure.4B.7a, b). RNF5 was increased to 119.16%, SYVN1 to 164.18%, UFD1 to 139.09%, and SEL1 to 122.29% compared to untreated group. Tangeretin could not significantly suppress the expression of RNF5 (114.75%) and SYVN1 (162.15%) compared to tunicamycin treated cells. In tangeretin treated cells, UFD1 expression was remarkably decreased to 94.22% and SEL1 to 108.21% compared to tunicamycin treated cells as depicted in Figure.4B.7a, b). PBA treatment decreased RNF5 levels to 109.85%, SEL1 to 92.41%, and UFD1 to 98.29%, however, SYVN1 (164.96%) levels were not downregulated compared to tunicamycin treated cells (Fig.4B.7a, b).

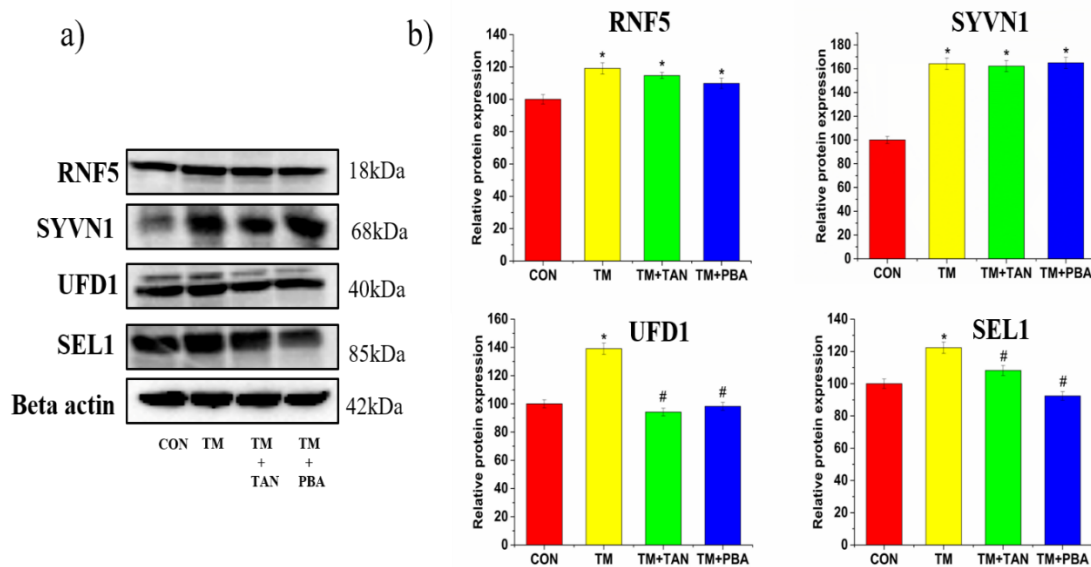


**Figure.4B.7. Effect of tangeretin on expression of RNF5, SYVN1, UFD1, SEL1 during ER stress.** a) Western blot analysis of RNF5, SYVN1, UFD1, SEL1 with beta actin as loading control. b) Densitometric analysis of proteins relative to beta actin. CON-untreated cells, TM-0.25 $\mu$ g/ml tunicamycin treatment, TM+TAN-0.25 $\mu$ g/ml tunicamycin tangeretin (50 $\mu$ M) co-treatment, TM+PBA-0.25 $\mu$ g/ml tunicamycin PBA (1mM) co-treatment. Values are expressed as mean $\pm$ SEM where n=3. \*p $\leq$ 0.05 significantly varies from untreated cells, #p $\leq$ 0.05 significantly different from tunicamycin treated cells.

#### 4B.3.4 Tangeretin upregulates the SERCA and concomitantly downregulates phospho-ryanodine receptors (p-RYR) expression levels under ER stress

SERCA expression, channel for uptake of calcium into the ER was remarkably suppressed to 77.2% on chronic exposure to tunicamycin compared to the control cells as observed in Figure.4B.8a, b, c. Co-treatment with tangeretin significantly improved the SERCA levels to 122.97% while PBA remarkably improved the levels to 253.34% compared to tunicamycin treated cells (Figure.4B.8a, b). The immunofluorescence staining of SERCA was also in agreement with the western blot data (Figure.4B.8c). p-

R-YR, channel for release of calcium from the ER was analysed. The expression of p-RYR was elevated in tunicamycin treated cells while co-treatment with tangeretin as well as PBA respectively, aided in suppressing the levels as evident from the immunofluorescence images in Figure.4B.8d.

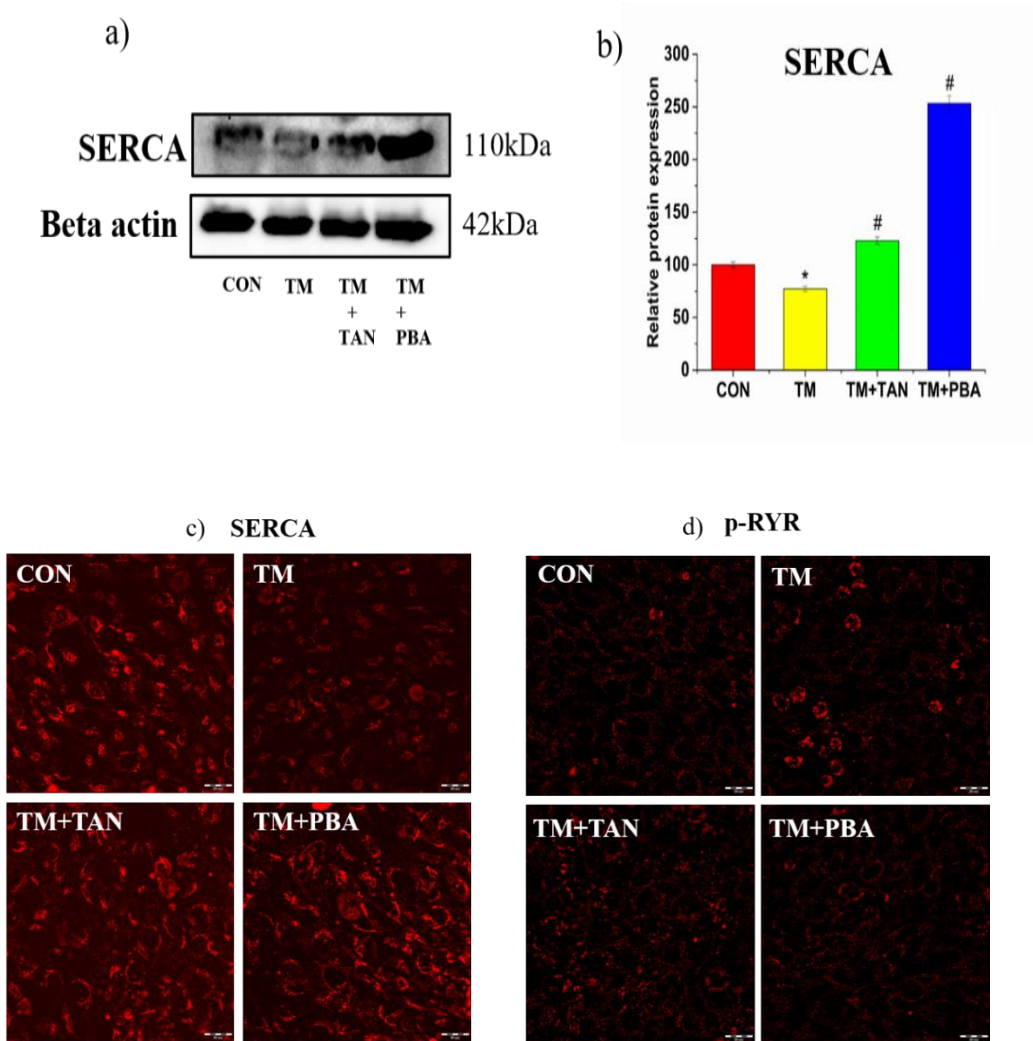


**Figure.4B.8. Effect of tangeretin on expression of ER calcium pumps, SERCA and p-RYR.** a) Western blot analysis of SERCA with beta actin as loading control. b) Densitometric analysis of SERCA relative to beta actin. c) Immunofluorescence imaging of SERCA using fluorescent microscopy. Magnification 20X. Scale corresponds to 20µm. d) Immunofluorescence imaging of p-RYR using fluorescent microscopy. Magnification 20X. Scale corresponds to 20µm. CON-untreated cells, TM-0.25µg/ml tunicamycin treatment, TM+TAN-0.25µg/ml tunicamycin tangeretin (50µM) co-treatment, TM+PBA-0.25µg/ml tunicamycin PBA (1mM) co-treatment. Values are expressed as mean±SEM where n=3. \*p≤0.05 significantly differs from control cells, #p≤0.05 significantly different from tunicamycin treated cells.



#### **4B.4 Discussion**

In the current study, the effect of tangeretin on the expression of the proteins involved in the two proteolytic systems, autophagy and ERAD were analysed. From the data obtained here, it was evident that prolonged exposure of L6 myotubes to tunicamycin resulted in upregulation of the autophagy and ERAD machinery indicating disturbances in the proteostasis network.

Here, enhanced expression of autophagy proteins, LC3-II and Beclin1 under ER stress was observed. LC3 is required for the elongation and maturation of the double membrane vesicle namely, autophagosome which engulfs the misfolded aggregates (Lee & Lee, 2016). During autophagosome formation, cytosolic LC3-I conjugated to phosphatidylethanolamine gets converted to membrane bound LC3-II via two ubiquitylation like reactions (Kabeya et al., 2000). The LC3-II gets degraded by the lysosomal proteases during fusion of autophagosome to lysosome, hence, the lysosomal turnover of LC3-II is a marker of autophagic activity (Tanida et al., 2008). Studies demonstrate the increase in LC3 expression in genetic model of muscle atrophy and its knockdown being associated with ablation of muscle mass loss (Sandri, 2010). Beclin1 is involved in the initial phase of autophagy and mediates the nucleation of the phagophore (initial double membrane structure) by forming complex with class III PI3K (Kang et al., 2011). The IRE-1 $\alpha$ -XBP-1 axis and the ATF6 arms of the UPR are known to activate Beclin1 and induce autophagy (Gade et al., 2012; Margariti et al., 2012). In the present study, co-treatment with tangeretin suppressed the expression of LC3-II and Beclin1 implying the amelioration of ER stress induced autophagy in muscle cells.

Autophagy is a tightly regulated process and the key mediators of this regulation are the mTOR and Akt (Deegan et al., 2013). mTOR is a master regulator of cellular metabolism

that upregulates the anabolic processes such as protein, lipid and nucleotide synthesis while inhibiting the catabolic processes such as autophagy (Deleyto-Seldas & Efeyan, 2021). ER stress induced UPR activates autophagy by suppressing the mTOR (Deegan et al., 2013). The mTOR is positively regulated by the Akt which has a pro-survival role by promoting growth and proliferation (Manning & Cantley, 2003). The Akt/mTOR signaling negatively controls the autophagy induction. ER stress abrogates the Akt activity via the upregulation of GRP78 and TRB3, the former inhibits the activity by preventing phosphorylation of Akt at Ser473 while the latter directly binds to Akt and suppresses its downstream functions (Du et al., 2003; Yung et al., 2011). In this study chronic exposure to tunicamycin significantly suppressed the p-Akt and mTOR levels indicating autophagy induction. Tangeretin was effective in improving the expression of p-Akt and mTOR which implies its therapeutic potential against autophagy mediated muscle mass loss and weakening.

Next, the therapeutic potential of tangeretin against tunicamycin induced ERAD or UPS mediated protein degradation was studied. Here, the expression of proteins involved in the different steps of ERAD were analysed. GRP94 and calnexin are ER chaperones that are part of the ER quality control system and involved in the protein recognition step of ERAD. These are upregulated in response to the UPR. Under physiological conditions, GRP94 is involved in selective protein folding which means that GRP94 is not required by several proteins unlike PDI and calreticulin which is omnipresent and it also functions as a calcium binding protein in the ER lumen (Eletto et al., 2010). Similarly, calnexin is also involved in mediating protein folding and demonstrates calcium binding properties, however unlike the classic molecular chaperones, calnexin, a lectin chaperone, binds to the N-linked carbohydrates or glycans attached to the proteins rather than the hydrophobic residues (Filipeanu, 2015; Lamriben et al., 2016). ERAD is triggered in response to ER

stress to facilitate the clearance of the misfolded proteins, and the first step involves the recognition of misfolded proteins by molecular and lectin chaperones. In this study prolonged treatment with tunicamycin upregulated the GRP94 and calnexin. A decrease in expression levels was observed on co-treatment with tangeretin which indicates alleviation of ER stress.

Properly folded proteins are directed by the ER resident chaperones to the Golgi apparatus for further processing, however, misfolded proteins are unable to exit the ER and re-enter the chaperone cycle or more precisely the calnexin cycle for further folding. If the folding remains unproductive, the misfolded proteins are targeted for demannosylation, and the trimmed mannose structure is then recognized by the EDEM1 and displaced from the calnexin cycle (Christianson et al. 2008). The proteins are then targeted to retro translocation in the cytoplasm. Here, an increase in expression of EDEM1 was observed on treatment with tunicamycin indicating induction of ERAD while tangeretin co-treatment exacerbated the levels.

HERPUD1, an ER membrane protein with a ubiquitin-like domain is involved in substrate protein retro translocation, ubiquitination and degradation (Schulze et al., 2005). It stabilises the ERAD multiprotein complex and interacts with E3 ubiquitin ligase HRD1/SYVN1 which is required for ubiquitination of misfolded proteins forming a part of the retro translocon channel along with SEL1 (Erzurumlu et al., 2022). Mammalian HRD1-SEL1L complex connects luminal substrates at the cytoplasmic surface for ubiquitination following their retro translocation across the ER membrane by acting as a scaffold for ERAD (Iida et al., 2011). The HRD1 and SEL1 expressions are mediated by the IRE-1 $\alpha$ -XBP-1 and ATF6 branches of the UPR respectively (Kaneko et al., 2007). Here, exposure to tunicamycin augmented the HERPUD1, SYVN1 and SEL1 expression

while tangeretin suppressed the HERPUD1, SEL1 expression but could not downregulate the SYVN1 levels.

RNF5, an ER membrane ubiquitin ligase mediates ubiquitination of misfolded proteins and inducible RNF5 expression correlated to degenerative myopathy and increased ER stress (Delaunay et al., 2008). UFD1, an ubiquitin recognition protein is also implicated in ERAD and it directs the ubiquitylated misfolded substrate proteins to the proteasome for degradation (Le et al., 2016). From the data obtained here, it was seen that tunicamycin treatment induced the expression levels of RNF5 and UFD1. Co-treatment with tangeretin could not downregulate the RNF5 expression, however, UFD1 levels were remarkably suppressed. The results for ERAD in this study indicate increased protein degradation in L6 myotubes on prolonged exposure to ER stress condition which can be detrimental leading to loss of muscle mass. Here, tangeretin could only partially suppress the tunicamycin induced ERAD as evident from the protein expression studies. Since, ERAD is primarily an adaptive mechanism to restore cellular homeostasis by reducing the protein load, proteins exacerbated on co-treatment with tangeretin may indicate an enhanced adaptive response in the presence of the methoxyflavones.

As already discussed in Section 4B.1, calcium leakage from the ER is a major trigger for both autophagy and ERAD. Hence, in the present study, the expression of the channels involved in the influx and efflux of calcium ions on the ER membrane was studied. In the skeletal muscle cells, SERCA is involved in transfer of calcium from the cytosol to the ER after contraction facilitating muscle relaxation and suppression of SERCA activity is associated with ER stress and muscle pathologies (Stammers et al., 2015). Thapsigargin, a pharmacological ER stress inducer facilitates ER stress by blocking the SERCA pump activity thereby leading to cytosolic calcium load (Sagara & Inesi, 1991). RyRs, on the other hand facilitate calcium ions out of the ER and the expression is augmented under

prolonged ER stress resulting in muscle pathologies (Greer et al., 2022). The data here indicates suppression of SERCA activity by incubation with tunicamycin as observed from the western blot and immunofluorescence data while p-RYR expression was enhanced as evident from the immunofluorescence results. This indicates a dysregulation of calcium homeostasis which acts as a stimulus for upregulation of proteolytic system. Tangeretin improved the SERCA levels while decreasing the p-RYR expression indicating its efficacy in improving the calcium homeostasis and subsequent suppression of protein degradation machinery. Both autophagy and ERAD represent putative therapeutic targets for management of ER stress induced muscle pathologies such as atrophy. Improvement of skeletal muscle health is a potent strategy for better management of diabetes related complications of muscle cells.

#### **4B.5 Summary**

The present study evaluated the therapeutic potential of tangeretin in improving the tunicamycin induced disrupted proteostasis network in skeletal muscle cells. Protein degradation pathways such as autophagy and ERAD are upregulated under prolonged ER stress and contribute to muscle mass loss and weakness. Tangeretin suppressed the tunicamycin induced autophagy markers and improved the expression of negative regulators of autophagy. However, tangeretin could only partially suppress the ERAD markers. Tangeretin also improved the calcium homeostasis as evident from the expression studies of ER calcium channels. Tangeretin can be a potential therapeutic lead for ER stress induced muscle pathologies. A summary of results is illustrated in Figure.4B.9.

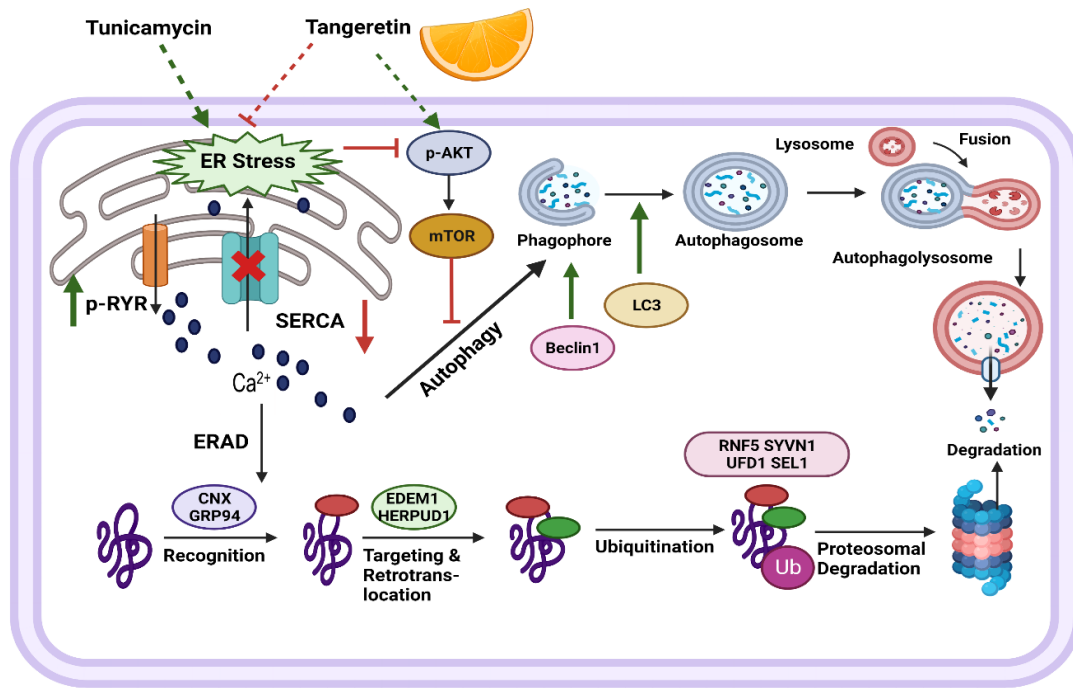


**Figure 4B.9. Effect of tangeretin on tunicamycin induced autophagy and ERAD in L6 myotubes.** Prolonged exposure to tunicamycin disturbs the proteostasis network and leads to upregulation of protein degradation pathways, autophagy and ERAD via disrupting the calcium homeostasis by suppression of SERCA pump and upregulation of ryanodine receptors. Tangeretin improved the calcium homeostasis by improving SERCA expression and suppressing p-RYR levels. Tangeretin also downregulated autophagy markers and partially rescued from ER stress induced ERAD.

## References

- Christianson, J. C., Shaler, T. A., Tyler, R. E., & Kopito, R. R. (2008). *OS-9 and GRP94 deliver mutant  $\alpha$  1-antitrypsin to the Hrd1-SEL1L ubiquitin ligase complex for ERAD*. <https://doi.org/10.1038/ncb1689>
- Daverkausen-Fischer, L., & Pröls, F. (2022). Regulation of calcium homeostasis and flux between the endoplasmic reticulum and the cytosol. *Journal of Biological Chemistry*, 298, 102061. <https://doi.org/10.1016/j.jbc.2022.102061>
- Deegan, S., Saveljeva, S., Gorman, A. M., & Samali, A. (2013). Stress-induced self-cannibalism: On the regulation of autophagy by endoplasmic reticulum stress. *Cellular and Molecular Life Sciences*, 70(14), 2425–2441. <https://doi.org/10.1007/s00018-012-1173-4>
- Delaunay, A. S., Bromberg, K. D., Hayashi, Y., Mirabella, M., & Burch, D. (2008). The ER-Bound RING Finger Protein 5 (RNF5/RMA1) Causes Degenerative Myopathy in Transgenic Mice and Is Deregulated in Inclusion Body Myositis. *PLoS ONE*, 3(2), 1609. <https://doi.org/10.1371/journal.pone.0001609>
- Deleyto-Seldas, N., & Efeyan, A. (2021). The mTOR–Autophagy Axis and the Control of Metabolism. *Frontiers in Cell and Developmental Biology*, 9(July), 1–9. <https://doi.org/10.3389/fcell.2021.655731>
- Du, K., Herzig, S., & Kulkarni, R. N. (2003). *TRB3 : A tribbles Homolog That Inhibits Akt / PKB Activation by*. 300(June), 1574–1578.
- Eletto, D., Dersh, D., & Argon, Y. (2010). GRP94 in ER quality control and stress responses. *Seminars in Cell and Developmental Biology*, 21(5), 479–485. <https://doi.org/10.1016/j.semcdb.2010.03.004>
- Erzurumlu, Y., Doganlar, Y., Dogan, H. K., Catakli, D., & Aydogdu, E. (2022). HERPUD1, a member of the Endoplasmic Reticulum Protein Quality Control Mechanism, may be a Good Target for Suppressing Tumorigenesis in Breast Cancer Cells. *Turkish Journal of Pharmaceutical Sciences*, 0(0), 0–0. <https://doi.org/10.4274/tjps.galenos.2022.71643>
- Filipeanu, C. M. (2015). Temperature-Sensitive Intracellular Traffic of  $\alpha$ 2C-Adrenergic Receptor. *Progress in Molecular Biology and Translational Science*, 132, 245–265.

<https://doi.org/10.1016/BS.PMBTS.2015.02.008>

- Gade, P., Ramachandran, G., Maachani, U. B., Rizzo, M. A., Okada, T., Prywes, R., Cross, A. S., Mori, K., & Kalvakolanu, D. V. (2012). *An IFN- $\gamma$ -stimulated ATF6-C/EBP- $\beta$ -signaling pathway critical for the expression of Death Associated Protein Kinase 1 and induction of autophagy*. <https://doi.org/10.1073/pnas.1119273109>
- Greer, L. K., Meilleur, K. G., Harvey, B. K., & Wires, E. S. (2022). Identification of ER/SR resident proteins as biomarkers for ER/SR calcium depletion in skeletal muscle cells. *Orphanet Journal of Rare Diseases*, *17*(1), 1–11. <https://doi.org/10.1186/s13023-022-02368-9>
- He, C., Bassik, M. C., Moresi, V., Sun, K., Wei, Y., Zhou, Z., An, Z., Loh, J., Fisher, J., Sun, Q., Korsmeyer, S., Packer, M., May, H. I., Hill, J. A., Virgin, H. W., Gilpin, C., Xiao, G., Bassel-Duby, R., Scherer, P. E., & Levine, B. (2012). *Exercise-induced BCL2-regulated autophagy is required for muscle glucose homeostasis*. *481*(7382), 511–515. <https://doi.org/10.1038/nature10758>
- Hetz, C., Zhang, K., & Kaufman, R. J. (2020). Mechanisms, regulation and functions of the unfolded protein response. *Nature Reviews Molecular Cell Biology* *2020* 21:8, *21*(8), 421–438. <https://doi.org/10.1038/s41580-020-0250-z>
- Iida, Y., Fujimori, T., Okawa, K., Nagata, K., Wada, I., & Hosokawa, N. (2011). SEL1L protein critically determines the stability of the HRD1-SEL1L Endoplasmic Reticulum-associated Degradation (ERAD) complex to optimize the degradation kinetics of ERAD substrates. *Journal of Biological Chemistry*, *286*(19), 16929–16939. <https://doi.org/10.1074/jbc.M110.215871>
- Johnston, H. E., & Samant, R. S. (2021). Alternative systems for misfolded protein clearance: life beyond the proteasome. *The FEBS Journal*, *288*(15), 4464–4487. <https://doi.org/10.1111/FEBS.15617>
- Kabeya, Y., Mizushima, N., Ueno, T., Yamamoto, A., Kirisako, T., Noda, T., Kominami, E., Ohsumi, Y., & Yoshimori, T. (2000). LC3, a mammalian homolog of yeast Apg8p, is localized in autophagosome membranes after processing. *EMBO Journal*, *22*(17), 4577. <https://doi.org/10.1093/emboj/cdg454>
- Kaneko, M., Yasui, S., Niinuma, Y., Arai, K., Omura, T., Okuma, Y., & Nomura, Y.



- (2007). A different pathway in the endoplasmic reticulum stress-induced expression of human HRD1 and SEL1 genes. *FEBS Letters*, *581*(28), 5355–5360. <https://doi.org/10.1016/J.FEBSLET.2007.10.033>
- Kang, R., Zeh, H. J., Lotze, M. T., & Tang, D. (2011). The Beclin 1 network regulates autophagy and apoptosis. *Cell Death and Differentiation*, *18*(4), 571–580. <https://doi.org/10.1038/cdd.2010.191>
- Kim, K. H., Jeong, Y. T., Oh, H., Kim, S. H., Cho, J. M., Kim, Y. N., Kim, S. S., Kim, D. H., Hur, K. Y., Kim, H. K., Ko, T., Han, J., Kim, H. L., Kim, J., Back, S. H., Komatsu, M., Chen, H., Chan, D. C., Konishi, M., ... Lee, M. S. (2013). Autophagy deficiency leads to protection from obesity and insulin resistance by inducing Fgf21 as a mitokine. *Nature Medicine*, *19*(1), 83–92. <https://doi.org/10.1038/nm.3014>
- Kocaturk, N. M., & Gozuacik, D. (2018). *Crosstalk Between Mammalian Autophagy and the Ubiquitin-Proteasome System*. <https://doi.org/10.3389/fcell.2018.00128>
- Lamriben, L., Graham, J. B., Adams, B. M., & Hebert, D. N. (2016). N-Glycan-based ER Molecular Chaperone and Protein Quality Control System: The Calnexin Binding Cycle. *Traffic*, *17*(4), 308–326. <https://doi.org/10.1111/tra.12358>
- Le, L. T. M., Kang, W., Kim, J. Y., Le, O. T. T., Lee, S. Y., & Yang, J. K. (2016). Structural Details of Ufd1 Binding to p97 and Their Functional Implications in ER-Associated Degradation. *PLOS ONE*, *11*(9), e0163394. <https://doi.org/10.1371/JOURNAL.PONE.0163394>
- Lee, Y.-K., & Lee, J.-A. (2016). Role of the mammalian ATG8/LC3 family in autophagy: differential and compensatory roles in the spatiotemporal regulation of autophagy. *BMB Rep*, *49*(8), 424–430. <https://doi.org/10.5483/BMBRep.2016.49.8.081>
- Manning, B. D., & Cantley, L. C. (2003). United at last: the tuberous sclerosis complex gene products connect the phosphoinositide 3-kinase/Akt pathway to mammalian target of rapamycin (mTOR) signalling. *Biochemical Society Transactions*, *31*(Pt 3), 573–578. <https://doi.org/10.1042/BST0310573>
- Margariti, A., Li, H., Chen, T., Martin, D., Vizcay-Barrena, G., Alam, S., Karamariti, E., Xiao, Q., Zampetaki, A., Zhang, Z., Wang, W., Jiang, Z., Gao, C., Ma, B., Chen, Y.-G., Cockerill ¶ ¶, G., Hu, Y., Xu, Q., & Zeng, L. (2012). *XBPI mRNA Splicing*

*Triggers an Autophagic Response in Endothelial Cells through BECLIN-1 Transcriptional Activation* \* □ S. <https://doi.org/10.1074/jbc.M112.412783>

Medinas, D. B., Hazari, Y., & Hetz, C. (2021). Disruption of Endoplasmic Reticulum Proteostasis in Age-Related Nervous System Disorders. *Progress in Molecular and Subcellular Biology*, 59, 239–278. [https://doi.org/10.1007/978-3-030-67696-4\\_12/COVER](https://doi.org/10.1007/978-3-030-67696-4_12/COVER)

Park, S.-J., Li, C., & Chen, Y. M. (2021). MINI-REVIEW Endoplasmic Reticulum Calcium Homeostasis in Kidney Disease Pathogenesis and Therapeutic Targets. *The American Journal of Pathology*, 191, 256–265.  
<https://doi.org/10.1016/j.ajpath.2020.11.006>

Sagara, Y., & Inesi, G. (1991). THE JOURNAL OF BIOLOGICAL CHEMISTRY Inhibition of the Sarcoplasmic Reticulum Ca<sup>2+</sup> Transport ATPase by Thapsigargin at Subnanomolar Concentrations\*. *Communication Val*, 266(21), 13503–13506.  
[https://doi.org/10.1016/S0021-9258\(18\)92726-2](https://doi.org/10.1016/S0021-9258(18)92726-2)

Sandri, M. (2010). Autophagy in skeletal muscle. *FEBS Letters*, 584(7), 1411–1416.  
<https://doi.org/10.1016/j.febslet.2010.01.056>

Sandri, M. (2013). Protein breakdown in muscle wasting: Role of autophagy-lysosome and ubiquitin-proteasome. *The International Journal of Biochemistry & Cell Biology*, 45(10), 2121. <https://doi.org/10.1016/J.BIOCEL.2013.04.023>

Schulze, A., Standera, S., Buerger, E., Kikkert, M., Van Voorden, S., Wiertz, E., Koning, F., Kloetzel, P. M., & Seeger, M. (2005). The Ubiquitin-domain Protein HERP forms a Complex with Components of the Endoplasmic Reticulum Associated Degradation Pathway. *Journal of Molecular Biology*, 354(5), 1021–1027.  
<https://doi.org/10.1016/J.JMB.2005.10.020>

Siekmann, I., Phillips, S. M., Lisboa, P. J., Shepherd, S., & Burniston, J. G. (2023). *Muscle of obese insulin-resistant humans exhibits losses in proteostasis and attenuated proteome dynamics that are improved by exercise training*. *Running title: Human muscle proteome dynamics*.

Stammers, A. N., Susser, S. E., Hamm, N. C., Hlynsky, M. W., Kimber, D. E., Kehler, D. S., & Duhamel, T. A. (2015). The regulation of sarco(endo)plasmic reticulum

- calcium-ATPases (SERCA)1. <https://doi.org/10.1139/Cjpp-2014-0463>, 93(10), 843–854. <https://doi.org/10.1139/CJPP-2014-0463>
- Sun, F., Xu, X., Wang, X., & Zhang, B. (2016). Regulation of autophagy by Ca<sup>2+</sup>. *Tumour Biology*, 37(12), 15467. <https://doi.org/10.1007/S13277-016-5353-Y>
- Tanida, I., Ueno, T., & Kominami, E. (2008). LC3 and autophagy. *Methods in Molecular Biology*, 445(2), 77–88. [https://doi.org/10.1007/978-1-59745-157-4\\_4](https://doi.org/10.1007/978-1-59745-157-4_4)
- Vervliet, T. (2018). Ryanodine Receptors in Autophagy: Implications for Neurodegenerative Diseases? *Frontiers in Cellular Neuroscience*, 12, 89. <https://doi.org/10.3389/FNCEL.2018.00089>
- Whittemore, S. R., Saraswat Ohri, S., Forston, M. D., Wei, G. Z., & Hetman, M. (2022). The Proteostasis Network: A Global Therapeutic Target for Neuroprotection after Spinal Cord Injury. *Cells*, 11(21), 1–25. <https://doi.org/10.3390/cells11213339>
- Wong, V. K. W., Li, T., Law, B. Y. K., Ma, E. D. L., Yip, N. C., Michelangeli, F., Law, C. K. M., Zhang, M. M., Lam, K. Y. C., Chan, P. L., & Liu, L. (2013). Saikosaponin-d, a novel SERCA inhibitor, induces autophagic cell death in apoptosis-defective cells. *Cell Death & Disease* 2013 4:7, 4(7), e720–e720. <https://doi.org/10.1038/cddis.2013.217>
- Yung, H. W., Charnock-Jones, D. S., & Burton, G. J. (2011). Regulation of AKT phosphorylation at Ser473 and Thr308 by endoplasmic reticulum stress modulates substrate specificity in a severity dependent manner. *PloS One*, 6(3). <https://doi.org/10.1371/JOURNAL.PONE.0017894>

# **Chapter 5**

**Effect of Tangeretin in improving the  
cellular function in pancreatic Beta-TC-6  
cells under ER stress condition**

## 5.1 Introduction

Diabetes mellitus is a chronic metabolic disease affecting people worldwide and both type 1 and type 2 diabetes are characterized by impaired insulin release from pancreatic beta cell islets. The pancreatic islets consist of a well-developed ER owing to their secretory function (Seo et al., 2008). Under physiological scenarios, the ER is involved in maintaining the beta cell function and maturation of insulin peptide, the major protein released by the pancreatic beta cells (Lipson et al., 2006). Any perturbations in the ER function can lead to ER stress which results in a buildup of misfolded or unfolded proteins in the ER lumen. This triggers a signaling cascade known as the unfolded protein response (UPR) which then functions to restore the ER homeostasis through activation of the three arms of the UPR, namely, IRE-1 $\alpha$ , ATF6, and PERK (Back & Kaufman, 2012). Chronic ER stress in pancreatic beta islets is associated with decreased beta cell mass, function, and impaired insulin production (Fonseca et al., 2011). Cellular stresses including obesity-mediated circulating saturated fatty acids (lipotoxicity) and high glucose-induced glucotoxicity have been reported to contribute to ER stress in beta cells as shown in Figure.5.1 (Wang et al., 2005; Zhu et al., 2021). In diabetic conditions, insulin resistance causes beta cell compensation by stimulating hypersecretion of insulin but after a point, loss of beta cells and function abrogate insulin secretion aggravating the disease condition (Kasuga, 2006). The impaired insulin secretion results in decreased glucose uptake in peripheral tissues leading to hyperglycemia. Sustained hyperglycemia and insulin resistance can contribute to ROS generation and mitochondrial dysfunction in pancreatic beta cells that ultimately result in beta cell apoptosis (Y. J. Park & Woo, 2019).

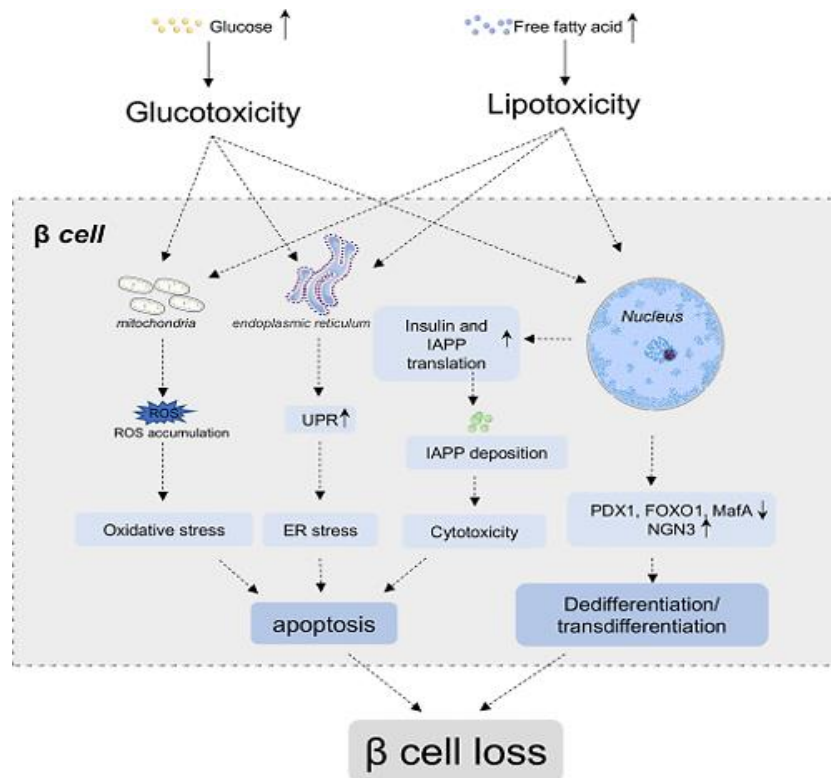


**Figure.5.1. Glucotoxicity and lipotoxicity induce ER stress in pancreatic beta cells** (Zhu et al., 2021)

In diabetic conditions, insulin resistance causes beta cell compensation by stimulating hypersecretion of insulin but after a point, loss of cells and function abrogate insulin secretion aggravating the disease condition (Kasuga, 2006). The impaired insulin secretion results in decreased glucose uptake in peripheral tissues leading to hyperglycaemia. Sustained hyperglycaemia and insulin resistance can contribute to ROS generation and mitochondrial dysfunction in pancreatic beta cells that ultimately result in beta cell apoptosis (Y. J. Park & Woo, 2019). Oxidative stress and ER stress are closely entwined events that are more prominent in pancreatic beta cells due to the relatively low antioxidant levels making them susceptible to oxidative damage (Lenzen et al., 1996). ER stress mediated mitochondrial dysfunction is also an important consequence in pancreatic beta cells due to the structural and functional proximity of ER and mitochondria (Vig et al., 2021). Prolonged ER stress interferes with the insulin biosynthesis via suppression of

insulin mRNA expression and insulin promoter activity by chronic IRE-1 $\alpha$  and ATF6 activation respectively (Lipson et al., 2006; Seo et al., 2008). Therapeutic intervention of ER stress and associated pathways may improve beta cell health which is an important prerequisite for normal insulin secreting potential of beta cells.

Currently, sulfonylureas are a class of drugs that are used as first line therapy to treat diabetes by improving insulin secretion from pancreatic beta cells (Chaudhury et al., 2017). However, its long-term use is associated with beta cell apoptosis and loss of function. This is due to the sustained increase in intracellular calcium ions to facilitate insulin secretion which may result in chronic ER stress as ER is a major reservoir of calcium and any perturbation in calcium metabolism leads to disruption of ER homeostasis (Rajan et al., 2007). Rather than only improving insulin secretion, focus should shift towards developing therapeutic strategies that aim to improve the overall pancreatic beta cell function by maintaining the ER homeostasis.

The present study was aimed at investigating the effect of tangeretin against tunicamycin induced ER stress in pancreatic Beta-TC-6 cell lines. Tangeretin has been in use as traditional Chinese medicine and it is also reported to have antioxidant, anti-inflammatory and anticancer activity (Arafa et al., 2021; Ashrafizadeh et al., 2020). Additionally, tangeretin has also been reported for improving the glucose uptake potential of C2C12 myotubes and 3T3-F442A adipocyte (M. S. Kim et al., 2012; Onda et al., 2013). Takano et. al reported the protective effect of methoxyflavones in pancreatic MIN6 cell lines against ER stress and oxidative stress (Takano et al., 2007). Our study aims to investigate the potential of tangeretin in alleviating the ER stress induced cellular perturbations including effect on insulin expression levels and overall cellular function in pancreatic Beta-TC-6 cell line.

## **5.2 Materials & Methods**

Fetal bovine serum, DMEM containing 4.5g/L glucose and 1.5g/L sodium bicarbonate, antimycotic antibiotic mix, triton X, glycine, sodium dodecyl sulphate, tris base, skimmed milk, phosphate buffered saline (PBS), DMSO, were procured from Himedia (Mumbai, India). Tunicamycin, PBA, tangeretin, HPLC grade methanol, DCFH-DA, protease inhibitor cocktail tablets were purchased from Sigma Aldrich Chemical (St. Louis Missouri, USA). JC-1 assay kit was purchased from Cayman Chemicals (Michigan, USA). RIPA lysis buffer, HBSS, BCA kit, were obtained from Thermo Fisher Scientific (Waltham, Massachusetts, USA). The antibodies insulin, GADD153, p-Akt, Akt, beta actin, HRP conjugated secondary antibodies, Alexa fluor conjugated secondary antibodies were bought from Cell Signaling Technologies (Danvers, Massachusetts, USA). Antibody TRB3 was purchased from Santa Cruz Biotechnology (Dallas, Texas, USA). Antibodies XBP-1, glucose transporter 2 (GLUT2), pancreatic duodenal homeobox-1 (Pdx-1), musculoaponeurotic fibrosarcoma (Maf A), GRP94, calnexin were purchased from Gbiosciences (St. Louis MO, USA). Mouse Beta-TC-6 cell lines were procured from National Centre for Cell Sciences, Pune, India.

### **5.2.1 Cell Culture**

Pancreatic Beta-TC6 cells were cultured in DMEM containing 15% fetal bovine serum and 1% antibiotic antimycotic mix. The cells were maintained in a humidified incubator at 37°C and 5% carbon dioxide. On reaching 90% confluence, the cells were treated with the experimental groups for a time period of 24 hours. After the treatment period, the cells were harvested for further analysis.



## 5.2.2 Experimental groups

- **CON-** untreated or control cells
- **TM-** tunicamycin (0.25µg/ml) treated cells
- **TM+TAN-** tunicamycin (0.25µg/ml) & tangeretin (10µM) co-treated cells
- **TM+PBA-** tunicamycin (0.25µg/ml) & PBA (100µM) co-treated cells (Positive control)

## 5.2.3 Experimental Design

A schematic work flow of this chapter is depicted in Figure.5.2.

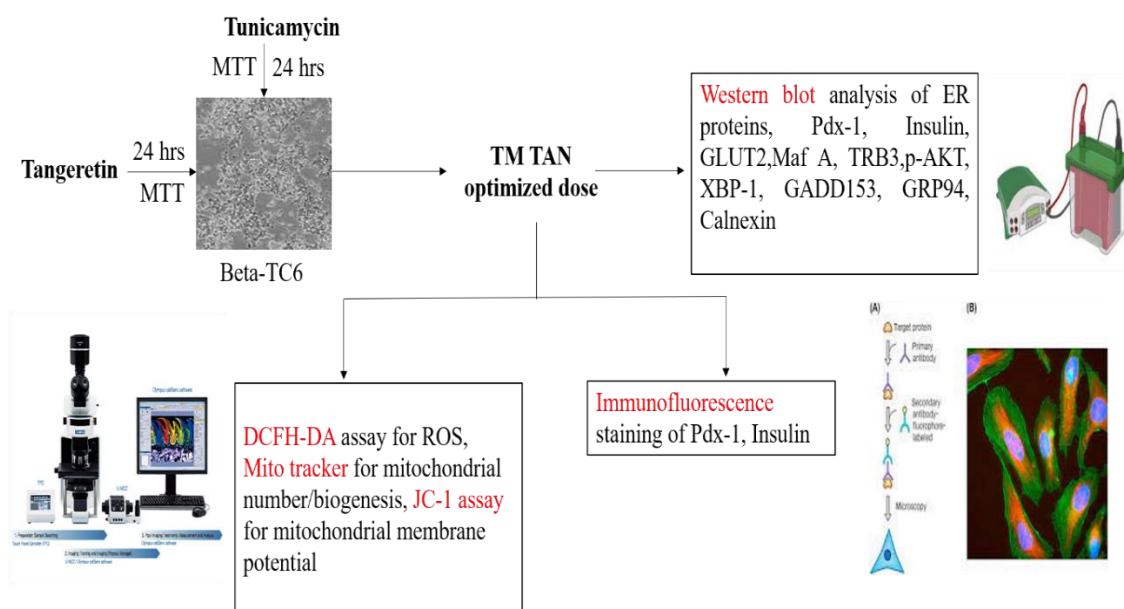


**Figure.5.2. Schematic representation of the experimental design**

## 5.2.4 Cytotoxicity studies of tunicamycin and tangeretin

Cells were seeded at a density of  $5 \times 10^3$  cells per well in 96 well plate. Tunicamycin was introduced to the cells in a range of concentrations (0.25 µg/ml to 10 µg/ml) for 24 hours in serum starved media. The cytotoxicity was evaluated using the MTT assay as described

by Mosmann (Mosmann, 1983). Cells were rinsed with HBSS following treatment, and incubated with MTT solution (0.5 mg/ml) dissolved in serum-free DMEM for 4 hours. After incubation, MTT solution was discarded and 100 $\mu$ L DMSO was added to each well. To ensure that the formazan crystals were completely dissolved, the plate was incubated on the shaker for 20 minutes and the absorbance was estimated at 570nm in multimode plate reader (Tecan infinite 200 PRO, Austria). In a separate experiment, cells were treated with different concentrations (10 $\mu$ M to 100 $\mu$ M) of tangeretin for 24 hours and cytotoxicity was determined. For optimising the dose of co-treatment, cells were treated with different doses (5 $\mu$ M, 10 $\mu$ M) of tangeretin and optimised dose of tunicamycin simultaneously and optimum dose for co-treatment was selected based on the MTT results.

### **5.2.5 Intracellular ROS generation**

The ROS levels were determined by the DCFH-DA staining. The cells were treated for 24 hours with the experimental groups. For DCFH-DA staining, protocol by Armstrong (2014) was followed in which cells were incubated with 10 $\mu$ M DCFH-DA staining solution for 20 minutes followed by gentle washing in HBSS (Armstrong, 2014) . Fluorescence images were acquired using the FITC filter in Fluorescence microscope (Olympus Life Science, Japan).

### **5.2.6 Determination of mitochondrial number/biogenesis and mitochondrial membrane potential**

Cells were seeded at a density of 5 $\times$ 10<sup>3</sup> cells per well in 96 black well plate. After treatment with respective experimental groups, the mitochondrial number/biogenesis was estimated by incubating cells with 100nM Mito tracker staining solution for 20 minutes followed by HBSS wash (Chazotte, 2011). The fluorescence images were acquired in

TRITC filter of fluorescence microscope and the intensity was determined using the cellSens software (Olympus Life Science, Japan). For measuring the mitochondrial membrane potential, following treatment period, cells were stained with cationic dye, JC-1 for 30 minutes (Sivandzade et al., 2019). Images of the aggregates were acquired in the TRITC filter whereas the monomer images were obtained using the FITC filter (Olympus Life Science, Japan).

### **5.2.7 Immunofluorescence staining of Beta-TC-6 cells**

After treatment period, cells were fixed in 4% paraformaldehyde solution for 15 minutes before being permeabilized in 0.1% Triton X for 10 minutes. Fixed cells were then incubated with the following antibodies, PDX-1(1:400) and insulin (1:400) antibodies, respectively. This was followed by incubation with suitable secondary antibodies conjugated with Alexa fluor (1:500). The cells were then counter stained with DAPI. The fluorescence images were acquired using fluorescence microscope (Olympus Life Science, Japan).

### **5.2.8 Western Blot analysis**

Cells were seeded in T25 flasks and after attaining 90% confluency were subjected to treatment with the experimental groups for 24 hours. Cells were then rinsed with HBSS and proteins were extracted using RIPA lysis buffer. Using the BCA assay kit and BSA as the standard, the extracted protein samples were quantitated and normalised. Protein samples were separated on 10% sodium dodecyl sulphate polyacrylamide gels. Proteins were then transferred onto PVDF membranes (Millipore, Merck, USA) and blocked for 1 hour in 5% skimmed milk. Membranes were then washed with TBST thrice before being incubated with the appropriate primary antibodies (1:1000 dilution), XBP-1, GADD153, GRP94, Calnexin, p-AKT, AKT, TRB3, insulin, GLUT2, Maf A, PDX-1

overnight at 4°C with agitation. The loading control used was beta actin. After that, the membranes were incubated for 2 hours at room temperature with suitable HRP-conjugated secondary antibodies. The ECL substrate solution was used to detect the blot bands, and image analysis was done in Chemidoc MP Imaging systems (Bio-Rad, USA). The resultant bands were quantified by densitometric analysis using the Image lab software version 6.1 (Bio-Rad, USA).

### **5.2.9 Statistical Analysis**

All experiments were performed in triplicates and three times, independently. Data was statistically analysed using one-way ANOVA and Duncan post hoc analysis in SPSS software. The results are represented as mean±SEM where p value≤0.05 was considered to be significant statistically.

## **5.3 Results**

### **5.3.1 Cytotoxicity studies of tunicamycin and tangeretin**

Tunicamycin was found to be non-toxic (induced less than 20% cell death) upto 0.25µg/ml in Beta-TC-6 cells after 24 hours treatment period with different concentrations ranging from 0.25µg/ml to 10µg/ml (Figure.5.3a). As we wanted to monitor the intracellular changes prior to induction of cell death, 0.25µg/ml tunicamycin was chosen as the optimum dose for ER stress induction in all future experiments. We also optimised the viable dose of tangeretin by treating cells with concentrations ranging from 10µM to 100µM. At a concentration of 10µM, tangeretin induced less than 20% cytotoxicity after 24 hours treatment period as seen in Figure.5.3b. The optimum dose of tangeretin under ER stress condition was determined by treating cells with different concentrations of tangeretin (5µM,10µM) in the presence of 0.25µg/ml tunicamycin. Tangeretin at a dose of 10µM was observed to induce less than 20% cytotoxicity in the

presence of 0.25 $\mu$ g/ml tunicamycin (Figure.5.3c). Therefore, 10 $\mu$ M tangeretin was used in all future experiments.

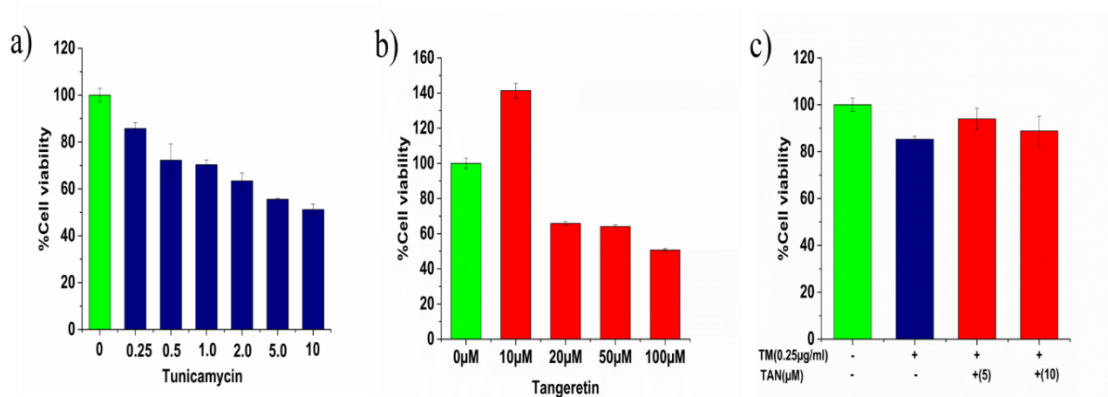


**Figure.5.3. Cytotoxicity analysis of tunicamycin and tangeretin.** a) Pancreatic Beta-TC-6 cells were treated with different doses of tunicamycin (0.25 $\mu$ g/ml to 10 $\mu$ g/ml) for 24 hrs. b) Pancreatic Beta-TC-6 cells were treated with various concentrations of tangeretin (10 $\mu$ M to 100 $\mu$ M) for 24 hours. This was followed by MTT analysis. c) Dose of co-treatment was determined by treating the cells with 5 $\mu$ M, 10 $\mu$ M tangeretin in the presence of 0.25 $\mu$ g/ml tunicamycin followed by MTT assay. CON represents untreated group, TM represents 0.25 $\mu$ g/ml tunicamycin treated group, TM+TAN represents TM tangeretin (10 $\mu$ M) co-treated group, TM+PBA represents TM 4-phenylbutyric acid (100 $\mu$ M) co-treated group. Values are represented as mean $\pm$ SEM where n=3.

### 5.3.2 Tangeretin suppresses tunicamycin induced intracellular ROS generation

ROS generation is a hallmark of cellular redox disturbances. From the fluorescence images in Figure.5.4a, it is observed that tunicamycin treated group showed an increased ROS generation compared to the control whereas co-treatment with tangeretin and PBA respectively brought down the ROS levels significantly. This was further demonstrated by the intensity histograms (Figure.5.4b) in which tunicamycin increased the ROS generation to 2222.5 a.u. (arbitrary units) (196.3%) compared to the control. The untreated cells showed a fluorescence of 1132.2 a.u. Co-treatment with tangeretin

significantly lowered the ROS levels to 1614.7 a.u. (142.6%) and PBA decreased the levels to 1499.62 a.u. (132.5%) compared to the tunicamycin treated cells.

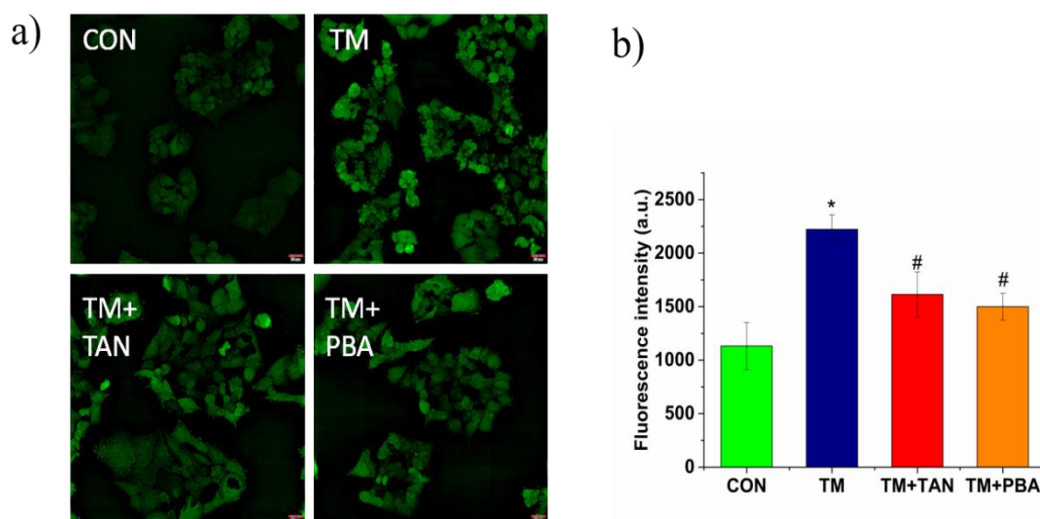


**Figure.5.4. Determination of intracellular ROS generation.** a) Effect of tangeretin on tunicamycin induced intracellular ROS was estimated using DCFH-DA dye and images acquired in fluorescence microscope. Magnification 20X. Scale corresponds to 20 $\mu$ m. b) DCFH-DA fluorescence intensity histogram. CON represents untreated group, TM represents 0.25 $\mu$ g/ml tunicamycin treated group, TM+TAN represents TM tangeretin (10 $\mu$ M) co-treated group, TM+PBA represents TM 4-phenylbutyric acid (100 $\mu$ M) co-treated group. Values are represented as mean $\pm$ SEM where n=3. \* $p\leq 0.05$  significantly different from control cells, # $p\leq 0.05$  significantly different from tunicamycin treated cells.

### 5.3.3 Changes in mitochondrial number/biogenesis and mitochondrial membrane potential

ER stress and mitochondrial dysfunction are closely linked events and both are involved in the pancreatic beta cell dysfunction and decreased insulin biosynthesis via the UPR activation (Luciani et al., 2009). Treatment with tunicamycin decreased the mitochondrial number/biogenesis as evident from the fluorescence images in Figure.5.5a, co-treatment with tangeretin and PBA improved the mitochondrial content (Figure.5.5a). From the

intensity histograms (Figure.5.5b), in tunicamycin treated group, mitochondrial biogenesis was decreased to 1448.7 a.u. (63.1%) compared to untreated cells (2297.5 a.u.). Co-treatment with tangeretin remarkably improved the fluorescence to 2107.1 a.u. (91.7%) while PBA increased the fluorescence to 1837.7 a.u. (79.9%) as seen in Figure.5.5a, b.

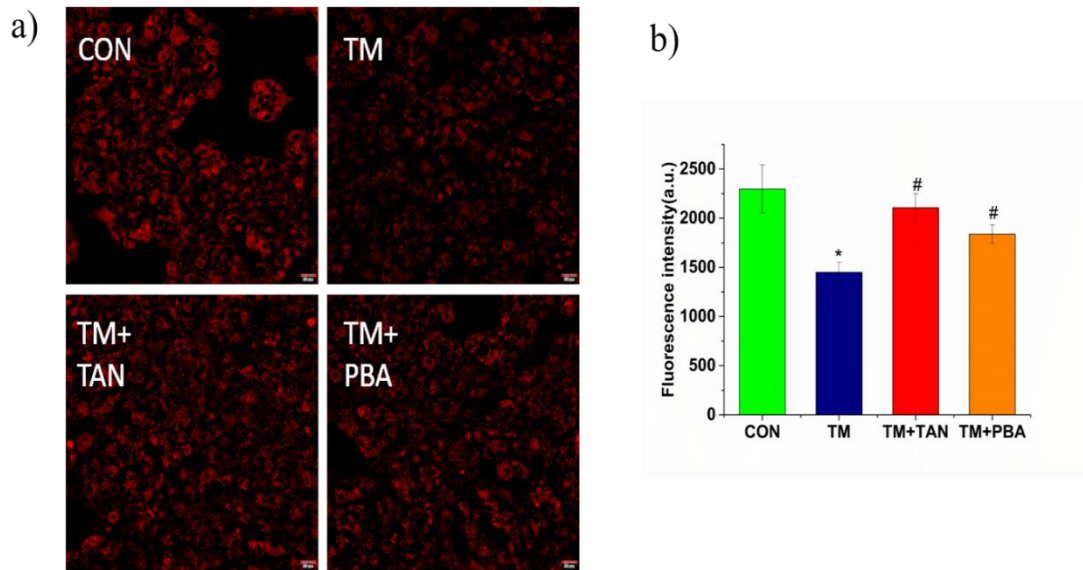


**Figure.5.5. Tangeretin improves mitochondrial number/biogenesis under ER stress.** a) Pancreatic Beta-TC-6 cells were treated with the experimental groups for 24 hours followed by incubation with Mito tracker dye. Imaging was performed in fluorescence microscope. Magnification 20X. Scale corresponds to 20 $\mu$ m. b) Mito tracker fluorescence intensity histogram analysis. CON represents untreated group, TM represents 0.25 $\mu$ g/ml tunicamycin treated group, TM+TAN represents TM tangeretin (10 $\mu$ M) co-treated group, TM+PBA represents TM 4-phenylbutyric acid (100 $\mu$ M) co-treated group. Values are expressed as mean $\pm$ SEM where n=3. \* $p\leq 0.05$  significantly different from control cells, # $p\leq 0.05$  significantly different from tunicamycin treated cells.

ER stress induction is associated with mitochondrial dysfunction and one of the early markers of the same is loss of mitochondrial membrane potential. The JC-1 dye exists as red aggregates in cells with healthy mitochondria while in depolarised mitochondrial

membrane it exists as green monomers. The aggregate to monomer ratio is an indicator of the mitochondrial well-being. Here, tunicamycin induced a depolarisation of the mitochondrial membrane as indicated by the fluorescence images and intensity histograms in Figure.5.6a & b, respectively. Tunicamycin treated cells showed a lower percentage of red to green ratio of 59.5% (1.5 ratio) compared to the untreated cells (2.6 ratio). Co-treatment with tangeretin induced a hyperpolarisation indicated by the higher percentage of the JC-1 aggregate to monomer ratio of 84.8% (2.2 ratio). Co-treatment with PBA improved the percentage ratio to 79.8% (2.1 ratio) as shown in Figure.5.6a, b.

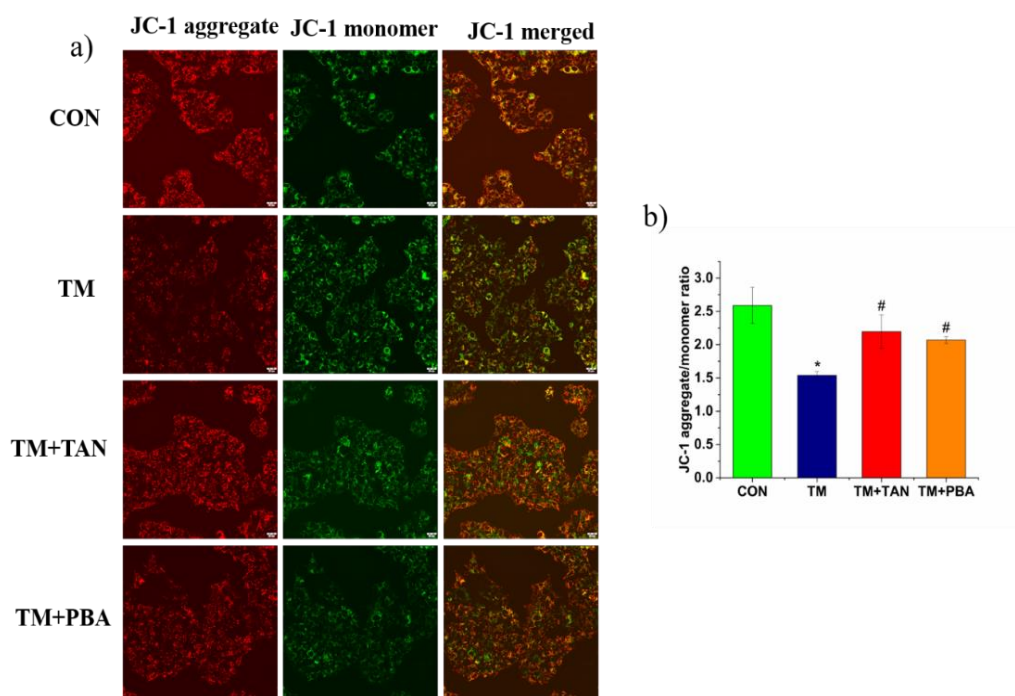


**Figure.5.6. Tangeretin improves tunicamycin induced loss of mitochondrial membrane potential.** a) Pancreatic Beta-TC-6 cells after treatment for 24 hours were incubated with JC-1 dye for 20 minutes. This was followed by imaging in fluorescence microscope. Magnification 20X. Scale corresponds to 20 $\mu$ m. b) Aggregate to monomer fluorescence intensity ratio analysis was performed in Cell Sens software (Olympus Life Science, Japan). CON represents untreated group, TM represents 0.25 $\mu$ g/ml tunicamycin treated group, TM+TAN represents TM tangeretin (10 $\mu$ M) co-treated group, TM+PBA represents TM 4-phenylbutyric acid (100 $\mu$ M) co-treated group. Values are expressed as mean $\pm$ SEM where n=3. \* $p\leq 0.05$  significantly different from control cells, # $p\leq 0.05$  significantly different from tunicamycin treated cells.



### **5.3.4 Tangeretin modulates the expression of XBP-1, ER resident chaperones and GADD153 during ER stress**

Under prolonged ER stress condition, the IRE-1 $\alpha$  arm of UPR induces the splicing of the XBP-1 mRNA, the spliced form translocates to the nucleus and regulates the genes encoding the ER resident chaperones such as GRP94, PDI, calreticulin and calnexin and components of ERAD (S. M. Park et al., 2021). In this study, tunicamycin significantly induced the expression of the following proteins, XBP-1 (164.1%), GRP94 (115.68%) and calnexin (114.64%), respectively (Figure.5.7a & b). Simultaneous treatment with tangeretin was effective in bringing down the levels of XBP-1 (128.25%) and GRP94 (99.687%) compared to tunicamycin treated group. However, calnexin levels were not downregulated significantly (106.53%). PBA did not alter the XBP-1 levels (163.66%) while GRP94 were reduced to 84.49% and calnexin to 83.22% respectively compared to tunicamycin treated cells as depicted in Figure.5.7a & b. As already stated, the primary aim of the UPR is restore the ER homeostasis but if the stress is chronic, the UPR becomes dysregulated and activates the apoptotic signalling (Nishitoh, 2012). GADD153 or CHOP is a hallmark of dysregulated UPR and amelioration of the same may aid in restoration of ER homeostasis. Tunicamycin significantly induced the expression of GADD153 (125.09%) compared to the control (Figure.5.7a & b). Tangeretin was effective in bringing down the levels of GADD153 (95.57%) while the levels were reduced by PBA treatment to 99.19% compared to tunicamycin treated cells (Figure.5.7a & b).

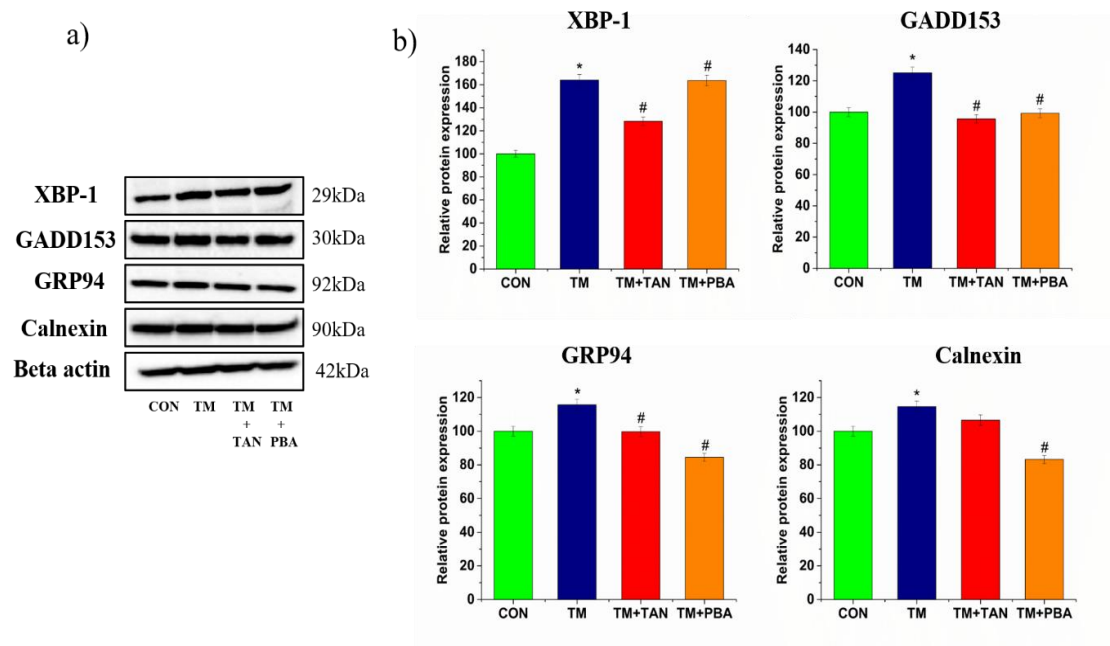


**Figure 5.7. Effect of tangeretin on tunicamycin induced expression of XBP-1, GADD153, ER resident chaperones (GRP94 & calnexin)** a) Western blot analysis of XBP-1, GADD153, GRP94 and calnexin was performed with beta actin as the loading control. b) Densitometric analysis of all proteins relative to beta actin. CON represents untreated group, TM represents 0.25 $\mu$ g/ml tunicamycin treated group, TM+TAN represents TM tangeretin (10 $\mu$ M) co-treated group, TM+PBA represents TM 4-phenylbutyric acid (100 $\mu$ M) co-treated group. Values are expressed as mean $\pm$ SEM where n=3. \*p $\leq$ 0.05 significantly different from control cells, #p $\leq$ 0.05 significantly different from tunicamycin treated cells.

### 5.3.5 Effect of Tangeretin on expression levels of TRB3, p-Akt, Pdx-1, Maf A and GLUT 2 during ER stress

Under ER stress conditions, TRB3 was found to be remarkably upregulated (122.49%) whereas phospho-Akt was found to be downregulated (72.39%) compared to the untreated cells as observed in Figure.5.8a, b. Treatment with tangeretin resulted in significant suppression of TRB3 levels (107.62%) while remarkably improving the phospho-Akt (108.24%) compared to tunicamycin treated group (Figure.5.7a, b). In PBA treated cells, TRB3 levels were decreased (102.26%) whereas phospho-Akt was improved (106.63%) compared to tunicamycin group as shown in Figure.5.8a, b.

Treatment with tunicamycin resulted in no significant change in expression of GLUT2 compared to the untreated cells (Figure.5.8c, d). Co-treatment with tangeretin also did not affect the GLUT2 levels significantly whereas PBA co-treatment however, suppressed the GLUT2 levels to 80.97% as seen in Figure.5.8c, d. The Maf A levels were observed to increase significantly (124.68%) on chronic treatment with tunicamycin compared to the control group (Figure.5.8c, d). The upregulated Maf A levels did not undergo any significant change on co-treatment with tangeretin (125.21%) compared to tunicamycin treated cells as seen in Figure.5.8c, d. PBA treatment exacerbated the Maf A levels to 137.43% compared to tunicamycin treated group (Figure.5.8c, d).

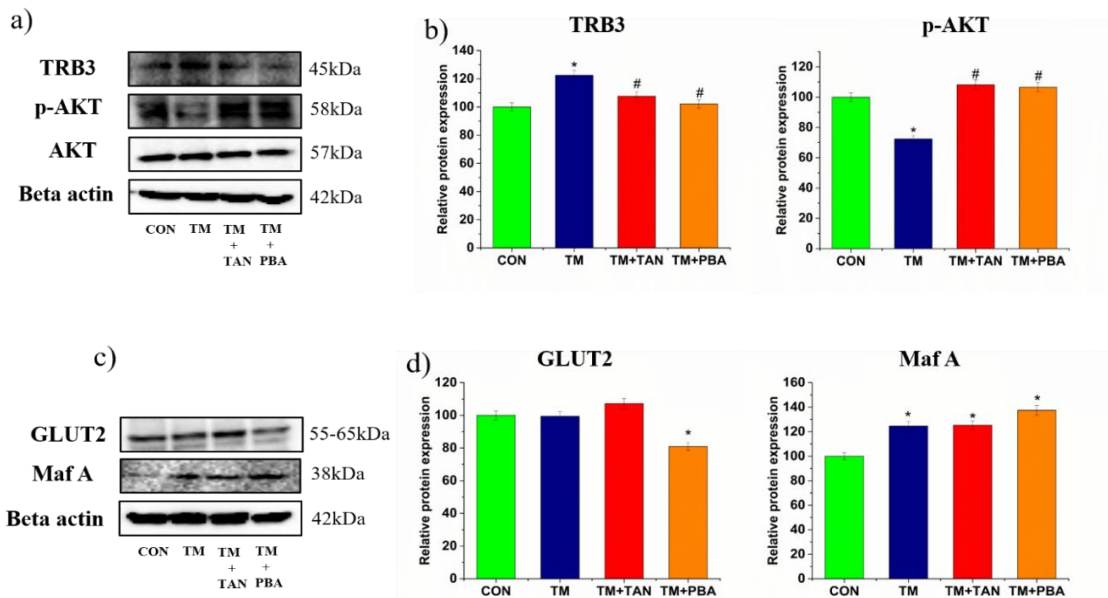


**Figure.5.8. Effect of tangeretin on expression levels of TRB3, p-Akt, Maf-A and GLUT 2 during ER stress.** a) Western blot analysis of TRB3 and p-AKT with beta actin and AKT as loading control respectively was performed. b) Densitometric analysis of TRB3 relative to beta actin and p-AKT relative to AKT. c) Western blot analysis of GLUT2 and Maf A with beta actin as loading control was performed. d) Densitometric analysis of GLUT2 and Maf A relative to beta actin. CON represents untreated group, TM represents 0.25 $\mu$ g/ml tunicamycin treated group, TM+TAN represents TM tangeretin (10 $\mu$ M) co-treated group, TM+PBA represents TM 4-phenylbutyric acid (100 $\mu$ M) co-treated group. Values are expressed as mean $\pm$ SEM where n=3. \* $p\leq 0.05$  significantly different from control cells, # $p\leq 0.05$  significantly different from tunicamycin treated cells.

Under ER stress conditions, the expression of Pdx-1 protein was significantly reduced (72.92%) compared to the untreated cells and treatment with tangeretin improved the Pdx-1 levels to 91.68% compared to tunicamycin treated cells as shown in Figure.5.9a, b. In PBA treated group the Pdx1 levels improved to 105.01% compared to tunicamycin treated cells (Figure.5.9a, b). Pdx-1 expression profile was confirmed by the immunofluorescence data as described in Figure.5.9c.

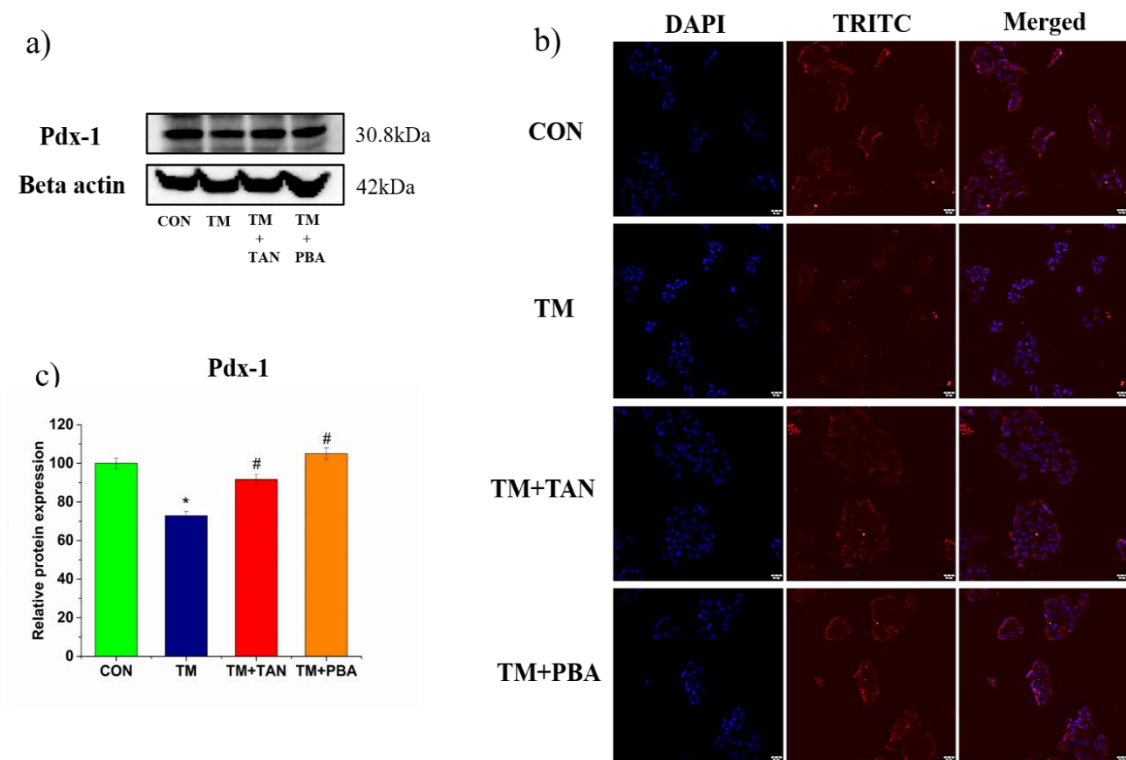


**Figure.5.9. Tangeretin improves Pdx-1 levels during ER stress in pancreatic Beta-TC-6 cells.** a) Pdx-1 levels was analysed using western blot analysis with beta actin as loading control. b) Densitometric analysis of Pdx-1 relative to beta actin. c) Immunofluorescence imaging of Pdx-1 using fluorescence microscopy. Magnification 20X. Scale corresponds to 20 $\mu$ m. CON represents untreated group, TM represents 0.25 $\mu$ g/ml tunicamycin treated group, TM+TAN represents TM tangeretin (10 $\mu$ M) co-treated group, TM+PBA represents TM 4-phenylbutyric acid (100 $\mu$ M) co-treated group. Values are expressed as mean $\pm$ SEM where n=3. \* $p\leq 0.05$  significantly different from control cells, # $p\leq 0.05$  significantly different from tunicamycin treated cells.

### 5.3.6 Effect of tangeretin on insulin expression during ER stress

Insulin expression was decreased to 86.32% as depicted in Figure.5.10a, b. Tangeretin improved the insulin levels to 92.18% but it was not significant compared to tunicamycin group as shown in Figure.10a, b. In PBA treated group, the insulin expression was decreased to 76.75% compared to the tunicamycin group (Figure.5.10a, b). These results were also corroborated by the immunofluorescence data of insulin expression (Figure.5.10c).

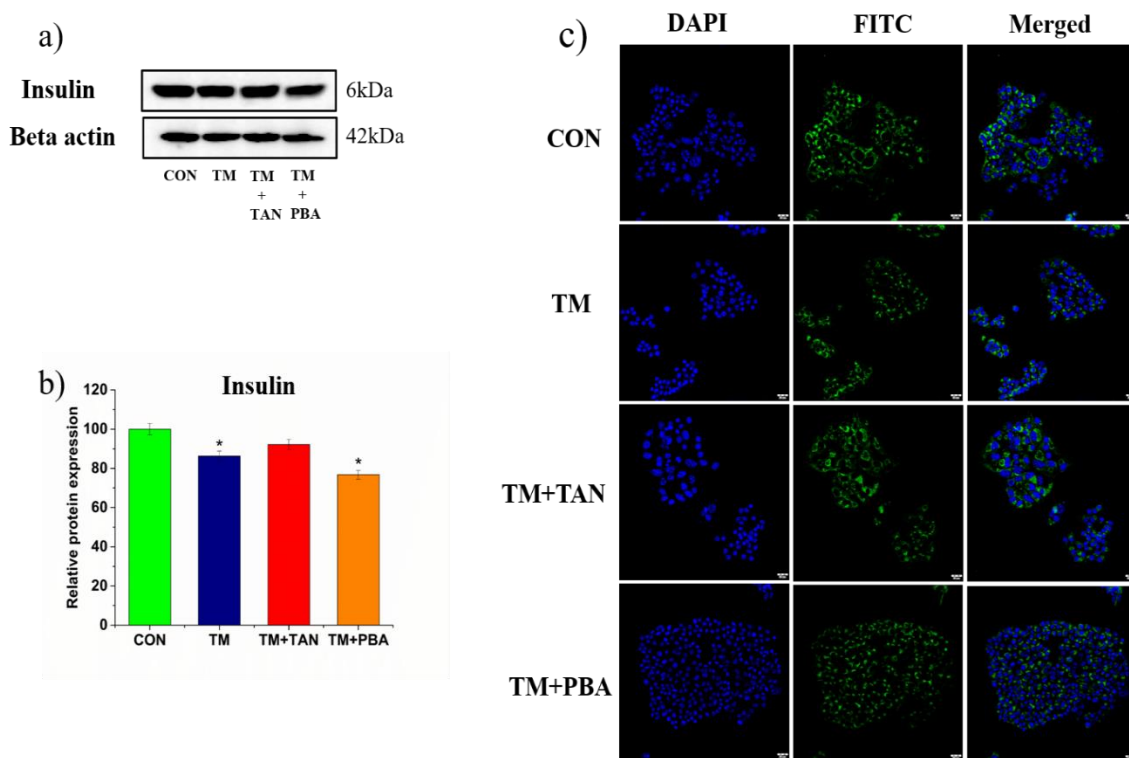


**Figure.5.10. Effect of tangeretin on insulin expression during ER stress.** a) Western blot analysis of insulin protein with beta actin as loading control. b) Densitometric analysis of insulin relative to beta actin. c) Immunofluorescence imaging of insulin using fluorescence microscope. Magnification 20X. Scale corresponds to 20 $\mu$ m. CON represents untreated group, TM represents 0.25 $\mu$ g/ml tunicamycin treated group, TM+TAN represents TM tangeretin (10 $\mu$ M) co-treated group, TM+PBA represents TM 4-phenylbutyric acid (100 $\mu$ M) co-treated group. Values are expressed as mean $\pm$ SEM where n=3. \* $p\leq 0.05$  significantly different from control cells, # $p\leq 0.05$  significantly different from tunicamycin treated cells.

## 5.4 Discussion

The present study attempted to evaluate the role of tangeretin in amelioration of tunicamycin induced perturbations in pancreatic Beta-TC-6 cells. Here, treatment of pancreatic beta cells with tunicamycin resulted in ROS generation, hallmark of oxidative stress. Co-treatment with tangeretin was effective in bringing down the ROS levels. As pancreatic beta cells express low levels of cellular antioxidants, they are more susceptible to redox disturbances (Hedge et al., 1997). ER stress and oxidative stress share a strong relationship in pancreatic beta cells where the prolonged exposure to former negatively affects insulin biosynthesis and beta cell function (Hasnain et al., 2016).

Cells under ER stress, generate more ROS due to the upregulation of the protein folding machinery which works to reduce the burden of misfolded proteins (Chong et al., 2017). In the present study, treatment with tunicamycin induced the expression of the protein folding machinery proteins namely XBP-1, GRP94 and calnexin. IRE-1 $\alpha$  arm of the UPR triggers the splicing of XBP-1 which then upregulates the ER resident chaperones to enhance the protein folding for alleviation of the ER stress (Calton et al., 2002). Overexpression of XBP-1 is also associated with decreased insulin levels, impaired glucose stimulated insulin secretion and beta cell apoptosis (Allagnat et al., 2010). GRP94 and calnexin are part of the quality control system in the ER and are induced during ER stress conditions (Maruri-Avidal et al., 2008). By remarkably reducing the levels of XBP-1 and GRP94, tangeretin inhibited the tunicamycin-induced activation of the protein folding machinery, indicating a reduction in the stress condition.

GADD153/CHOP expression is an indication of maladaptive or dysregulated UPR which subsequently results in cellular dysfunction (Hu et al., 2019). Here, we observed an increased expression of GADD153 on prolonged exposure to tunicamycin which was

suppressed on tangeretin co-treatment. Song et al. have reported the role of GADD153 in linking protein misfolding to oxidative stress in pancreas. CHOP or GADD153 deletion was associated with reduced oxidative stress and improved beta cell function in *in vivo* models (Song et al., 2008). Targeting the CHOP can be a therapeutic approach to improve beta cell function.

Recent studies indicate a role of both ER stress and oxidative stress in the loss of mitochondrial membrane potential (Fang et al., 2020; Xiao et al., 2020). Our findings demonstrate an improvement in mitochondrial membrane potential by tangeretin under ER stress conditions. Mitochondrial membrane hyperpolarization and downstream increase in ATP/ADP ratio is a necessary step in the canonical glucose stimulated insulin secretion (GSIS) (Gerencser, 2018). Under diabetic conditions, there is a loss of mitochondrial membrane potential which may hamper the insulin secretion. Loss in mitochondrial biogenesis or number due to mitochondrial dysfunction is manifested in diabetic condition (Kelley et al., 2002). Improving the mitochondrial biogenesis can aid in better management of the disease (Singh et al., 2021). In this study, under ER stress conditions the mitochondrial biogenesis was found to be significantly reduced indicating mitochondrial dysfunction as evident from the Mito tracker red fluorescence data whereas co-treatment with tangeretin remarkably improved the same. This data is consistent with the GADD153 expression levels in tunicamycin treated group which indicates beta cell dysfunction upon induction of ER stress.

Under physiological conditions, the Akt signaling plays an important role in beta cell proliferation, function and insulin secretion (Balcazar Morales et al., 2012; Cheng et al., 2012). Akt function is negatively regulated by oxidative stress and ER stress and improving the Akt function will contribute to improvement of beta cell function (Elghazi & Bernal-Mizrachi, 2009). TRB3, an ER stress marker protein that is involved in the

suppression of the Akt active form, is activated by the ATF4/GADD153 arm of the UPR (Ohoka et al., 2005). We have already reported the upregulation of GADD153 in tunicamycin treated group. Here we observed a concomitant increase in the expression of TRB3 and a downregulation in p-Akt levels in cells treated with tunicamycin. Tangeretin significantly brought down the TRB3 levels while increasing the p-Akt levels which indicates the efficacy of the citrus flavone in promoting beta cell survival and function under ER stress condition by suppressing the TRB3 levels and improving the p-Akt levels.

The main stimulus for pancreatic insulin secretion is the glucose which is taken into the cells by the GLUT2 transporter on the plasma membrane of rodent cells. It has low affinity (high Km) for glucose and is not the primary glucose transporter in human beta cells where GLUT1 and GLUT3 are prominently involved in GSIS (McCulloch et al., 2011). Unlike GLUT4 which gets activated in response to insulin, GLUT2 is activated by the extracellular glucose (Thorens, 2015). After reaching the cytosol, the glucose is phosphorylated by the glucokinase enzyme for glycolysis for generation of ATP and subsequently aids in insulin secretion (Bensellam et al., 2018). Here, we studied the expression of GLUT2 as we have used mouse insulinoma Beta-TC-6 cells for our study, the protein levels did not change significantly under ER stress conditions. This was even observed in cells co-treated with tangeretin. This is in contrast to previous reports where the GLUT2 expression is significantly reduced under ER stress condition in pancreatic beta cells (Allagnat et al., 2010; Chen et al., 2022). However, few previous studies have also reported the unchanged GLUT2 levels in response to tunicamycin (Ferrer et al., 1993; Zhang, 2020). This can be because GLUT2 is not the rate limiting step in the insulin biosynthesis signaling as it mediates passive glucose diffusion. In our study this can be due to the subtoxic levels of tunicamycin and also because GLUT2 expression is not



directly related to ER stress (Zhou et al., 2021). Another reason could be the high glucose concentration in the growth medium which acts as a trigger for GLUT2 expression and the subtoxic concentration of tunicamycin was unable to significantly lower the expression.

Here, the expression of Pdx-1, a transcriptional factor required for insulin gene expression and beta cell survival, was investigated. Pdx-1 controls development, maturation, and differentiation of beta cells and low expression levels are linked to beta cell malfunction (S. K. Kim & Hebrok, 2001). In this study, the expression of Pdx-1 was significantly suppressed on treatment with tunicamycin while co-treatment with tangeretin improved the Pdx-1 levels as evident from the western blot results. This was in agreement with Yao et al., who demonstrated the efficacy of an O-methylated isoflavone in promoting the activity of Pdx-1 under glucotoxic and lipotoxic conditions in *in vitro* and *in vivo* models (Yao et al., 2020). The expression of Maf A that is required for insulin gene expression and overall beta cell function was studied here (Matsuoka et al., 2007). Surprisingly, unlike Pdx-1, we observed an increase in Maf A levels in tunicamycin treated cells when compared to the basal levels in the control cells. Tangeretin did not have any significant effect on the upregulated Maf A levels. This is in contrast to past reports that have demonstrated a reduction in Maf A levels during diabetic condition (Guo et al., 2013; Matsuoka et al., 2010). However, Kitamura et al. have reported enhanced expression of Maf A as a protective mechanism against under stress conditions (Kitamura et al., 2005). This could be because the cellular defense mechanisms may get activated on exposure to tunicamycin and upregulation of Maf A can be a coping mechanism to suppress the stress conditions. Aguayo-Mazzucato et al., demonstrated that overexpression of Pdx-1 is associated with improved insulin content but not glucose responsiveness whereas

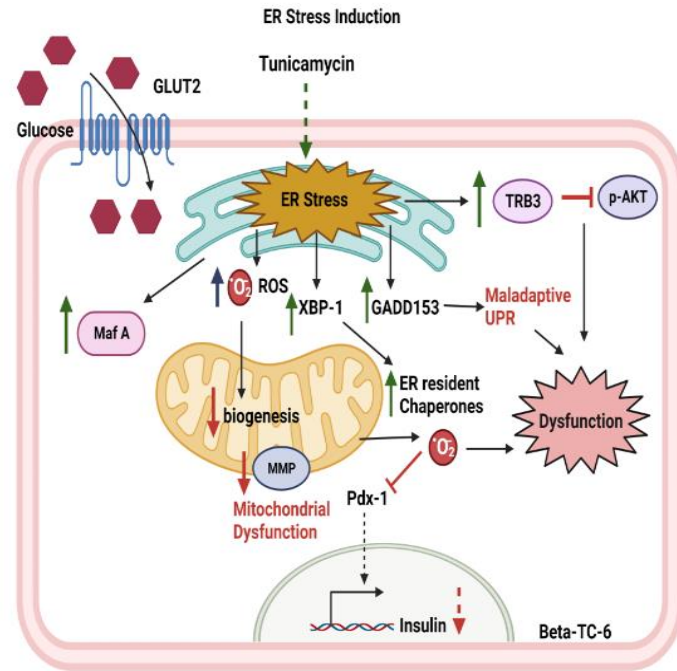
overexpression of Maf A enhanced glucose responsive insulin secretion while insulin content remained unaltered in neonatal beta cells (Aguayo-Mazzucato et al., 2011).

The major function of pancreatic beta cells involves insulin biosynthesis and secretion in response to elevated blood glucose levels. During chronic ER stress conditions, pancreatic beta cell function is compromised resulting in reduced levels of insulin synthesis as well as insulin secretion (Fonseca et al., 2011). From the results here, it is evident that expression of the insulin protein was modestly downregulated upon treatment with tunicamycin. This modest decrease may be due to the subtoxic dose of tunicamycin used in the study, that was sufficient for ER stress induction but not strong enough to fully curtail the insulin expression. Co-treatment with tangeretin could only marginally improve the insulin levels. This was even confirmed by the immunofluorescence data. Tangeretin was effective in ameliorating the ER stress and improving the overall beta cell function, however, it could only modestly improve the insulin levels.

## **5.5 Summary**

ER stress in pancreatic beta cells compromises their function by upregulating maladaptive UPR, inducing oxidative stress, mitochondrial dysfunction and suppressing insulin expression. Tangeretin was effective in mitigating ER stress induced cellular disturbances and improving beta cell health under ER stress condition and hence, tangeretin can be proposed as a potential candidate in mitigating ER stress induced damage in pancreatic beta cells. A schematic summary of the results is depicted in Figure.5.11.

a)



b)

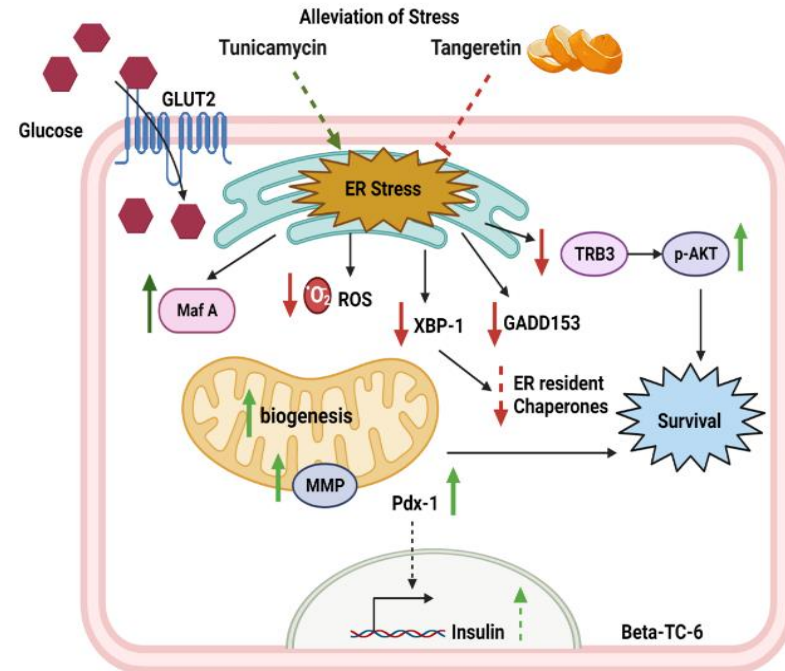


**Figure.5.11. Effect of tangeretin on pancreatic Beta-TC-6 function during tunicamycin induced ER stress.** a) ER stress induction in Beta-TC-6 cells by tunicamycin. b) Alleviation of stress condition in Beta-TC-6 cells by tangeretin. Prolonged exposure to tunicamycin induced ER stress, upregulated the protein folding machinery, increased ROS generation, decreased mitochondrial biogenesis, membrane potential and modestly suppressed insulin expression. Co-treatment with tangeretin ameliorated the ER stress, suppressed the protein folding machinery, decreased the ROS levels, improved mitochondrial function and modestly upregulated the insulin expression.

## References

- Aguayo-Mazzucato, C., Koh, A., El Khattabi, I., Li, W. C., Toschi, E., Jermendy, A., Juhl, K., Mao, K., Weir, G. C., Sharma, A., & Bonner-Weir, S. (2011). Mafa expression enhances glucose-responsive insulin secretion in neonatal rat beta cells. *Diabetologia*, *54*(3), 583–593. <https://doi.org/10.1007/s00125-010-2026-z>
- Allagnat, F., Christulia, F., Ortis, F., Pirot, P., Lortz, S., Lenzen, S., Eizirik, D. L., & Cardozo, A. K. (2010). Sustained production of spliced X-box binding protein 1 (XBP1) induces pancreatic beta cell dysfunction and apoptosis. *Diabetologia*, *53*(6), 1120–1130. <https://doi.org/10.1007/s00125-010-1699-7>
- Arafa, E. S. A., Shurrab, N. T., & Buabeid, M. A. (2021). Therapeutic Implications of a Polymethoxylated Flavone, Tangeretin, in the Management of Cancer via Modulation of Different Molecular Pathways. *Advances in Pharmacological and Pharmaceutical Sciences*, *2021*. <https://doi.org/10.1155/2021/4709818>
- Armstrong, D. (2014). Advanced protocols in oxidative stress III, Methods in Molecular Biology,. *Advanced Protocols in Oxidative Stress III*, *594*, 1–477. <https://doi.org/10.1007/978-1-60761-411-1>
- Ashrafizadeh, M., Ahmadi, Z., Mohammadinejad, R., & Ghasemipour Afshar, E. (2020). Tangeretin: a mechanistic review of its pharmacological and therapeutic effects. *Journal of Basic and Clinical Physiology and Pharmacology*, *31*(4). <https://doi.org/10.1515/JBCPP-2019-0191>
- Back, S., & Kaufman, R. (2012). Endoplasmic reticulum stress and type 2 diabetes. *Annual Review of Biochemistry*, *4*, 767–793. <https://doi.org/10.1146/annurev-biochem-072909-095555>.
- Balcazar Morales, yahoos, de Plata, A., & Colombia Médica, C. (2012). Role of AKT/mTORC1 pathway in pancreatic  $\beta$ -cell proliferation Participación de la vía de señalización AKT/mTORC1 en la proliferación de las células  $\beta$  del páncreas. *Colomb Med*, *43*(3), 235–243.
- Bensellam, M., Jonas, J. C., & Laybutt, D. R. (2018). Mechanisms of  $\beta$ -cell dedifferentiation in diabetes: Recent findings and future research directions. *Journal of Endocrinology*, *236*(2), R109–R143. <https://doi.org/10.1530/JOE-17-0516>

- Calfon, M., Zeng, H., Urano, F., Till, J. H., Hubbard, S. R., Harding, H. P., Clark, S. G., & Ron, D. (2002). IRE1 couples endoplasmic reticulum load to secretory capacity by processing the XBP-1 mRNA. *Nature*, *415*(6867), 92–96. <https://doi.org/10.1038/415092A>
- Chaudhury, A., Duvoor, C., Reddy Dendi, V. S., Kraleti, S., Chada, A., Ravilla, R., Marco, A., Shekhawat, N. S., Montales, M. T., Kuriakose, K., Sasapu, A., Beebe, A., Patil, N., Musham, C. K., Lohani, G. P., & Mirza, W. (2017). Clinical Review of Antidiabetic Drugs: Implications for Type 2 Diabetes Mellitus Management. *Frontiers in Endocrinology*, *8*(January). <https://doi.org/10.3389/fendo.2017.00006>
- Chazotte, B. (2011). Labeling mitochondria with mitotracker dyes. *Cold Spring Harbor Protocols*, *6*(8), 990–992. <https://doi.org/10.1101/pdb.prot5648>
- Chen, C. W., Guan, B. J., Alzahrani, M. R., Gao, Z., Gao, L., Bracey, S., Wu, J., Mbow, C. A., Jobava, R., Haataja, L., Zalavadia, A. H., Schaffer, A. E., Lee, H., LaFramboise, T., Bederman, I., Arvan, P., Mathews, C. E., Gerling, I. C., Kaestner, K. H., ... Hatzoglou, M. (2022). Adaptation to chronic ER stress enforces pancreatic  $\beta$ -cell plasticity. *Nature Communications*, *13*(1), 1–18. <https://doi.org/10.1038/s41467-022-32425-7>
- Cheng, K. K. Y., Lam, K. S. L., Wu, D., Wang, Y., Sweeney, G., Hoo, R. L. C., Zhang, J., & Xu, A. (2012). APPL1 potentiates insulin secretion in pancreatic  $\beta$  cells by enhancing protein kinase Akt-dependent expression of SNARE proteins in mice. *Proceedings of the National Academy of Sciences of the United States of America*, *109*(23), 8919–8924. <https://doi.org/10.1073/PNAS.1202435109/-/DCSUPPLEMENTAL/PNAS.201202435SI.PDF>
- Chong, W. C., Shastri, M. D., & Eri, R. (2017). Endoplasmic Reticulum Stress and Oxidative Stress: A Vicious Nexus Implicated in Bowel Disease Pathophysiology. *International Journal of Molecular Sciences*, *18*(4). <https://doi.org/10.3390/IJMS18040771>
- Elghazi, L., & Bernal-Mizrachi, E. (2009). Akt and PTEN:  $\beta$ -cell mass and pancreas plasticity. In *Trends in Endocrinology and Metabolism* (Vol. 20, Issue 5, pp. 243–

251). <https://doi.org/10.1016/j.tem.2009.03.002>

Fang, X., Zhang, X., & Li, H. (2020). Oxidative stress and mitochondrial membrane potential are involved in the cytotoxicity of perfluorododecanoic acid to neurons. *Toxicology and Industrial Health*, 36(11), 892–897.

<https://doi.org/10.1177/0748233720957534>

Ferrer, J., Gomis, R., Alvarez, J. F., Casamitjana, R., & Vilardell, E. (1993). Signals Derived From Glucose Metabolism Are Required for Glucose Regulation of Pancreatic Islet GLUT2 mRNA and Protein. *Diabetes*, 42(9), 1273–1280. <https://doi.org/10.2337/DIAB.42.9.1273>

Fonseca, S. G., Gromada, J., & Urano, F. (2011). Endoplasmic reticulum stress and pancreatic  $\beta$ -cell death. *Trends in Endocrinology and Metabolism*, 22(7), 266–274. <https://doi.org/10.1016/j.tem.2011.02.008>

Gerencser, A. A. (2018). Metabolic activation-driven mitochondrial hyperpolarization predicts insulin secretion in human pancreatic beta-cells. *Biochimica et Biophysica Acta (BBA) - Bioenergetics*, 1859(9), 817–828.

<https://doi.org/10.1016/J.BBABIO.2018.06.006>

Guo, S., Dai, C., Guo, M., Taylor, B., Harmon, J. S., Sander, M., Robertson, R. P., Powers, A. C., & Stein, R. (2013). Inactivation of specific  $\beta$  cell transcription factors in type 2 diabetes. *The Journal of Clinical Investigation*, 123.

<https://doi.org/10.1172/JCI65390>

Hasnain, S. Z., Prins, J. B., & McGuckin, M. A. (2016). Oxidative and endoplasmic reticulum stress in  $\beta$ -cell dysfunction in diabetes. *Journal of Molecular Endocrinology*, 56(2), R33–R54. <https://doi.org/10.1530/JME-15-0232>

Hedge, M., Lortz, S., Drinkgern, J., & Lenzen, S. (1997). *Relation Between Antioxidant Enzyme Gene Expression and Antioxidative Defense Status of Insulin-Producing Cells*. 46(February).

Hu, H., Tian, M., Ding, C., & Yu, S. (2019). The C/EBP homologous protein (CHOP) transcription factor functions in endoplasmic reticulum stress-induced apoptosis and microbial infection. *Frontiers in Immunology*, 10(JAN), 1–13.

<https://doi.org/10.3389/fimmu.2018.03083>

- Kasuga, M. (2006). Insulin resistance and pancreatic  $\beta$  cell failure. *Journal of Clinical Investigation*, 116(7), 1756. <https://doi.org/10.1172/JCI29189>
- Kelley, D. E., He, J., Menshikova, E. V., & Ritov, V. B. (2002). Dysfunction of Mitochondria in Human Skeletal Muscle in Type 2 Diabetes. *Diabetes*, 51(10), 2944–2950. <https://doi.org/10.2337/DIABETES.51.10.2944>
- Kim, M. S., Hur, H. J., Kwon, D. Y., & Hwang, J. T. (2012). Tangeretin stimulates glucose uptake via regulation of AMPK signaling pathways in C2C12 myotubes and improves glucose tolerance in high-fat diet-induced obese mice. *Molecular and Cellular Endocrinology*, 358(1), 127–134. <https://doi.org/10.1016/j.mce.2012.03.013>
- Kim, S. K., & Hebrok, M. (2001). *Intercellular signals regulating pancreas development and function*. <https://doi.org/10.1101/gad.859401>
- Kitamura, Y. I., Kitamura, T., Kruse, J.-P., Raum, J. C., Stein, R., Gu, W., & Accili, D. (2005). *FoxO1 protects against pancreatic  $\beta$  cell failure through NeuroD and MafA induction*. <https://doi.org/10.1016/j.cmet.2005.08.004>
- Lenzen, S., Drinkgern, J., & Tiedge, M. (1996). Low antioxidant enzyme gene expression in pancreatic islets compared with various other mouse tissues. *Free Radical Biology & Medicine*, 20(3), 463–466. [https://doi.org/10.1016/0891-5849\(96\)02051-5](https://doi.org/10.1016/0891-5849(96)02051-5)
- Lipson, K. L., Fonseca, S. G., Ishigaki, S., Nguyen, L. X., Foss, E., Bortell, R., Rossini, A. A., & Urano, F. (2006). Regulation of insulin biosynthesis in pancreatic beta cells by an endoplasmic reticulum-resident protein kinase IRE1. *Cell Metabolism*, 4(3), 245–254. <https://doi.org/10.1016/j.cmet.2006.07.007>
- Luciani, D. S., Gwiazda, K. S., Yang, T.-L. B., Kalynyak, T. B., Bychkivska, Y., Frey, M. H. Z., Jeffrey, K. D., Sampaio, A. V., Underhill, T. M., & Johnson, J. D. (2009). *Roles of IP 3 R and RyR Ca 2 Channels in Endoplasmic Reticulum Stress and-Cell Death*. <https://doi.org/10.2337/db07-1762>
- Maruri-Avidal, L., López, S., & Arias, C. F. (2008). Endoplasmic Reticulum Chaperones Are Involved in the Morphogenesis of Rotavirus Infectious Particles. *Journal of Virology*, 82(11), 5368–5380. <https://doi.org/10.1128/jvi.02751-07>

- Matsuoka, T. A., Kaneto, H., Miyatsuka, T., Yamamoto, T., Yamamoto, K., Kato, K., Shimomura, I., Stein, R., & Matsuhisa, M. (2010). Regulation of MafA expression in pancreatic  $\beta$ -cells in db/db mice with diabetes. *Diabetes*, *59*(7), 1709–1720. <https://doi.org/10.2337/db08-0693>
- Matsuoka, T. A., Kaneto, H., Stein, R., Miyatsuka, T., Kawamori, D., Henderson, E., Kojima, I., Matsuhisa, M., Hori, M., & Yamasaki, Y. (2007). MafA regulates expression of genes important to islet  $\beta$ -cell function. *Molecular Endocrinology*, *21*(11), 2764–2774. <https://doi.org/10.1210/me.2007-0028>
- McCulloch, L. J., van de Bunt, M., Braun, M., Frayn, K. N., Clark, A., & Gloyn, A. L. (2011). GLUT2 (SLC2A2) is not the principal glucose transporter in human pancreatic beta cells: Implications for understanding genetic association signals at this locus. *Molecular Genetics and Metabolism*, *104*(4), 648–653. <https://doi.org/10.1016/j.ymgme.2011.08.026>
- Mosmann, T. (1983). Rapid colorimetric assay for cellular growth and survival: Application to proliferation and cytotoxicity assays. *Journal of Immunological Methods*, *65*(1–2), 55–63. [https://doi.org/10.1016/0022-1759\(83\)90303-4](https://doi.org/10.1016/0022-1759(83)90303-4)
- Nishitoh, H. (2012). CHOP is a multifunctional transcription factor in the ER stress response. *Journal of Biochemistry*, *151*(3), 217–219. <https://doi.org/10.1093/jb/mvr143>
- Ohoka, N., Yoshii, S., Hattori, T., Onozaki, K., & Hayashi, H. (2005). TRB3, a novel ER stress-inducible gene, is induced via ATF4-CHOP pathway and is involved in cell death. *EMBO Journal*, *24*(6), 1243–1255. <https://doi.org/10.1038/sj.emboj.7600596>
- Onda, K., Horike, N., Suzuki, T. I., & Hirano, T. (2013). Polymethoxyflavonoids tangeretin and nobiletin increase glucose uptake in murine adipocytes. *Phytotherapy Research*, *27*(2), 312–316. <https://doi.org/10.1002/ptr.4730>
- Park, S. M., Kang, T. Il, & So, J. S. (2021). Roles of XBP1s in transcriptional regulation of target genes. *Biomedicines*, *9*(7), 1–26. <https://doi.org/10.3390/biomedicines9070791>
- Park, Y. J., & Woo, M. (2019). Pancreatic  $\beta$  cells: Gatekeepers of type 2 diabetes. *J. Cell*



*Biol*, 218, 1094–1095. <https://doi.org/10.1083/jcb.201810097>

Rajan, S. S., Srinivasan, V., Balasubramanyam, M., & Tatu, U. (2007). *Endoplasmic reticulum ( ER ) stress & diabetes. March*, 411–424.

Seo, H. Y., Yong, D. K., Lee, K. M., Min, A. K., Kim, M. K., Kim, H. S., Won, K. C., Park, J. Y., Lee, K. U., Choi, H. S., Park, K. G., & Lee, I. K. (2008). Endoplasmic Reticulum Stress-Induced Activation of Activating Transcription Factor 6 Decreases Insulin Gene Expression via Up-Regulation of Orphan Nuclear Receptor Small Heterodimer Partner. *Endocrinology*, 149(8), 3832.

<https://doi.org/10.1210/EN.2008-0015>

Singh, R., Mohapatra, L., & Tripathi, A. S. (2021). *Targeting mitochondrial biogenesis: a potential approach for preventing and controlling diabetes.*

<https://doi.org/10.1186/s43094-021-00360-x>

Sivandzade, F., Bhalerao, A., & Cucullo, L. (2019). Analysis of the Mitochondrial Membrane Potential Using the Cationic JC-1 Dye as a Sensitive Fluorescent Probe. *Bio-Protocol*, 9(1). <https://doi.org/10.21769/BIOPROTOC.3128>

Song, B., Scheuner, D., Ron, D., Pennathur, S., & Kaufman, R. J. (2008). *Chop deletion reduces oxidative stress. 118*(10). <https://doi.org/10.1172/JCI34587DS1>

Takano, K., Tabata, Y., Kitao, Y., Murakami, R., Suzuki, H., Yamada, M., Inuma, M., Yoneda, Y., Ogawa, S., & Hori, O. (2007). Methoxyflavones protect cells against endoplasmic reticulum stress and neurotoxin. *American Journal of Physiology - Cell Physiology*, 292(1), 353–361.

[https://doi.org/10.1152/AJPCELL.00388.2006/SUPPL\\_FILE/FIGURE](https://doi.org/10.1152/AJPCELL.00388.2006/SUPPL_FILE/FIGURE)

Thorens, B. (n.d.). *GLUT2, glucose sensing and glucose homeostasis.* <https://doi.org/10.1007/s00125-014-3451-1>

Vig, S., Lambooi, J. M., Zaldumbide, A., & Guigas, B. (2021). *Endoplasmic Reticulum-Mitochondria Crosstalk and Beta-Cell Destruction in Type 1 Diabetes.* <https://doi.org/10.3389/fimmu.2021.669492>

Wang, H., Kouri, G., & Wollheim, C. B. (2005). ER stress and SREBP-1 activation are implicated in beta-cell glucolipotoxicity. *Journal of Cell Science*, 118(Pt 17), 3905–

3915. <https://doi.org/10.1242/JCS.02513>

- Xiao, T., Liang, X., Liu, H., Zhang, F., Meng, W., & Hu, F. (2020). Mitochondrial stress protein HSP60 regulates ER stress-induced hepatic lipogenesis. *Journal of Molecular Endocrinology*, *64*(2), 67–75. <https://doi.org/10.1530/JME-19-0207>
- Yao, X., Li, K., Liang, C., Zhou, Z., Wang, J., Wang, S., Liu, L., Yu, C. L., Song, Z. B., Bao, Y. L., Zheng, L. H., Sun, Y., Wang, G., Huang, Y., Yi, J., Sun, L., & Li, Y. (2020). Tectorigenin enhances PDX1 expression and protects pancreatic b-cells by activating ERK and reducing ER stress. *Journal of Biological Chemistry*, *295*(37), 12975–12992. <https://doi.org/10.1074/JBC.RA120.012849>
- Zhang, I. X. (2020). *Investigating the Role of ER Stress on Mouse Pancreatic Beta-Cell Function*.
- Zhou, X., Xu, Y., Gu, Y., & Sun, M. (2021). 4-Phenylbutyric acid protects islet  $\beta$  cell against cellular damage induced by glucocorticoids. *Molecular Biology Reports*, *48*(2), 1659–1665. <https://doi.org/10.1007/s11033-021-06211-5>
- Zhu, M., Liu, X., Liu, W., Lu, Y., Cheng, J., & Chen, Y. (2021). B Cell Aging and Age-Related Diabetes. *Aging*, *13*(5), 7691–7706. <https://doi.org/10.18632/aging.202593>

# **Chapter 6**

## **Summary & Conclusion**

## Summary & Conclusion

Diabetes mellitus is a lifelong condition that deteriorates over time because it is a chronic metabolic syndrome with complex pathogenesis. Anti-diabetic medications are used as first-line therapy to achieve proper glycemic control primarily by improving insulin secretion from the pancreas and suppressing insulin resistance in peripheral tissues, but the prevalence of the disease and the financial burden associated with providing care for diabetics are rising at an alarming rate. Therefore, the focus should shift towards identifying novel targets and cheaper alternatives than the currently used drugs. ER stress has emerged as a putative mechanism underlying diabetes pathogenesis. Natural compounds can be used to pharmacologically manipulate ER stress, which can help in the development of improved treatment approaches with less financial burden for disease management.

In the present study, *in vitro models* for ER stress induction using skeletal muscle L6 cell line and pancreatic Beta-TC-6 cell line were established by treating the cells for a period of 24 hours with 0.25 $\mu$ g/ml tunicamycin, a pharmacological ER stress inducer that blocks the first step of the N-linked glycosylation. We then studied the efficacy of three selected flavones, apigenin, luteolin, and tangeretin in ameliorating the maladaptive UPR and redox imbalances in L6 myotubes. The flavones were used at the following concentrations for co-treatment with tunicamycin, apigenin (20 $\mu$ M), luteolin (10 $\mu$ M), and tangeretin (50 $\mu$ M). PBA (1mM), a chemical chaperone was used as the positive control in all the experiments.

Skeletal muscle cells are relevant targets for diabetes related as well as ER stress related studies. This is because they are the main sites for insulin stimulated glucose utilization

and also, they have an elaborate ER known as sarcoplasmic reticulum which serves as calcium reservoir facilitating muscle contractions. This makes skeletal muscle cells ideal targets for pharmacological manipulation of ER stress and diabetes related pathways. ER stress and oxidative stress are closely associated events where the induction of the former upregulates the protein folding machinery which in turn generates ROS, a hallmark of oxidative stress and disturbed redox homeostasis. In our study, we observed an upregulation in the expression of PDI and ERp72, members of the protein folding machinery which was accompanied by increased ROS generation and decreased SOD and glutathione reductase antioxidant activities indicating disruption of redox homeostasis. The selected flavones were observed to suppress the PDI, Erp72 levels and also improve the antioxidant activities. However, only luteolin and tangeretin could significantly suppress the ER stress induced ROS levels whereas apigenin could not suppress the levels significantly. In this study, TrxR activity was exacerbated on treatment with tunicamycin while downregulation of activity was observed on co-treatment with the flavones. This was because TrxR is involved in reducing the non-native disulfide bonds which would be higher during ER stress. The antioxidant potential of the flavones was confirmed through the molecular docking studies where the binding interaction of the flavones with various antioxidant enzymes (catalase, glutathione peroxidase, SOD1, and SOD2) was analyzed by the autodock and pyMOL software.

Prolonged ER stress leads to maladaptive UPR which is indicated by the upregulation of GADD153/CHOP expression. Here, chronic treatment with tunicamycin induced the CHOP expression. Tangeretin and luteolin suppressed the CHOP levels while apigenin was not effective against tunicamycin induced upregulated CHOP levels. We also studied the expression of major MAP kinase proteins (p-JNK, p-p38MAPK, and ERK1/2) that are activated in response to ER stress and ROS generation and contribute to cellular

dysfunction. Here, tunicamycin treatment upregulated the p-JNK, p-p38MAPK, and ERK1/2 levels. Apigenin did not induce any lowering effect on the MAP kinase proteins. Luteolin could only suppress the ERK1/2 levels whereas tangeretin was shown to ameliorate the expression of all three MAP kinase proteins. From the results obtained, it is evident that tangeretin was most effective in alleviating ER stress related redox imbalances in skeletal muscle cells.

ER stress is a mechanism underlying insulin resistance and hence targeting ER stress can aid in mitigation of insulin resistance and the improvement of glucose uptake in skeletal muscles. Here we observed the induction of insulin resistance in L6 myotubes on prolonged treatment with tunicamycin and co-treatment with tangeretin was effective in improving the glucose uptake. However, apigenin and luteolin did not show any efficacy against tunicamycin induced insulin resistance. Hence, we selected tangeretin for all future studies and proceeded to elucidate its mechanism of action in ameliorating ER stress induced insulin resistance. In the present study, we observed an amelioration in the expression of ER stress markers (GRP78, IRE-1 $\alpha$ , p-PERK, ATF6, XBP-1, and ATF4) on co-treatment with tangeretin which indicates its potential in downregulating the ER stress. Here, we studied the expression of proteins involved in insulin-stimulated as well as insulin-independent glucose uptake under ER stress. The expression of the proteins namely, p-IRS1(tyr), PI3K, GLUT4, and AMPK were suppressed under ER stress. From the results, it was observed that tangeretin was not effective in improving p-IRS1(tyr), PI3K expression levels which are components of insulin-stimulated signaling. This was also confirmed by studying the expression of PTEN, a negative regulator of insulin signaling. Tangeretin did not suppress the PTEN levels. However, tangeretin improved glucose uptake by activating the AMPK signaling as shown by the improved expression

of p-LKB1, p-AMPK, and AS160 proteins. The role of AMPK was also validated by the AMPK inhibitor studies using dorsomorphin.

The close proximity and the functional interaction between the ER and mitochondria, make it susceptible to pathological insults in the ER. Skeletal muscle cells are metabolically active and have high energy consumption which makes them vulnerable to mitochondrial dysfunction. In the present study, we observed the mitochondrial changes that occur in response to ER stress, and the potential of tangeretin in modulating these changes was analyzed. Here, we observed that tunicamycin augmented the mitochondrial ROS levels, decreased the SOD1 and 2 levels, induced loss of mitochondrial membrane potential, upregulated the mitochondrial dynamics, increased the UCP-3, and XIAP levels (indication of stress condition), and modulated the MAMs protein expression which included the IP<sub>3</sub>R, VDAC, GRP75, PACS2 and FUNDC1. However, tunicamycin treatment did not induce any significant changes in mitochondrial biogenesis, cytochrome c levels, oxygen consumption rate, and corresponding COXIV activity. This could be due to the subtoxic dose of tunicamycin used in our study. Tangeretin was able to suppress the mitochondrial ROS levels which was accompanied by improvement in the SOD levels. Tangeretin suppressed the expression of OPA1, DRP1, and FIS1 (proteins involved in mitochondrial dynamics) while also improving the mitochondrial membrane potential. Tangeretin further augmented mitochondrial uncoupling protein UCP-3 which may be an adaptive mechanism to suppress the ROS generation. The upregulated anti-apoptotic factor XIAP was suppressed on treatment with tangeretin which implies the alleviation of stress.

One of the consequences of ER stress is the disruption of the proteostasis network (equilibrium between protein synthesis and protein degradation). In the present study, we evaluated the effect of tangeretin on ER stress induced autophagy and ERAD proteolytic

pathways. Increased protein degradation in skeletal muscles leads to loss of muscle mass or muscle wasting also known as atrophy. It is a comorbidity related to diabetes that can impact muscle function. Here, tangeretin improved the proteostasis network by downregulating the expression of autophagy proteins LC3-II and Beclin1 while improving the expression of autophagy regulators, p-Akt and mTOR. Tangeretin suppressed the levels of GRP94, calnexin, HERPUD1, SEL1, and UFD1 involved in the ERAD while it could not lower the expression of EDEM1, SYVN1, and RNF5. Depletion of calcium ions from the ER is a stimulus for the activation of protein degradation pathways. Hence, in our study, we analyzed the expression of SERCA (calcium influx channel) and p-RYR (calcium efflux channel), calcium transporters on the ER membrane. From the results, it was observed that tangeretin improved the SERCA expression and suppressed p-RYR expression implying restoration of calcium homeostasis and subsequently proteostasis network. A schematic result summary highlighting the findings in L6 myotubes is represented in Figure.6.1.



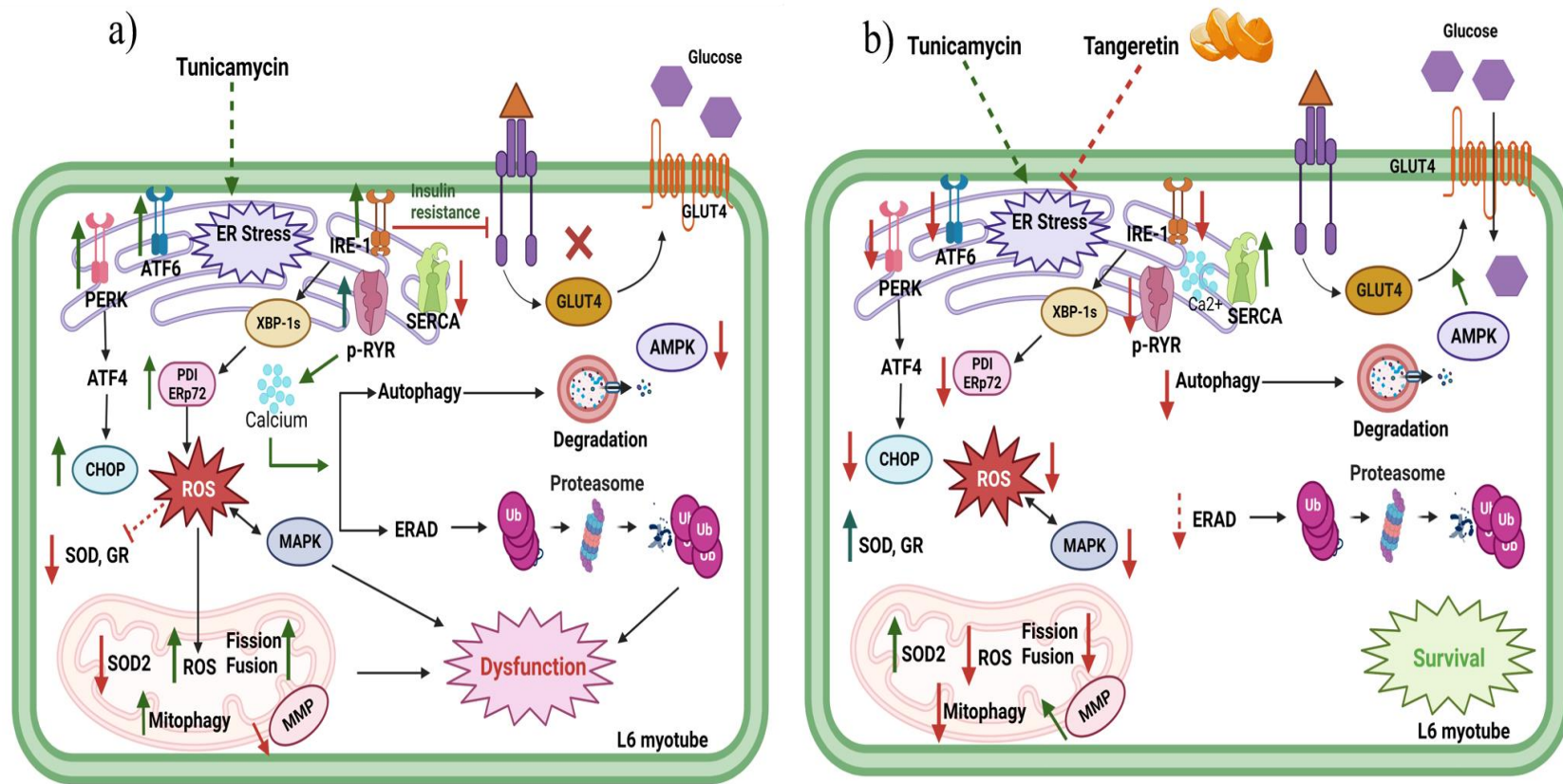


**Figure.6.1. Schematic result summary in rat skeletal muscle L6 cells.** a) Chronic treatment with tunicamycin induces maladaptive UPR, redox imbalances, insulin resistance, mitochondrial dysfunction, and protein degradation pathways mediating cellular dysfunction. b) Tangeretin co-treatment ameliorates ER stress induced maladaptive UPR, redox imbalances, insulin resistance, mitochondrial dysfunction, and protein degradation pathways promoting cellular survival.

Pancreatic beta cells are important targets for both ER stress as well as diabetes due to an elaborate ER which can be attributed to its insulin-secreting potential. Pathological insults in the pancreatic beta cells result in impaired insulin biosynthesis as well as beta cell dysfunction. Hence, here we studied the efficacy of tangeretin in mitigating the ER stress induced perturbations in pancreatic Beta-TC-6 cells. An optimised dose of 0.25µg/ml tunicamycin for a time period of 24 hours was used for ER stress induction. Tangeretin co-treatment dose was determined as 10µM. PBA (100µM) was used as the positive control in all the experiments. From the results, it was observed that prolonged exposure to tunicamycin resulted in increased ROS generation, upregulated the protein folding machinery (XBP-1, GRP94, calnexin), increased the GADD153/CHOP, TRB3, and Maf A levels. Whereas it decreased mitochondrial biogenesis, mitochondrial membrane potential, p-Akt, Pdx-1, and insulin protein expression. The GLUT2 levels did not undergo significant change in response to tunicamycin and this could be due to the subtoxic dose of inducer used and also the fact that GLUT2 expression is not directly related to ER stress. Co-treatment with tangeretin suppressed the ROS levels, protein folding machinery, CHOP, and TRB3 levels while improving the mitochondrial function, p-Akt, and Pdx-1 levels. Tangeretin was able to improve insulin levels only modestly. An overall summary of the findings in pancreatic Beta-TC-6 cells is schematically depicted in Figure.6.2.

Although ER stress plays a pivotal role in the development and evolution of diabetes mellitus, the disease is still not completely recognized as a protein misfolding disorder, and the markers of ER stress are not fully utilized as therapeutic targets. Based on our study in both rat skeletal muscle L6 and pancreatic Beta-TC-6 cells, we propose tangeretin as a potential candidate against ER stress induced diabetic complications. Further detailed studies in suitable *in vivo* models are needed to validate the findings here.

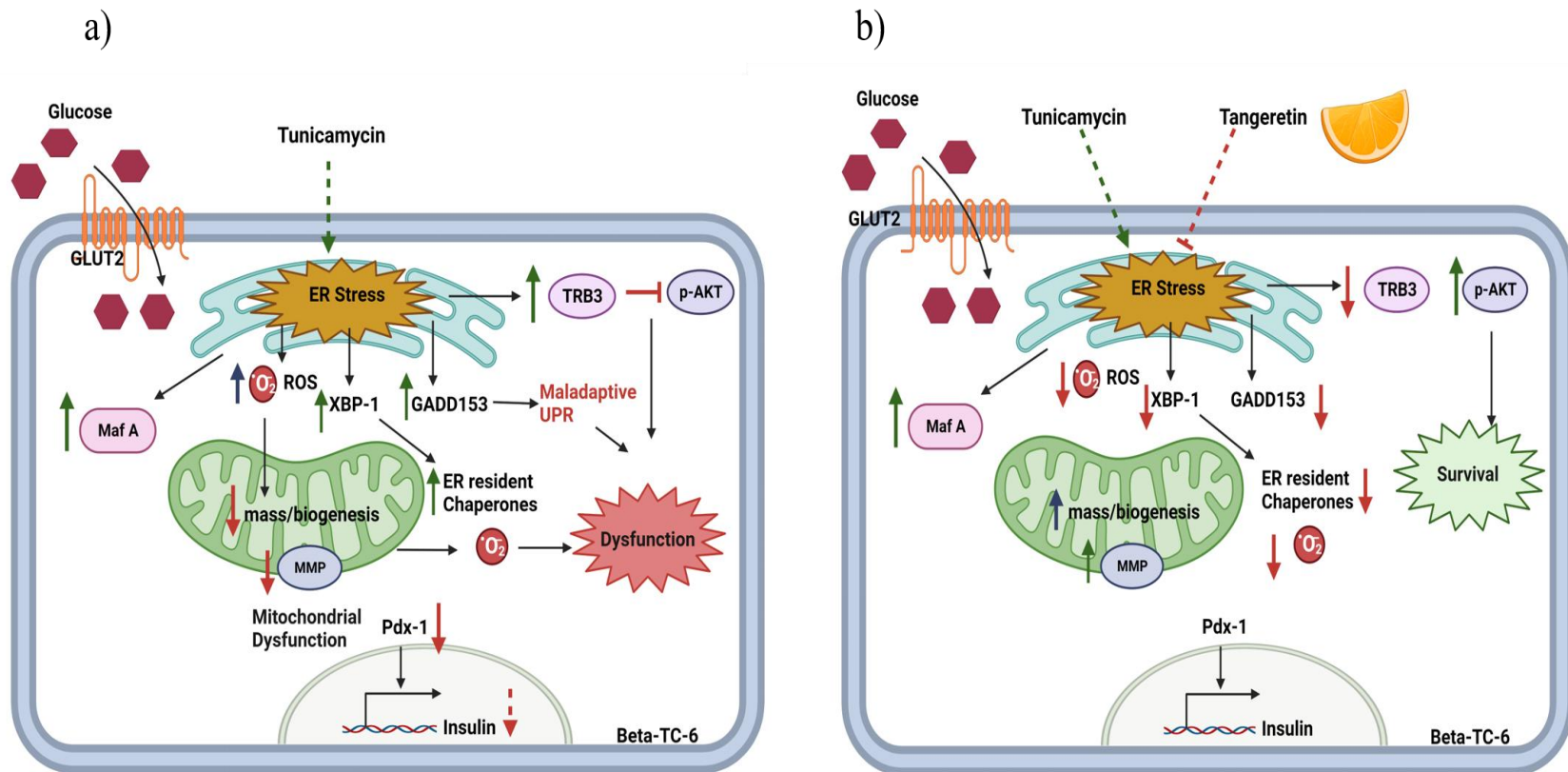


**Figure.6.2. Schematic result summary in pancreatic Beta-TC-6 cells.** a) Prolonged exposure to tunicamycin induces maladaptive UPR, protein folding machinery, redox imbalances, and mitochondrial dysfunction and mediates beta cell dysfunction by augmenting TRB3 levels. b) Tangeretin co-treatment alleviates ER stress induced maladaptive UPR, protein folding machinery, redox imbalances, and mitochondrial dysfunction and promotes cell survival by augmenting p-Akt and Pdx-1 levels.

## ABSTRACT

Name of the Student: Eveline M Anto

Registration no. 10BB17J39011

Faculty of study: Biological Sciences

Year of Submission: 2023

CSIR Lab: NIIST

Name of the supervisor: Dr. P Jayamurthy

**Title of the thesis: Investigation on the role of Tangeretin in alleviation of ER stress induced diabetic complications: An *in vitro* approach**

Diabetes mellitus is a chronic disorder defined by sustained hyperglycemia. Despite the availability of numerous antidiabetic drugs, the disease prevalence as well as the economic burden imposed by diabetes healthcare is on the rise. There is a need to identify newer targets and cheaper alternatives for disease intervention. ER stress has emerged as an underlying mechanism in the development of the two clinical manifestations of diabetes, insulin resistance in peripheral tissues such as skeletal muscles (the most prominent site for glucose uptake and utilization) and impaired insulin secretion from the pancreatic beta cells. In the present study, we evaluated the potential of tangeretin, a citrus methoxy flavone found abundantly in orange fruit peels against tunicamycin (pharmacological ER stress inducer) induced diabetes-related complications in rat skeletal muscle L6 cells and mouse insulinoma pancreatic Beta-TC-6 cells. We observed an amelioration in ER stress-mediated oxidative stress in L6 cells on treatment with tangeretin. This was indicated by the reduction in ROS levels, increased antioxidant levels, suppressed PDI and ERp72 levels, suppressed MAP Kinase levels and decreased GADD153/CHOP expression. We also observed alleviation of tunicamycin induced insulin resistance by treatment with tangeretin via suppression of ER stress markers and activation of AMPK-mediated glucose uptake. The present study evaluated the effect of tangeretin on ER stress-mediated mitochondrial dysfunction. Here, we observed an improvement in mitochondrial function on co-treatment with tangeretin as evident from the suppressed mitochondrial ROS, downregulation of mitochondrial fission, fusion, improvement in SOD levels, hyperpolarization of mitochondrial membrane potential, and modulation of MAMs proteins. Enhanced protein degradation by autophagy and ERAD machinery is a consequence of ER stress which if sustained can lead to proteolysis in skeletal muscles resulting in a condition termed as muscle atrophy or wasting, a comorbidity associated with diabetes. Here, we observed increased autophagy and ERAD signaling on prolonged exposure to tunicamycin. Tangeretin co-treatment suppressed the autophagy machinery by downregulating the expression of LC3-II, and Beclin1 (autophagy proteins) and upregulating the expression of autophagy negative regulators, p-Akt and mTOR. Tangeretin also modulated the ERAD signaling by suppressing some of the proteins including GRP94, calnexin, SEL1, HERPUD1 and UFD1. In the present study, tangeretin treatment was able to improve pancreatic beta cell function during ER stress by improving the p-AKT, Pdx-1 levels and mitochondrial function while suppressing the ROS levels, GADD153 and protein folding machinery. Our results propose tangeretin as a potential candidate against ER stress induced diabetes related complications.

# List of Publications

## Publications emanating from thesis work

**Eveline M Anto**, Sruthi CR, Lekshmy Krishnan, Raghu KG, Jayamurthy Purushothaman.

“Tangeretin alleviates Tunicamycin-induced endoplasmic reticulum stress and associated complications in skeletal muscle cells”. *Cell Stress & Chaperones*, 2023.

<https://doi.org/10.1007/s12192-023-01322-3>

**Eveline M Anto**, P.Jayamurthy. “Tangeretin enhances pancreatic beta-TC-6 function by ameliorating tunicamycin-induced cellular perturbations”. *Molecular Biology Reports*, 2023. DOI 10.1007/s11033-023-09013-z

DOI 10.1007/s11033-023-09013-z

## Publications not related to thesis work

**Eveline M Anto**, Anaga Nair, and Jayamurthy Purushothaman. "Role of Nanotechnology in Diagnosis and Treatment of Diabetes, 2022." In *Nanophytomedicine*, pp. 131-140. CRC Press.

**Eveline M Anto**, Anaga Nair, and Jayamurthy Purushothaman. "Emerging Role of Circulating Tumour DNA in Treatment Response Prognosis in Colon Cancer." In *Colon Cancer Diagnosis and Therapy*, pp. 257-270. Springer, Cham, 2021.

Anaga Nair, **Eveline M Anto**, and Jayamurthy Purushothaman. "Probiotics in Colon Cancer: A Therapeutic Approach." In *Colon Cancer Diagnosis and Therapy*, pp. 421-434. Springer, Cham, 2021.

## Conference Presentations

17th Annual Meeting of the Society for Free Radical Research India (SFRR-INDIA-2020) & Conference on "Role and Management of Oxidative Stress in Human Disease" held during Feb. 12-15, 2020 at DAE Convention Centre, BARC, Anushaktinagar, Mumbai (Poster Presentation)

33<sup>rd</sup> Kerala Science Congress held on 25-28 January, 2021 at Thiruvananthapuram (Online Poster Presentation)

Two Days National Seminar on Fundamental and Applied Dimensions in Plant Sciences held on 24-25 March, 2022 at JNTBGRI, Palode, Thiruvananthapuram (**Best Paper**)

International Seminar on Plant Chemistry, Gene Prospecting and Clinical Biology organized by Kerala Academy of Sciences and Department of Chemistry, Mar Ivanios College, Thiruvananthapuram from 10-11 November, 2022 (**Best Paper**)

National Seminar on Recent Trends in Disease Prevention and Health Management at CSIR-National Institute for Interdisciplinary Science and Technology, Thiruvananthapuram, Kerala on 14 & 15 December 2022 (**Best Poster**)



# Tangeretin alleviates Tunicamycin-induced endoplasmic reticulum stress and associated complications in skeletal muscle cells

Eveline M. Anto<sup>1,2</sup> · C. R. Sruthi<sup>1,2</sup> · Lekshmy Krishnan<sup>1</sup> · K. G. Raghu<sup>1,2</sup> · Jayamurthy Purushothaman<sup>1,2</sup>

Received: 14 June 2022 / Revised: 10 November 2022 / Accepted: 10 January 2023  
© The Author(s), under exclusive licence to Cell Stress Society International 2023

## Abstract

Endoplasmic reticulum (ER) stress and associated oxidative stress are involved in the genesis and progression of skeletal muscle diseases such as myositis and atrophy or muscle wasting. Targeting the ER stress and associated downstream pathways can aid in the development of better treatment strategies for these diseases with limited therapeutic approaches. There is a growing interest in identifying natural products against ER stress due to the lower toxicity and cost effectiveness. In the present study, we investigated the protective effect of Tangeretin, a citrus methoxyflavone found in citrus peels against Tunicamycin (pharmacological ER stress inducer)–induced ER stress and associated complications in rat skeletal muscle L6 cell lines. Treatment with Tunicamycin for a period of 24 h resulted in the upregulation of ER stress marker proteins, ER resident oxidoreductases and cellular reactive oxygen species (ROS). Co-treatment with Tangeretin was effective in alleviating Tunicamycin-induced ER stress and associated redox-related complications by significantly downregulating the unfolded protein response (UPR), ER resident oxidoreductase proteins, cellular ROS and improving the antioxidant enzyme activity. Tunicamycin also induced upregulation of phosphorylated p38 MAP Kinase and loss of mitochondrial membrane potential. Tangeretin significantly reduced the levels of phosphorylated p38 MAP Kinase and improved the mitochondrial membrane potential. From the results, it is evident that Tangeretin can be explored further as a potential candidate for skeletal muscle diseases involving protein misfolding and ER stress.

**Keywords** ER stress · Oxidative stress · Tangeretin · Tunicamycin · L6 cell lines

## Introduction

Endoplasmic reticulum (ER) is one of the largest and complex organelle in eukaryotic cells which is committed to multiple functions such as protein synthesis, folding, transport, lipid metabolism and calcium storage (Schwarz and Blower 2015). ER stress is a condition which ensues when the protein folding demand exceeds the protein folding capacity leading to build-up of misfolded/unfolded protein

aggregates (Lin et al. 2007). This triggers a cascade of signalling pathways broadly termed as the unfolded protein response (UPR). The UPR is the cell's coping mechanism to deal with the ER stress. There are three main branches of UPR which are implicated during ER stress, namely the inositol-requiring kinase 1 alpha (IRE-1  $\alpha$ ), the protein kinase ribonucleic acid (RNA)-activated-like ER kinase (PERK) and activating transcription factor 6 (ATF6) (Parmar and Schröder 2012). In unstressed conditions, these three sensors are sequestered by the Bip protein also known as GRP78. Upon induction of ER stress, these three sensors dissociate from Bip and are activated leading to downstream signalling pathways that are involved in protein synthesis attenuation, removal of misfolded proteins and upregulation of protein folding machinery which may result in either cell survival or cell apoptosis (Rutkowski and Kaufman 2004). Maladaptive and sustained UPR is associated with several pathological scenarios such as neurodegenerative diseases, metabolic disorders and skeletal muscle diseases (Lin et al. 2007; Rayavarapu et al. 2012; Afroze et al. 2019).

✉ K. G. Raghu  
raghugopal@niist.res.in

✉ Jayamurthy Purushothaman  
pjayamurthy@niist.res.in

<sup>1</sup> Department of Biochemistry, Agro-Processing & Technology Division, CSIR-National Institute for Interdisciplinary Science & Technology, Thiruvananthapuram 695019, Kerala, India

<sup>2</sup> Academy of Scientific and Innovative Research (AcSIR), Ghaziabad 201002, India



Skeletal muscle is a vital organ involved in multiple functions, primarily, whole body glucose homeostasis, body movement and thermoregulation (Gallot and Bohnert 2021). A specialised ER known as the sarcoplasmic reticulum (SR) exists in the skeletal muscles which acts as a reservoir of calcium ions thereby playing a pivotal role in muscle contraction and subsequently skeletal muscle function (Mensch and Zierz 2020). Also, skeletal muscle tissue is a prominent site for protein metabolism accounting for storage of 50–70% of total body protein (Bohnert et al. 2018). ER stress in skeletal muscle arises in response to numerous stimuli such as high nutritional intake, exercise, oxygen starvation, disruption of redox homeostasis and fluctuation in calcium levels (Deldicque et al. 2013). Once triggered, the ER stress induces the oxidative stress by enhancing the protein folding machinery of ER which in turn generates ROS as byproducts of disulphide exchange reactions mediated by protein disulphide isomerase (PDI) family of proteins causing disturbances in the cellular redox state (Haynes et al. 2004). A vicious cycle exists between ER stress and ROS production where the former can initiate as well as be augmented by the latter (Chong et al. 2017). Increased ROS generation weakens the cellular antioxidant defense and also induces mitochondrial dysfunction owing to the close structural proximity of the ER and mitochondria via the mitochondrial associated membranes (MAMs) (Silva-Palacios et al. 2020). All these factors contribute to the pathogenesis of skeletal muscle diseases such as myositis and atrophy or muscle wasting. Currently exercising, nutrient supplementation and drug therapy are the major treatment strategies; however, exercise may not be a feasible option for many patients with severe symptoms (Yin et al. 2021). Therefore, major emphasis is on the drugs but these are limited by the associated adverse effects (Carstens and Schmidt 2014; Oddis 2016; Sartori et al. 2021).

Pharmacological intervention of ER stress and associated downstream pathways may aid in the development of better treatment strategies. Exploring plant-based alternatives has been a prominent area of research owing to their economic feasibility and minimum side effects. However, their mode of action at the cellular level needs to be explored thoroughly in order to determine the efficacy. Flavonoids due to their abundance in fruits and vegetables and associated health benefits have become an integral aspect of nutraceutical and medicinal applications (Panche et al. 2016). In the present study, we have evaluated the potential of Tangeretin, a polymethoxyflavone found abundantly in citrus fruits and fruit peels against the ER stress-induced cellular alterations in rat skeletal muscle L6 cell lines (Li et al. 2007). Tangeretin is well reported for its antioxidant, antidiabetic, anticancer, anti-inflammatory and neuroprotective activities (Ashrafizadeh et al. 2020; Boye et al. 2021). It is also reported for its ER protective effects in MIN6 and PC-12 cell lines (Takano et al. 2007). However, there are no reports indicating the

potential of Tangeretin against ER stress and its effect in downstream associated pathways in skeletal muscle cells.

Here, we have attempted to investigate the molecular mechanism of Tangeretin in mitigating ER stress-associated redox perturbations in rat skeletal muscle L6 cell lines. For ER stress induction, Tunicamycin, a chemical which blocks the first step in the N-linked glycosylation of proteins resulting in build-up of misfolded proteins, was used (Oslowski and Urano 2011). This study may contribute towards gaining a deeper insight into the ER protective effect of Tangeretin in skeletal muscle cells.

## Materials and methods

Dulbecco's modified Eagle's medium (DMEM) containing 4.5 g/L glucose and 1.5 g/L sodium bicarbonate, fetal bovine serum, Horse serum, antimycotic antibiotic mix and dimethyl sulfoxide (DMSO), Triton X, Glycine, Tris base, Skimmed milk, Sodium dodecyl sulphate were purchased from Himedia (Mumbai, India). Tangeritin, Tunicamycin, 4-Phenyl butyric acid (PBA), HPLC grade methanol, protease inhibitor cocktail tablets were purchased from Sigma Aldrich Chemical (St. Louis, Missouri, USA). Dihydroethidium (DHE) assay kit, Glutathione reductase assay kit, Thioredoxin reductase assay kit, superoxide dismutase assay kit, JC-1 assay kit were obtained from Cayman Chemicals (Michigan, USA). Radioimmunoprecipitation assay buffer (RIPA lysis buffer), Bicinchoninic acid assay kit (BCA kit) were purchased from Thermo Fisher Scientific (Waltham, Massachusetts, USA). The antibodies ATF4, IRE-1 alpha, Beta actin, p38MAPK, PDI, Antirabbit and Antimouse HRP conjugated antibodies were purchased from Cell Signaling Technologies (Danvers, Massachusetts, USA). Antibodies ATF6, GRP78, and p-p38MAPK were purchased from Santa Cruz Biotechnology (Dallas, Texas, USA). Antibodies XBP-1 and ERp72 were purchased from Gbiosciences (St. Louis, MO, USA). Rat skeletal muscle cell lines, L6 myoblasts were purchased from National Centre for Cell Sciences, Pune, India.

## Cell culture

L6 myoblasts were maintained at 37 °C (5% carbon dioxide) in DMEM containing 10% fetal bovine serum and 1% antibiotic mix. For differentiation, myoblasts were grown upto 70% confluency and medium was replaced with DMEM containing 2% horse serum and the medium was changed alternatively for 4 days. Following the cell viability assays, all the experiments were conducted in differentiated myotubes. The experimental design for the study has been represented in Fig. 1.



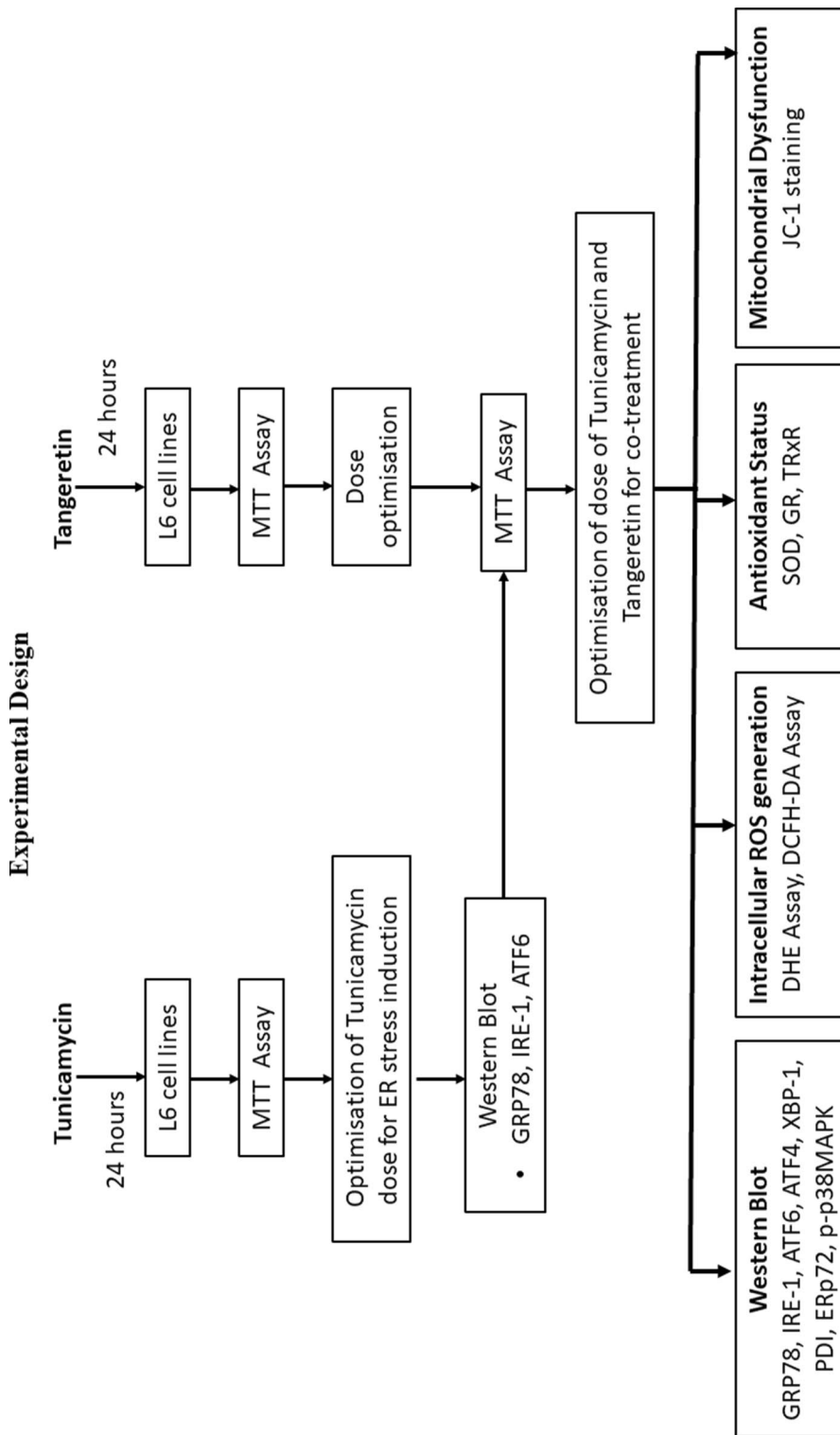


**Fig. 1** Experimental design for the study. Effect of Tangeretin against Tunicamycin-induced stress-related complications was evaluated in L6 cell lines by studying the alterations in the ER proteins, the redox status and mitochondrial membrane potential

## Dose optimization of Tunicamycin

### MTT assay

Cytotoxicity of Tunicamycin was determined by the MTT assay (Mosmann 1983). To be precise, myoblasts were seeded in 96 well plate at a density of  $5 \times 10^3$  cells per well. After attaining confluence, myoblasts were treated with various concentrations of Tunicamycin (0.25 to 4  $\mu\text{g/ml}$ ) for a time period of 24 h. Post treatment, cells were washed with HBSS and incubated with MTT solution (0.5 mg/ml) dissolved in serum free DMEM for 4 h. Following incubation, MTT solution was aspirated and 100  $\mu\text{L}$  DMSO was added per well. Plate was then kept on shaker for 20 min to ensure complete dissolution of the formazan crystals. The absorbance was read at 570 nm in multimode plate reader (Tecan infinite 200 PRO, Austria).

### Western blot analysis for ER stress induction

After 24 h treatment with respective doses of Tunicamycin, myotubes were washed with Hank's balanced salt solution (HBSS) followed by extraction of proteins using RIPA lysis buffer. The extracted protein samples were quantitated using the BCA assay kit with bovine serum albumin as the standard and were normalised. Protein samples were separated on a 10% sodium dodecyl sulphate polyacrylamide gels (Bio rad, USA). Following this, proteins were transferred onto PVDF membranes (Millipore, Merck, USA) and then blocked in 5% skimmed milk for 1 h. Membranes were then washed with TBST three times and incubated at 4 °C overnight with suitable primary antibodies against ER stress markers such as GRP78, ATF6, IRE-1 $\alpha$  (dilution 1:1000). Beta actin was used as the loading control. Membranes were then incubated with appropriate HRP conjugated secondary antibodies (dilution 1:1000 to 1:2000) for 2 to 3 h at room temperature. Membranes were then probed with ECL substrate (Thermo Fisher Scientific, Massachusetts, USA) in Chemidoc MP Imaging systems (BioRad, USA). Densitometric analysis of the obtained bands were performed using the Image lab software version 6.1 (BioRad, USA).

## Dose optimization of Tangeretin

### MTT assay

L6 myoblasts were seeded in 96 well plate at  $5 \times 10^3$  cells per well and were treated with various concentrations of Tangeretin (10 to 100  $\mu\text{M}$ ) for 24 h and MTT assay was performed (as previously discussed in the "MTT Assay" section). Cell viability of Tangeretin was also investigated in the presence of Tunicamycin by treating cells with the

optimised dose of Tunicamycin in combination with various concentrations of Tangeretin (10 to 100  $\mu\text{M}$ ) for 24 h followed by MTT assay. Plate was read at 570 nm in multimode plate reader (Tecan infinite 200 PRO, Austria).

## Protective effect of Tangeretin against Tunicamycin-induced stress and associated perturbations

### Western blot

Western blot was performed to study the expression of proteins related to ER stress and oxidative stress. Myoblasts were cultured in T25 flasks and were differentiated for 4 days after reaching 80% confluence. Myotubes were then treated with 0.25  $\mu\text{g/ml}$  Tunicamycin in the presence and absence of 50  $\mu\text{M}$  Tangeretin for 24 h. 1 mM 4-Phenylbutyric acid (PBA), an FDA approved chemical chaperone was used as the positive control for all the assays. After the treatment period, cells were lysed for protein extraction for western blot (as described in the "Western blot analysis for ER stress induction" section). The proteins studied included GRP78, IRE-1, XBP-1, ATF6, ATF4, PDI, ERp72, p38MAP kinase, p-p38MAP kinase and Beta actin.

### Detection of intracellular reactive oxygen species ions by Dihydroethidium assay and DCFH-DA assay

L6 myoblasts were seeded in 96 black well plate. After differentiation, myotubes were treated with respective groups for a period of 24 h. Following the treatment, cells were assayed following the manufacturer's protocol. Briefly, myotubes were incubated with dihydroethidium (DHE) staining buffer for 1.5 h at 37 °C in dark. Following this, staining solution was removed and cells were overlaid with 100  $\mu\text{l}$  cell based assay buffer and fluorescence was measured at an excitation and emission wavelength of 480–520 nm and 570–600 nm respectively, using a multimode plate reader (Tecan infinite 200 PRO, Austria).

Alternatively, after 24 h co-treatment, myotubes were incubated with 10  $\mu\text{M}$  DCFH-DA staining solution for 20 min. Following which cells were washed with HBSS and overlaid with 100  $\mu\text{l}$  plain DMEM and taken for imaging in fluorescence microscope using the FITC filter (Olympus Life Science, Japan). The fluorescence intensity was quantitated using the Cell sense software (Olympus Life Science, Japan).

### Modulation of the cellular antioxidant enzymes

**Glutathione reductase** Glutathione reductase (GR) levels were measured as per the manufacturer's protocol (Cayman Chemicals, USA). The assay measures the rate of oxidation

of NADPH to NADP<sup>+</sup> by GR which was monitored by a decrease in absorbance. Treated myotubes were homogenised in ice cold 50 mM potassium phosphate buffer containing 1 mM EDTA (pH 7.5) followed by centrifugation at 10,000 × g for 15 min at 4 °C. The supernatants were collected and used for the assay. The reaction was initiated by the addition of NADPH (50 µl) to wells containing a mix of samples (20 µl), assay buffer (100 µl) and GSSG (20 µl). Absorbance was read kinetically at 340 nm (Tecan infinite 200 PRO, Austria) at an interval of 1 min for 5 timepoints.

**Superoxide dismutase** Cellular superoxide dismutase (SOD) levels were determined following the manufacturer's protocol (Cayman Chemicals, USA). Treated myotubes were collected in ice cold PBS (IX) by centrifugation at 1000 × g for 5 min at 4 °C. The cell pellets were then homogenised in 20 mM cold HEPES buffer (pH 7.2) followed by centrifugation at 1500 × g for 5 min at 4 °C and supernatant was collected. The assay mix consisted of 10 µl samples and 200 µl radical detector. The reaction was initiated by the addition of 20 µl xanthine oxidase to each well. After 30 min incubation at room temperature, absorbance was read at 440 nm in a plate reader (Tecan infinite 200 PRO, Austria).

**Thioredoxin reductase** Thioredoxin reductase (TrxR) levels were estimated according to the manufacturer's protocol (Cayman Chemicals, USA). Post 24 h co-treatment, myotubes were collected by centrifugation at 1000 × g for 5 min and the cell pellets were homogenised in cold buffer (50 mM potassium phosphate buffer, pH 7.4, containing 1 mM EDTA). Followed by centrifugation at 10,000 × g for 15 min at 4 °C. The supernatants were assayed for the TrxR activity. Reaction was initiated by the addition of NADPH and 5,5'-dithio-bis(2-dinitro benzoic acid) (DTNB) to assay mix consisting of diluted assay buffer (140 µl) and samples (20 µl). Absorbance was read kinetically at 405 nm at an interval of 1 min to obtain 5 timepoints.

### JC-1 staining

Myoblasts were seeded in 96-well plate and subjected to differentiation post 80% confluence. Myotubes after incubation with respective treatment groups were stained with JC-1 staining solution (Cayman Chemicals, USA) in dark and kept in CO<sub>2</sub> incubator at 37 °C for 20 min. Cells were then analysed in fluorescence microscope (Olympus Life Science, Japan). In healthy cells, JC-1 accumulates as red aggregates in the mitochondria which can be detected at an excitation/emission wavelength of 540/570 nm whereas in disease condition due to a loss of mitochondrial membrane potential ( $\Delta\psi_m$ ), JC-1 remains

as monomers emitting green fluorescence which can be detected at an excitation/emission of 485/535 nm and quantitated using Cell sense software (Olympus Life Science, Japan).

### Statistical analysis

All the experiments were performed independently three times in triplicates. All data was statistically analysed by one way ANOVA followed by Duncan post hoc test in SPSS software. All results are expressed as mean ± SEM. In all experiments, a *p* value ≤ 0.05 was regarded as statistically significant.

## Results

### Optimisation of Tunicamycin dose

#### MTT assay

In order to select appropriate dose of Tunicamycin for our study, cells were incubated with 0.25 µg/ml, 0.5 µg/ml, 1 µg/ml, 2 µg/ml, 3 µg/ml, 4 µg/ml of Tunicamycin for a period of 24 h. The concentrations which induced less than 20% toxicity were considered viable. Tunicamycin upto 1 µg/ml was found to induce less than 20% cytotoxicity (80.24 ± 1.79%) as shown in Fig. 2.

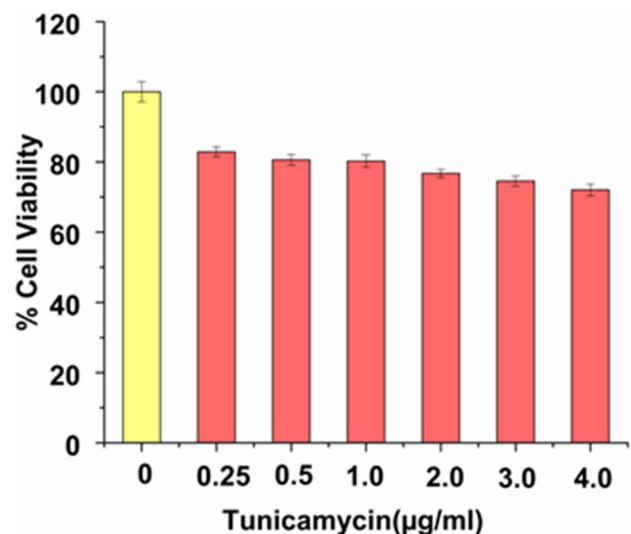


**Fig. 2** Cytotoxicity and microscopic analysis of Tunicamycin. L6 myoblasts treated with different doses of Tunicamycin (0.25 to 4 µg/ml) for 24 h, Values are expressed as mean ± SEM, where *n* = 3

### Western blot analysis for upregulation of ER stress markers

The expression of ER stress marker proteins namely GRP78, IRE-1 and ATF6 were significantly increased on treatment with both doses of tunicamycin as compared to the control cells as shown in Fig. 3a. GRP78 expression was increased to  $359.9 \pm 10.392\%$  and  $314.8 \pm 9.0902\%$  on treatment with  $0.25 \mu\text{g/ml}$  and  $1.0 \mu\text{g/ml}$  tunicamycin, respectively (Fig. 3b). IRE-1 $\alpha$  was found to be elevated on treatment with both doses of tunicamycin ( $176.9 \pm 5.107\%$  with  $0.25 \mu\text{g/ml}$  and  $173.1 \pm 4.998\%$  with  $1.0 \mu\text{g/ml}$ ) (Fig. 3b). ATF6, another ER stress sensor protein was also expressed in its active cleaved form post treatment with both doses of Tunicamycin,

$125.4 \pm 3.622\%$  and  $131.9 \pm 3.809\%$  for  $0.25 \mu\text{g/ml}$  and  $1.0 \mu\text{g/ml}$  tunicamycin, respectively (Fig. 3b). Since, the lower dose of Tunicamycin, i.e.,  $0.25 \mu\text{g/ml}$  was observed to be sufficient for induction of ER stress for a prolonged duration of 24 h without causing significant cell death, hence this concentration was selected for future experiments.

### Optimization of Tangeretin dose

#### MTT assay

Cell viability of Tangeretin was evaluated via MTT assay by treating cells with various concentrations of Tangeretin

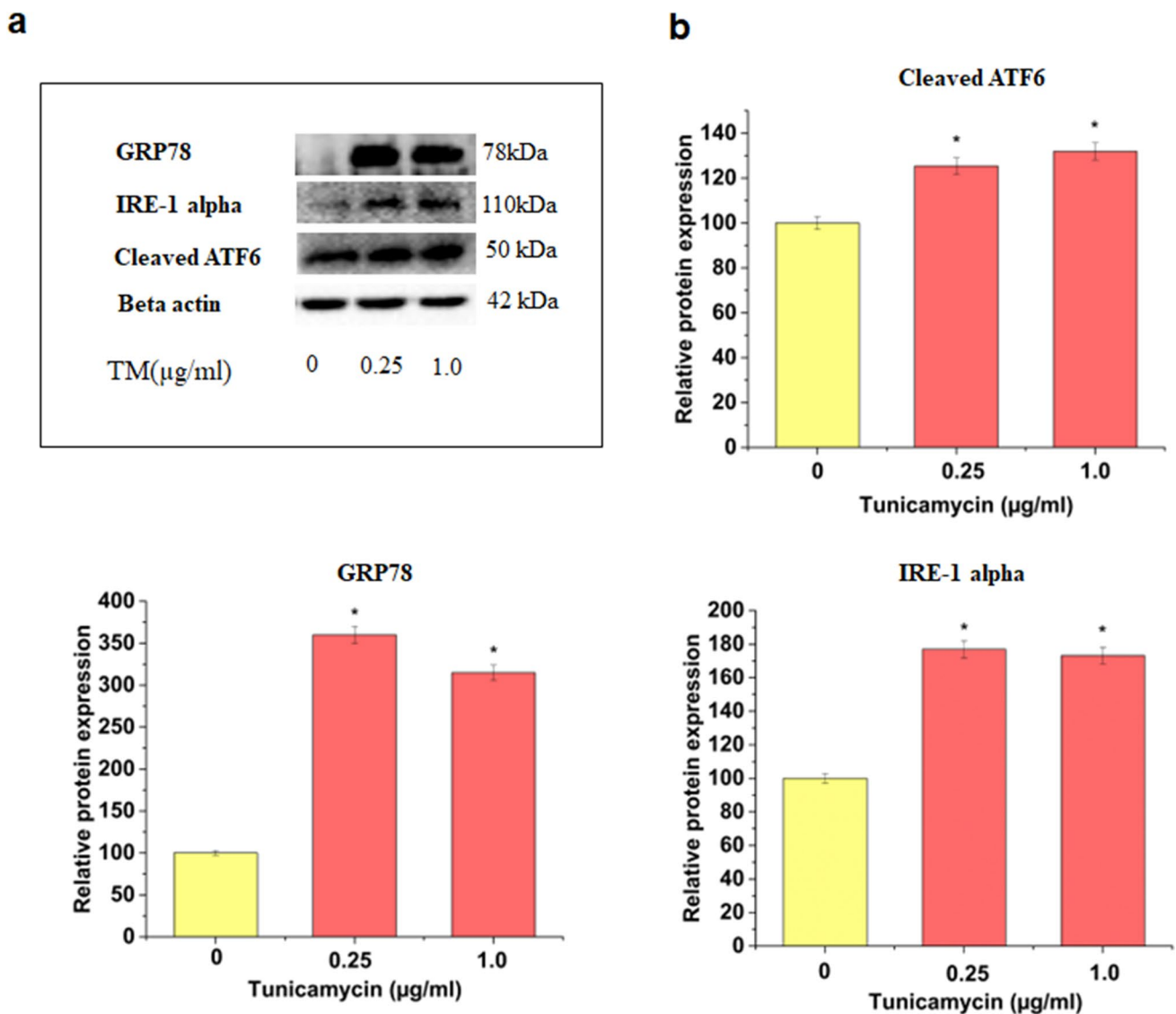


**Fig. 3** Optimization of Tunicamycin dose for induction of ER stress. **(a)** L6 myotubes were treated with selected doses of Tunicamycin ( $0.25$  and  $1 \mu\text{g/ml}$ ) for 24 h followed by western blot analysis of ER stress proteins, GRP78, IRE-1 $\alpha$  and ATF6, Beta actin was used as

the loading control. **(b)** Densitometric analysis of all proteins relative to Beta actin. TM represents Tunicamycin. Values are expressed as mean  $\pm$  SEM where  $n=3$ .  $*p \leq 0.05$  significantly different from control group

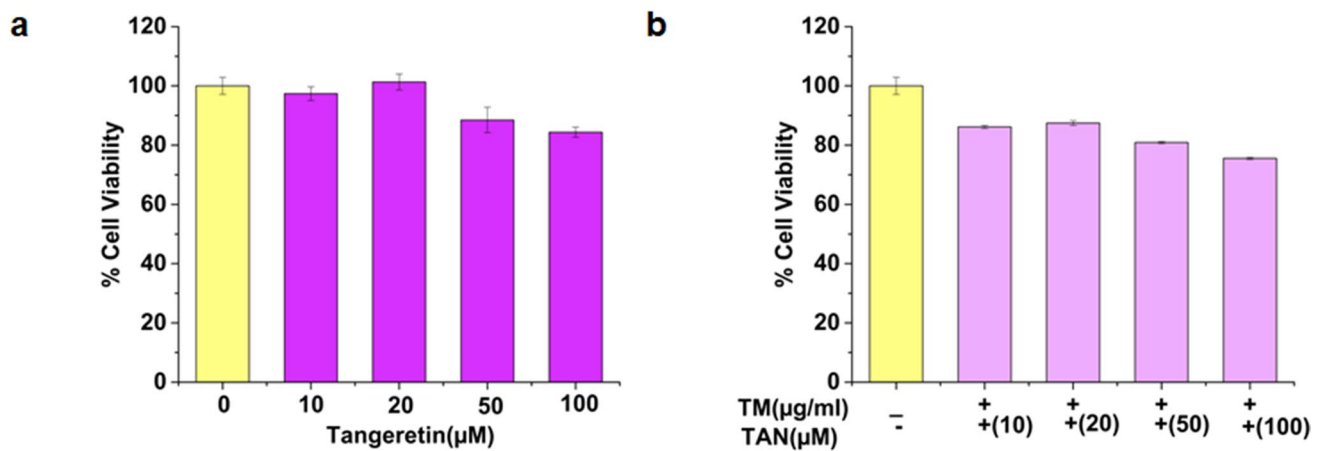


**Fig. 4** Cytotoxicity studies of Tangeretin **(a)** L6 myoblasts were treated with different doses of Tangeretin (10 to 100 μM) for 24 h. Cytotoxicity of compounds was evaluated using MTT assay. **(b)** L6 myoblasts were co-treated with 0.25 μg/ml Tunicamycin and differ-

ent concentrations of Tangeretin (10 to 100 μM) for 24 h. Cytotoxicity was determined using MTT assay, TM-0.25 μg/ml Tunicamycin, TAN-Tangeretin. Values are expressed as mean ± SEM, where  $n = 3$

(10 μM, 20 μM, 50 μM and 100 μM) for 24 h followed by MTT assay. Cells were found to be  $84.38 \pm 1.67\%$  viable upto 100 μM Tangeretin (Fig. 4a). Cell viability of Tangeretin in the presence of Tunicamycin was evaluated by treating cells with various concentrations of Tangeretin in the presence of 0.25 μg/ml Tunicamycin for 24 h. In the presence of Tunicamycin, cells were found to be  $80.9 \pm 0.37\%$  viable upto 50 μM Tangeretin. Based on the result of MTT assay, 50 μM Tangeretin was selected for further studies as shown in Fig. 4b.

### Tangeretin protects myotubes against Tunicamycin-induced stress and associated perturbations

#### Tangeretin suppresses Tunicamycin-induced stress via downregulation of the proteins involved in the UPR signalling cascade

Prolonged incubation of myotubes with Tunicamycin results in unresolved ER stress which was confirmed by the upregulation of ER stress proteins (Fig. 5a). The expression of GRP78 was significantly increased to  $638 \pm 18.419\%$  on treatment with Tunicamycin compared to control. Treatment with Tangeretin downregulated the expression levels remarkably by 90.4% ( $547.6 \pm 15.809\%$ ) while treatment with PBA brought down the levels by 171.8% ( $466.17 \pm 13.457\%$ ), respectively, compared to the Tunicamycin-treated group (Fig. 5b). Tunicamycin enhanced the IRE-1α expression to  $180.5 \pm 5.21\%$  when compared to the control. Treatment with Tangeretin brought down the levels to  $108.3 \pm 3.128\%$  and PBA reduced the expression to  $65.5 \pm 1.905\%$ , respectively, compared to

Tunicamycin-treated cells (Fig. 5b). Upon induction of ER stress by Tunicamycin, IRE-1α induces splicing of XBP-1. The expression of both unspliced and spliced forms of XBP-1 were upregulated in Tunicamycin-treated cells ( $123.2 \pm 3.557\%$  and  $138.2 \pm 3.988\%$ , respectively). Tangeretin treatment significantly lowered the levels of both unspliced and spliced forms of XBP-1 by 36% ( $87.24 \pm 2.518\%$ ) and 31.7% ( $106.57 \pm 3.077\%$ ), respectively, compared to Tunicamycin group. PBA downregulated the expression levels by 38.1% ( $98.89 \pm 2.456\%$ ) and 81.1% ( $57.09 \pm 1.648\%$ ) respectively as seen in Fig. 5b. Another ER stress sensor, ATF6 was notably upregulated by 52.3% ( $152.3 \pm 4.399\%$ ) on treatment with Tunicamycin compared to the control. Co-treatment with Tangeretin reduced the expression levels by 15.9% ( $136.4 \pm 3.938\%$ ) while PBA treatment resulted in a decrease of 8.4% ( $143.9467 \pm 4.155\%$ ), respectively, compared to the Tunicamycin group (Fig. 5a, b). Tunicamycin-treated myotubes showed a  $145.09 \pm 4.189\%$  increase in the ATF4 expression compared to the control cells. In cells co-treated with Tangeretin, the expression levels were downregulated to  $97.7 \pm 2.821\%$  and with PBA, it was reduced to  $120.7 \pm 3.486\%$ , respectively, compared to the Tunicamycin group (Fig. 5a, 5b).

#### Tangeretin mitigates Tunicamycin-induced oxidative stress via downregulating the ER resident oxidoreductases

Treatment with Tunicamycin resulted in a significant upregulation of PDI ( $126 \pm 3.64\%$ ) compared to the control cells. Tangeretin was able to lower the expression by 26.2% ( $99.8 \pm 2.882\%$ ) and treatment with PBA caused a 33.5% ( $92.5 \pm 2.67\%$ ) decrease in expression,

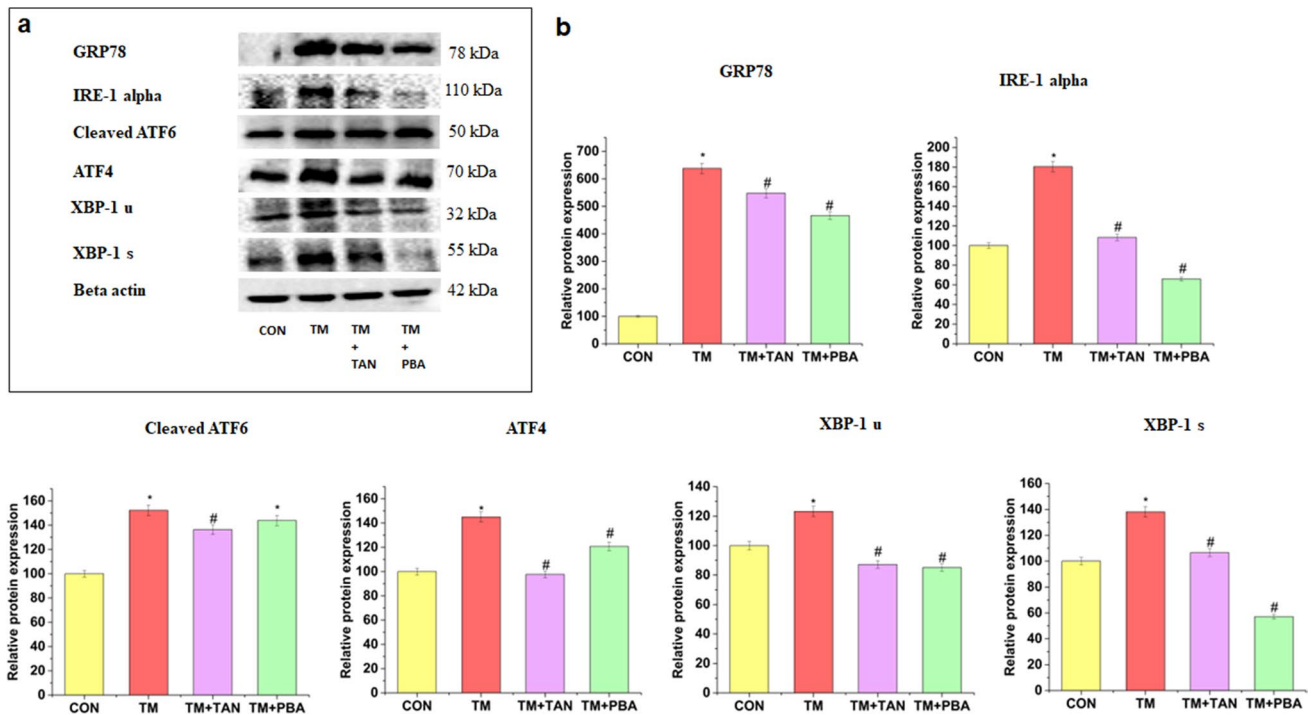


**Fig. 5** Effect of Tangeretin on Tunicamycin-induced upregulated ER stress markers. **(a)** Western blot analysis of ER stress markers, GRP78, IRE-1 $\alpha$ , ATF6, XBP-1 and ATF4 was performed with Beta actin as the loading control. **(b)** Densitometric analysis of all proteins relative to beta actin. CON represents untreated group, TM represents 0.25  $\mu$ g/ml Tunicamycin-treated group, TM+TAN represents

TM Tangeretin (50  $\mu$ M) co-treated group, TM+PBA represents TM 4-Phenylbutyric acid (1 mM) co-treated group. Values are expressed as mean  $\pm$  SEM where  $n=3$ . \* $p \leq 0.05$  significantly different from control group, # $p \leq 0.05$  significantly different from Tunicamycin group

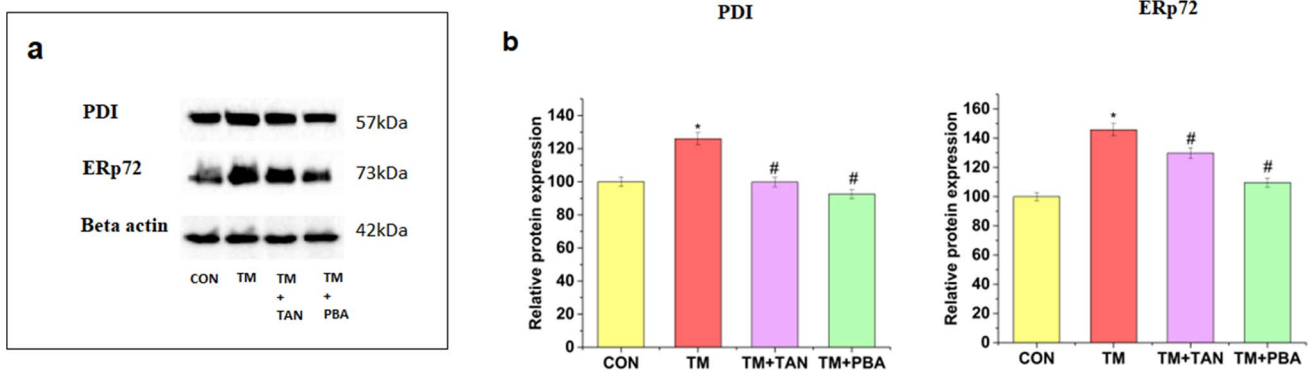


**Fig. 6** Treatment with Tangeretin suppresses expression of TM induced upregulated PDI and ERp72. **(a)** Western blot analysis of PDI & ERp72 protein expression, beta actin was used as the loading control. **(b)** Densitometric analysis of proteins relative to beta actin. CON represents untreated group, TM represents 0.25  $\mu$ g/ml Tunicamycin-treated group, TM+TAN represents TM Tangeretin (50  $\mu$ M) co-treated group, TM+PBA represents TM 4-Phenylbutyric acid (1 mM) co-treated group. Values are expressed as mean  $\pm$  SEM where  $n=3$ . \* $p \leq 0.05$  significantly different from control group, # $p \leq 0.05$  significantly different from Tunicamycin group

mycin-treated group, TM+TAN represents TM Tangeretin (50  $\mu$ M) co-treated group, TM+PBA represents TM 4-Phenylbutyric acid (1 mM) co-treated group. Values are expressed as mean  $\pm$  SEM where  $n=3$ . \* $p \leq 0.05$  significantly different from control group, # $p \leq 0.05$  significantly different from Tunicamycin group

respectively, compared to the Tunicamycin-treated cells as depicted in Fig. 6a and b. Myotubes treated with Tunicamycin showed higher expression levels of ERp72 by 45.7% ( $145.7 \pm 4.208\%$ ) compared to control. Treatment

with Tangeretin resulted in subsequent downregulation of ERp72 by 15.9% ( $129.87 \pm 3.749\%$ ) whereas PBA-treated cells showed a 36.1% ( $109.66 \pm 3.166\%$ ) decrease compared to Tunicamycin group (Fig. 6a and b).



## Abatement of Tunicamycin-induced oxidative stress by Tangeretin

ER stress induces oxidative stress which is manifested by the generation of reactive oxygen species. In this assay, DHE was used as a fluorescent probe for ROS detection. Cells treated with Tunicamycin showed increased intracellular ROS generation by 69.4% ( $169.4 \pm 4.89\%$ ) compared to the control (Fig. 7a). Co-treatment with Tangeretin significantly suppressed the ROS levels to 12.7% ( $112.7 \pm 4.111\%$ ) whereas PBA treatment brought down the ROS levels to 16.1% ( $116.1 \pm 3.351\%$ ), respectively

compared to the tunicamycin-treated group. The Tunicamycin-induced ROS generation was also detected by the DCFHDA staining. In Tunicamycin-treated groups, there was a significant increase in ROS generation compared to the untreated cells as evident from Fig. 7b and c. Co-treatment with Tangeretin and PBA respectively, demonstrated a significantly lowered ROS generation (Fig. 7b and c). Differentiated myotubes treated with Tunicamycin significantly decreased the SOD activity to  $37.2 \pm 1.073\%$  compared to the control. Treatment with Tangeretin improved the SOD activity to  $69.3 \pm 2.001\%$ . Treatment with PBA improved the activity to  $68.4 \pm 1.976\%$ , respectively, in a significant

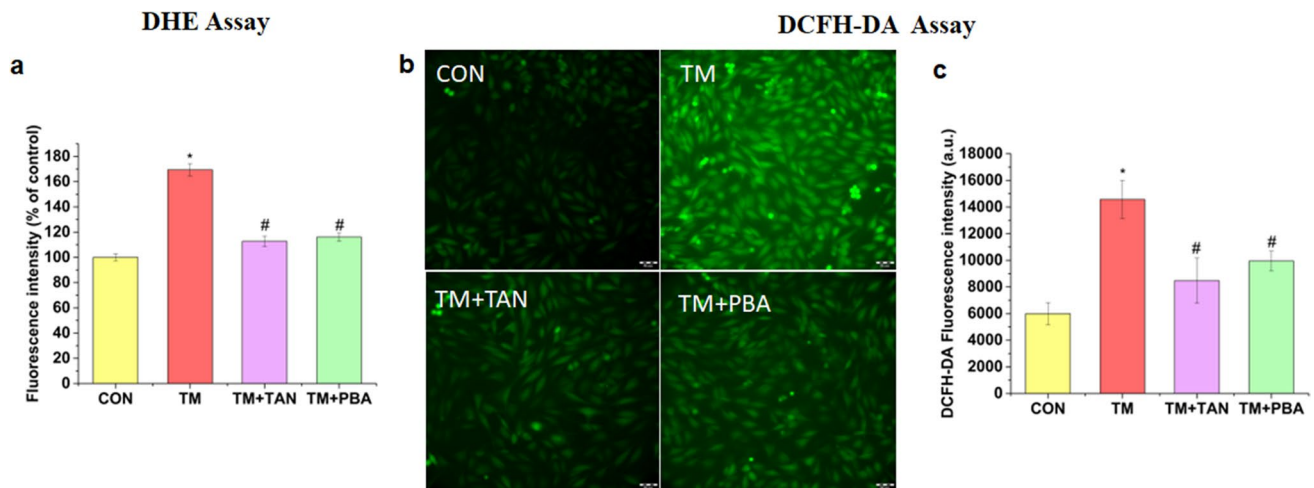


**Fig. 7** Tangeretin alleviates Tunicamycin-induced intracellular redox disturbances. Effect of Tangeretin on Tunicamycin-induced cellular reactive oxygen species production was determined using dihydroethidium (DHE) assay and dichlorodihydrofluorescein diacetate (DCFH-DA) assay. (a) DHE fluorescence intensity measurement of cells. (b) DCFH-DA stained fluorescence microscopic images of cells. Magnification 20 $\times$ . Scale corresponds to 50  $\mu$ m. (c) DCFH-DA fluo-

rescence intensity measurement of cells. CON represents untreated group, TM represents 0.25  $\mu$ g/ml Tunicamycin-treated group, TM+TAN represents TM Tangeretin (50  $\mu$ M) co-treated group, TM+PBA represents TM 4-Phenylbutyric acid (1 mM) co-treated group. Values are expressed as mean  $\pm$  SEM where  $n=3$ . \* $p \leq 0.05$  significantly different from control group, # $p \leq 0.05$  significantly different from Tunicamycin group

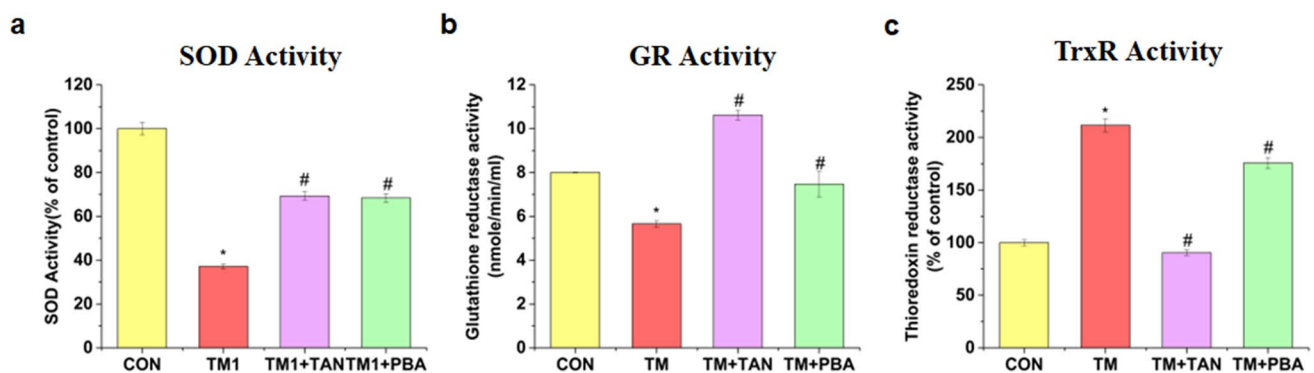


**Fig. 8** Tangeretin improves cellular antioxidant status. Effect of Tangeretin on (a) Superoxide Dismutase (SOD) activity, (b) Glutathione reductase (GR) activity, (c) Thioredoxin reductase (TrxR) activity in the presence of Tunicamycin was evaluated. CON represents untreated group, TM represents 0.25  $\mu$ g/ml Tunicamycin-treated

group, TM+TAN represents TM Tangeretin (50  $\mu$ M) co-treated group, TM+PBA represents TM 4-Phenylbutyric acid (1 mM) co-treated group. Values are expressed as mean  $\pm$  SEM where  $n=3$ . \* $p \leq 0.05$  significantly different from control group, # $p \leq 0.05$  significantly different from Tunicamycin group

manner compared to Tunicamycin-treated group (Fig. 8a). In cells treated with Tunicamycin, GR activity decreased by 29.3% ( $5.66 \pm 0.1471$  nmoles/min/ml) compared to control cells ( $8.01 \pm 0.0166$  nmoles/min/ml) whereas treatment with Tangeretin remarkably improved the same by 62% ( $10.623 \pm 0.2218$  nmoles/min/ml) and PBA improved the GR activity by 22.6% ( $7.473 \pm 0.5871$  nmoles/min/ml) compared to the Tunicamycin-treated group as seen in Fig. 8b. Thioredoxin reductase activity was determined following the manufacturer's protocol (Cayman Chemicals, USA). TrxR activity was significantly increased by 111.6% ( $211.6 \pm 6.109\%$ ) in Tunicamycin-treated group as compared to the control group. It was decreased to  $90.5 \pm 2.61\%$  on treatment with Tangeretin and by 35.9% ( $175.7 \pm 5.07\%$ ) on treatment with PBA compared to Tunicamycin-treated cells (Fig. 8c).

#### Tangeretin decreases Tunicamycin-induced ROS-associated p38 MAP Kinase activation

Here, we investigated the effect of Tunicamycin in the presence and absence of Tangeretin on the activation of this protein. Cells treated with Tunicamycin showed increased expression levels of phosphorylated p38MAP-kinase ( $139.5 \pm 6.973\%$ ) compared to the control. Treatment with Tangeretin and PBA significantly downregulated the protein expression levels to  $112.4 \pm 3.244\%$  and

$105.7 \pm 3.051\%$  respectively, compared to Tunicamycin-treated group (Fig. 9a and b).

#### Tangeretin reduces Tunicamycin-induced loss of mitochondrial membrane potential

Here, changes in  $\Delta\psi_m$  were determined using the JC-1 staining dye. Under normal conditions JC-1 (cationic, lipophilic dye) enters the mitochondria and accumulates to form aggregates which emit fluorescence in the red spectrum. In unhealthy cells, JC-1 accumulates to a lesser extent as monomers inside the mitochondria due to loss of  $\Delta\psi_m$  and increased membrane permeability thereby emitting green fluorescence (Sivandzade et al. 2019). Tunicamycin treatment induced loss of  $\Delta\psi_m$  compared to the control which was restored on co-treatment with Tangeretin (Fig. 10a). The JC-1 aggregate to monomer ratio or red to green fluorescence ratio is a parameter for gauging the mitochondrial function. The ratio significantly declined to 60.5% ( $1.4702 \pm 0.0327$ ) in Tunicamycin-treated cells due to membrane depolarization compared to the control ( $2.4292 \pm 0.04975$ ). Tangeretin significantly improved the red to green fluorescence to 96.2% ( $2.3392 \pm 0.0789$ ) compared to Tunicamycin group. PBA increased the JC-1 aggregate to monomer ratio to 78.1% ( $1.8971 \pm 0.0388$ ) compared to Tunicamycin-treated group as depicted in Fig. 10b.

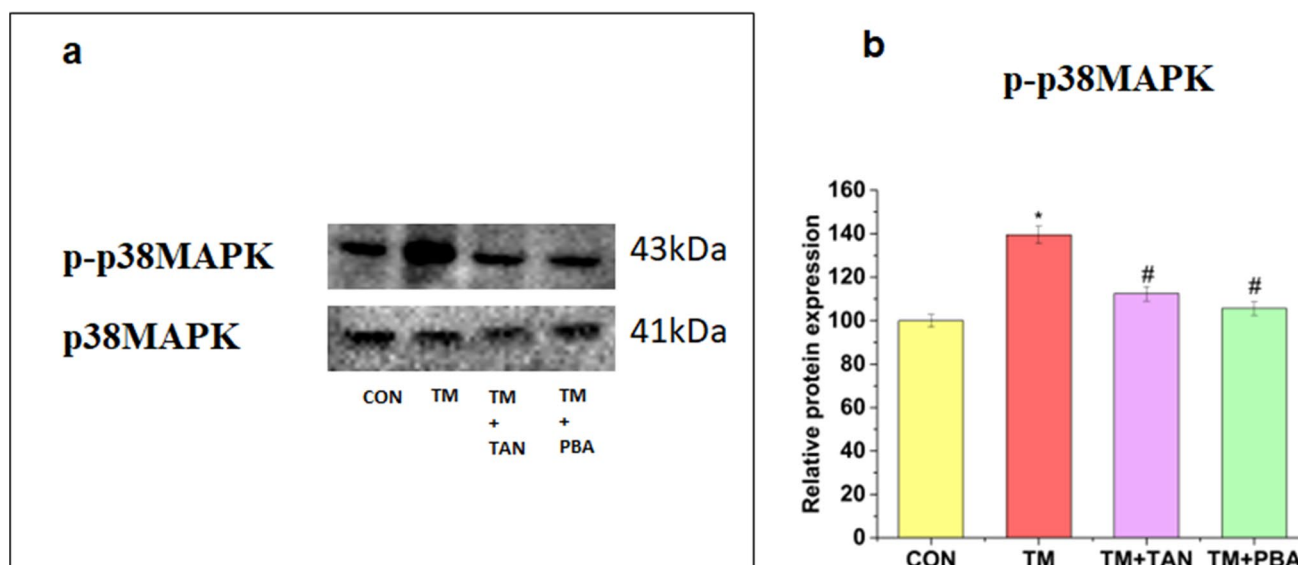


**Fig. 9** Tangeretin suppresses the levels of phosphorylated p38MAP Kinase. **(a)** Western blot analysis of phospho-p38Map Kinase, p38 Map Kinase was used as loading control. **(b)** Densitometric analysis of p-p38Map Kinase relative to p38Map Kinase. CON represents untreated group, TM represents 0.25  $\mu$ g/ml Tunicamycin-treated

group, TM+TAN represents TM Tangeretin (50  $\mu$ M) co-treated group, TM+PBA represents TM 4-Phenylbutyric acid (1 mM) co-treated group. Values are expressed as mean  $\pm$  SEM where  $n=3$ , \* $p \leq 0.05$  significantly different from control group, # $p \leq 0.05$  significantly different from Tunicamycin group



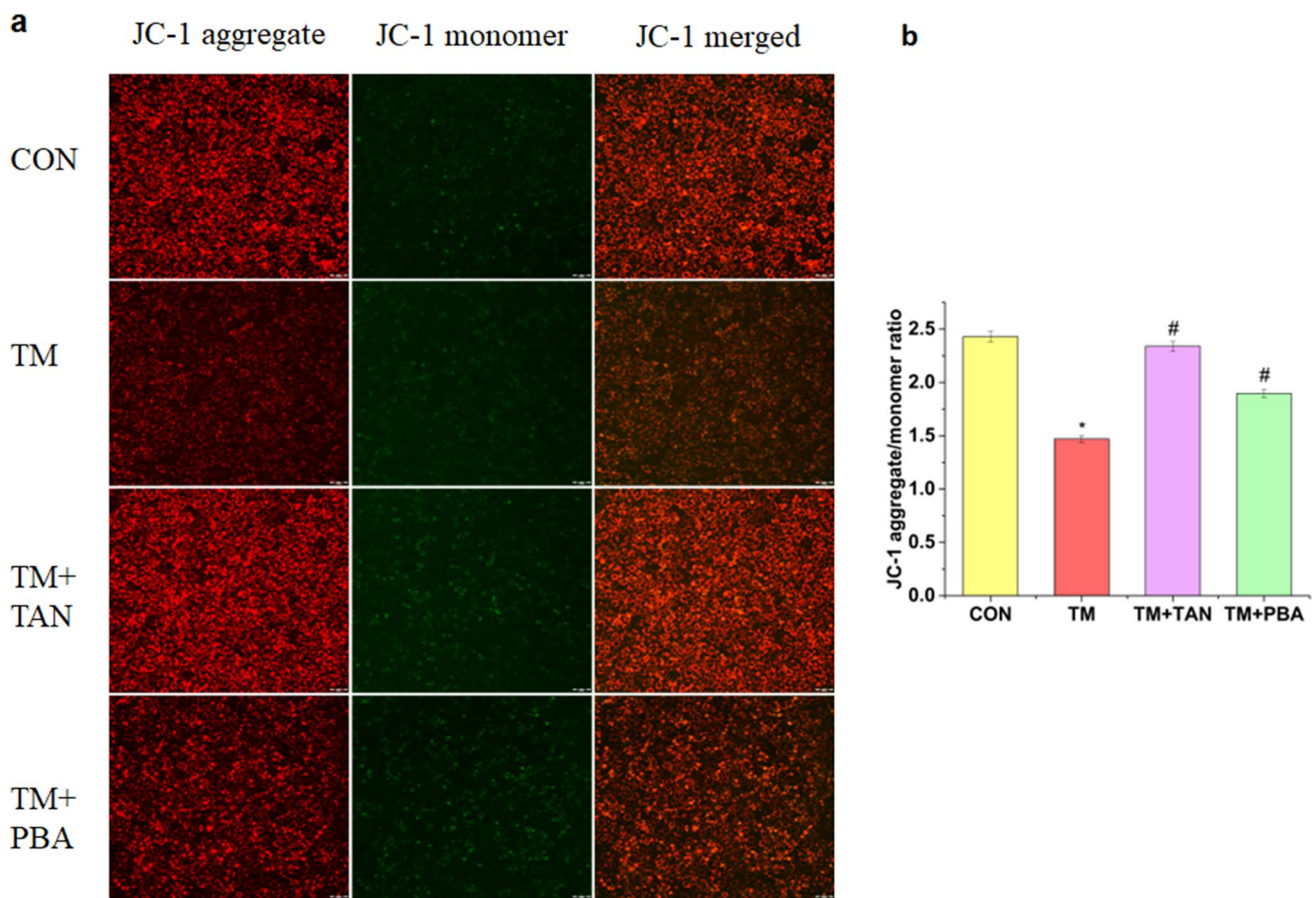


**Fig. 10** Effect of Tangeretin on Tunicamycin-induced loss of  $\Delta\psi_m$ . **(a)** L6 myotubes after treatment with respective groups for 24 h were incubated with JC-1 staining solution for 20 min. Imaging was performed in fluorescence microscope. Magnification 20 $\times$ . Scale corresponds to 50  $\mu$ m. **(b)** Red to green fluorescent intensity ratio. CON represents untreated group, TM represents 0.25  $\mu$ g/ml Tunicamycin-treated group, TM+TAN represents TM Tangeretin (50  $\mu$ M) co-treated group, TM+PBA represents TM 4-Phenylbutyric acid (1 mM) co-treated group. Values are expressed as mean  $\pm$  SEM where  $n=3$ . \* $p \leq 0.05$  significantly different from control group, # $p \leq 0.05$  significantly different from Tunicamycin group

mycin-treated group, TM+TAN represents TM Tangeretin (50  $\mu$ M) co-treated group, TM+PBA represents TM 4-Phenylbutyric acid (1 mM) co-treated group. Values are expressed as mean  $\pm$  SEM where  $n=3$ . \* $p \leq 0.05$  significantly different from control group, # $p \leq 0.05$  significantly different from Tunicamycin group

## Discussion

In this study, we have evaluated the protective effect of Tangeretin, a citrus methoxyflavone against ER stress-induced signalling pathways and associated redox perturbations in rat skeletal muscle L6 cell lines. ER stress-induced ROS generation and associated mitochondrial dysfunction in skeletal muscles are well known contributors in the pathogenesis of myositis and atrophy (Mensch and Zierz 2020; Gallot and Bohnert 2021; Lightfoot et al. 2015). There are several chemical chaperones such as Tauroursodeoxycholic acid (TUDCA) and PBA which are reported to reduce ER stress by interacting with the hydrophobic sites of misfolded proteins but their therapeutic potential is limited by the high doses required for exerting ER protective effects and (Cortez and Sim 2014). Natural products have always piqued the curiosity of researchers. Targeting the ER stress pathway components by natural compounds has been a compelling

area of research and can be an effective treatment strategy for several pathologies (Martucciello et al. 2020). In this study, we focussed on gaining a deeper insight into the mechanism of action of Tangeretin against ER stress-induced cellular alterations in L6 cell lines.

In our study, prolonged incubation of myotubes with the optimised dose of Tunicamycin (0.25  $\mu$ g/ml), results in the upregulation of ER stress-induced UPR markers and this was evident by the upregulation of the proteins involved in the UPR such as GRP78, the ER stress master regulator protein (Cullinan and Diehl 2006). This is in agreement with a previous study by Vattemi et al., where upregulation of GRP78 was reported in muscle biopsies with inclusion body myositis (Vattemi et al. 2004). IRE-1 $\alpha$ , the most conserved ER stress sensor (Mohan et al. 2019), XBP-1 which is downstream of IRE-1 $\alpha$  that gets spliced by the latter in response to ER stress were also significantly upregulated in response to Tunicamycin (Uemura et al. 2009). Bohnert

et al., demonstrated the IRE-1 XBP-1 signalling as a mediator of muscle atrophy in Lewis lung carcinoma mice model (Bohnert et al. 2018). In our study, we observed an upregulation in ATF6 protein which in response to ER stress dissociates from Bip protein and translocates to the golgi apparatus where it is cleaved by site1 and site2 proteases. The cleaved form then enters the nucleus and triggers downstream signalling pathways (Taouji et al. 2013). Our results indicate an upregulation in ATF4, which is activated by the PERK arm of the UPR and may trigger adaptive or apoptotic pathways depending on the strength and duration of ER stress (Wortel et al. 2017). Ebert et al., described the role of ATF4 in progression of muscle atrophy via the Gadd45a protein (Ebert et al. 2020). Therefore, downregulation of these ER stress components may prove to be successful in relieving muscular pathologies. In the present study, treatment with Tangeretin significantly mitigated the Tunicamycin-induced stress by downregulating these ER stress marker proteins. This data is consistent with previous studies where targeting ER stress in skeletal muscles has significantly reduced the UPR stimulation and associated cellular alterations such as insulin resistance, ROS generation and mitochondrial dysfunction (Eo and Valentine 2021; Thoma et al. 2020a).

One of the consequences as well as initiator of ER stress is the oxidative stress which is characterised by aberrant ROS generation leading to disruption of redox homeostasis. In skeletal muscles, low levels of ROS are induced during exercise-mediated muscle contraction (Davies et al. 1982). This moderate amount of ROS confers better muscle health (Scicchitano et al. 2018). However, abnormally high levels of ROS may result in skeletal muscle damage through activation of signalling pathways exacerbating mitochondrial dysfunction and inflammatory mediators (Marzetti et al. 2013). Therefore, targeting the proteins involved in the ER stress-mediated oxidative stress can be a therapeutic strategy for disease intervention.

PDI, an ER resident oxidoreductase mediates the disulphide bond reduction, formation and isomerisation during protein folding (Malhotra and Kaufman 2007). Under ER stress conditions, IRE-1 alpha-stimulated spliced form of XBP-1 upregulates the PDI, which in turn promotes correct folding of misfolded proteins and also reprimands the non-native disulphide bonds (França et al. 2019; Khan and Mutus 2014). In doing so, PDI itself undergoes an aberrant cycle of oxidation reduction leading to surplus generation of ROS as byproducts leading to a hyperoxidised ER lumen which further augments ER stress by interfering with proper PDI function resulting in more misfolded proteins (Burgos-Morón et al. 2019). Overexpression of PDI is linked to increased cellular ROS generation (Khan and Mutus 2014). In our study, we found that treatment with Tunicamycin significantly induced the expression of PDI and ERp72, another member of the PDI family

which has functions similar to PDI (Zhou et al. 2017). Our results showed that treatment with Tangeretin remarkably lowered the levels of both PDI and ERp72, effectively bringing down the ROS levels. This data corroborates the findings of Pan et al. who have reported the efficacy of bioactives extracted from *Scutellariae radix* and *Rhei rhizoma* in attenuating oxidative stress by downregulating the dimethylnitrosamine-induced upregulation of PDI expression through the proteome analysis in an in vivo model (Pan et al. 2015).

Tunicamycin-induced ROS generation debilitates the redox homeostasis in the cells by downregulating the cellular antioxidant defense system. From the results, it is clear that myotubes treated with Tunicamycin alone showed an increased ROS generation, which was evident from the DHE and the DCFH-DA assay and also by decline in the levels of glutathione reductase and superoxide dismutase enzymes. Treatment with Tangeretin significantly lowered the ROS levels and improved the antioxidant status of the cells as was evident by the improvement in glutathione reductase and superoxide dismutase activity. Glutathione reductase is associated with the reduction of oxidised glutathione (GSSG) to reduced glutathione while superoxide dismutase lowers the cellular ROS levels by conversion of superoxides to oxygen and hydrogen peroxide, respectively (Couto et al. 2016; Wang et al. 2018). Tunicamycin was found to induce upregulation of Thioredoxin reductase enzyme and subsequent downregulation was observed on treatment with Tangeretin. This can be justified by assessing the function of thioredoxin reductase which involves reduction of non-native disulphide bonds (Poet et al. 2017). In ER stress conditions there is a build-up of misfolded proteins with several non-native disulphide bonds so there is a need to reduce these bonds and this may account for the increased thioredoxin reductase activity in Tunicamycin-treated groups. Tangeretin significantly lowered the thioredoxin reductase activity which can be attributed to Tangeretin's ability in reducing the ER stress pathway.

Disturbances in redox homeostasis also triggers the MAP Kinase signalling, especially p38MAPK which is involved in augmenting mitochondrial ROS and downstream activation of diverse pathways such as inflammation, insulin resistance and mitochondrial dysfunction (Ashraf et al. 2014; Brown et al. 2014; Yu et al. 2017). p38 MAPK which belongs to the mitogen activated family of proteins is also implicated in skeletal muscle diseases and suppression of p38MAPK can be a potential therapeutic approach (Brennan et al. 2021; Cuenda and Rousseau 2007; Yuasa et al. 2018). p38MAPK is known to be activated by ROS generation and also by the IRE-1 alpha arm of UPR (Jia et al. 2007). In the present study, we found that Tunicamycin induced significant upregulation in p38MAPK expression and Tangeretin was effective in bringing down the levels of this protein.

Therefore, targeting the p38MAPK can aid in suppressing ER stress-induced skeletal muscle dysfunction.

Mitochondrial dysfunction in skeletal muscles is a consequence of prolonged ER stress and associated oxidative stress and this was determined by studying the effect of Tunicamycin on mitochondrial membrane potential, a hallmark of mitochondrial health (Thoma et al. 2020a). Due to the close association of ER and mitochondria through MAMs, perturbations in the ER can cause mitochondrial dysfunction. As already stated, changes in mitochondrial membrane potential is an indicator of the mitochondrial well-being, where depolarisation of  $\Delta\psi_m$  indicates mitochondrial dysfunction (Connolly et al. 2018). Here in this study, it is clear that Tunicamycin induced a loss of  $\Delta\psi_m$  which was improved on treatment with Tangeretin. From the results obtained, it is evident that Tunicamycin-induced

UPR-mediated oxidative stress and mitochondrial dysfunction in L6 cell lines were attenuated on treatment with Tangeretin. A summary of the results is represented in Fig. 11. The findings pave way for considering Tangeretin as a potential candidate for ER stress-related skeletal muscle dysfunction.

## Conclusion

Targeting ER stress which is upstream of several pathological conditions is emerging as a therapeutic strategy in the management of several diseases. ER stress and associated oxidative stress in L6 myotubes was remarkably alleviated on treatment with Tangeretin, a citrus methoxyflavone. Tangeretin exerted its protective effects in L6 myotubes

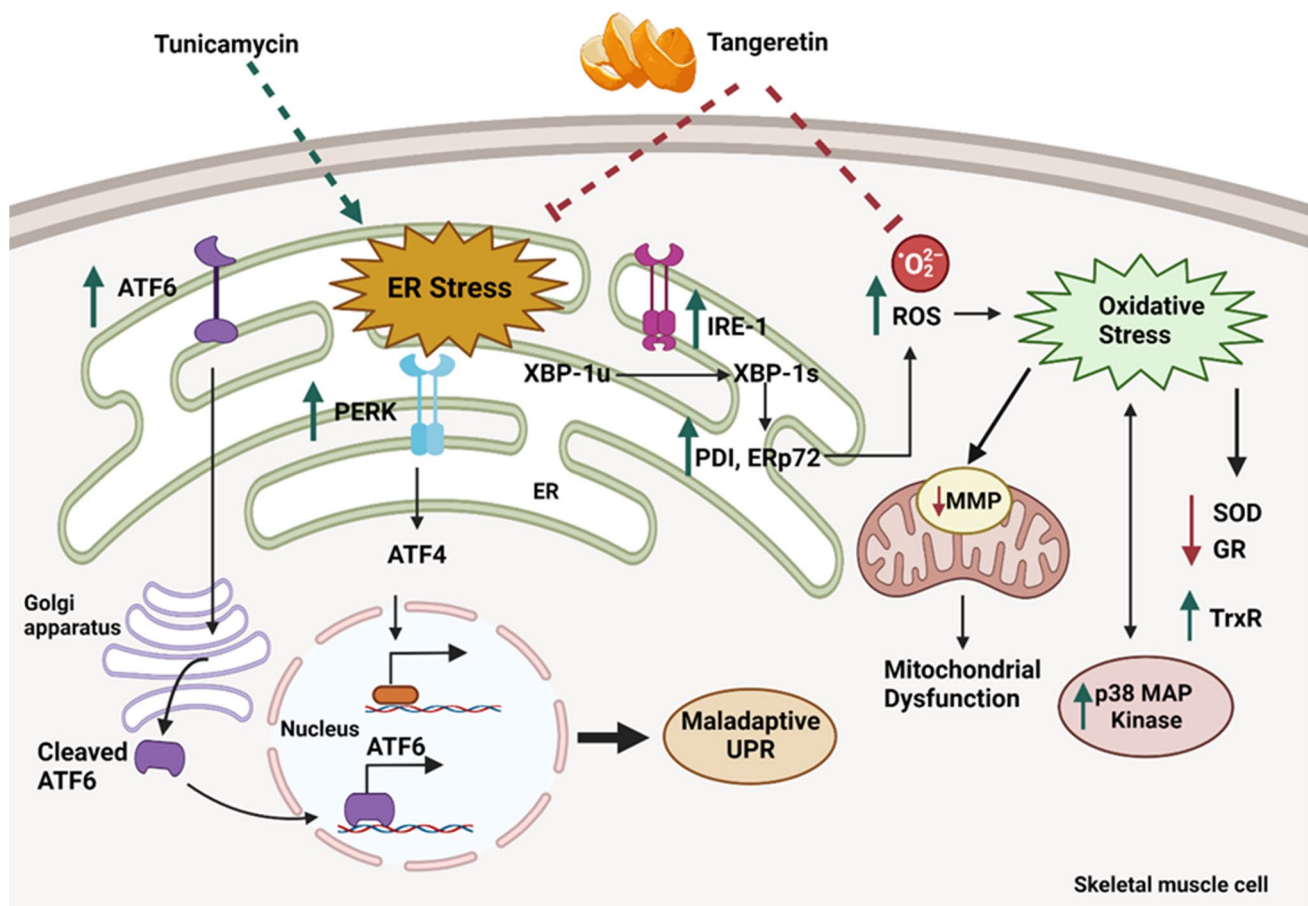


**Fig. 11** Proposed mechanism of action of Tangeretin in alleviating Tunicamycin-induced ER stress and associated complications. Tunicamycin-treated myotubes showed an increase in the levels of the proteins involved in the ER stress induction namely ATF6, IRE-1 alpha, XBP-1 and ATF4 resulting in maladaptive UPR. The XBP-1 induction leads to an upregulation of the ER resident oxidoreductases, PDI and ERp72 for enhancing the protein folding machinery thereby resulting in ROS generation. This causes disturbances in the cellular

redox homeostasis leading to loss of mitochondrial membrane potential, upregulation of phosphorylated p38 MAP kinase and suppression of the antioxidant defense system. All these factors contribute to the progression of skeletal muscle pathologies. Tangeretin protected the myotubes from Tunicamycin insult via downregulation of the ER stress proteins, ER resident oxidoreductases, also by suppression of the ROS generation, downregulation of phosphorylated p38 MAP kinase and improving the antioxidant defense system



via downregulation of the UPR pathway, ER resident oxidoreductases (PDI and ERp72) and phospho-p38MAPK. Tangeretin also mitigated Tunicamycin-induced ROS generation, improved the antioxidant system and mitochondrial function. The findings of the study indicate that Tangeretin can be considered as a potential lead against ER stress-induced pathological outcomes in skeletal muscles.

**Acknowledgements** Eveline M Anto thanks the University Grants Commission (UGC), New Delhi, India, for providing fellowship. P. Jayamurthy thanks CSIR, India for the financial assistance to conduct the research.

**Data Availability** The authors are willing to provide all the data generated and/or analysed during the study on reasonable request.

## Declarations

**Conflict of interest** The authors declare no competing interests.

## References

- Afroze D, Kumar A (2019) ER stress in skeletal muscle remodeling and myopathies. *FEBS J* 286(2):379–398
- Ashraf MI, Ebner M, Wallner C, Haller M, Khalid S, Schwelberger H, Koziel K et al (2014) A P38MAPK/MK2 signaling pathway leading to redox stress, cell death and ischemia/reperfusion injury. <http://www.biosignaling.com/content/12/1/6>. Accessed June 2022
- Ashrafizadeh M, Ahmadi Z, Mohammadinejad R, Afshar EG (2020) Tangeretin: a mechanistic review of its pharmacological and therapeutic effects. *J Basic Clin Physiol Pharmacol* 31(4). <https://doi.org/10.1515/JBCPP-2019-0191/MACHINEREADABLECITATION/RIS>
- Bohnert KR, McMillan JD, Kumar A (2018) Emerging roles of ER stress and unfolded protein response pathways in skeletal muscle health and disease. *J Cell Physiol* 233(1):67–78. <https://doi.org/10.1002/jcp.25852>
- Boye A, Ahmad I, Fakhri S, Hussain Y, Khan H (2021) Incipient citrus polymethoxylated flavone tangeretin as anticancer drug candidate: mechanistic insights, limitations and possible solutions. *Adv Cancer Biol-Metastasis* 3(September):100010. <https://doi.org/10.1016/j.adcanc.2021.100010>
- Brennan CM, Emerson CP, Owens J, Christoforou N (2021) P38 MAPKs — roles in skeletal muscle physiology, disease mechanisms, and as potential therapeutic targets. *JCI Insight* 6(12). <https://doi.org/10.1172/JCI.INSIGHT.149915>
- Brown AE, Palsgaard J, Borup R, Avery P, Gunn DA, De Meyts P, Yeaman SJ, Walker M (2014) P38 MAPK activation upregulates proinflammatory pathways in skeletal muscle cells from insulin-resistant type 2 diabetic patients. *Am J Physiol. Endocrinol Metab* 308(1):E63–70. <https://doi.org/10.1152/AJPENDO.00115.2014>
- Burgos-Morón E, Abad-Jiménez Z, Martínez de Marañón A, Iannantuoni F, Escribano-López I, López-Domènech S, Salom C et al (2019) Relationship between oxidative stress, ER stress, and inflammation in type 2 diabetes: the battle continues. *J Clin Med* 8(9):1385. <https://doi.org/10.3390/JCM8091385>
- Carstens PO, Schmidt J (2014) Diagnosis, pathogenesis and treatment of myositis: recent advances. *Clin Exp Immunol* 175(3):349–358. <https://doi.org/10.1111/cei.12194>
- Chong WC, Shastri MD, Eri R (2017) Molecular sciences endoplasmic reticulum stress and oxidative stress: a vicious nexus implicated in bowel disease pathophysiology. <https://doi.org/10.3390/ijms18040771>
- Connolly NMC, Theurey P, Adam-Vizi V, Bazan NG, Bernardi P, Bolaños JP, Culmsee C et al (2018) Guidelines on experimental methods to assess mitochondrial dysfunction in cellular models of neurodegenerative diseases. *Cell Death Differ* 25(3):542–572. <https://doi.org/10.1038/S41418-017-0020-4>
- Cortez L, Sim V (2014) The therapeutic potential of chemical chaperones in protein folding diseases. *Prion* 8(2):197. <https://doi.org/10.4161/PRI.28938>
- Couto N, Wood J, Barber J (2016) The role of glutathione reductase and related enzymes on cellular redox homeostasis network. *Free Radic Biol Med* 95(June):27–42. <https://doi.org/10.1016/J.FREERADBIOMED.2016.02.028>
- Cuenda A, Rousseau S (2007) P38 MAP-Kinases pathway regulation, function and role in human diseases. *Biochim Biophys Acta-Mol Cell Res* 1773(8):1358–1375. <https://doi.org/10.1016/J.BBAMCR.2007.03.010>
- Cullinan SB, Alan Diehl J (2006) Coordination of ER and oxidative stress signaling: the PERK/Nrf2 signaling pathway. *Int J Biochem Cell Biol* 38(3):317–332. <https://doi.org/10.1016/J.BIOCEL.2005.09.018>
- Davies KJA, Quintanilha AT, Brooks GA, Packer L (1982) Free radicals and tissue damage produced by exercise. *Biochem Biophys Res Commun* 107(4):1198–1205. [https://doi.org/10.1016/S0006-291X\(82\)80124-1](https://doi.org/10.1016/S0006-291X(82)80124-1)
- Deldicque L, Guimarães-Ferreira L, Paolucci N (2013) Endoplasmic reticulum stress in human skeletal muscle: any contribution to sarcopenia? <https://doi.org/10.3389/fphys.2013.00236>
- Ebert SM, Bullard SA, Basisty N, Marcotte GR, Skopec ZP, Dierdorff JM, Al-Zougbi A et al (2020) Activating transcription factor 4 (ATF4) promotes skeletal muscle atrophy by forming a heterodimer with the transcriptional regulator C/EBPβ. *J Biol Chem* 295(9):2787–2803. <https://doi.org/10.1074/JBC.RA119.012095>
- Eo H, Valentine RJ (2021) Imoxin inhibits tunicamycin-induced endoplasmic reticulum stress and restores insulin signaling in C2C12 myotubes. *Am J Physiol Cell Physiol* 321(2):C221–C229
- França LM, Coêlho CFF, Freitas LNC, Souza ILS, Chagas VT, Debbas V, De TM Lima TM, De Souza HP, Laurindo FRM, De Andrade Paes AM (2019) Syzygium cumini leaf extract reverts hypertriglyceridemia via downregulation of the hepatic XBP-1s/PDI/MTP axis in monosodium L-glutamate-induced obese rats. *Oxidative Med Cell Longev*. <https://doi.org/10.1155/2019/9417498>.
- Gallot YS, Bohnert KR (2021) Confounding roles of er stress and the unfolded protein response in skeletal muscle atrophy. *Int J Mol Sci* 22(5):1–18. <https://doi.org/10.3390/ijms22052567>
- Haynes CM, Titus EA, Cooper AA (2004) Degradation of misfolded proteins prevents ER-derived oxidative stress and cell death employ a quality control mechanism that recognizes and degrades (ERAD) aberrantly folded proteins to prevent the aggregation and/or delivery of potentially dysfunc. *Mol Cell* 15:767–76. <http://www.molecule.org/cgi/content/>. Accessed June 2022
- Jia Y-T, Wei W, Ma B, Xu Y, Liu W-J, Wang Y, Lv K-Y, Tang H-T, Wei D, Xia Z-F (2007) Activation of P38 MAPK by reactive oxygen species is essential in a rat model of stress-induced gastric mucosal injury. *J Immunol (Baltimore, Md. : 1950)* 179(11):7808–19. <https://doi.org/10.4049/JIMMUNOL.179.11.7808>
- Khan HA, Mutus B (2014) Protein disulfide isomerase a multifunctional protein with multiple physiological roles. *Front Chem* 2(AUG):70. <https://doi.org/10.3389/FCHEM.2014.00070/BIBTEX>
- Li S, Lambros T, Wang Z, Goodnow R, Ho CT (2007) Efficient and scalable method in isolation of polymethoxyflavones from orange peel extract by supercritical fluid chromatography. *J Chromatogr*

- b: *Anal Technol Biomed Life Sci* 846(1–2):291–297. <https://doi.org/10.1016/j.jchromb.2006.09.010>
- Lightfoot AP, McArdle A, Jackson MJ, Cooper RG (2015) In the idiopathic inflammatory myopathies (IIM), do reactive oxygen species (ROS) contribute to muscle weakness? *Ann Rheum Dis* 74(7):1340–1346. <https://doi.org/10.1136/annrheumdis-2014-207172>
- Lin JH, Walter P, Benedict Yen TS (2007) Endoplasmic reticulum stress in disease pathogenesis. <https://doi.org/10.1146/annurev.pathmechdis.3.121806.151434>
- Malhotra JD, Kaufman RJ (2007) Endoplasmic reticulum stress and oxidative stress: a vicious cycle or a double-edged sword? <https://Home.Liebertpub.com/Ars> 9 (12):2277–93. <https://doi.org/10.1089/ARS.2007.1782>
- Martucciello S, Masullo M, Cerulli A, Piacente S (2020) Natural products targeting ER stress, and the functional link to mitochondria. *Int J Mol Sci* 21(6). <https://doi.org/10.3390/IJMS21061905>
- Marzetti E, Calvani R, Cesari M, Buford TW, Lorenzi M, Behnke BJ, Leeuwenburgh C (2013) Mitochondrial dysfunction and sarcopenia of aging: from signaling pathways to clinical trials. *Int J Biochem Cell Biol* 45(10):2288–2301. <https://doi.org/10.1016/j.BIOCEL.2013.06.024>
- Mensch A, Zierz S (2020) Cellular stress in the pathogenesis of muscular disorders—from cause to consequence. *Int J Mol Sci* 21(16):1–27. <https://doi.org/10.3390/ijms21165830>
- Mohan S, Preetha Rani MR, Brown L, Ayyappan P, Raghu KG (2019) Endoplasmic reticulum stress: a master regulator of metabolic syndrome. *Eur J Pharmacol* 860 (October). <https://doi.org/10.1016/J.EJPHAR.2019.172553>
- Mosmann T (1983) Rapid colorimetric assay for cellular growth and survival: application to proliferation and cytotoxicity assays. *J Immunol Methods* 65(1–2):55–63. [https://doi.org/10.1016/0022-1759\(83\)90303-4](https://doi.org/10.1016/0022-1759(83)90303-4)
- Oddis CV (2016) Update on the pharmacological treatment of adult myositis. <https://doi.org/10.1111/joim.12511>
- Oslowski CM, Urano F (2011) Measuring ER stress and the unfolded protein response using mammalian tissue culture system. *Methods Enzymol* 490:71–92
- Pan TL, Wang PW, Huang CH, Leu YL, Wu TH, Wu YR, You JS (2015) Herbal formula, *Scutellariae Radix* and *Rhei Rhizoma* attenuate dimethylnitrosamine-induced liver fibrosis in a rat model. *Sci Rep* 5(1):1–11. <https://doi.org/10.1038/srep11734>
- Panche AN, Diwan AD, Chandra SR (2016) Flavonoids: an overview. *J Nutr Sci* 5:1–15. <https://doi.org/10.1017/jns.2016.41>
- Parmar VM, Schröder M (2012) Sensing endoplasmic reticulum stress. *Adv Exp Med Biol* 738:153–168. [https://doi.org/10.1007/978-1-4614-1680-7\\_10](https://doi.org/10.1007/978-1-4614-1680-7_10)
- Poet GJ, Oka OBV, Lith M, Cao Z, Robinson PJ, Pringle MA, Arnér ESJ, Bulleid NJ (2017) Cytosolic thioredoxin reductase 1 is required for correct disulfide formation in the ER. *EMBO J* 36(5):693–702. <https://doi.org/10.15252/EMBJ.201695336>
- Rayavarapu S, Coley W, Nagaraju K (2012) Endoplasmic reticulum stress in skeletal muscle homeostasis and disease. *Curr Rheumatol Rep* 14(3):238–243. <https://doi.org/10.1007/s11926-012-0247-5>
- Rutkowski DT, Kaufman RJ (2004) A trip to the ER: coping with stress. *Trends Cell Biol* 14(1):20–28. <https://doi.org/10.1016/j.tcb.2003.11.001>
- Sartori R, Romanello V, Sandri M (2021) Mechanisms of muscle atrophy and hypertrophy: implications in health and disease. <https://doi.org/10.1038/s41467-020-20123-1>
- Schwarz DS, Blower MD (2015) The endoplasmic reticulum: structure, function and response to cellular signaling. *Cell Mol Life Sci* 73. <https://doi.org/10.1007/s00018-015-2052-6>
- Scicchitano BM, Pelosi L, Sica G, Musarò A (2018) The physiopathologic role of oxidative stress in skeletal muscle. *Mech Ageing Dev* 170(March):37–44. <https://doi.org/10.1016/J.MAD.2017.08.009>
- Silva-Palacios A, Zazueta C, Pedraza-Chaverri J (2020) ER membranes associated with mitochondria: possible therapeutic targets in heart-associated diseases. *Pharmacol Res* 156:104758. <https://doi.org/10.1016/j.phrs.2020.104758>
- Sivandzade F, Bhalerao A, Cucullo L (2019) Analysis of the mitochondrial membrane potential using the cationic JC-1 dye as a sensitive fluorescent probe. *Bio-Protocol* 9 (1). <https://doi.org/10.21769/BIOPROT.3128>
- Takano K, Tabata Y, Kitao Y, Murakami R, Suzuki H, Yamada M, Iinuma M, Yoneda Y, Ogawa S, Hori O (2007) Methoxyflavones protect cells against endoplasmic reticulum stress and neurotoxin. *Am J Phys Cell Physiol* 292(1):353–361. [https://doi.org/10.1152/AJPCELL.00388.2006/SUPPL\\_FILE/FIGURE](https://doi.org/10.1152/AJPCELL.00388.2006/SUPPL_FILE/FIGURE)
- Taouji S, Wolf S, Chevet E (2013) Oligomerization in endoplasmic reticulum stress signaling. *Prog Mol Biol Transl Sci* 117:465–484. <https://doi.org/10.1016/B978-0-12-386931-9.00017-9>
- Thoma A, Lyon M, Al-Shanti N, Nye GA, Cooper RG, Lightfoot AP (2020) Eukarion-134 attenuates endoplasmic reticulum stress-induced mitochondrial dysfunction in human skeletal muscle cells. *Antioxidants* 9(8):1–19. <https://doi.org/10.3390/antiox9080710>
- Uemura A, Oku M, Mori K, Yoshida H (2009) Unconventional splicing of XBP1 mRNA occurs in the cytoplasm during the mammalian unfolded protein response. *J Cell Sci* 122(16):2877–2886. <https://doi.org/10.1242/JCS.040584>
- Vattemi G, King Engel W, McFerrin J, Askanas V (2004) Endoplasmic reticulum stress and unfolded protein response in inclusion body myositis muscle. *Am J Pathol* 164(1):1–7. [https://doi.org/10.1016/S0002-9440\(10\)63089-1](https://doi.org/10.1016/S0002-9440(10)63089-1)
- Wang Y, Branicky R, Noë A, Hekimi S (2018) Superoxide dismutases: dual roles in controlling ROS damage and regulating ROS signaling. *J Cell Biol* 217(6):1915–1928. <https://doi.org/10.1083/JCB.201708007>
- Wortel IMN, Van Der Meer LT, Kilberg MS, Van Leeuwen FN (2017) Surviving stress: modulation of ATF4-mediated stress responses in normal and malignant cells. <https://doi.org/10.1016/j.tem.2017.07.003>
- Yin L, Li N, Jia W, Wang N, Liang M, Yang X, Du G (2021) Skeletal muscle atrophy: from mechanisms to treatments. *Pharmacol Res* 172(August). <https://doi.org/10.1016/j.phrs.2021.105807>
- Yu Q, Fang Du, Douglas JT, Yu H, Yan SS, Yan SF (2017) Mitochondrial dysfunction triggers synaptic deficits via activation of P38 MAP Kinase signaling in differentiated Alzheimer's disease trans-mitochondrial cybrid cells HHS public access. *J Alzheimers Dis* 59(1):223–239. <https://doi.org/10.3233/JAD-170283>
- Yuasa K, Okubo K, Yoda M, Otsu K, Ishii Y, Nakamura M, Itoh Y, Horiuchi K (2018) Targeted ablation of p38 $\alpha$  MAPK suppresses denervation-induced muscle atrophy OPEN. <https://doi.org/10.1038/s41598-018-26632-w>
- Zhou J, Yi Wu, Fengwu Chen Lu, Wang LR, Hayes VM, Poncz M et al (2017) The disulfide isomerase ERp72 supports arterial thrombosis in mice. *Blood* 130(6):817. <https://doi.org/10.1182/BLOOD-2016-12-755587>

**Publisher's note** Springer Nature remains neutral with regard to jurisdictional claims in published maps and institutional affiliations.

Springer Nature or its licensor (e.g. a society or other partner) holds exclusive rights to this article under a publishing agreement with the author(s) or other rightsholder(s); author self-archiving of the accepted manuscript version of this article is solely governed by the terms of such publishing agreement and applicable law.



# Tangeretin enhances pancreatic beta-TC-6 function by ameliorating tunicamycin-induced cellular perturbations

Eveline M Anto<sup>1,2</sup> · P. Jayamurthy<sup>1,2</sup>

Received: 31 August 2023 / Accepted: 6 November 2023  
© The Author(s), under exclusive licence to Springer Nature B.V. 2023

## Abstract

**Background** Pancreatic beta cell health and its insulin-secreting potential are severely compromised under the diabetic condition. One of the key mediators of beta cell dysfunction is endoplasmic reticulum (ER) stress. Pharmacological intervention of ER stress and associated complications in pancreatic beta cells may be an effective strategy for the management of diabetes. In the present study, we evaluated the efficacy of tangeretin, a citrus pentamethoxyflavone, in the alleviation of ER stress and associated perturbations in pancreatic Beta-TC-6 cell lines.

**Methods and results** Tunicamycin (pharmacological ER stress inducer) at subtoxic levels was observed to induce beta cell dysfunction by upregulation of intracellular ROS levels, lowering mitochondrial number/biogenesis and membrane potential, elevation of UPR markers, XBP-1, GADD153, and ER resident chaperones. Treatment with tangeretin was successful in improving the beta cell function by lowering the ROS levels and improving the mitochondrial biogenesis and mitochondrial membrane potential. Tangeretin also downregulated the expression levels of XBP-1, GADD153, and ER resident chaperones. GLUT2 expression, however, did not undergo any significant change under ER stress. We also observed altered expression of Pdx-1, TRB3, and p-Akt under the ER stress condition. Tangeretin augmented the expression levels of Pdx-1, and p-Akt while curtailing the expression of TRB3 in beta cells. Tunicamycin treatment suppressed the insulin levels, however, co-treatment with tangeretin could only marginally improve the levels.

**Conclusion** Targeting ER stress and associated pathways in pancreatic Beta-TC-6 cell lines by tangeretin can be an effective strategy for improving beta cell function.

**Keywords** ER stress · Tangeretin · Beta-TC-6 cell line · Tunicamycin

## Introduction

Diabetes mellitus is a chronic metabolic disease affecting people worldwide and both type 1 and type 2 diabetes are characterized by impaired insulin release from pancreatic beta cell islets. The pancreatic islets consist of a well-developed ER owing to their secretory function [1]. Under physiological scenarios, the ER is involved in maintaining the beta cell function and maturation of insulin peptide, the

major protein released by the pancreatic beta cells [2]. Any perturbations in the ER function can lead to ER stress which results in a buildup of misfolded or unfolded proteins in the ER lumen. The unfolded protein response (UPR), a signaling cascade that is triggered by this, works to restore ER homeostasis by activating its three arms, IRE-1, ATF6, and PERK [3]. These three proteins work in concert to reduce the ER burden by attenuating the protein translation, induction of the ER-resident chaperones, and upregulation of the endoplasmic reticulum-associated degradation [4].

Chronic ER stress in pancreatic beta islets is associated with decreased beta cell mass, function, and impaired insulin production [5]. Cellular stresses including obesity-mediated circulating saturated fatty acids (lipotoxicity) and high glucose-induced glucotoxicity have been reported to contribute to ER stress in beta cells [6]. In diabetic conditions, insulin resistance causes beta cell compensation by stimulating hypersecretion of insulin but after a point, loss of beta cells

✉ P. Jayamurthy  
pjayamurthy@niist.res.in

<sup>1</sup> Agro-Processing & Technology Division,  
Department of Biochemistry, CSIR-National  
Institute for Interdisciplinary Science & Technology,  
Thiruvananthapuram, Kerala 695019, India

<sup>2</sup> Academy of Scientific and Innovative Research (AcSIR),  
Ghaziabad 201002, India

and function abrogate insulin secretion aggravating the disease condition [7]. The impaired insulin secretion results in decreased glucose uptake in peripheral tissues leading to hyperglycemia. Sustained hyperglycemia and insulin resistance can contribute to reactive oxygen species (ROS) generation and mitochondrial dysfunction in pancreatic beta cells that ultimately result in beta cell apoptosis [8].

Oxidative stress and ER stress are closely entwined events that are more prominent in pancreatic beta cells due to the relatively low antioxidant levels making them susceptible to oxidative damage [9]. ER stress mediated mitochondrial dysfunction is also an important consequence in pancreatic beta cells due to the structural and functional proximity of ER and mitochondria [10]. Prolonged ER stress interferes with the insulin biosynthesis via suppression of insulin mRNA expression and insulin promoter activity by chronic IRE-1 $\alpha$  and ATF6 activation respectively [1, 2]. Therapeutic intervention of ER stress and associated pathways may improve beta cell health which is an important prerequisite for normal insulin secreting potential of beta cells.

Currently, sulfonylureas are a class of drugs that are used as first line therapy to treat diabetes by improving insulin secretion from pancreatic beta cells [11]. However, its long-term use is associated with beta cell apoptosis and loss of function. This is due to the sustained increase in intracellular calcium ions to facilitate insulin secretion which may result in chronic ER stress as ER is a major reservoir of calcium and any perturbation in calcium metabolism leads to disruption of ER homeostasis [12]. Rather than only improving insulin secretion, focus should shift towards developing therapeutic strategies that aim to improve the overall pancreatic beta cell function by maintaining the ER homeostasis. Identifying plant-based alternatives with ER protective effects to improve the pancreatic beta cell function will be an effective treatment strategy due to the economic feasibility and lesser adverse effects.

Flavonoids are polyphenols which are widely present in fruits and vegetables and form an integral part of the daily human diet. Flavonoids are reported to have broad spectrum biological activities [13]. Tangeretin is a pentamethoxyflavone belonging to the flavone subclass of flavonoids and abundantly found in the peels of citrus fruits [14]. The present study was aimed at investigating the effect of tangeretin against tunicamycin induced ER stress in pancreatic Beta-TC-6 cell lines. Tangeretin has been in use as traditional Chinese medicine and it is also reported to have antioxidant, anti-inflammatory and anticancer activity [14, 15]. Takano et al. reported the protective effect of methoxyflavones in pancreatic MIN6 cell lines against ER stress and oxidative stress [16]. Our group has also reported the protective effect of tangeretin against ER stress induced cellular dysfunction in skeletal muscle L6 cells [17]. This study aims to investigate the potential of tangeretin in alleviating the ER stress

induced cellular perturbations including effect on insulin expression levels and overall cellular function in pancreatic Beta-TC-6 cell line.

## Materials and methods

Tangeretin (Cat no.T8951), 4-phenyl butyric acid (PBA) (Cat no.P21005), tunicamycin (Cat no.T7765), HPLC grade methanol (Cat no.60600710001730), dichlorodihydrofluorescein diacetate (DCFH-DA) (Cat no.D6883), protease inhibitor cocktail tablets (Cat no.S8830) were bought from Sigma Aldrich Chemical (St. Louis, Missouri, USA). Dulbecco's modified Eagle's medium (DMEM) (Cat no.AL007S) containing 4.5 g/L glucose and 1.5 g/L sodium bicarbonate, antimycotic antibiotic mix (Cat no.A002A), fetal bovine serum (Cat no.RM10432), dimethyl sulfoxide (DMSO) (Cat no.TC185), triton X (Cat no.TC286), glycine (Cat no.MB013), sodium dodecyl sulphate (Cat no.GRM6218), tris base (Cat no.TC072), skimmed milk (Cat no.GRM1254), phosphate buffered saline (PBS) (Cat no.ML023) were procured from Himedia (Mumbai, India). Bicinchoninic acid assay kit (BCA kit) (Cat no.23225), radioimmunoprecipitation assay buffer (RIPA lysis buffer) (Cat no.89900), hank's balanced salt solution (HBSS) (Cat no.14025092) was obtained from Thermo Fisher Scientific (Waltham, Massachusetts, USA). JC-1 assay kit (Cat no.10009172) was obtained from Cayman Chemicals (Michigan, USA). The antibodies insulin (Cat no.8138), p-Akt (Cat no.4058), Akt (Cat no.4685), beta actin (Cat no.4967), HRP conjugated secondary antibodies (Cat no.7074,7076), Alexa Fluor conjugated secondary antibodies (Cat no.4412, 4408) were purchased from Cell Signaling Technologies (Danvers, Massachusetts, USA). Antibodies TRB3 (Cat no.sc-365842), GADD153 (Cat no.sc-7351), were purchased from Santa Cruz Biotechnology (Dallas, Texas, USA). Antibodies XBP-1 (Cat no.ITT05110), GLUT2 (Cat no.ITT07510), Pdx-1 (Cat no.ITT07170), GRP94 (Cat no.ITT05287), calnexin (Cat no.ITT05362) were purchased from Gbiosciences (St. Louis, MO, USA). Mouse Beta-TC-6 cell lines were purchased from National centre for cell sciences, Pune, India.

## Cell culture

Pancreatic Beta-TC-6 cells were cultured in DMEM containing 15% fetal bovine serum and 1% antibiotic antimycotic mix. The cells were maintained in a humidified incubator at 37 °C and 5% carbon dioxide. On reaching 90% confluence, the cells were treated with the experimental groups for a time period of 24 h. After the treatment period, the cells were harvested for further analysis.



## Experimental groups

- CON—untreated or control cells
- TM—tunicamycin (0.25 µg/ml) treated cells
- TM + TAN—tunicamycin (0.25 µg/ml) & tangeretin (10 µM) co-treated cells
- TM + PBA—tunicamycin (0.25 µg/ml) & PBA (100 µM) co-treated cells (positive control)

## Dose optimization of tunicamycin and tangeretin

Cells were seeded at a density of  $5 \times 10^3$  cells per well in 96 well plate. The cells were treated with different doses of tunicamycin (0.25–10 µg/ml), for a time period of 24 h in serum starved medium. The cytotoxicity was evaluated using the MTT assay as described by Mosmann et al. [18]. Following the treatment period, medium was aspirated and cells were given HBSS wash followed by incubation with 0.5 mg/ml MTT solution for 2–4 h. After the incubation period, MTT solution was replaced with 100 µl DMSO per well. Plate was then incubated on shaker for 20 min and absorbance reading was taken at 570 nm in Tecan plate reader (Tecan infinite 200 PRO, Austria). In a separate experiment, cells were treated with different concentrations of tangeretin (10–100 µM) for 24 h and cytotoxicity was determined. The optimal dose for co-treatment studies was determined by treating the cells with different concentrations (5 µM and 10 µM) of tangeretin in the presence of optimised dose of tunicamycin for 24 h followed by MTT assay. The optimal dose of tangeretin for co-treatment studies was selected based on the MTT results.

## Intracellular ROS generation

The ROS levels were determined by the DCFH-DA staining. The cells were treated for 24 h with the experimental groups. For DCFH-DA staining, protocol by Armstrong was followed in which cells were incubated with 10 µM DCFH-DA staining solution for 20 min followed by gentle washing in HBSS [19]. Fluorescence images were acquired using the FITC filter in fluorescence microscope and intensity was quantitated using the cell sens software (Olympus Life Science, Japan).

## Determination of mitochondrial content and mitochondrial membrane potential

After treatment with respective experimental groups, the mitochondrial content was estimated by incubating with 100 nM Mito tracker staining solution for 20 min followed by HBSS wash [20]. The fluorescence images were acquired in TRITC filter of fluorescence microscope and the intensity was determined using the cell Sens software (Olympus Life

Science, Japan). For measuring the mitochondrial membrane potential, following treatment period, cells were stained with cationic dye, JC-1 for 30 min [21]. Images of the aggregates were acquired in the TRITC filter whereas the monomer images were obtained using the FITC filter (Olympus Life Science, Japan).

## Immunofluorescence staining of beta-TC-6 cells

After treatment period, cells were fixed for 15 min in paraformaldehyde solution (4%) before being permeabilized for 10 min in 0.1% Triton X. This was followed by incubation of the fixed cells with the following antibodies, Pdx-1 (1:400) and Insulin (1:400) antibodies, respectively. The cells were then incubated with specific secondary antibody conjugated with Alexa Fluor (1:500). The cells were then counter stained with DAPI. The fluorescence images were acquired using fluorescence microscope (Olympus Life Science, Japan).

## Western blot analysis

Cells were seeded in T25 flasks and after attaining 90% confluency, they were subjected to treatment with the experimental groups for 24 h. Cells were then rinsed with HBSS and proteins were extracted using RIPA lysis buffer. Using the BCA assay kit and BSA as the standard, the extracted protein samples were quantitated and normalised. Protein samples were separated on 10% sodium dodecyl sulphate polyacrylamide gels. This was followed by transfer of proteins to PVDF membranes (Millipore, Merck, USA) and blocking for 60 min in 5% skimmed milk. Membranes were then given TBST wash three times followed by incubation with the appropriate primary antibodies (1:1000 dilution), XBP-1, GADD153, GRP94, calnexin, p-Akt, Akt, TRB3, insulin, GLUT2, Pdx-1 overnight at 4 °C with agitation. The loading control used was beta actin. After that, the membranes were incubated for 2 h at room temperature with suitable HRP-conjugated secondary antibodies. The ECL substrate solution was used to detect the blot bands, and image analysis was done in Chemidoc MP Imaging systems (Bio-Rad, USA). The resultant bands were quantified by densitometric analysis using the Image lab software version 6.1 (Bio-Rad, USA).

## Statistical analysis

All experiments were performed in triplicates and three times, independently. Data was statistically analysed using one-way ANOVA and Duncan post hoc analysis in SPSS software. The results are represented as mean  $\pm$  SEM where p value  $\leq 0.05$  was considered to be significant statistically.



## Results

### Cytotoxicity studies of tunicamycin and tangeretin

Tunicamycin was found to be non-toxic (induced less than 20% cell death) upto 0.25  $\mu\text{g/ml}$  in Beta-TC-6 cells after 24 h treatment period with different concentrations ranging from 0.25 to 10  $\mu\text{g/ml}$  (Fig. 1a). As we wanted to monitor the intracellular changes prior to induction of cell death, 0.25  $\mu\text{g/ml}$  tunicamycin was chosen as the optimum dose for ER stress induction in all experiments. We also optimised the viable dose of tangeretin by treating cells with concentrations ranging from 10 to 100  $\mu\text{M}$ . At a concentration of 10  $\mu\text{M}$ , tangeretin induced less than 20%

cytotoxicity after 24 h treatment period as seen in Fig. 1b. The optimum dose of tangeretin under ER stress condition was determined by treating cells with different doses of tangeretin (5  $\mu\text{M}$ , 10  $\mu\text{M}$ ) along with 0.25  $\mu\text{g/ml}$  tunicamycin. At a dose of 10  $\mu\text{M}$  tangeretin, cells were found to be viable under ER stress (Fig. 1c). Therefore, 10  $\mu\text{M}$  tangeretin was used in all future experiments. PBA was found to be non-toxic upto 100  $\mu\text{M}$  concentration (Supplementary Fig. 1).

### Intracellular ROS generation

ROS generation is a hallmark of cellular redox disturbances. From the fluorescence images in Fig. 2a, it is evident that tunicamycin treated group showed an increased

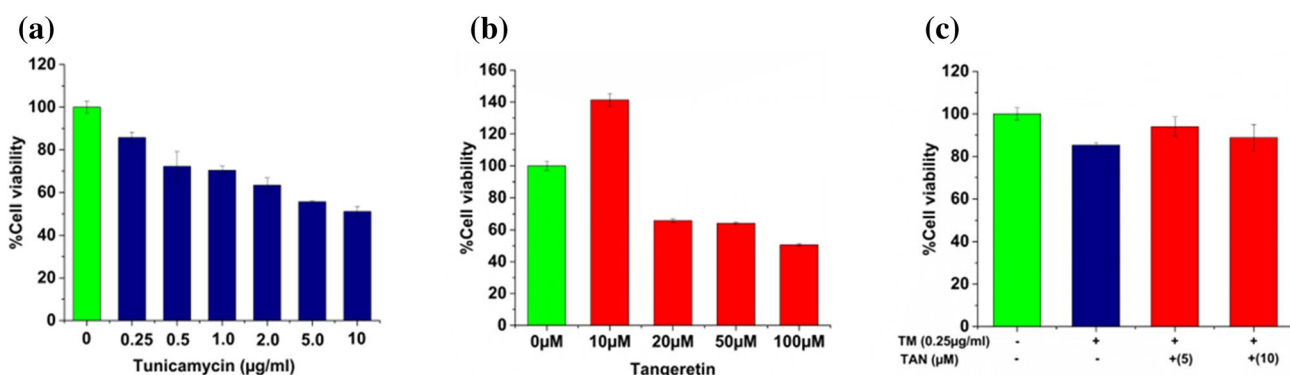


**Fig. 1** Cytotoxicity studies. **a** Pancreatic Beta-TC-6 cells were treated with different doses of tunicamycin (0.25–10  $\mu\text{g/ml}$ ) for 24 h. **b** Pancreatic Beta-TC-6 cells were treated with various concentrations of tangeretin (10–100  $\mu\text{M}$ ) for 24 h. This was followed by MTT analy-

sis. **c** Dose of co-treatment was determined by treating the cells with 5  $\mu\text{M}$ , 10  $\mu\text{M}$  tangeretin in the presence of 0.25  $\mu\text{g/ml}$  tunicamycin followed by MTT assay. Values are represented as mean  $\pm$  SEM where  $n=3$

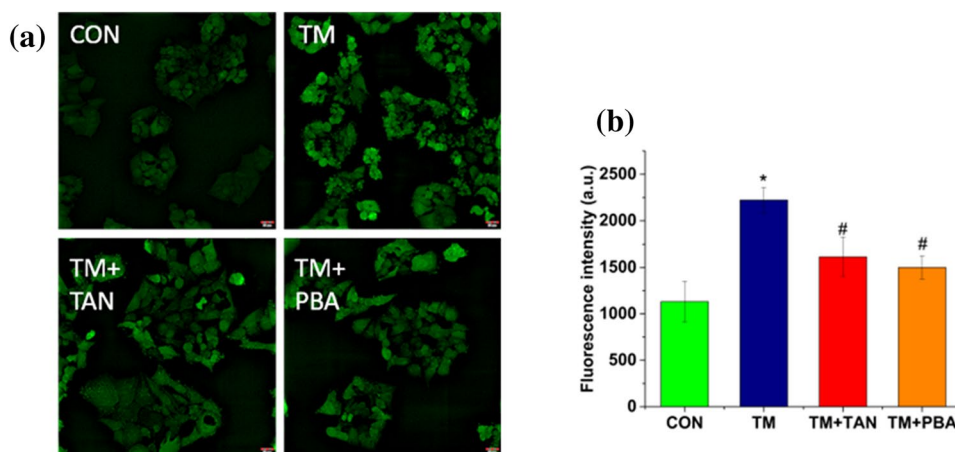


**Fig. 2** Determination of intracellular ROS generation. **a** Effect of tangeretin on tunicamycin induced intracellular ROS was estimated using DCFH-DA dye and images acquired in fluorescence microscope. Magnification  $\times 20$ . Scale corresponds to 20  $\mu\text{m}$ . **b** DCFH-DA fluorescence intensity histogram. CON represents untreated group, TM represents 0.25  $\mu\text{g/ml}$  tunicamycin treated group, TM+TAN

represents TM tangeretin (10  $\mu\text{M}$ ) co-treated group, TM+PBA represents TM 4-phenylbutyric acid (100  $\mu\text{M}$ ) co-treated group. Values are represented as mean  $\pm$  SEM where  $n=3$ . \* $p \leq 0.05$  significantly different from control cells, # $p \leq 0.05$  significantly different from tunicamycin treated cells

ROS generation compared to the control as indicated by the increased fluorescence whereas co-treatment with tangeretin and PBA respectively brought down the ROS levels significantly. This was further demonstrated by the fluorescence intensity histograms (Fig. 2b) in which tunicamycin increased the ROS generation to 2222.5 a.u. (arbitrary units) compared to the control. The untreated cells showed a fluorescence intensity of 1132.2 a.u. Co-treatment with tangeretin significantly lowered the ROS levels to 1614.7 a.u. and PBA decreased the levels to 1499.62 a.u. which was significantly lower than the tunicamycin treated group.

### Changes in mitochondrial content and mitochondrial membrane potential

ER stress and mitochondrial dysfunction are closely linked events and both are involved in the pancreatic beta cell dysfunction and decreased insulin biosynthesis via the UPR activation [22]. Treatment with tunicamycin decreased the mitochondrial number/biogenesis as evident from the fluorescence images in Fig. 3a, co-treatment with tangeretin and PBA improved the mitochondrial content. From the intensity histograms (Fig. 3b), in tunicamycin treated group, mitochondrial biogenesis was decreased to 1448.7 a.u. compared to untreated cells (2297.5 a.u.). Co-treatment with tangeretin remarkably improved the fluorescence to 2107.1 a.u. while PBA increased the fluorescence to 1837.7 a.u. as seen in Fig. 3a, b.

ER stress induction is associated with mitochondrial dysfunction and one of the early markers of the same is loss of mitochondrial membrane potential. The JC-1 dye exists

as red aggregates in cells with healthy mitochondria while in depolarised mitochondrial membrane it exists as green monomers. The aggregate to monomer ratio is an indicator of the mitochondrial well-being. Here, tunicamycin induced a depolarisation of the mitochondrial membrane as indicated by the fluorescence images and intensity histograms in Fig. 4a, b respectively. Tunicamycin treated group showed a lower red to green ratio of 1.5 compared to the untreated cells having aggregate to monomer ratio of 2.6. Co-treatment with tangeretin induced a hyperpolarisation indicated by the higher JC-1 aggregate to monomer ratio of 2.2. Co-treatment with PBA improved the ratio to 2.1 as shown in Fig. 4b.

### Modulation of XBP-1, ER resident chaperones and GADD153 expression during ER stress by tangeretin

Under prolonged ER stress condition, the IRE-1 $\alpha$  arm of UPR induces the splicing of the XBP-1 mRNA to a highly active form. Following translation, the spliced form translocates to the nucleus and regulates the genes encoding the ER resident chaperones such as GRP94, PDI, calreticulin and calnexin and components of the endoplasmic reticulum associated degradation [23]. In this study, tunicamycin significantly induced the expression of the following proteins, XBP-1 (164.1%), GRP94 (115.68%) and calnexin (114.64%) respectively compared to the control (Fig. 5a, b). Co-treatment with tangeretin was effective in significantly bringing down the levels of XBP-1 by 35.85% and GRP94 by 64.41% compared

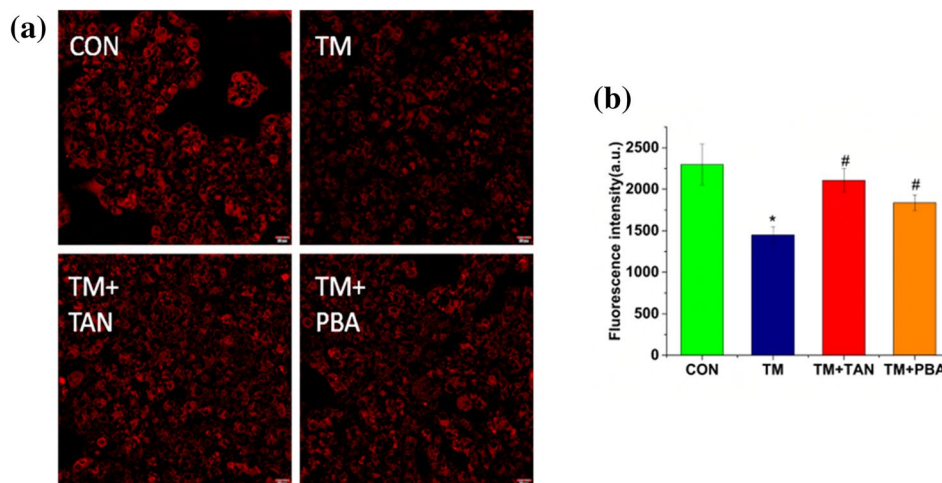


**Fig. 3** Tangeretin improves mitochondrial number/biogenesis under ER stress. **a** Pancreatic Beta-TC-6 cells were treated with the experimental groups for 24 h followed by incubation with Mito tracker dye. Imaging was performed in fluorescence microscope. Magnification  $\times 20$ . Scale corresponds to 20  $\mu\text{m}$ . **b** Mito tracker fluorescence intensity histogram analysis. CON represents untreated group, TM repre-

sents 0.25  $\mu\text{g/ml}$  tunicamycin treated group, TM+TAN represents TM tangeretin (10  $\mu\text{M}$ ) co-treated group, TM+PBA represents TM 4-phenylbutyric acid (100  $\mu\text{M}$ ) co-treated group. Values are expressed as mean  $\pm$  SEM where  $n=3$ . \* $p \leq 0.05$  significantly different from control cells, # $p \leq 0.05$  significantly different from tunicamycin treated cells

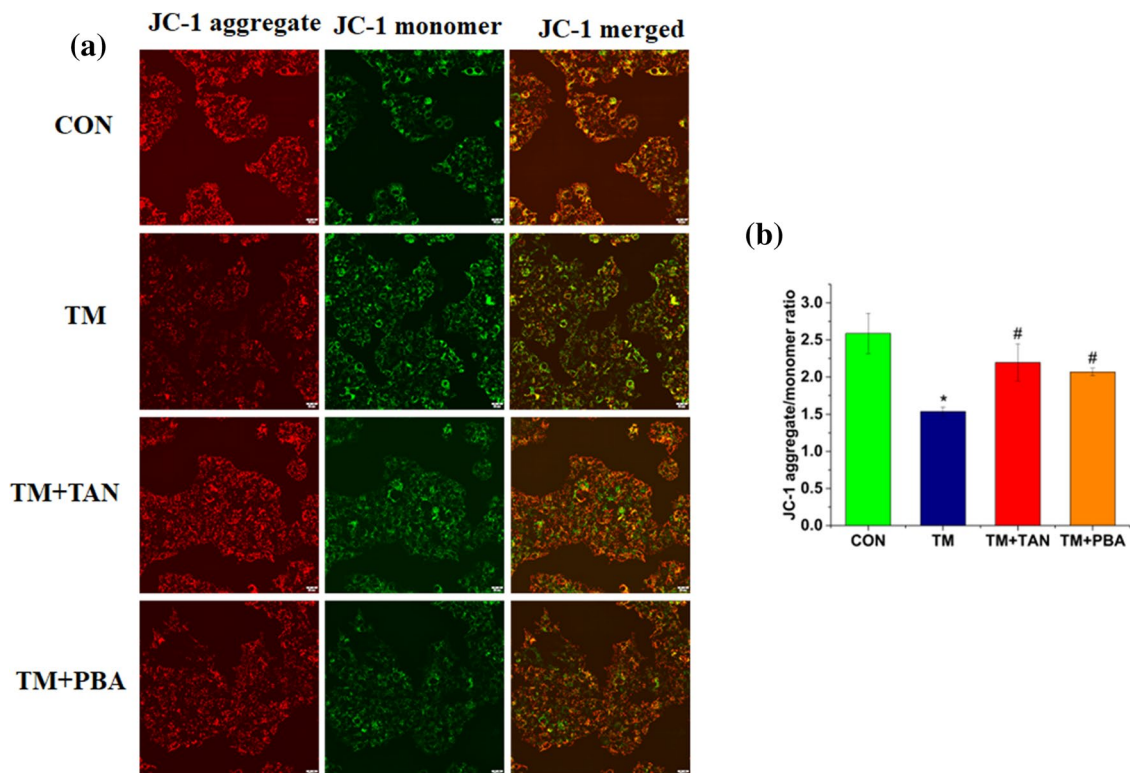


**Fig. 4** Tangeretin improves tunicamycin induced loss of mitochondrial membrane potential. **a** Pancreatic Beta-TC-6 cells after treatment for 24 h were incubated with JC-1 dye for 20 min. This was followed by imaging in fluorescence microscope. Magnification $\times 20$ . Scale corresponds to 20  $\mu\text{m}$ . **b** Aggregate to monomer fluorescence intensity ratio analysis was performed in Cell Sens software (Olympus Life Science, Japan). CON represents untreated group, TM rep-

resents 0.25  $\mu\text{g/ml}$  tunicamycin treated group, TM+TAN represents TM tangeretin (10  $\mu\text{M}$ ) co-treated group, TM+PBA represents TM 4-phenylbutyric acid (100  $\mu\text{M}$ ) co-treated group. Values are expressed as mean $\pm$ SEM where  $n=3$ . \* $p\leq 0.05$  significantly different from control cells, # $p\leq 0.05$  significantly different from tunicamycin treated cells

to tunicamycin treated group, however, calnexin levels were not downregulated significantly (106.53%). PBA did not alter the XBP-1 levels (163.66%) while GRP94 were significantly reduced by 31.19% and calnexin by 32.46% respectively compared to tunicamycin treated group as depicted in Fig. 5a, b.

As already stated, the primary aim of the UPR is to restore the ER homeostasis but if the stress is chronic, the UPR becomes dysregulated and activates the apoptotic signalling [24]. GADD153 or CHOP is a hallmark of dysregulated UPR and amelioration of the same may aid in restoration of ER homeostasis. Tunicamycin significantly induced the expression of GADD153 (125.09%) compared to the control (Fig. 5a, b). Tangeretin was effective in bringing down the levels of GADD153 significantly by 29.52% whereas GADD153 levels were reduced remarkably by 25.9% in PBA treated group compared to tunicamycin treated group (Fig. 5a, b).

### Effect of tangeretin on proteins involved in beta cell survival and insulin biosynthesis

Under ER stress conditions, TRB3 was found to be remarkably upregulated (122.49%) whereas phospho-Akt was found to be significantly downregulated (72.39%) compared to the control as seen in Fig. 6a, b. Treatment with tangeretin resulted in significant suppression of TRB3 levels by 14.87% while remarkably improving the phospho-Akt by 35.85% compared to tunicamycin treated group (Fig. 6a, b). In PBA treated cells, TRB3 levels were significantly decreased by 20.23% whereas phospho-Akt was remarkably improved by 34.24% as shown in Fig. 6a, b.

Treatment with tunicamycin resulted in no significant change in expression of GLUT2 (Fig. 6a, b). Co-treatment with tangeretin also did not affect the levels significantly as seen in Fig. 6a, b. Under ER stress conditions, the expression of Pdx-1 protein was significantly reduced (72.92%)

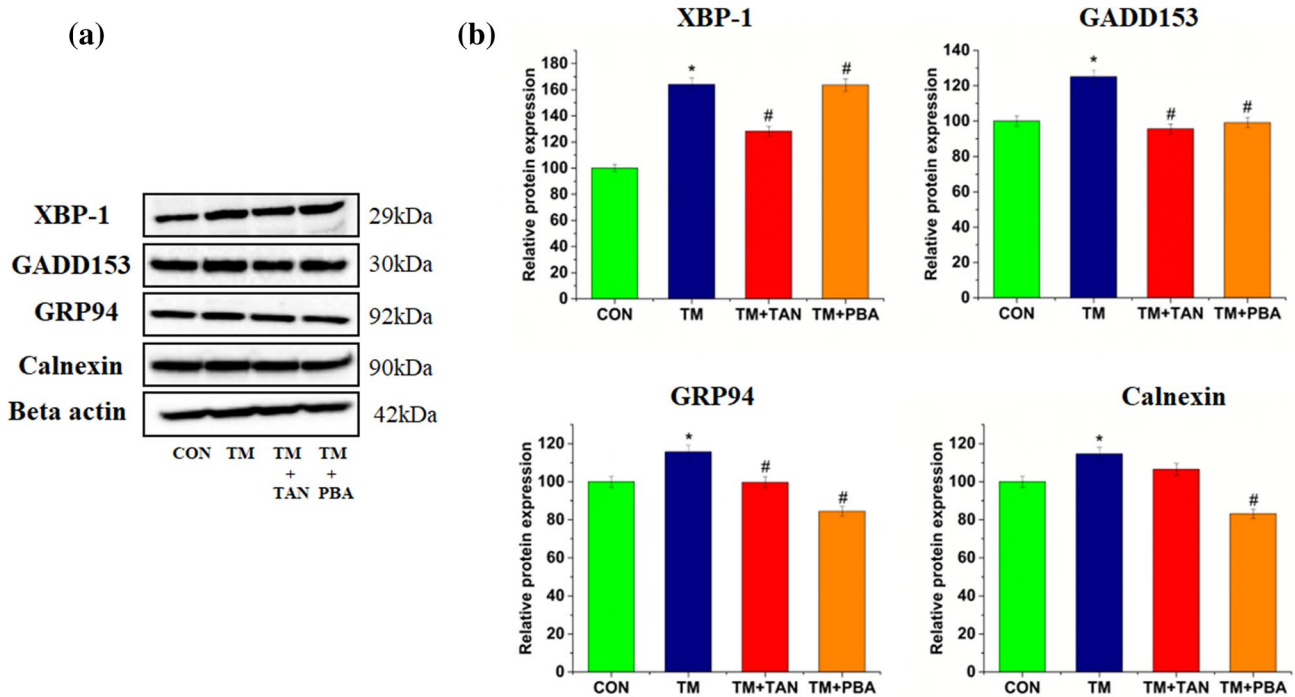


**Fig. 5** Effect of tangeretin on tunicamycin induced expression of XBP-1, GADD153, ER resident chaperones (GRP94 & calnexin). **a** Western blot analysis of XBP-1, GADD153, GRP94 and calnexin was performed with beta actin as the loading control. **b** Densitometric analysis of all proteins relative to beta actin. CON represents untreated group, TM represents 0.25 µg/ml tunicamycin treated

group, TM+TAN represents TM tangeretin (10 µM) co-treated group, TM+PBA represents TM 4-phenylbutyric acid (100 µM) co-treated group. Values are expressed as mean ± SEM where n=3. \*p ≤ 0.05 significantly different from control cells, #p ≤ 0.05 significantly different from tunicamycin treated cells

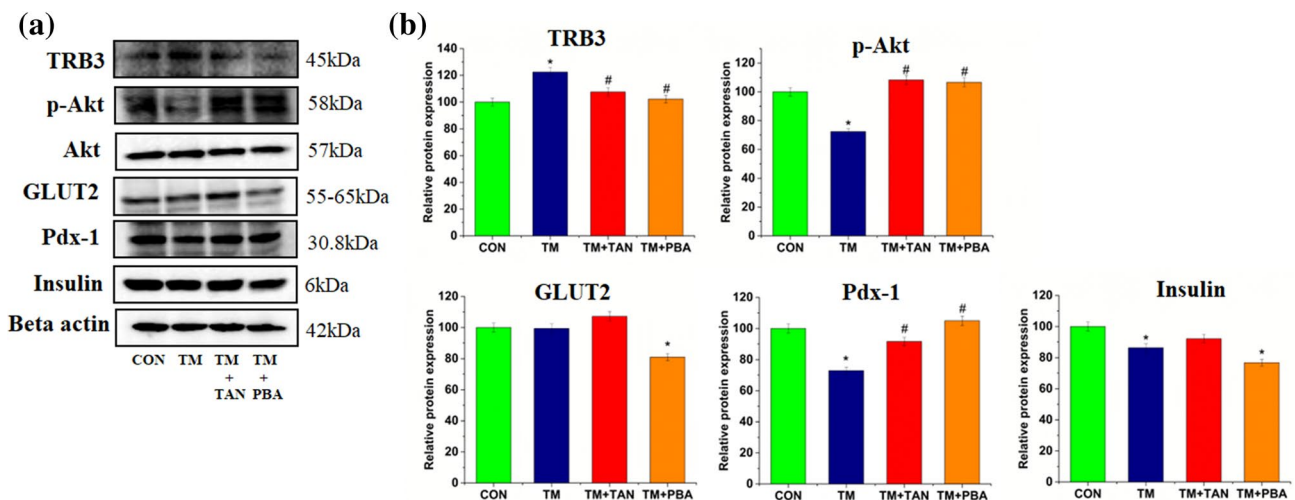


**Fig. 6** Effect of tangeretin on expression levels of TRB3, p-Akt, GLUT 2, Pdx-1, insulin during ER stress. **a** Western blot analysis of TRB3, p-Akt, GLUT2, Pdx-1 and insulin was performed. Beta actin was the loading control for TRB3, GLUT2, Pdx-1 and insulin while Akt was the loading control for p-Akt. **b** Densitometric analysis of TRB3, GLUT2, Pdx-1, insulin relative to beta actin and p-Akt rela-

tive to Akt. CON represents untreated group, TM represents 0.25 µg/ml tunicamycin treated group, TM+TAN represents TM tangeretin (10 µM) co-treated group, TM+PBA represents TM 4-phenylbutyric acid (100 µM) co-treated group. Values are expressed as mean ± SEM where n=3. \*p ≤ 0.05 significantly different from control cells, #p ≤ 0.05 significantly different from tunicamycin treated cells



and insulin expression were also decreased significantly to 86.32% compared to control cells as depicted in Fig. 6a, b. Treatment with tangeretin improved the Pdx-1 levels significantly by 18.76% compared to tunicamycin treated cells (Fig. 6a, b). Tangeretin improved the insulin levels by 5.86% but it was not significant compared to tunicamycin group as shown in Fig. 6a, b. In PBA treated group the Pdx-1 levels were remarkably improved by 32.09% whereas insulin expression was decreased by 9.57% compared to tunicamycin treated group (Fig. 6a, b). These results were also corroborated by the immunofluorescence data of Pdx-1 (Fig. 7a) and insulin (Fig. 7b).

## Discussion

ER stress is a key mediator of insulin biosynthesis impairment and subsequent pancreatic beta cell dysfunction, a major event in diabetic progression. Identifying ER protective agents that target the ER stress and related signaling mechanisms may aid in novel therapeutic strategies for disease management. The present study attempted to evaluate the role of tangeretin in amelioration of tunicamycin induced perturbations in pancreatic Beta-TC-6 cells. Here, treatment of pancreatic beta cells with tunicamycin resulted in ROS generation, hallmark of oxidative stress. Co-treatment with tangeretin was effective in bringing down the ROS levels. As pancreatic beta cells express low levels of cellular

antioxidants, they are more susceptible to redox disturbances [25]. ER stress and oxidative stress share a strong relationship in pancreatic beta cells where the prolonged exposure to former negatively affects insulin biosynthesis and beta cell function [26].

Cells under ER stress, generate more ROS due to the upregulation of the protein folding machinery which works to reduce the burden of misfolded proteins [27]. In the present study, treatment with tunicamycin induced the expression of the protein folding machinery proteins namely XBP-1, GRP94 and calnexin. IRE-1 $\alpha$  arm of the UPR triggers the splicing of XBP-1 which then upregulates the ER resident chaperones to enhance the protein folding for alleviation of the ER stress [28]. Overexpression of XBP-1 is also associated with decreased insulin levels, impaired glucose stimulated insulin secretion and beta cell apoptosis [29]. GRP94 and calnexin are part of the quality control system in the ER and are induced during ER stress conditions [30]. By remarkably reducing the levels of XBP-1 and GRP94, tangeretin inhibited the tunicamycin-induced activation of the protein folding machinery, indicating a reduction in the stress condition.

GADD153/CHOP expression is an indication of maladaptive or dysregulated UPR which subsequently results in cellular dysfunction [31]. Here, we observed an increased expression of GADD153 on prolonged exposure to tunicamycin which was suppressed on tangeretin co-treatment. Song et al. have reported the role of GADD153 in linking

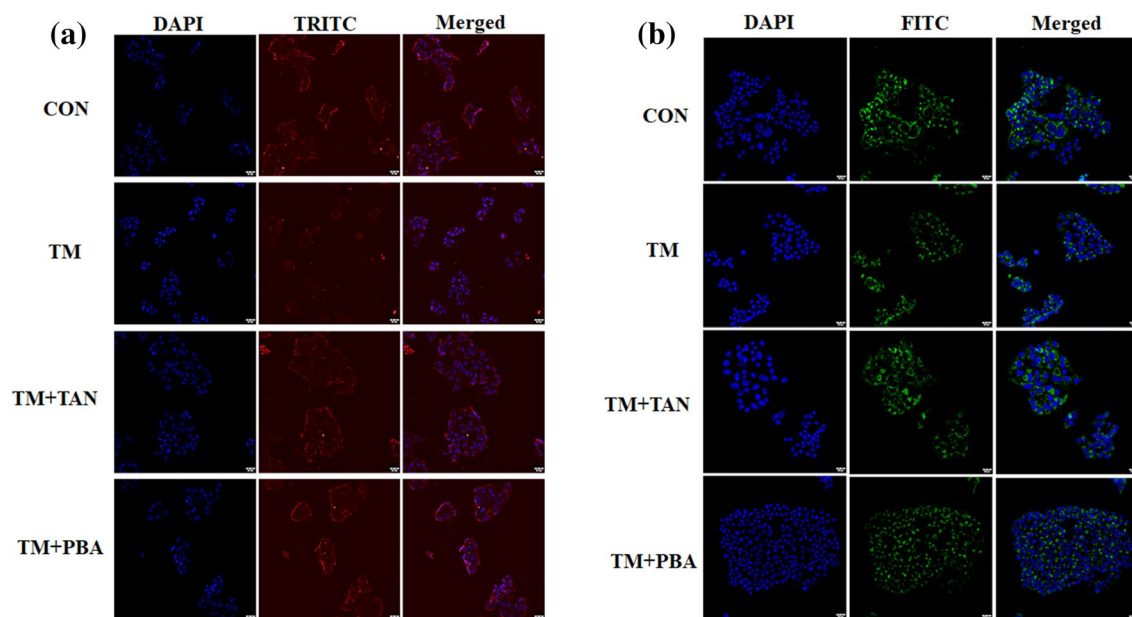


**Fig. 7** Immunofluorescence expression studies of Pdx-1 and insulin during ER stress. Immunofluorescence imaging of **a** Pdx-1 and **b** insulin, using fluorescence microscope. Magnification  $\times 20$ . Scale corresponds to 20  $\mu\text{m}$ . CON represents untreated group, TM represents 0.25  $\mu\text{g}/\text{ml}$  tunicamycin treated group, TM + TAN represents TM tan-

geretin (10  $\mu\text{M}$ ) co-treated group, TM + PBA represents TM 4-phenylbutyric acid (100  $\mu\text{M}$ ) co-treated group. Values are expressed as mean  $\pm$  SEM where  $n = 3$ . \* $p \leq 0.05$  significantly different from control cells, # $p \leq 0.05$  significantly different from tunicamycin treated cells

protein misfolding to oxidative stress in pancreas. CHOP or GADD153 deletion was associated with reduced oxidative stress and improved beta cell function in in vivo models [32]. Targeting the CHOP can be a therapeutic approach to improve beta cell function.

Recent studies indicate a role of both ER stress and oxidative stress in the loss of mitochondrial membrane potential [33, 34]. Our findings demonstrate an improvement in mitochondrial membrane potential by tangeretin under ER stress conditions. Mitochondrial membrane hyperpolarization and downstream increase in ATP/ADP ratio is a necessary step in the canonical glucose stimulated insulin secretion (GSIS) [35]. Under diabetic conditions there is a loss of mitochondrial membrane potential which may hamper the insulin secretion. Loss in mitochondrial biogenesis or number due to mitochondrial dysfunction is manifested in diabetic condition [36]. Improving the mitochondrial biogenesis can aid in better management of the disease [37]. In our study, under ER stress conditions the mitochondrial biogenesis was found to be significantly reduced indicating mitochondrial dysfunction as evident from the Mito tracker red staining whereas co-treatment with tangeretin remarkably improved the same. This data is consistent with the GADD153 expression levels in tunicamycin treated group which indicates beta cell dysfunction upon induction of ER stress.

Under physiological conditions the Akt signaling plays an important role in beta cell proliferation, function and insulin secretion [38, 39]. Akt function is negatively regulated by oxidative stress and ER stress and improving the Akt function will contribute to beta cell function [40]. TRB3, an ER stress marker protein that is involved in the suppression of the Akt active form, is activated by the ATF4/GADD153 arm of the UPR [41]. Here we observed a concomitant increase in the expression of TRB3 and a downregulation in p-Akt levels in cells treated with tunicamycin only. Tangeretin significantly brought down the TRB3 levels while increasing the p-Akt levels which indicates the efficacy of the citrus flavone in promoting beta cell survival and function under ER stress condition by suppressing the TRB3 levels and improving the p-Akt levels.

The main stimulus for pancreatic insulin secretion is the glucose which is taken into the cells by the GLUT2 transporter on the plasma membrane of rodents. Unlike GLUT4 which gets activated in response to insulin, GLUT2 is activated by the extracellular glucose [42]. After reaching the cytosol, the glucose is phosphorylated by the glucokinase enzyme for glycolysis for generation of ATP and subsequently aids in insulin secretion [43]. Here, the expression of GLUT2 did not change significantly under ER stress conditions. This was even observed in cells co-treated with tangeretin. This is in contrast to previous reports where the GLUT2 expression was significantly reduced under ER stress condition in pancreatic beta cells [29, 44]. However,

few previous studies have also reported the unchanged GLUT2 levels in response to tunicamycin [45, 46]. This can be because GLUT2 is not the rate limiting step in the insulin biosynthesis signaling as it mediates passive glucose diffusion. In our study this can be due to the subtoxic levels of tunicamycin and also because GLUT2 expression is not directly related to ER stress [47].

We also studied the expression of Pdx-1, a transcriptional factor which is essential for insulin gene expression and also required for beta cell survival by regulating development, maturation and differentiation and reduced Pdx-1 expression is associated with beta cell dysfunction [48]. In this study, the expression of Pdx-1 was significantly suppressed on treatment with tunicamycin while co-treatment with tangeretin restored the Pdx-1 levels as evident from the Western blot results. This was in agreement with Yao et al., who demonstrated the efficacy of an *O*-methylated isoflavone in promoting the activity of Pdx-1 under glucotoxic and lipotoxic conditions in in vitro and in vivo models [49]. The major function of pancreatic cells involves insulin biosynthesis and secretion in response to elevated blood glucose levels. During chronic ER stress conditions, pancreatic beta cell function is compromised resulting in reduced levels of insulin synthesis as well as insulin secretion. From our results it was seen that expression of the insulin protein was modestly but significantly downregulated upon treatment with tunicamycin. This modest decrease may be due to the subtoxic dose of tunicamycin used in the study, that was sufficient for ER stress induction but not strong enough to fully curtail the insulin expression. Co-treatment with tangeretin could only marginally improve the insulin levels. ER stress contributes to both reduced insulin expression and beta cell damage while tangeretin ameliorated the pancreatic beta cell damage by suppressing maladaptive UPR, oxidative stress and mitochondrial damage, it could only moderately improve the insulin levels. A summary of the results is schematically depicted in Fig. 8. Findings from this study indicate the ER protective role of tangeretin in improving pancreatic beta cell survival.

## Conclusion

ER stress in pancreatic beta cells compromise their function by upregulating maladaptive UPR, inducing oxidative stress, mitochondrial dysfunction and suppressing insulin expression. Tangeretin was effective in mitigating ER stress induced cellular disturbances and improving beta cell survival under ER stress condition and hence, we propose tangeretin as ER protective agent and a potential candidate in mitigating ER stress induced pancreatic Beta-TC-6 cell dysfunction.

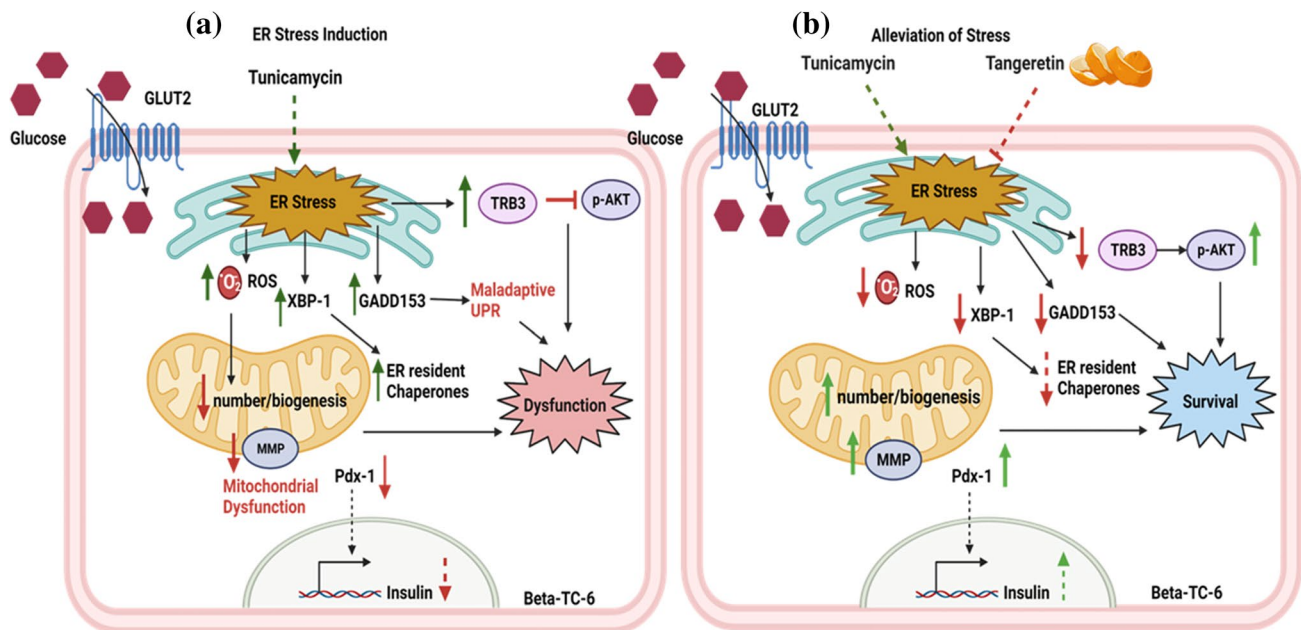


**Fig. 8** Effect of tangeretin on pancreatic Beta-TC-6 function during tunicamycin induced ER stress. **a** ER stress induction in Beta-TC-6 cells by tunicamycin. **b** Alleviation of stress condition in Beta-TC-6 cells by tangeretin. Prolonged exposure to tunicamycin induced ER stress, upregulated the protein folding machinery, increased ROS gen-

eration, decreased mitochondrial biogenesis, membrane potential and modestly suppressed insulin expression. Co-treatment with tangeretin ameliorated the ER stress, suppressed the protein folding machinery, decreased the ROS levels, improved mitochondrial function and modestly upregulated the insulin expression

**Supplementary Information** The online version contains supplementary material available at <https://doi.org/10.1007/s11033-023-09013-z>.

**Acknowledgements** Eveline M Anto is indebted to the University Grants Commission (UGC), New Delhi, India, for providing fellowship. P. Jayamurthy is grateful to Council of Scientific & Industrial Research (CSIR), India for financial assistance to conduct the research.

**Author contributions** EMA has contributed to the study design, data collection, analysis, interpretation and manuscript preparation. PJ has contributed to the data approval, interpretation, manuscript preparation and correction.

**Funding** The authors have received funding from the University Grants Commission (UGC) and Council of Scientific & Industrial Research (CSIR), New Delhi, India.

**Data availability** The authors are willing to provide all the data generated and/or analysed during the study on reasonable request.

## Declarations

**Competing interests** The authors declare no competing interests.

**Ethical approval** Not applicable.

## References

1. Seo HY et al (2008) Endoplasmic reticulum stress-induced activation of activating transcription factor 6 decreases insulin gene

- expression via up-regulation of orphan nuclear receptor small heterodimer partner. *Endocrinology* 149(8):3832. <https://doi.org/10.1210/EN.2008-0015>
2. Lipson KL et al (2006) Regulation of insulin biosynthesis in pancreatic beta cells by an endoplasmic reticulum-resident protein kinase IRE1. *Cell Metab* 4(3):245–254. <https://doi.org/10.1016/j.cmet.2006.07.007>
3. Back S, Kaufman R (2012) Endoplasmic reticulum stress and type 2 diabetes. *Annu Rev Biochem*. <https://doi.org/10.1146/annurev-biochem-072909-095555>. *Endoplasmic*
4. Berry C, Lal M, Binukumar BK (2018) Crosstalk between the unfolded protein response, microRNAs, and insulin signaling pathways: in search of biomarkers for the diagnosis and treatment of type 2 diabetes. *Front Endocrinol (Lausanne)*. <https://doi.org/10.3389/fendo.2018.00210>
5. Fonseca SG, Gromada J, Urano F (2011) Endoplasmic reticulum stress and pancreatic  $\beta$ -cell death. *Trends Endocrinol Metab* 22(7):266–274. <https://doi.org/10.1016/j.tem.2011.02.008>
6. Zhu M, Liu X, Liu W, Lu Y, Cheng J, Chen Y (2021) B cell aging and age-related diabetes. *Aging (Albany, NY)* 13(5):7691–7706. <https://doi.org/10.18632/aging.202593>
7. Kasuga M (2006) Insulin resistance and pancreatic  $\beta$  cell failure. *J Clin Invest* 116(7):1756. <https://doi.org/10.1172/JCI29189>
8. Park YJ, Woo M (2019) Pancreatic  $\beta$  cells: gatekeepers of type 2 diabetes. *J Cell Biol* 218:1094–1095. <https://doi.org/10.1083/jcb.201810097>
9. Lenzen S, Drinkgern J, Tiedge M (1996) Low antioxidant enzyme gene expression in pancreatic islets compared with various other mouse tissues. *Free Radic Biol Med* 20(3):463–466. [https://doi.org/10.1016/0891-5849\(96\)02051-5](https://doi.org/10.1016/0891-5849(96)02051-5)
10. Vig S, Lambooj JM, Zaldumbide A, Guigas B (2021) Endoplasmic reticulum-mitochondria crosstalk and beta-cell destruction

- in type 1 diabetes. *Front Immunol*. <https://doi.org/10.3389/fimmu.2021.669492>
11. Chaudhury A et al (2017) Clinical review of antidiabetic drugs: implications for type 2 diabetes mellitus management. *Front Endocrinol (Lausanne)*. <https://doi.org/10.3389/fendo.2017.00006>
  12. Sundar Rajan S, Srinivasan V, Balasubramanyam M, Tatu U (2007) Endoplasmic reticulum (ER) stress & diabetes. *Indian J Med Res* 125(3):411–424
  13. Panche AN, Diwan AD, Chandra SR (2016) Flavonoids: an overview. *J Nutr Sci* 5:1–15. <https://doi.org/10.1017/jns.2016.41>
  14. Arafa ESA, Shurrab NT, Buabeid MA (2021) Therapeutic implications of a polymethoxylated flavone, tangeretin, in the management of cancer via modulation of different molecular pathways. *Adv Pharmacol Pharm Sci*. <https://doi.org/10.1155/2021/4709818>
  15. Ashrafizadeh M, Ahmadi Z, Mohammadinejad R, Ghasempour Afshar E (2020) Tangeretin: a mechanistic review of its pharmacological and therapeutic effects. *J Basic Clin Physiol Pharmacol*. <https://doi.org/10.1515/JBCPP-2019-0191>
  16. Takano K et al (2007) Methoxyflavones protect cells against endoplasmic reticulum stress and neurotoxin. *Am J Physiol Cell Physiol* 292(1):353–361. [https://doi.org/10.1152/AJPCELL.00388.2006/SUPPL\\_FILE/FIGURE](https://doi.org/10.1152/AJPCELL.00388.2006/SUPPL_FILE/FIGURE)
  17. Anto EM, Sruthi CR, Krishnan L, Raghu KG, Purushothaman J (2023) Tangeretin alleviates tunicamycin-induced endoplasmic reticulum stress and associated complications in skeletal muscle cells. *Cell Stress Chaperones*. <https://doi.org/10.1007/s12192-023-01322-3>
  18. Mosmann T (1983) Rapid colorimetric assay for cellular growth and survival: application to proliferation and cytotoxicity assays. *J Immunol Methods* 65(1–2):55–63. [https://doi.org/10.1016/0022-1759\(83\)90303-4](https://doi.org/10.1016/0022-1759(83)90303-4)
  19. Armstrong D (2014) Advanced protocols in oxidative stress III, methods in molecular biology. *Adv Protoc Oxid Stress III* 594:1–477. <https://doi.org/10.1007/978-1-60761-411-1>
  20. Chazotte B (2011) Labeling mitochondria with mitotracker dyes. *Cold Spring Harb Protoc* 6(8):990–992. <https://doi.org/10.1101/pdb.prot5648>
  21. Sivandzade F, Bhalerao A, Cucullo L (2019) Analysis of the mitochondrial membrane potential using the cationic JC-1 dye as a sensitive fluorescent probe. *Bio Protoc*. <https://doi.org/10.21769/BIOPROT.3128>
  22. Luciani DS et al (2009) Roles of IP<sub>3</sub>R and RyR Ca<sup>2+</sup> channels in endoplasmic reticulum stress and beta-cell death. *Diabetes* 58(2):422–432. <https://doi.org/10.2337/db07-1762>
  23. Park SM, Il Kang T, So JS (2021) Roles of XBPIs in transcriptional regulation of target genes. *Biomedicines* 9(7):1–26. <https://doi.org/10.3390/biomedicines9070791>
  24. Nishitoh H (2012) CHOP is a multifunctional transcription factor in the ER stress response. *J Biochem* 151(3):217–219. <https://doi.org/10.1093/jb/mvr143>
  25. Tiedge M, Lortz S, Drinkgern J, Lenzen S (1997) Relation between antioxidant enzyme gene expression and antioxidative defense status of insulin-producing cells. *Diabetes* 46(11):1733–742. <https://doi.org/10.2337/diab.46.11.1733>
  26. Hasnain SZ, Prins JB, McGuckin MA (2016) Oxidative and endoplasmic reticulum stress in  $\beta$ -cell dysfunction in diabetes. *J Mol Endocrinol* 56(2):R33–R54. <https://doi.org/10.1530/JME-15-0232>
  27. Chong WC, Shastri MD, Eri R (2017) Endoplasmic reticulum stress and oxidative stress: a vicious nexus implicated in bowel disease pathophysiology. *Int J Mol Sci*. <https://doi.org/10.3390/IJMS18040771>
  28. Calfon M et al (2002) IRE1 couples endoplasmic reticulum load to secretory capacity by processing the XBP-1 mRNA. *Nature* 415(6867):92–96. <https://doi.org/10.1038/415092A>
  29. Allagnat F et al (2010) Sustained production of spliced X-box binding protein 1 (XBP1) induces pancreatic beta cell dysfunction and apoptosis. *Diabetologia* 53(6):1120–1130. <https://doi.org/10.1007/s00125-010-1699-7>
  30. Maruri-Avidal L, López S, Arias CF (2008) Endoplasmic reticulum chaperones are involved in the morphogenesis of rotavirus infectious particles. *J Virol* 82(11):5368–5380. <https://doi.org/10.1128/jvi.02751-07>
  31. Hu H, Tian M, Ding C, Yu S (2019) The C/EBP homologous protein (CHOP) transcription factor functions in endoplasmic reticulum stress-induced apoptosis and microbial infection. *Front Immunol* 10(JAN):1–13. <https://doi.org/10.3389/fimmu.2018.03083>
  32. Song B, Scheuner D, Ron D, Pennathur S, Kaufman RJ (2008) Chop deletion reduces oxidative stress, improves beta cell function, and promotes cell survival in multiple mouse models of diabetes. *J Clin Invest* 118(10):3378–3389. <https://doi.org/10.1172/JCI34587>
  33. Xiao T, Liang X, Liu H, Zhang F, Meng W, Hu F (2020) Mitochondrial stress protein HSP60 regulates ER stress-induced hepatic lipogenesis. *J Mol Endocrinol* 64(2):67–75. <https://doi.org/10.1530/JME-19-0207>
  34. Fang X, Zhang X, Li H (2020) Oxidative stress and mitochondrial membrane potential are involved in the cytotoxicity of perfluorododecanoic acid to neurons. *Toxicol Ind Health* 36(11):892–897. <https://doi.org/10.1177/0748233720957534>
  35. Gerencser AA (2018) Metabolic activation-driven mitochondrial hyperpolarization predicts insulin secretion in human pancreatic beta-cells. *Biochim Biophys Acta* 1859(9):817–828. <https://doi.org/10.1016/j.bbabi.2018.06.006>
  36. Kelley DE, He J, Menshikova EV, Ritov VB (2002) Dysfunction of mitochondria in human skeletal muscle in type 2 diabetes. *Diabetes* 51(10):2944–2950. <https://doi.org/10.2337/DIABES.51.10.2944>
  37. Singh R, Mohapatra L, Tripathi AS (2021) Targeting mitochondrial biogenesis: a potential approach for preventing and controlling diabetes. *Future J Pharm Sci*. <https://doi.org/10.1186/s43094-021-00360-x>
  38. Cheng KKY et al (2012) APPL1 potentiates insulin secretion in pancreatic  $\beta$  cells by enhancing protein kinase Akt-dependent expression of SNARE proteins in mice. *Proc Natl Acad Sci USA* 109(23):8919–8924. <https://doi.org/10.1073/PNAS.1202435109/-DCSUPPLEMENTAL/PNAS.201202435SI.PDF>
  39. Balcazar Morales N, Aguilar de Plata C (2012) Role of AKT/mTORC1 pathway in pancreatic  $\beta$ -cell proliferation. *Colomb Med (Cali)* 43(3):235–243
  40. Elghazi L, Bernal-Mizrachi E (2009) Akt and PTEN:  $\beta$ -cell mass and pancreas plasticity. *Trends Endocrinol Metab* 20(5):243–251. <https://doi.org/10.1016/j.tem.2009.03.002>
  41. Ohoka N, Yoshii S, Hattori T, Onozaki K, Hayashi H (2005) TRB3, a novel ER stress-inducible gene, is induced via ATF4-CHOP pathway and is involved in cell death. *EMBO J* 24(6):1243–1255. <https://doi.org/10.1038/sj.emboj.7600596>
  42. Thorens B (2015) GLUT2, glucose sensing and glucose homeostasis. *Diabetologia* 8(2):221–232. <https://doi.org/10.1007/s00125-014-3451-1>
  43. Bensellam M, Jonas JC, Laybutt DR (2018) Mechanisms of  $\beta$ -cell dedifferentiation in diabetes: recent findings and future research directions. *J Endocrinol* 236(2):R109–R143. <https://doi.org/10.1530/JOE-17-0516>
  44. Chen CW et al (2022) Adaptation to chronic ER stress enforces pancreatic  $\beta$ -cell plasticity. *Nat Commun* 13(1):1–18. <https://doi.org/10.1038/s41467-022-32425-7>
  45. Ferrer J, Gomis R, Alvarez JF, Casamitjana R, Vilardell E (1993) Signals derived from glucose metabolism are required for glucose regulation of pancreatic islet GLUT2 mRNA and protein. *Diabetes* 42(9):1273–1280. <https://doi.org/10.2337/DIAB.42.9.1273>



46. Zhang IX (2020) Investigating the role of ER stress on mouse pancreatic beta-cell function
47. Zhou X, Xu Y, Gu Y, Sun M (2021) 4-Phenylbutyric acid protects islet  $\beta$  cell against cellular damage induced by glucocorticoids. *Mol Biol Rep* 48(2):1659–1665. <https://doi.org/10.1007/s11033-021-06211-5>
48. Kim SK, Hebrok M (2001) Intercellular signals regulating pancreas development and function. *Genes Dev* 15(2):111–127. <https://doi.org/10.1101/gad.859401>
49. Yao X et al (2020) Tectorigenin enhances PDX1 expression and protects pancreatic  $\beta$ -cells by activating ERK and reducing ER stress. *J Biol Chem* 295(37):12975–12992. <https://doi.org/10.1074/JBC.RA120.012849>

**Publisher's Note** Springer Nature remains neutral with regard to jurisdictional claims in published maps and institutional affiliations.

Springer Nature or its licensor (e.g. a society or other partner) holds exclusive rights to this article under a publishing agreement with the author(s) or other rightsholder(s); author self-archiving of the accepted manuscript version of this article is solely governed by the terms of such publishing agreement and applicable law.